



UiT The Arctic University of Norway

Faculty of Health Sciences

Department of Medical Biology

Evolutionary genomics of cowpox virus and recombination *in vitro* between a naturally occurring cowpox virus and a vaccinia virus vectored influenza vaccine

Diana Karina Diaz Cánova

A dissertation for the degree of Philosophiae Doctor (PhD)

April 2023



A dissertation for the degree of Philosophiae Doctor

**Evolutionary genomics of cowpox virus and recombination *in vitro*
between a naturally occurring cowpox virus and a vaccinia virus
vectored influenza vaccine**

Diana Karina Diaz Cánova



**Molecular Inflammation Research Group
Department of Medical Biology
Faculty of Health Sciences
UiT- The Arctic University of Norway**

April 2023

*To my grandmother, Josefa N. Mendoza
Zavala vda. de Diaz.*

Acknowledgements

This PhD project was performed at the Molecular Inflammation Research Group (MIRG), Department of Medical Biology, Faculty of Health Sciences, the Arctic University of Norway-UiT.

First and foremost, I would like to express my profound gratitude to my two wonderful supervisors, Ugo Moens and Malachy Okeke. I am infinitely grateful for all the support, patience and encouragement that you gave me during this journey that was not an easy one, but we succeeded!

Thank you Ugo, for always having the door to your office open so I could run to you when I had a problem or a silly question to ask. You were always there for me despite your busy schedule. I really appreciate your kind words of encouragement in our meetings that made me realize how much I have achieved and learnt. I am really impressed by how efficient you are. When I asked for a document, five minutes later you were knocking at my office door with the signed document!

Malachy, despite you not being here in Tromsø, I could always count on you! The distance was not a problem and you managed to supervise well me during these years. Even when something went wrong in my experiments you could guide me from Nigeria. Thanks for allowing me to contact you anytime. You were always available and ready to answer my questions. Sometimes I thought you would get mad because of my millions of questions, but you did not! You were always so kind and patient.

Both of you, Ugo and Malachy, were the right match. You complemented each other and made a great team! Thanks for having me as your PhD student, for sharing all your knowledge with me and believing in me.

I would like to thank Andreas Nitsche for giving me the opportunity to visit the Robert Koch Institute in Berlin. The research stay in your institute was a cornerstone in my PhD. Also, I want to give my infinite gratitude to Annika Brinkmann for introducing me to this new world called “bioinformatics”. I really appreciate your patience during those two weeks in Berlin. Without you I would not have been able to analyze all my sequencing data.

I want to thank Carla Mavian. I am so grateful that we worked together, and you shared your knowledge in BEAST to me.

I want to thank Rolf Andersen from the Orakelet, you were just a star! When I had a problem with the server or any programs, you were always there helping me, providing solutions and you made my PhD life much easier by introducing me to the UiT server. Thanks a lot!!

Juan Daniel Montenegro thanks for being so patient and helping me with my bioinformatics troubles. You taught me new bioinformatics programs that are now part of the methodology used in my articles ¡Eres un capo!

Thanks to the past members of the Molecular Inflammation Research Group (Conny, Kashif, Aelita, Baldur, Dag, Marianne, Maria and Gianina) for creating a nice atmosphere in the lab. A special thanks to my lovely and sweet friend Connyzita, thanks for all the love, hugs and chocolates. I miss your priceless hugs!

I would like to thank to the Old and New “Lab-gang” of the 9th floor (Adri, Clement, Jessin, Ekaterina, Ahmed, Bishnu, Srijana, Jeanette, Jalal, Maria, Gaute, Kjersti, Mushtaq, Hermoine, Theresa, Bhupender, Dorothea, Jonathan, Ken, Martin, Erick and Mikal), Almudena and Swapnil for the delicious common lunches, parties, coffee/cake breaks, laughs, talks, etc. Thanks for all the nice memories.

Clementine, thanks for being a wonderful friend, for being by my side in the most difficult moments. I could always count on you. You were like a big brother always advising me when I needed it most. Also, thanks for all the amazing memories (our trips, parties, birthday dinners, burgers, laughs, etc.), you just made my PhD journey and my life much lighter and easier, thank you from the bottom of my heart!

Adri, thanks a lot for being the big sister that I needed in Norway. Despite you moving to Oslo, you always called me, checked on me, advised me and supported me when I needed it the most, thanks, thanks, thanks!! You don't know how much I treasure you! I love you, my Adri!. My dear friend Jessin, thanks for sharing your bioinformatics knowledge with me and helping me when I was going crazy with the bioinformatics programs. Also, thanks for spoiling me with your delicious Indian food.

I also want to thank my lovely ladies (Alejandra, Karla and Angie) that made my life in Tromsø very pleasant with their great sense of humor and warm company. Sometimes life is not easy, but you showed me that women are extremely strong, brave, and courageous and can overcome any obstacle in life. Alejandra (Margothcita), thanks for the wonderful gift that you gave me (my cute Godson Sander) and for pampering me when I really needed it, you made me feel at home.

Thanks to my lovely family, especially to my beloved dad, grandmother and my sister Susan, for their endless love, always believing in me and cheering me up. Grandma thanks for always supporting me to pursue my dreams and keeping me in your prayers. If it was not for you, I could not be writing these words ¡Te amo con todo mi ser!

Above all, I want to thank God for being with me and guiding me during this journey and blessing me with wonderful people around me.

¡Gracias totales!

D.K.D.C

Table of Contents

LIST OF ABBREVIATIONS	iii
LIST OF FIGURES.....	v
LIST OF PAPERS.....	vi
SUMMARY	1
1. INTRODUCTION.....	3
1.1 Poxvirus.....	3
1.2 Orthopoxvirus.....	3
1.2.1 <i>Variola virus</i>	3
1.2.2 <i>Cowpox virus</i>	4
1.2.3 <i>Vaccinia virus</i>	5
1.2.4 <i>Monkeypox virus</i>	7
1.2.5 <i>Ectromelia virus</i>	8
1.2.6 <i>Alaskapox virus</i>	8
1.3 Virus structure	9
1.3.1 Genome organization	9
1.4 Viral cycle	10
1.4.1 Virus entry and uncoating	11
1.4.2 Viral DNA replication	11
1.4.3 Virus assembly and egress.....	12
1.5 Viral tropism.....	13
1.6 Evolution and phylogeny of orthopoxviruses.....	15
1.7 Hazard characterization of Modified Vaccinia virus Ankara.....	17
1.7.1 Host cell restriction of MVA.....	18
1.7.2 Nature and distribution of naturally circulating orthopoxviruses.....	19
1.7.3 Recombination in co-infection and superinfection.....	19
1.7.4 Homogeneity and genetic stability of MVA.....	21
2. RATIONALE OF THIS STUDY	22
3. GENERAL OBJECTIVE	24
4. METHODOLOGY	25
4.1 Viruses, cells, co-infection and superinfection experiments	25
4.2 Viral DNA extraction	27
4.3 Sequencing	27
4.4 Genome assembling and annotation.....	28

4.5	Gene content comparison	28
4.6	Recombination analysis.....	29
4.7	Phylogenetic analysis, patristic and genetic distances.....	29
4.8	Phyldynamic evolutionary analysis of CPXV	31
5.	SUMMARY OF THE MAIN RESULTS	32
6.	GENERAL DISCUSSION	34
7.	CONCLUSION AND FUTURE PERSPECTIVES	40
8.	REFERENCES	41

LIST OF ABBREVIATIONS

AKMV	Ahkmeta virus
AKPV	Alaskapox virus
ATI	A-type inclusion
BPXV	Buffalopox virus
BHK	Baby hamster kidney
BI	Bayesian inference
CAM	Chorioallantoic membrane
CDS	Coding sequence
CEF	Chicken embryo fibroblast
CEV	Cell-associated enveloped virus
CHO	Chinese hamster ovary
ChPV	Chordopoxvirinae
CMLV	Camelpox virus
CNPV	Canarypox virus
CPXV	Cowpox virus
CrmB	Cytokine response modifier B
CrmD	Cytokine response modifier D
CVA	Chorioallantois VACV Ankara
dsDNA	double-stranded DNA
ECTV	Ectromelia virus
EEV	Extracellular enveloped virus
ER	Endoplasmic reticulum
ERA	Environmental risk assessment
EU	European Union
GATU	Genome Annotation Transfer Utility
GMO	Genetically modified organism
HA	Hemagglutinin
HPD	High posterior density interval
HSPV	Horsepox virus
ICTV	International Committee on Taxonomy of Viruses
IEV	Intracellular enveloped virus
IMV	Intracellular mature virus
ITR	Inverted terminal repeat
IV	Immature virus
IVN	Immature virus with nucleoid
LSDV	lumpy skin disease virus
MAFFT	Multiple Alignment Fast Fourier Transform
ML	Maximum Likelihood
moi	Multiplicity of infection
MPXV	Monkeypox virus
MVA	Modified Vaccinia virus Ankara
MVA-HANP	MVA vectored influenza vaccine
NGS	Next-generation sequencing
NP	Nucleoprotein
OPXV	Orthopoxvirus
ORF	Open reading frame
ppi	Post primary infection
RCNV	Raccoonpox virus

RDP	Recombination detect program
RSV	Respiratory Syncytial virus
SKPV	Skunkpox virus
TATV	Taterapox virus
TGS	Third generation sequencing
tMRCA	Time to the most recent common ancestor
UK	United Kingdom
VACV	Vaccinia virus
VARV	Variola virus
VOCs	Viral Orthologous Clusters database
VPXV	Volepox virus
WHO	World health organization

LIST OF FIGURES

Figure 1. Schematic representation of the CVA and MVA genomes. The pink boxes represent the deleted regions in the CVA genome. The blue arrows represent ITR.....	7
Figure 2. Schematic diagram of Vaccinia virus structure.....	9
Figure 3. Schematic overview of the Vaccinia virus life cycle. IV, immature virion; IVN, immature virion with nucleoid; IMV, intracellular mature virion; IEV, intracellular enveloped virus; CEV, cell-associated enveloped virus; EEV, extracellular enveloped virus.	10
Figure 4. Co-infection and superinfection experiments in Vero cells. Co-infection, Vero cells were co-infected with CPXV-No-F1 and MVA-HANP. Superinfection 1, primary infection with CPXV-No-F1 and secondary infection with MVA-HANP at 4h post primary infection (ppi); Superinfection 2, primary infection with MVA-HANP and secondary infection with CPXV-No-F1 at 4h ppi; Superinfection 3, primary infection with CPXV-No-F1 and secondary infection with MVA-HANP at 6h ppi; Superinfection 4, primary infection with MVA-HANP and secondary infection with CPXV-No-F1 at 6h ppi.....	26

LIST OF TABLES

Table 1. Cell lines susceptibility to MVA	14
--	----

LIST OF PAPERS

Paper I

Diaz-Cánova, D., Moens, U. L., Brinkmann, A., Nitsche, A., and Okeke, M. I. (2022). Genomic Sequencing and Analysis of a Novel Human Cowpox Virus With Mosaic Sequences From North America and Old World Orthopoxvirus. *Front. Microbiol.* 13. doi:10.3389/FMICB.2022.868887

Paper II

Diaz-Cánova, D., Mavian, C., Brinkmann, A., Nitsche, A., Moens, U., and Okeke, M. I. (2022). Genomic Sequencing and Phylogenomics of Cowpox Virus. *Viruses* 2022, Vol. 14, Page 2134 14, 2134. doi:10.3390/V14102134.

Paper III

Diaz-Cánova, D., Brinkmann, A., Nitsche, A., Moens, U., and Okeke, M. I. Whole genome sequencing of recombinant viruses obtained from co-infection and superinfection of Vero cells with Modified Vaccinia virus Ankara vectored influenza vaccine and a naturally occurring *Cowpox virus*. Manuscript

SUMMARY

Modified vaccinia virus Ankara (MVA) is a promising orthopoxvirus (OPXV) vector vaccine candidate due to its host range restriction and good safety profile as a smallpox vaccine. It has been widely tested in clinical trials as a recombinant vector for vaccination against infectious diseases and cancers in humans and animals. Furthermore, it is being used as smallpox and Mpox vaccine. However, the extensive use of MVA and MVA vectored vaccines have the potential for MVA or MVA vectored vaccine to recombine with naturally circulating OPXV. *Cowpox virus* (CPXV) as a close relative of MVA is a potential candidate for recombination. Hence, the genetic diversity and evolution of CPXV was assessed in this work, as well as recombination *in vitro* between a naturally occurring CPXV and MVA vectored vaccine in cells in which MVA multiplies poorly. CPXV is classified as a single species; however, we demonstrated that CPXV might be an assemblage of several species based on its high genetic diversity, lack of monophyly, and close phylogenetic relationship with other OPXV. CPXV strains were separated into five major clusters rather than one monophyletic cluster. Furthermore, we described a new, distinct cluster closely related to *Ectromelia virus* (ECTV) and *Abatino macacapox virus* (Abatino) named “ECTV-Abatino-like CPXV”. Additionally, we showed evidence that a Norwegian CPXV isolate was a natural occurring recombinant CPXV that might have emerged following multiple recombination events between different OPXV species from the Old World and North America. Under *in vitro* conditions, the progeny viruses obtained from co-infection and superinfection of Vero cells with MVA-HANP and CPXV-No-F1 had mosaic genomes and displayed parental and non-parental plaque phenotypes. Furthermore, some progeny viruses contained the transgene from MVA-HANP and regained genes that were deleted or fragmented in MVA-HANP. Overall, these findings will contribute to the environmental risk assessment of MVA and MVA vectored vaccines and to the improvement of the biosafety of MVA vectored vaccines.

1. INTRODUCTION

1.1 Poxvirus

Poxviridae is a family of large double-stranded DNA (dsDNA) viruses¹. The family is divided into two subfamilies based on its host range: *Chordopoxvirinae* (*ChPV*), viruses that infect vertebrates, and *Entomopoxvirinae*, viruses that infect insects. There are four and eighteen genera within *Entomopoxvirinae* and *Chordopoxvirinae*, respectively (<https://ictv.global/taxonomy>). Among *Chordopoxvirinae*, only species of the genera *Orthopoxvirus*, *Parapoxvirus*, *Molluscipoxvirus*, and *Yatapoxvirus* are known to cause human infections². The best characterized genus within vertebrate poxviruses is *Orthopoxvirus* (OPXV). Some OPXV including *Variola virus* (VARV), *Vaccinia virus* (VACV)-like, *Cowpox virus* (CPXV), *Monkeypox virus* (MPXV), and *Camelpox virus* (CMLV) can cause human diseases³. The genus *Orthopoxvirus* includes twelve species. According to their endemism, OPXV are divided into the New World and the Old World OPXV. The Old World or African-Eurasian OPXV group contains: CPXV, VACV, MPXV, VARV, CMLV, *Taterapox virus* (TATV) and *Ectromelia virus* (ECTV). The New world OPXV group comprises three species that are endemic to North America: *Raccoonpox virus* (RCNV), *Volepox virus* (VPXV) and *Skunkpox virus* (SKPV)⁴. Recently, three novel OPXV species have been discovered in different locations: *Abatino macacapox virus* (Abatino) in Italy, *Ahkmeta virus* (AKMV) in Georgia and *Alaskapox virus* (AKPV) in the United States⁵⁻⁷, although AKPV is still not formally classified as an OPXV species.

1.2 Orthopoxvirus

1.2.1 *Variola virus*

VARV is the most notorious OPXV, as it is the causative of smallpox. VARV has humans as an exclusive host and no animal reservoirs have been found⁸. Smallpox is a highly contagious airborne disease with high mortality rates (15-45%)^{9,10} that caused around 300-500 million deaths world-wide in the 20th century¹¹. The term “variola” for smallpox was derived from the latin word *various* (meaning spotted) or from *varus* (meaning pimples)¹², and refers to the pustules that appears on the body and face. Later, the term “small pockes” (pocke means sac) was used to differentiate it from syphilis, “great pockes”¹³. The first historical record of smallpox was in Egypt from the mummy of Ramses V, who died 1157 BC¹⁴. From Egypt, the disease started to spread to other parts of the world. One of the first methods to mitigate smallpox was variolation, which consisted in the inoculation of smallpox pus or scabs into the skin (Indian method) or in intranasal insufflation of dried smallpox scabs (Chinese method) to a healthy person¹⁵. It was an effective method to prevent smallpox, but the mortality rate was approximately 2%^{9,10}. After 1798, variolation was gradually replaced by a safer procedure called vaccination¹⁰. Compared to variolation, vaccination gave the same protection, but with less severe symptoms. In 1959, the World Health organization (WHO) launched a Global

Smallpox Eradication Program with the aim to eradicate smallpox ¹⁰. From 1959 to 1977, the WHO organized vaccination campaigns world-wide. The last natural smallpox case was recorded in 1977 ¹⁶, and in 1980 the WHO formally declared the eradication of smallpox, and the routine smallpox vaccination ceased ¹⁷.

Prior to the eradication of smallpox, there were multiple VARV strains that were circulating. However, there were two main variants: *variola major* with a mortality rate of 20-45% (which is the most common cause of death related to smallpox) and *variola minor* or *alastrim*, characterized by a much lower mortality rate (1-2%) ^{9,10}. The latter variant was common in Western Africa and America and appeared in the end of the 19th century ¹⁰. After smallpox eradication, the WHO decided that all VARV stocks should be destroyed or deposited in two international centers in the State Research Center of Virology and Biotechnology in Russia and the Center for Disease Control and Prevention in the United States ¹⁸. Those are the only two WHO-approved centers that can conduct research on VARV. The WHO had planned to destroy all VARV stocks but given the potential for a bioterrorist attack, the destruction has been postponed for a few years until the development of new antiviral agents against smallpox and until the committee decides the best options for global public health ¹⁹.

1.2.2 Cowpox virus

CPXV is a zoonotic OPXV that is the causative agent of the disease cowpox. Historically, cowpox has been associated with the first vaccine used by the English physician Edward Jenner who established a safer method called “vaccination” to protect against smallpox in 1798. He had heard the folk tale that anyone who contracted cowpox could not catch smallpox ²⁰. Based on this belief, in 1796, he inoculated the boy James Phipps with cowpox pustules from the hand of the milkmaid Sara Nelmes. Some weeks after, Jenner infected the boy with smallpox pus and the boy did not develop the disease. After this finding, he repeated the same procedure with other children and concluded that vaccination offers a full protection against smallpox ^{21,22}. Jenner called the pustular material “*variolae vaccinae*” (smallpox of the cow) to make reference to the cow (latin word *vacca*) ^{23,24} and later the “*variolae vaccinae*” was referred to as vaccine ²⁵. However, until now, there is still uncertainty about the nature of the virus that Jenner used as a first vaccine. Probably he might have used VACV or *Horsepox virus* (HSPV) ^{22,26-28}. In 1798, Jenner published his discovery, which was the basis for vaccination and immunology ²². Although vaccination had been first used by Benjamin Jesty 22 years before Jenner ^{29,30}, there is no evidence that Jenner knew about Jesty’s vaccinations ²⁹. Thus, the credits for developing vaccination were given to Jenner ^{29,30}.

CPXV is endemic of Eurasia, mainly in Europe ³¹⁻³⁷. CPXV has the broadest host range among OPXV ^{3,38}, which is thought to be associated with its high number of host range genes ^{39,40}. Its natural reservoir hosts are probably wild rodents such as bank voles (*Myodes glareolus*), common voles (*Microtus arvalis*) and field voles (*Microtus agrestis*) ^{31,41,42}. CPXV infects many non-reservoir species such as felines, monkeys, dogs, alpacas, rats, cats and horses ^{36,42-47}. CPXV even causes spillover infections from infected animals to humans ^{34,48-59}. Most human

CPXV cases were caused by contact with infected cats^{49,59,60}. In humans, the disease is usually self-limiting with pox lesions and mild symptoms, but it can lead to fatal infections, especially in immune-compromised individuals^{61–63}. The first zoonotic case was reported in the Netherlands in 1985, in which a woman was infected with CPXV from a domestic cat⁶⁴. In the last decades, multiple lethal and non-lethal CPXV outbreaks in animals have been reported as well as human cases of CPXV infections^{42,61–63,65–67}. In the Fennoscandian region, CPXV infections in humans and felines have been reported (CPXV-No-H1, CPXV-No-H2, CPXV-Swe-H1, CPXV-Swe-H2, CPXV-No-F1 and CPXV-No-F2)^{45 45,68–72}. Interestingly, one of these Fennoscandian CPXV isolates, CPXV-No-H2, was a peculiar CPXV strain⁷¹. The phylogenetic analysis using the *p4c* gene revealed that CPXV-No-H2 was clustered separate from the other CPXV isolates. This was evidence of the genetic diversity among CPXV isolates. Other studies have also revealed that CPXV is genetically heterogeneous^{70,72–78}.

The traditional nomenclature used in poxvirus taxonomy, that is naming the virus after the host from which it was isolated, brought confusion in the classification of cowpox. For instance, cows are susceptible to both CPXV and VACV. Jenner described cowpox as a disease characterized by pustules on the nipples and utters of cows that were infected from horses²². Later, Downie defined CPXV as strains that were isolated from the spontaneous disease in cattle or from human lesions caused by directly infection from that source. Additionally, he described some biological properties of CPXV such as the presence of A-type inclusion bodies (ATI) and red hemorrhagic pocks on the chorioallantoic membrane (CAM) of chicken eggs after infection⁷⁹. Since then, the classification of CPXV has been based on host specificity and the two main criteria described by Downie. As a consequence, several viruses have been classified as CPXV^{80–83}. The classification of CPXV is still a matter of debate. It has been proposed that CPXV is not one single species and it may contain more than one species^{70,72,73,75,76,84}.

1.2.3 *Vaccinia virus*

VACV has been used as a vaccine against smallpox in the 20th century⁷⁹. Although it is still not clear when VACV started to be used, it is thought that at some point during 19th century cowpox was swapped for VACV¹⁰. However, recent evidence showed that old smallpox vaccines were more similar to HSPV^{22,26–28}, which is more closely related to VACV than to CPXV. Therefore, it has been suspected that Jenner may have used a HSPV-like virus instead of CPXV^{26,85,86}.

The exact origin of VACV is still unknown as well as its natural reservoir, even though VACV is the most studied OPXV. Since VACV strains have been attenuated in the laboratory, it was thought that VACV strains were unable to establish an infection in nature³. However, VACV-like infections have been reported in multiple species (such as cat, cattle, buffaloes and rabbit) and in different places throughout the world^{3,47,87–93}. VACV and VACV-like have a broad host range^{3,94} and are considered endemic in South America and Asia⁹⁴.

There are several variants of VACV-like that have been described such as HSPV, Buffalopox virus (BPXV) and Brazilian VACV-like^{3,47,87}. BPXV outbreaks have occurred in several countries, affecting mainly buffaloes but also humans^{89,95,96}. In South America, multiple outbreaks of VACV-like infections have been recorded, especially in Brazil^{3,97-99}. Brazilian VACV-like strains were mainly isolated from cattle and humans, although they have been detected in other animals^{3,100-102}. It is likely that Brazilian VACV-like derived from a spillback of a vaccine strain to wild hosts rather than being natural VACV populations circulating in an unknown reservoir^{3,85,103}. VACV-like infections in humans were associated with infected animals (zoonotic transmission)^{104,105}. Although human-to-human transmission (interhuman transmission) has also been reported^{106,107}.

Several VACV strains have been used to develop smallpox vaccines. There are four major types of VACV vaccines: first-, second-, third- and fourth-generation vaccines^{108,109}. The first-generation vaccines were live vaccines produced in live animals and were used during the Global Smallpox Eradication campaign^{10,110}. Many VACV strains were used to develop first-generation vaccines, for instance the New York City Board of Health (NYCBH) strain was used in the USA, the Temple of Heaven (Tian Tan) strain was used in China and the Lister strain was used in Africa, Asia, Europe and the USA^{10,109,111}. Nonetheless, these vaccines were not recommended due to safety problems. The second-generation vaccines were produced in tissue culture with good manufacturing practices¹⁰⁹. However, like first generation vaccines, they may still cause severe side effects^{109,112}. The poor safety profile of VACV second-generation vaccines led to the third-generation vaccines. These vaccines are live but attenuated VACV that maintained their immunogenicity and protection against smallpox¹⁰⁸. The attenuation was obtained after multiple passages of the parental virus in cell cultures, which generated random mutations in its genome¹⁰⁹. Several attenuated VACV strains have been developed such as modified Vaccinia virus Ankara (MVA) and Lister-16m8 (LC16m8)^{113,114}. In the fourth-generation vaccines, the attenuation is achieved using genetic engineering. The genomes of the fourth-VACV strains are manipulated by, for example, inserting, deleting or interrupting specific genes¹⁰⁹. An example of these vaccines is NYVACV¹¹⁵. Moreover, subunit-based vaccines are included within the fourth-generation vaccines^{116,117}. Recombinant DNA technology has played an important role in the development of VACV-based vaccines. The ability of incorporate foreign DNA (up to 25kb) into the VACV genome¹¹⁸ opened the opportunity of using VACV as viral vector against other diseases.

Modified Vaccinia virus Ankara

MVA was originally developed in the 1970s as a smallpox vaccine. MVA is an attenuated VACV strain derived from Chorioallantois VACV Ankara (CVA). CVA was passaged more than 500 times in primary chicken embryo fibroblasts (CEF) to be attenuated. After 516 passages, an attenuated virus was obtained and CVA was renamed MVA¹¹⁹. Upon more than 570 passages, the CVA genome had suffered six major deletions as well as minor deletions, insertions and point mutations (Figure 1). As a result, the CVA genome was reduced by around 13%, from 208 kbp (CVA) to 178 kbp (MVA)¹²⁰⁻¹²². The mutations led to the deletion, fragmentation and disruption of multiple genes in MVA responsible for evasion of the host

immune response and regulating the viral host range, such as the *K1L*, *C12L* and *C16L* genes^{122,123}. Although the six major deletions took place in genomic regions of CVA where truncated or fragmented genes pre-existed (e.g. *A39R* and *A55R* gene). The small mutations affected 122 of the 195 genes in MVA¹²². It is presumed that the genetic modifications render MVA incapable to multiply in most mammalian and human cells^{121,124,125}.

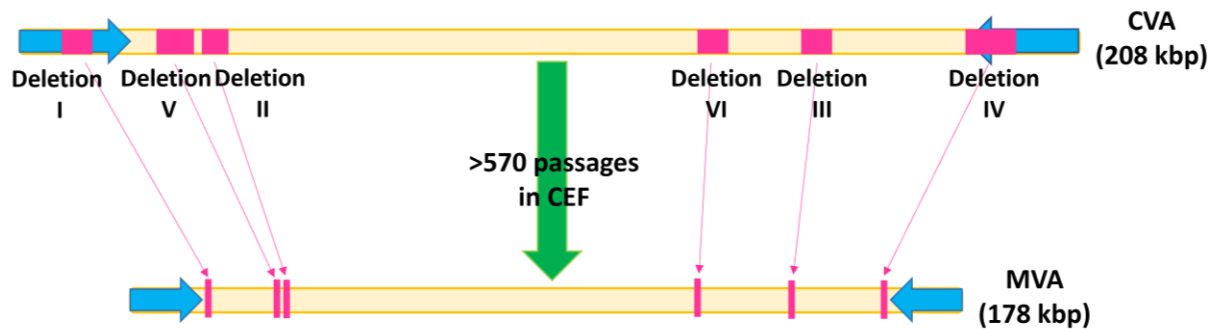


Figure 1. Schematic representation of the CVA and MVA genomes. The pink boxes represent the deleted regions in the CVA genome. The blue arrows represent ITR.

MVA was administered to over 120,000 people in Germany when smallpox was not endemic in the country. Among those vaccinated were children, immunocompromised individuals and elderly people. The vaccines showed mild or moderate adverse effects, such as local reaction (redness) and fever^{114,126–128}. MVA-BN has been authorized for use as a smallpox vaccine in Europe (with the trade name Imvanex), Canada (with the trade name Imvamune) and in USA (with the trade name Jynneos)^{129,130}. Furthermore, it has been approved as a Mpox vaccine¹³¹. MVA-BN is derived from the MVA-584 strain, following six rounds of plaque purification. It has a more restricted host range than other MVA strains¹³². Due to its excellent safety profile, attenuation *in vivo*, immunogenicity *in vivo*, and the ability to incorporate and express foreign DNA with correct post-translational modification, MVA is one of the promising viral vectors for development of recombinant vaccines and gene delivery^{133,134}. MVA has been used to develop recombinant vaccines against numerous diseases, both in humans and animals, and cancers. The development of vaccines using MVA vectors are in different phases of clinical trials, including MVA vaccines against HIV^{135,136}, Ebola^{137–140}, respiratory syncytial virus¹⁴¹, Middle East Respiratory Syndrome¹⁴², cytomegalovirus¹⁴³, influenza^{144,145}, tuberculosis¹⁴⁶ and malaria^{147–149}.

1.2.4 Monkeypox virus

Mpox is a zoonotic disease caused by MPXV. The virus causes mild symptoms but in immunosuppressed patients, individuals with pre-existing medical conditions, elderly people and young children the disease can be more severe with fatal outcomes^{150–153}. Similar to smallpox, Mpox is more often lethal in children than in adults^{151,154,155}. Mpox is endemic in

West and Central Africa ¹⁵⁶. MPXV strains are divided into Clade I (formerly Central African clade) and Clade II (formerly West African clade) ¹⁵⁷. The Clade I has a higher fatality rate (10.6%) than the Clade II (3.6%) ¹⁵⁸. There are two routes of MPXV transmission: (1) from animal to human (zoonotic) and (2) from human to human (interhuman), which includes mother-to-child (vertical transmission) ^{153,155,158}.

MPXV was first identified in captive monkeys in Denmark in 1958 ¹⁵⁹. Natural infections of MPXV have been detected in other mammalian species ¹⁶⁰. Although there is no definitive reservoir of MPXV, it is presumed that African rodents are the reservoir ¹⁶⁰. The first human Mpox case was reported in the Democratic Republic of Congo in 1970 ¹⁶¹. After this, human cases of Mpox have been reported in endemic countries ^{160,162,163}. From 2013 to 2021, sporadic non-endemic cases imported from endemic countries were reported in the USA, Singapore, Israel and the United Kingdom (UK) ¹⁶⁴⁻¹⁶⁸. It is thought that those MPXV outbreaks were spillovers from animals to humans ^{157,169}. In May 2022, the global Mpox outbreak started in the UK ¹⁷⁰, and since then 86,724 cases have been confirmed in 110 countries ¹⁷¹.

1.2.5 *Ectromelia virus*

ECTV is the causative agent of mousepox, a lethal, acute exanthematous disease of laboratory mouse colonies ^{172,173}. The natural reservoir of ECTV is likely wild mice. One ECTV strain was isolated from wild mice in Germany ¹⁷⁴. ECTV has a very narrow host range, its host is the mouse. However, human cases of ECTV infection have been reported in China and one case in fox ¹⁷⁵⁻¹⁷⁷. The first ECTV strain (ECTV-Hampstead) was discovered in a laboratory mouse colony in Hampstead, the UK ¹⁷³. After that, several outbreaks occurred in Europe, Japan, China and the USA ^{174,178,179}. ECTV-Hampstead was the progenitor of the outbreaks in Europe. It is thought that ECTV-Hampstead was also responsible for the outbreaks in Russia, Japan and the USA (from the 1980s) ¹⁷⁴. The ECTV outbreaks in the USA caused high mortality in laboratory mice and losses of millions of dollars ¹⁸⁰. Mousepox was a serious threat to laboratory mice, but it has been eliminated due to increased health surveillance and improvements in animal facilities ¹⁸⁰. However, mousepox is still relevant as it is the best small animal model of smallpox. In addition, it has been used in studies of OPXV infection and pathogenesis ^{172,181,181,182}. Compared to CPXV, ECTV produces white lesions on chorioallantoic membrane (CAM) of chicken eggs and V⁻ ATI phenotype. However, ECTV-Hampstead produced the wild type V⁺ ATI and the atypical V^{+/-} ATI. Furthermore, it contained a complete *p4c* gene. Whereas the other ECTV strains contained a truncated *p4c* gene and produced V⁻ ATI ^{174,183}.

1.2.6 *Alaskapox virus*

AKPV has not been classified as OPXV, but it has been suggested that it represents a novel OPXV. AKPV was isolated from a patient in Alaska, the USA. The distribution of AKPV is unknown as well the infection source of the patient. It has been speculated that either the patient was in contact with fomites brought from abroad or the virus was circulating in small mammals,

like other OPXV, in the areas close to the residence of the patient. The sampling of small mammals and the fomites tested negative for OPXV, although the sampling was limited^{7,184}.

1.3 Virus structure

Poxviruses are ovoid or brick-shaped viruses (220-450 nm x 140-260 nm)¹⁸⁵. The virions are composed of three main substructures: viral core, one or two lateral bodies and the viral membrane(s) (Figure 2)¹⁸⁶⁻¹⁸⁸. The core contains the dsDNA genome, structural proteins and enzymes needed for the transcription of early viral genes¹⁸⁹⁻¹⁹¹. The core is encased by a core wall that has a biconcave shape¹⁸⁶. The core wall is composed of two layers: the inner layer or “smooth layer”, formed by A3; and the outer layer or “palisade layer”, formed by A10 and A4¹⁹². The lateral bodies reside on the concave regions of the core^{187,193}. They are proteinaceous structures that carry host modulatory proteins such as the phosphoprotein F17R, the phosphatase H1 and a glutaredoxin-2 (G4L)¹⁹³. The virus is surrounded by one lipoprotein bilayer membrane and one additional outer membrane (envelope)¹⁹⁴.

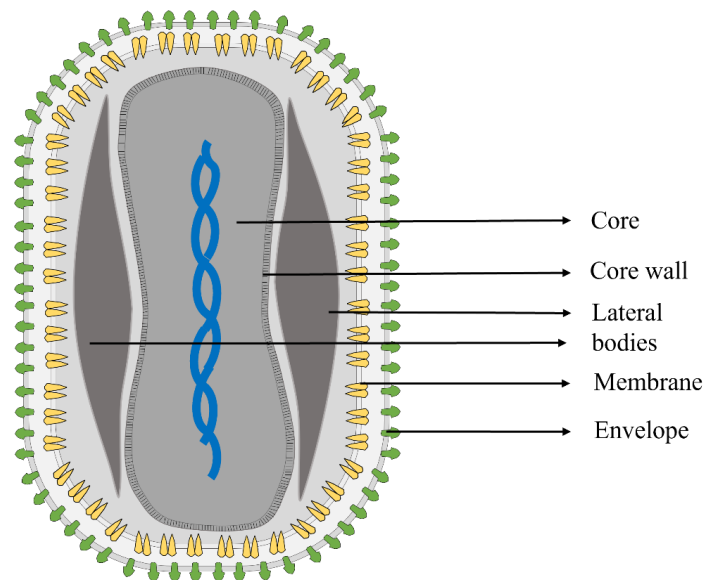


Figure 2. Schematic diagram of *Vaccinia virus* structure.

1.3.1 Genome organization

The genome of poxviruses is a double strand DNA that varies in length from 122 kbp, in *Cetacean poxvirus* of OPXV genus¹⁹⁵, to 360 kbp, in *Canarypox virus* (CNPV) of the *Avipoxvirus* genus¹⁹⁶. Poxvirus genomes contain from approximately 133 genes (in *Yatapoxvirus* and Parapoxvirus) to 328 genes (in CNPV)¹⁹⁶. Their genome consists of the central region and two variable regions at the termini. The end of the variable region contains inverted terminal regions (ITR). ITR are identical sequences in inverse direction at the opposite end with hairpin loops that join the two DNA strands¹. ITR are variable in size between species, and can contain genes that are present in diploid copies in the genome or not contain genes, as in VARV¹⁹⁷⁻¹⁹⁹.

The central region of the genome is highly conserved between the poxviruses, sharing similar gene location (synteny) and genome organization^{84,198}. In this region, there are 49, 90 and 109 genes that are conserved among poxviruses, chordopoxviruses and OPXV, respectively^{198,200–202}. The conserved genes are involved in essential functions such as DNA replication, transcription, and virion assembly^{84,200,202}. In contrast, the variable regions comprise genes that encode proteins involved in the interaction with the host including host range, immunomodulation and pathogenicity. These genes are termed as “non-conserved genes” or “accessory genes”^{8,198,200,201}. Compared to the conserved genes, those genes are more divergent and not highly conserved between poxviruses^{198,202,203}. Furthermore, those genes have more variability in gene length than the genes in the central region¹⁹⁸. Thus, the main differences in the genome of OPXV species are in the terminal variable genomic regions²⁰⁴.

1.4 Viral cycle

The prototype of the OPXV is VACV. Thus, the viral cycle is described with reference to VACV. The complete viral cycle of VACV occurs in the cytoplasm of the host cell¹ (Figure 3).

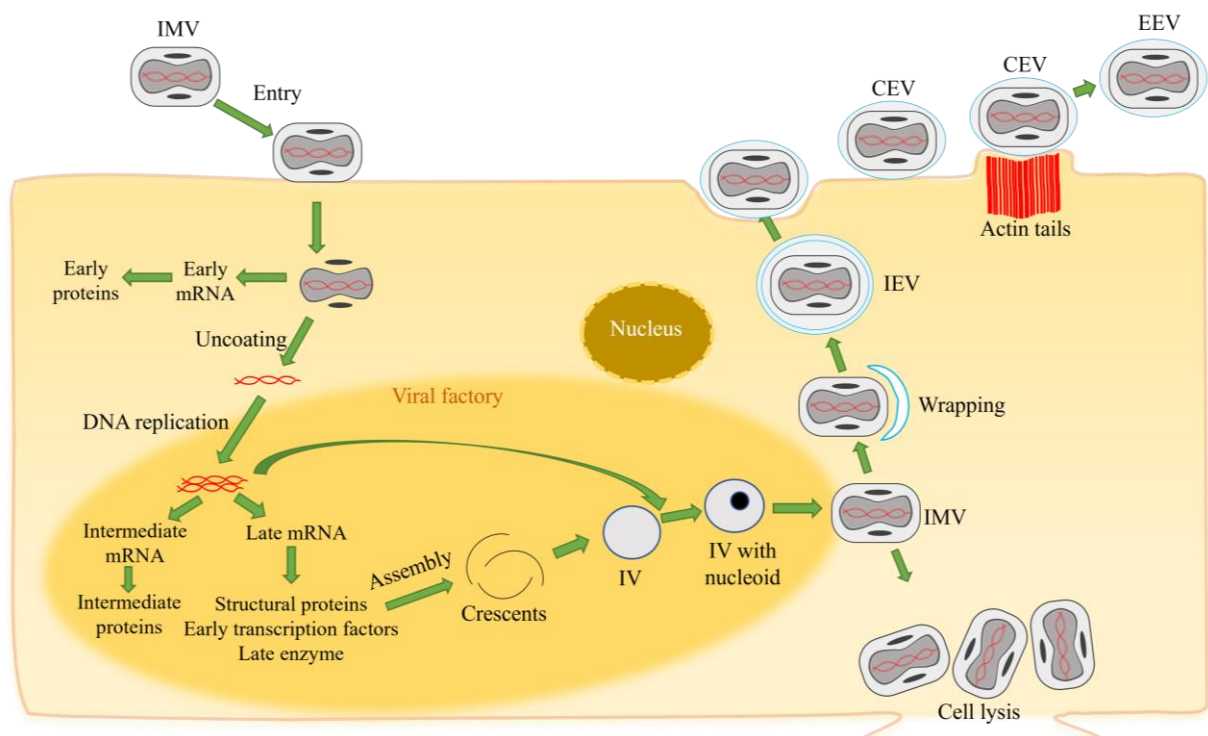


Figure 3. Schematic overview of the *Vaccinia virus* life cycle. IV, immature virion; IVN, immature virion with nucleoid; IMV, intracellular mature virion; IEV, intracellular enveloped virus; CEV, cell-associated enveloped virus; EEV, extracellular enveloped virus.

1.4.1 Virus entry and uncoating

The viral cycle starts with the viral entry (binding and fusion) (Figure 3). VACV attaches to the cell through the interaction of glycosaminoglycans and viral membrane proteins. There are at least 15 proteins involved in the viral entry: four proteins used for binding to the cell (D8, A27 and H3 and A26) and eleven required for viral fusion (A16L, A21L, A28L, F9, G3L, G9R, H2, J5, L1R, L5R and O3L)²⁰⁵. The last ones are called the entry-fusion complex (EFC). The virion entry occurs either through macropinocytosis or direct fusion of the viral membrane with the cell membrane^{1,206}.

Upon entry, the core and the lateral bodies are released in the cytoplasm²⁰⁵. The lateral bodies are dissociated from the core and disassembled²⁰⁷. The core is released in the cytoplasm and transported by microtubules close to the endoplasmic reticulum or perinuclear region of the cytoplasm^{208–210}, followed by the transcription of early viral genes²¹¹. The expression of early genes does not require *de novo* protein synthesis because the viral particles contain their own transcription machinery^{1,212}. More than 100 genes are transcribed inside the viral core²¹³ and the early mRNAs are detected within 20 min post infection^{214,215}. The transcripts are extruded from the core and translated in the cytosol. The core is uncoated and the viral genome is released to the cytoplasm (Figure 3)²¹¹.

When the cell is infected with VACV, superinfection can be prevented by the interaction of A56 and K2 proteins on the membrane of the infected cell with the A16-G9 subcomplex of EFC of subsequent viruses, which blocks the viral entry after membrane fusion^{216,217}. The mechanism by which viruses prevents superinfection with a second virus is called superinfection exclusion. There is another mechanism of superinfection exclusion that does not require the A56 or K2 proteins and prevents the viral fusion of the superinfecting virion and the infected cells, but this mechanism is not completely elucidated, yet²¹⁸.

1.4.2 Viral DNA replication

After the genome has been released, viral DNA replication starts, followed by the expression of intermediate and late genes²¹¹. The viral genome in the cytoplasm is surrounded by membranes derived from the rough endoplasmic reticulum (ER), forming a “virus factory” or “replication factories” in the cytoplasm (Figure 3)^{187,219,220}. It has been proposed that the ER membranes might protect the viral genome from cellular recognition and degradation. Viral DNA replication occurs in the viral factories²¹¹. Each viral factory is derived from one viral particle^{208,221}. Since the cell DNA machinery is located in the nucleus, VACV produces its own viral DNA replication machinery before viral DNA synthesis. The early viral proteins that mediate the viral DNA replication are: B1, I3, H5, G5, A50, E9, A20, D4 and D5^{221–232}.

Transcription and translation of intermediate and late proteins also take places in the viral factories as well as the viral assembly²³³. The activation of intermediate and late genes requires viral DNA replication²³⁴ as the newly replicated DNA serves as a template for the transcription of these genes²³⁵. Most intermediate and late mRNAs are detected at 100 min post infection

^{214,234}. The intermediate viral genes encode DNA binding and packaging proteins, core-associated proteins and late transcription factors ²¹³, whereas the late viral genes encode structural proteins, the viral RNA transcription machinery, early gene transcription factors and proteins involved in morphogenesis and entry ^{236,237}.

1.4.3 Virus assembly and egress

The viral assembly occur in the viral factories (Figure 3) ²³⁸. During the morphogenesis VACV produces four types of virions: intracellular mature virion (IMV), intracellular enveloped virus (IEV), cell-associated enveloped virus (CEV) and extracellular enveloped virus (EEV) ²³⁹. IMV has a single lipid bilayer membrane compared to CEV and EEV that contain one additional membrane (envelope), derived from either endosomes or trans-golgi ^{240,241}. The virion morphogenesis begins with the formation of viral crescents, which are open membranes derived from the ER ²⁴². The crescent grows until it forms a spherical immature virion (IV). Before it closes the viral genome is packaged into IV. These IV are called IV with nucleoid (IVN). Then IVN matures to intracellular mature virion (IMV) (Figure 3) ²⁴³.

IMVs are released from the viral factory. The majority of IMV stay inside the cell until cell lysis. In species such as CPXV, ECTV and AKPV, IMV are occluded within a dense protein matrix in the cytoplasm called ATI bodies ^{79,174,184}. Three phenotypes of ATI exist: IMV are inside the ATI matrix (V⁺), ATI with no IMV inside or on its surface (V⁻) and IMV are only in the periphery of ATI (V^{+/-}) ^{244,245}. The *atip*, *p4c* and *A27L* genes are involved in the production of the wild type V⁺ ATI ²⁴⁶⁻²⁴⁸. The other IMV are transported from the viral factories to the site of wrapping on microtubules. IMV are wrapped by a double membrane derived from either endosomes or trans-golgi ^{240,241}, resulting in intracellular enveloped virus (IEV). The double membrane contains nine proteins (A33, A34, A36, A56, B5, E2, F12, F13 and K2). The deletion of any of these proteins, except for A56 and K2, causes a small plaque phenotype ¹. The deletion or mutation of A56 or K2 causes the formation of syncytia (fusion of infected cells) ^{249 250-253}.

The transportation of the IEV to the cell surface and egression needs three proteins A36, F12 and E2 ^{254,255}. A36 and F12 are only present on the outer membrane of the IEV ²⁵⁶. IEV is moved to the cell surface and its outer membrane fuses with the cell membrane, exposing the virion on the cell membrane ²³⁹. Upon fusion A36 is accumulated in cell membrane ²⁵⁷. The viral particle has one lesser membrane and if it is retained on the surface is called cell-associated enveloped virus (CEV). When CEV is released from the cell, it is known as extracellular enveloped virus (EEV) ²³⁹. CEV is important for cell-to-cell spread ^{239,258}. A33, A34 and B5 proteins are required for efficient cell-to-cell spread ²⁵⁹⁻²⁶¹. These proteins are associated with the formation of comet-shaped plaques ^{259,262,263}. When EEV reaches an infected cell, the infected cell expressing A33 and A36 on the membrane to repel the superinfecting EEV. A33 and A36 induce actin tails to spread EEV to neighboring cells ²⁶⁴. This is another form of superinfection exclusion.

1.5 Viral tropism

The poxvirus tropism can be classified in three levels: cell tropism, tissue tropism and host tropism²⁶⁵. The cell tropism refers to the ability of the virus to infect cell cultures. Based on this ability, cells can be defined as permissive, semi-permissive and non-permissive. The tissue and host tropism are the ability of the virus to infect tissue and host species, respectively²⁶⁵. The initiation of the viral cycle for many viruses begins with the binding to the cell. Thus, it is considered that the viral binding has an important role in cell and tissue tropism²⁶⁵. However, several poxviruses can successfully enter to non-permissive cells^{266–269}, as it has been observed for MVA¹¹⁹. This indicates that cell tropism is affected by other downstream events^{8,270}. The cell tropism depends on the ability of the virus to manipulate the intracellular antiviral pathways that is activated upon viral entry, the ability of the cell to provide complementing host factors needed for the viral multiplication^{8,271,272} as well as the presence/absence of antiviral genes²⁷². In the poxviral genome, within the non-conserved genes, there are genes involved in the modulation of the host antiviral response. These genes are defined as virulence genes^{8,38}. Within the virulence genes, the ones that are required for the successful multiplication of poxviruses in a set of cultured cells are referred to as “host range genes”^{8,38}. The host range genes encode proteins called host range factors that target antiviral and anti-inflammatory host pathways³⁸ and influence the virus tropism⁸. In poxvirus, 38 host range gene homologs have been identified and are classified in 12 gene families^{38,39,271}. The most studied host range genes are *E3L* and *K3L*³⁸.

VACV can productively multiply in most mammalian and avian cells, but not in Chinese hamster ovary (CHO) cells²⁷³. The insertion of the CPXV Chinese hamster ovary host range gene (*CP77*) permitted VACV to multiply in CHO cells²⁷⁴. The first host range genes identified in VACV that are required for multiplication in human cells were *KIL* and *C7L*^{275–277}. It has been shown that the deletion of *KIL* and *C7L* in VACV leads to abortive infection in human cells, pig kidney cells and rabbit kidney RK13 cells^{275–278}. The multiplication deficient in human and pig kidney cells is overcome by the insertion of either *KIL*, *C7L* or *CP77* gene, whereas multiplication in rabbit kidney cells is restored by the insertion of either *KIL* or *CP77* gene, but not the *C7L* gene^{273,277,278}. Other host range genes have been identified in VACV, *E3L* and *C12L* (encoding serine protease inhibitor-1, SPI-1). The *E3L* gene is required to grow VACV in Vero cells and human HeLa cells, but not in rabbit RK-13 cells, hamster BHK cells and CEF cells^{279–281}. *C12L* is needed for VACV multiplication in human A549 cells^{282,283}.

MVA has a restricted host range and is unable to productively infect human and most mammalian cells^{121,124,284}. However, MVA still multiplies in human cells such as osteosarcoma TK–143B cells^{123,124,132,284,285}. Furthermore, it has been observed that MVA strains differ in their ability to multiply in different human cell lines¹³². MVA also multiplies efficiently in some non-human mammalian cell lines such as baby hamster kidney (BHK-21) cells (Table 1)^{121,124,284–288}.

Table 1. Cell lines susceptibility to MVA

Cell lines	Species	Multiplication of MVA strains								
		MVA ^a	MVA-II/85	MVA-VR1508	MVA-BN	MVA-B	MVA-572	MVA-1721	MVA-574	MVA-LZ
MDCK	Canine; kidney	SP							NP	
Ederm	Equine; skin								NP	
RO5R	Fruit bat Egyptian			P						
RO5T	Fruit bat Egyptian			P						
RO6E	Fruit bat Egyptian			P						
CHL	Hamster Chinese; lung	NP								
CHO	Hamster Chinese; ovaries	NP		NP						
BHK-21	Hamster Syrian; kidney	P		P	P	P				P
HEK-293	Human; kidney	NP		NP	NP	NP	NP	P		SP
HeLa	Human; cervix	NP	SP		NP	NP	NP	P	NP	SP
SW839	Human; kidney	NP								
TK-143B	Human; bone	P	SP		NP		NP	P		
MRC-5	Human; lung		NP		NP	NP			NP	
FS-2	Human; skin		NP							
Caco-2	Human; colorectal			NP						
FHs74int	Human; esophagus			NP						
Hutu-80	Human; small intestine			NP						
A549	Human; lung			SP						
HaCaT	Human; skin				NP		SP	P		
HRT18	Human; colon								NP	
Hep-2	Human; larynx								NP	
SK 29 MEL 1	Human; skin									NP
LC5	Human; lung									NP
85 HG 66	Human; brain									NP
U138	Human; brain									NP
C8166	Human; blood (T-cell)									NP
HUT 78	Human; blood (T-cell)									NP
SY9287	Human; blood (B-cell)									NP
MA104	Monkey; kidney								P	
MIB	Monkey; blood (B-cell)									NP
BSC-1	Monkey African Green; kidney	SP								
CV1	Monkey African Green; kidney	SP,P								P
Vero	Monkey African Green; kidney	SP		SP	SP	SP			SP	
FRhK-4	Monkey Rhesus; kidney	NP								
Balb3t3	Mouse; embryonal fibroblast		NP			NP				

NMULI	Mouse; glandular epithelial			SP					
AG101	Mouse; skin				NP		NP	NP	
DBT	Mouse; brain								NP
PK(15)	Pig; kidney	NP		NP					
BEL	Pig; lung								SP
MDBK	Pig; kidney								NP
RK13	Rabbit; kidney	NP		NP					NP
RAB-9	Rabbit; skin	NP							
SIRC	Rabbit; cornea	NP							
IEC-6	Rabbit; small intestine			P		SP			
H4IIE	Rat; liver			NP					

P: permissive, SP: semi-permissive, NP: non-permissive. ^a MVA whose strain, variant or passage number was not stated. Data are summarized from Okeke *et al.* ¹³³.

In non-permissive cells, the viral cycle of MVA follows the same first steps of the VACV life cycle. MVA enters to the cell, expresses the early genes, replicates the viral genome, expresses the intermediate and late genes, but the cycle is blocked in the viral assembly, leading to immature virus particles that stay inside the infected cells ¹¹⁹ or dense particles ^{287,289}. Thus, MVA cannot produce infectious progeny ^{124,284,286,287}. Recombinant MVA vectored influenza vaccine (MVA-HANP) has a similar cell permissiveness compared to MVA, except in A549 and NMULI that are non-permissive to MVA-HANP ²⁸⁷.

1.6 Evolution and phylogeny of orthopoxviruses

The orthopoxviruses, as dsDNA viruses with proofreading DNA polymerases, evolve slowly compared to RNA viruses ²⁹⁰. However, OPXV are not static, they can suffer genomic and phenotypic changes. The evolution of OPXV is driven by several molecular mechanisms such as point mutations, gene duplication, gene loss, homologous and non-homologous recombination and gene gain by horizontal gene transfer ²⁹¹. These mechanisms play an important role in the evolution of OPXV ^{200,291}.

The substitution rate of OPXV have been estimated as $1.7-6.5 \times 10^{-6}$ substitutions per site per year (subs/site/year) ²⁹²⁻²⁹⁵. It is thought that OPXV evolve slowly because of the high fidelity of DNA replication by DNA polymerase ²⁵⁶. However, despite of their low mutation rate, OPXV can evolve rapidly as it has been observed in MPXV ²⁹¹. Since 2018, the MPXV genomes have accumulated 50 single nucleotide polymorphisms (SNP). These number of SNP is higher with respect of the estimated substitution rate of OPXV. The rapid evolution of the recent MPXV outbreak may be due to human adaptation ²⁹⁶. In contrast, the VARV genome has been quite stable over the years as it was well adapted to its host (humans) ¹⁹⁹. However, point mutations have also been observed in the OPXV genomes during the course of passaging in the laboratory ²⁹⁷⁻²⁹⁹.

Another mechanism that plays a significant role in OPXV evolution is recombination^{84,200}. Recombination has been observed *in vitro* and *in vivo* between strains of the same species (intraspecies) and between different species (interspecies)^{7,71,72,77,300–304}. Additionally, recombination between OPXV species with non-OPXV has been described³⁰⁵. Among CPXV strains, there is evidence of recombination between different CPXV clusters⁷⁷. Similarly, recombination has been observed between VACV strains^{303,306}. Furthermore, interspecies recombination has been reported between AKPV and ECTV⁷. The study of Gigante *et al.* demonstrated that ECTV may contain AKPV genome sequence⁷. Another study also showed recombination between ECTV and other OPXV (i.e., CPXV)⁷¹. This work demonstrated evidence of recombination in a CPXV strain that contained an ECTV-like *atip* gene⁷¹. Another study described that AKMV may have undergone recombination with CPXV. Some AKMV isolates contained a sequence of 6 kbp similar to CPXV in the left terminal region^{6,302}.

The phylogenetic analyses of OPXV showed that its members were split into two groups: the New World OPXV (RCNV, SKPV and VPXV) and the Old World OPXV (MPXV, CPXV, VACV, TATV, CMLV, VARV, ECTV, Abatino and AKMV)^{7,74,78,307}. AKPV branched separately between the two groups despite its place of isolation (the USA)^{7,74,307}. Based on the AKPV gene content, AKPV was more similar to the Old World OPXV than the New World OPXV. However, AKPV contained seven genes (*AKPV009*, *010*, *024*, *025*, *203*, *204* and *205*) that encoded proteins most similar to proteins of Murmansk and NY_014 poxviruses. The presence of these genes in the AKPV genome might be a result of more than one recombination event with Murmansk. Moreover, two putative recombinant regions between ECTV and AKPV were also found in the AKPV genome⁷.

Within the Old World OPXV, AKMV formed the deepest branch^{6,7,74,184,302,307}. The isolates from the same species formed monophyletic clades, except for CPXV that did not cluster as a monophyletic group^{7,73–75,77,78,307}. CPXV isolates were closely related to the Old World OPXV, except for AKMV^{7,74,78,302}. Despite the similar genomic region (recombinant region) between some AKMV isolates and CPXV, AKMV did not cluster with CPXV in the study of Jeske *et al.* that used the complete genomes⁷⁸.

The phylogenetic studies showed that CPXV isolates were separated into at least five clusters named CPXV-like 1, CPXV-like 2, CPXV-like 3, VACV-like CPXV and VARV-like CPXV^{72–78,308}.^{77,78,308}. The phylogenetic relationship between CPXV-like 1, 2 and 3 and the other OPXV varied in the phylogenetic studies^{74,77,78,307,309}. VACV-like CPXV had a close phylogenetic relationship with VACV. VARV-like CPXV was closely related to VARV, TATV and CMLV^{73,74,77,78,302,307}.

Various phylogenetic studies showed that CPXV was the only polyphyletic member of OPXV and also demonstrated the genetic diversity in CPXV isolates^{70,72–78}. Carrol *et al.* showed the diversity of CPXV isolates using the genetic and patristic distances between CPXV isolates using as threshold values the distances between TATV and VARV. Their study also revealed that CPXV comprised several (up to 5) species⁷⁵. Another study also revealed that CPXV was

genetically heterogeneous and could be divided into six cluster species based on the phylogeny and the genetic and patristic distances (using the distances between TATV and CMLV as a threshold)⁷². Mauldin *et al.* suggested that there are five (up to 14) lineages in CPXV based on monophyly and genetic distance criteria⁷³.

Compared to the other OPXV, CPXV had the largest genome, containing an almost full repertoire of OPXV genes (including OPXV accessory genes) and had the widest host range^{40,84,198,201}. Based on that, it has been proposed that the common ancestor of the Old world OPXV (except for AKMV) is a CPXV-like virus^{40,84,198,201}. The molecular evolution of OPXV is still unclear. A study of the molecular evolution of OPXV revealed that the emergence of OPXV took place about 42,000 years ago³⁰⁷. An earlier study of Babkin *et al.* showed that OPXV emerged 51,000 years ago, although the new OPXV species (i.e. AKMV, AKPV and Abatino) were not part of the dataset²⁹². The New World OPXV first separated from the other OPXV³⁰⁷. Then, AKPV diverged from the Old World OPXV approximately 19,000 years ago. The emergence of the Old World OPXV was about 11,000 years ago. Within the Old World OPXV, the first to diverge was AKMV and its emergence was at around 11,000 years ago. The remaining of the Old World OPXV emerged about 6,000 years ago. Then, ECTV, Abatino and CPXV-GerMKY2010 clade diverged from other OPXV, and their estimated time to the most recent common ancestor (tMRCA) was approximately 5,000 years ago. Later CPXV-like 2 segregated from other OPXV approximately 5,400 years ago. The tMRCA of MPXV, VACV and VACV-like CPXV was estimated as 3,500 years ago. MPXV originated approximately 600 years ago, ~1444 AD³⁰⁷. However, a more recent study suggested that MPXV emerged in 1970 AD³¹⁰, although this estimation is later than the date of the first MPXV isolation¹⁵⁹. CPXV-like1 diverged from VARV, TATV, CMLV and VARV-like CPXV about 3,700 years ago. VARV originated approximately 1,746 years ago³⁰⁷. Although a recent study reported that VARV has emerged 4,000 years ago, which is consistent with the records of smallpox in Egyptian mummies³¹¹.

1.7 Hazard characterization of Modified Vaccinia virus Ankara

Recombinant viral vector vaccines, such as recombinant MVA, are considered as genetically modified organisms (GMO). In the European Union (EU), the marketing authorization of recombinant vaccines are subject to additional requirements compared to non-recombinant vaccines, which are stipulated in Directive 2001/18/EC³¹². The directive seeks to protect human health and the environment when a GMO is placed on the market and released into the environment by requiring an Environmental risk assessment (ERA) for the approval of the recombinant vaccine. The purpose of the ERA is to assess potential risks to human health and the environment that may arise from the use and release of GMOs into environment. The ERA consists of six steps: hazard identification, hazard characterization, evaluation of the likelihood of the hazard, risk characterization, proposal of risk management strategies and determination of overall risk conclusion³¹². Step 2 (hazard characterization) consists of the evaluation of the

potential consequences of each possible adverse effect of a GMO on human health and the environment.

Despite the strong safety profile of MVA, there are still some knowledge gaps regarding MVA and MVA vectored vaccines such as recombination of MVA vectored vaccines with naturally circulating OPXV, nature and distribution of naturally occurring OPXV, the molecular basis of MVA host range restriction as well as the genetic stability of MVA and MVA vectored vaccines¹³³. Hence, addressing these knowledge gaps through carefully planned experiments in cell cultures and animal models is essential for the hazard characterization of MVA and MVA vectored vaccines. Therefore, it would contribute to achieving a more robust ERA and further optimizations of MVA as a safe vaccine vector¹³³.

1.7.1 Host cell restriction of MVA

The host restriction range of MVA is one of the characteristics that make MVA a good candidate for the development of vaccines against infectious diseases. However, the genetic basis for MVA restriction is not completely elucidated. MVA has suffered six major deletions that may cause its restricted host range. However, the introduction of six major MVA deletions into CVA was not enough to recover the complete host range of MVA²⁸⁵. Similarly, the restoration of large deleted regions containing *KIL* and *C12L* did not restore wild type host range³¹³, but improved the ability of MVA to multiply in human cells³¹³. However, the introduction of the *C12L* gene rescued MVA multiplication in only human MRC-15 cells³¹⁴. Additionally, the insertion of *KIL* in MVA did not restore the capacity to productively grow in human cells^{121,313,315}, but restored the multiplication of MVA in rabbit RK13 cells³¹⁵.

Another host range gene that plays a role in multiplication of MVA in human cells is *C16L*. The repair of both the *C16L* and *C12L* genes rescued the ability of MVA to multiply in human cell lines (HeLa, 293T, A549 and MRC-5 cells)³¹⁶. Although the insertion of both genes, unlike the introduction of only *C16*, did not enhance the multiplication of MVA in monkey BS-C-1 cells³¹⁶. Nevertheless, the multiplication competent VACV-WR lacked the *C16L* gene, which suggested that it contained another gene with redundant function^{316,317}. Yet, the role of the major deletions and small mutations in the host range defect of MVA it is still unclear.

A study by Erez *et al.* has shown that spontaneous single mutations altered the host range of MVA. These single mutations in the *D10L* gene arose during passaging of MVA in BS-C-1 cells and increased multiplication of MVA in monkey BS-C-1 cells and slightly in human cells³¹⁸. Even though the *D10L* gene has never been associated with the host range. Another study demonstrated that it is possible to re-adapt MVA to human Caco2-cells by serial passages in Caco2-cells. MVA variants were able to undergo productive infection in human Caco2-cells¹³³. These studies indicate that host defect of MVA could be reversible and the host range restriction of MVA might not be a stable feature³¹⁸. Alternatively, most MVA strains may be polyclonal containing many variants and adaption in human and mammalian cells through serial

passages might have selected a variant with enhanced fitness and multiplication abilities in human cells.

1.7.2 Nature and distribution of naturally circulating orthopoxviruses

For the hazard characterization of the MVA and MVA vectored vaccines, it is necessary to have information about the nature and distribution of naturally occurring OPXV in the area where the recombinant vaccine is to be deployed due to potential recombination of MVA vectored vaccines with a multiplication competent OPXV, which may lead to restoration of MVA to wild type and transfer of the transgene into a competent OPXV ¹³³.

Despite the relevance of OPXV, there is still lack of information regarding the natural reservoir, host range and geographic distribution of some OPXV ^{184,319}. The surveillance efforts and isolation of OPXV both in humans and animals are limited, except for a few countries ¹³³. In addition, many places where OPXV are endemic lack infrastructure and resources. Most information about OPXV has been collected after outbreaks, for instance, the current global Mpox outbreak. Thus, known OPXV are not a representation of what is in nature because most OPXV strains were isolated from humans and from a few places. The lack of information about the nature, distribution and evolution of OPXV hinders the prediction of emergence OPXV ³¹⁹.

Moreover, there is also lack of information about the consequences of the possible adverse effects after releasing the OPXV vectored vaccines. There is no monitoring of the adverse effects associated with the interaction of the recombinant vaccine and naturally occurring OPXV. One example is the recombinant vaccinia-rabies vaccine (Raboral-VRG) used in foxes ³²⁰. It has been monitored for efficacy of vaccination but not for the interaction of the vaccine with the wild OPXV in foxes as well as its possible adverse effects ³²¹. It is important to establish monitoring plans in place prior to releasing the recombinant vaccines as, for example, the spillover from vaccinated animals to the environment could cause changes in the diversity of the wild OPXVs.

It is difficult to make inference about adverse effects due to the interaction of OPXV vectored vaccines and the wild type OPXV when there is few or lack of information about the nature and distribution of naturally occurring OPXV before and after the release of OPXV vectored vaccines. Those are knowledge gaps in the hazard characterization of MVA vectored vaccines ¹³³.

1.7.3 Recombination in co-infection and superinfection

The recombination between MVA vectored vaccines and naturally occurring OPXV could result in the restoration of MVA to wild type (due to the rescue of deleted and fragmented genes), the transfer of the transgene into a naturally occurring OPXV and the generation of progeny viruses with altered properties (such as virulence and host range) ^{133,322}. The information about the potential for recombination between OPXV vectored vaccines and naturally occurring OPXV are not mandatory in the ERA ¹³³. Even though the genetic transfer

could be a consequence of recombination and it is stipulated in the Directive 2001/18/EC as an indirect effect.

There is dearth of information about the potential for recombination between the poxvirus vectored vaccines and naturally occurring OPXV as well as its consequences. The recombination events between MVA vectored vaccines and naturally occurring OPXV are considered negligible because (1) the co-localization of the viruses in the same cell is unlikely, (2) MVA lost the ability to produce infectious virions in human and most mammalian cells, (3) OPXV are short-lived and (4) superinfection exclusion prevents the second infection of infected cells³²³. However, the likelihood of co-localization increases when there are OPXV circulating in the area of administration of MVA and when the vaccines are administered to domesticated animals and wildlife since animals are the reservoirs and accidental hosts of natural OPXV^{133,322}. Even the ongoing global Mpox outbreak would create scenarios for the interaction of MVA and zoonotic OPXV in humans due to the extensive use of MVA vaccines. Despite the short-lived of OPXV, DNAemia of CPXV can last until four weeks³²⁴, which is a lapse of time for virus-virus interactions¹³³. Even though MVA is unable to complete the viral cycle in non-permissive cells, the infection is blocked on the morphogenesis, thereby the viral DNA replication is unimpaired¹¹⁹. Hence, the recombination could take place in non-permissive cells because only 12 bp of overlapping homologous sequences in DNA sequences are sufficient for recombination³²⁵. In case of superinfections, the mechanisms of superinfection exclusion are not absolute as few viral cores of the superinfecting virions were observed in the cytoplasm of superinfected cells²¹⁸.

A study of *in vitro* co-infection with MVA vectored vaccines and naturally occurring OPXV showed that the viruses underwent recombination³²⁶. The co-infection was performed in permissive BHK-21 cells. The recombination resulted in hybrid viruses that displayed parental and non-parental characteristics^{326,327}. The genomic characterization of these progeny viruses would give a better understanding of the recombination between these viruses.

Evidence for the natural recombination between a wild strain of capripoxvirus and a live attenuated vaccine in Russia has been reported³²⁸. The recombinant vaccine-like lumpy skin disease virus (LSDV) might be the result of the recombination between field LSDV strain and LSD vaccine. It was isolated after the introduction of the vaccine. The next outbreaks were caused by vaccine-like LSDV strains and not by wild LSDV strains that were observed in the previous years before the vaccination campaigns^{329,330}. Although it has been suggested that the recombinant vaccine-like LSDV strains could be a spillover from vaccinated animals³³¹.

Despite of the relevance of the recombination between OPXV vaccines or OPXV vectored vaccine and naturally circulating OPXV, the studies about this topic are scarce. Therefore, more studies examining recombination should be performed to obtain data about the potential hazard arising from recombination between MVA vectored vaccine and naturally occurring OPXV. Furthermore, the biological and genetic characterization of recombinant progeny viruses should

be performed to understand the recombination process, poxvirus host range, cytopathogenicity and transgene stability and integrity.

1.7.4 Homogeneity and genetic stability of MVA

The homogeneity and the genetic stability of OPXV vectored vaccines are the major concerns during the production of vaccines in large-scale. It is deemed that MVA was homogenous and stable after 570 passages in CEF and plaque purified³³². Comparison of the genome sequence of five MVA strains showed that their genomes (excluding the ITR) were similar³³³. Another study showed that the genomes of three MVA strains were genetically identical, but the strains showed different phenotypic properties and safety profiles. The method employed in that study did not detect the variants in the MVA strains (which were polyclonal mixtures of viruses) because the method only evaluated the majority of viral genome in the sample¹³². In order to identify variants in the MVA strains and confirm the homogeneity, the strains should be subjected to deep sequencing¹³³.

The genetic instability could occur within and outside the transgene. One of the desirable characteristics for a virus to be used as recombinant vector vaccines is to be genetically stable. It has been observed that the MVA genome suffers spontaneous mutations during serial passages^{318,334} and, hence, some variants could be raised during the production of the vaccine or recombinant vaccine stocks. The stability and integrity of the transgene is particular important in the development of recombinant viral vaccines to avoid losing or reducing expression of the transgene. Thus, understanding the viral and host determinants involved in the genetic instability will facilitate the development of MVA vectored vaccines.

Some studies have showed instability of the transgene in recombinant MVA vaccines³³⁵⁻³³⁸. A study by Wyatt *et al.* showed that the transgene expression changed during serial passages due to spontaneous mutations³³⁸. The mutations were found inside and outside the transgene³³⁸. The transgene stability of MVA-HANP has been examined in permissive IEC-6 cells. The expression of the transgene was unstable, after the third passage the expression was undetectable³²⁷. Similarly, it has been observed in the hybrid progeny viruses obtained from co-infection *in vitro* with MVA-HANP and a wild type CPXV. One hybrid virus completely lost the transgene expression after the third or fourth passage. Whereas the stability of transgene of other hybrid progeny viruses varied across different cell lines^{326,327}. From a biosafety point of view the loss of the transgene is relevant because the transgene serves as a tool to monitor the spread of the recombinant vaccine to target and non-target organisms as well as its non-target effects.

In order to confirm the genome stability of recombinant MVA vaccine, it has been recommended to perform the genome sequencing of master seed virus for up to five passages¹³³. In the ERA it is required to assess the adverse effects caused by the genetic stability but it is not mandatory to provide that information as well as whole genome sequences of the stocks to confirm homogeneity¹³³.

2. RATIONALE OF THIS STUDY

OPXV based vaccines, especially MVA, are being used as recombinant vector vaccine against infectious diseases and neoplasm in humans and animals. OPXV vectored vaccines are also being developed against well-known and emerging human diseases caused by viruses such as HIV, influenza virus, Ebola virus, Zika virus, respiratory syncytial virus and SARS-coronavirus-2. Moreover, oncolytic chimeric OPXV are in clinical trials for the treatment of cancer. It is worth considering some biosafety issues that may arise if OPXV vaccines or OPXV vectored vaccines are deployed extensively in the treatment of infectious diseases and cancers. MVA is considered an attractive vector for vaccination due to its host range restriction in human and mammalian cell lines. During the attenuation process MVA lost some virulence genes. However, various mammalian cells, even human cells, are still permissive and semi-permissive to MVA infection.

There are still knowledge gaps with respect to the hazard characterization of MVA. One of the biosafety concerns about the use of MVA vectored vaccine is the potential for recombination between MVA vectored vaccine and a naturally occurring OPXV in cells/hosts in which it multiplies poorly (semi-permissive/non-permissive cells). The recombination with multiplication competent OPXV during co-infection and superinfection may lead the rescue of deleted and/or truncated host range genes in MVA and, therefore, restore the ability to multiply efficiently in human and mammalian cells. The hybrid progenies could display higher virulence and non-parental characteristics, lose the transgene (which hinders the monitoring of OPXV vectored vaccine) and/or transfer the transgene to a multiplication competent OPXV.

In vitro studies on recombination between OPXV vectored vaccine and wild type OPXV are scarce because the risk of recombination has been considered negligible. This argument is based on MVA host restriction and superinfection exclusion. Nevertheless, viral DNA replication still occurs in non-permissive cells which is enough for recombination to take place. Therefore, studies of recombination *in vitro* between MVA vectored vaccine and natural circulating OPXV in semi-permissive cells during co-infection and superinfection should be performed. These studies are relevant to hazard characterization of MVA vectored vaccines.

There are putative scenarios where recombination between OPXV vectored vaccines and other OPXV such as post-exposure therapies of MVA to treat pre-existing OPXV infection in animals or humans can occur. A robust characterization of the potential for recombination between MVA vectored vaccines and naturally occurring OPXVs will require knowledge of the genetic diversity and evolution of naturally circulating OPXVs in regions in which the vaccine will be released since endemic OPXVs will serve as parental strains for recombination. Natural infection with an OPXV (for example MPXV) and vaccination with MVA vaccine (for example JYNEOUS) or prophylactic vaccination with MVA vaccine and natural infection with OPXV are plausible scenarios for co-infection and superinfection which may result in recombination. The surveillance and characterization of OPXV are limited, except for MPXV whose surveillance has increased recently due to the current global outbreak in several non-endemic

countries. OPXV circulated on every continent except Antarctica. For instance, CPXV is endemic to Eurasia. CPXV is a peculiar species among OPXV because it is genetically diverse and polyphyletic. It contains almost the full set of OPXV genes. Moreover, there is evidence of natural recombination in CPXV and between CPXV and other OPXV. The genomic characterization of CPXV isolates would provide insights into OPXV evolution, phylogeny and phylodynamic. Experimental *in vitro* co-infection and superinfection of cell cultures with naturally occurring CPXV and MVA vectored vaccine will serve as a model in which the potential for recombination and genome wide pattern of recombination will be explored. Taken together, the study of the diversity and evolution of OPXV circulating in the location of in which MVA vaccines may be released should be investigated because they are the baseline data to evaluate the potential for recombination and interrogate the genetic heterogeneity of CPXV.

3. GENERAL OBJECTIVE

The main objective of this thesis is to study the evolution and the genetic diversity of CPXV and examine recombination *in vitro* between a naturally occurring CPXV and MVA vectored vaccine in cells that MVA multiplies poorly. Thus, this study is aimed at improving OPXV vectored vaccine biosafety through genomic characterization of wild type CPXV and CPXV/MVA progeny viruses.

PAPER I

Hypothesis: Recombinant CPXV viruses are circulating in nature.

Specific objectives:

- To perform genomic characterization of a novel human CPXV.
- To detect potential recombination events in the genome of novel human CPXV.
- To determine the phylogenetic relationship of a novel human CPXV with other representative CPXV and OPXV strains.

PAPER II

Hypothesis: CPXV isolates have high genetic diversity and CPXV is not a single species.

Specific objectives:

- To determine the phylogenetic relationship of the Fennoscandian CPXV isolates with other representative CPXV and OPXV strains.
- To evaluate the genetic diversity in CPXV isolates
- To study the evolutionary history of CPXV.

PAPER III

Hypothesis: Recombination between MVA-HANP and a naturally occurring CPXV during co-infection and superinfection of cells (in which MVA multiplies poorly) leads the generation of progeny virus with novel genetic and biological characteristics.

Specific objectives:

- To examine the recombination *in vitro* MVA-HANP and naturally occurring Norwegian feline CPXV during co-infection and superinfection of semi-permissive Vero cells.
- To perform genome characterization of parental MVA-HANP and progeny viruses.

4. METHODOLOGY

4.1 Viruses, cells, co-infection and superinfection experiments

In **paper I**, we used the naturally occurring Norwegian human CPXV-No-H2 to examine the possibility of natural recombination in circulating Fennoscandian CPXV and map genome-wide recombination events. Evidence of natural recombination in CPXV-No-H2 based on limited genetic characterization was previously demonstrated ⁷¹. CPXV was propagated in African green monkey kidney Vero cells because these cells are fully permissive to CPXV infection ^{121,124,284–287,327} (**paper I and II**).

In **paper II**, we characterized five naturally circulating CPXV strains (CPXV-No-H1, CPXV-No-F1, CPXV-No-F2, CPXV-Swe-H1 and CPXV-Swe-H2) that were isolated in the Fennoscandian region (Norway and Sweden) from human and felines ^{45,68–71}. Genome sequencing of these Fennoscandian CPXV, and phylogenomic analysis with other OPXV strains would contribute to the understanding of the diversity, phylogenetic relationship of CPXV and other OPXV and evolutionary history of CPXV.

In **paper III**, we evaluated the recombination between CPXV-No-F1 and MVA-HANP during *in vitro* co-infection and superinfection of semi-permissive cells to MVA-HANP. Vero cells were selected for these experiments because they are semi-permissive to MVA-HANP infection ²⁸⁷. The feline isolate CPXV-No-F1 was selected instead of the human isolate CPXV-No-H1 because a possible scenario of human CPXV infection is by direct contact with infected domestic pets like cats. In addition, this is also a naturally occurring Fennoscandian CPXV.

MVA-HANP was previously chosen as a OPXV vectored vaccine since (1) MVA is used as smallpox vaccine and viral vector vaccine, (2) MVA is a multiplication incompetent poxvirus vector, and (3) MVA-HANP contains the influenza virus *hemagglutinin* (HA; A/PR/8/34) and *nucleoprotein* (NP) gene inserts, which makes it easier to monitor the transgenes by immunostaining. Overall, this is a safe model to test recombination *in vitro*.

The selection of the progeny viruses was in Vero cells. Unlike CPXV, MVA does not form plaques in Vero cells but expresses HA ³²⁶, which facilitates the identification (and selection) of the plaques from hybrid viruses and differentiate them from parental virus plaques by plaque phenotype and the HA expression. Two criteria used to select the progeny viruses were: plaque phenotype and the expression of the influenza virus HA protein.

The co-infection and superinfection experiments were done at a multiplicity of infection (moi) of 5.0 for each parental virus. Although the high moi of 5 might not be reflect the moi. under natural co-infection/superinfection, it assures the infection of all the cells in the primary infection and, therefore, guarantee the superinfection of Vero cells. Additionally, we performed different superinfection experiments: (1) primary infection with CPXV-No-F1 and superinfection with MVA-HANP after 4 hrs post primary infection (ppi), (2) primary infection with CPXV-No-F1 and superinfection with MVA-HANP after 6 hrs ppi, (3) primary infection

with MVA-HANP and superinfection with CPXV-No-F1 after 4 hrs ppi and (4) primary infection with MVA-HANP and superinfection with CPXV-No-F1 after 6 hrs ppi (Figure 4). These experiments would simulate different possible scenarios such as (1) the person/animal is infected with CPXV and receives the vaccine (MVA) and (2) when the person/animal received the vaccine (MVA) and then is infected with CPXV. The least possible scenario would be the co-infection when the person is infected by both viruses at the same time. But these experiments constitute cell culture-based models to examine recombination of MVA with other OPXV during co-infection of semi-permissive cells as well as evaluate the possibility of superinfection exclusion in preventing recombination.

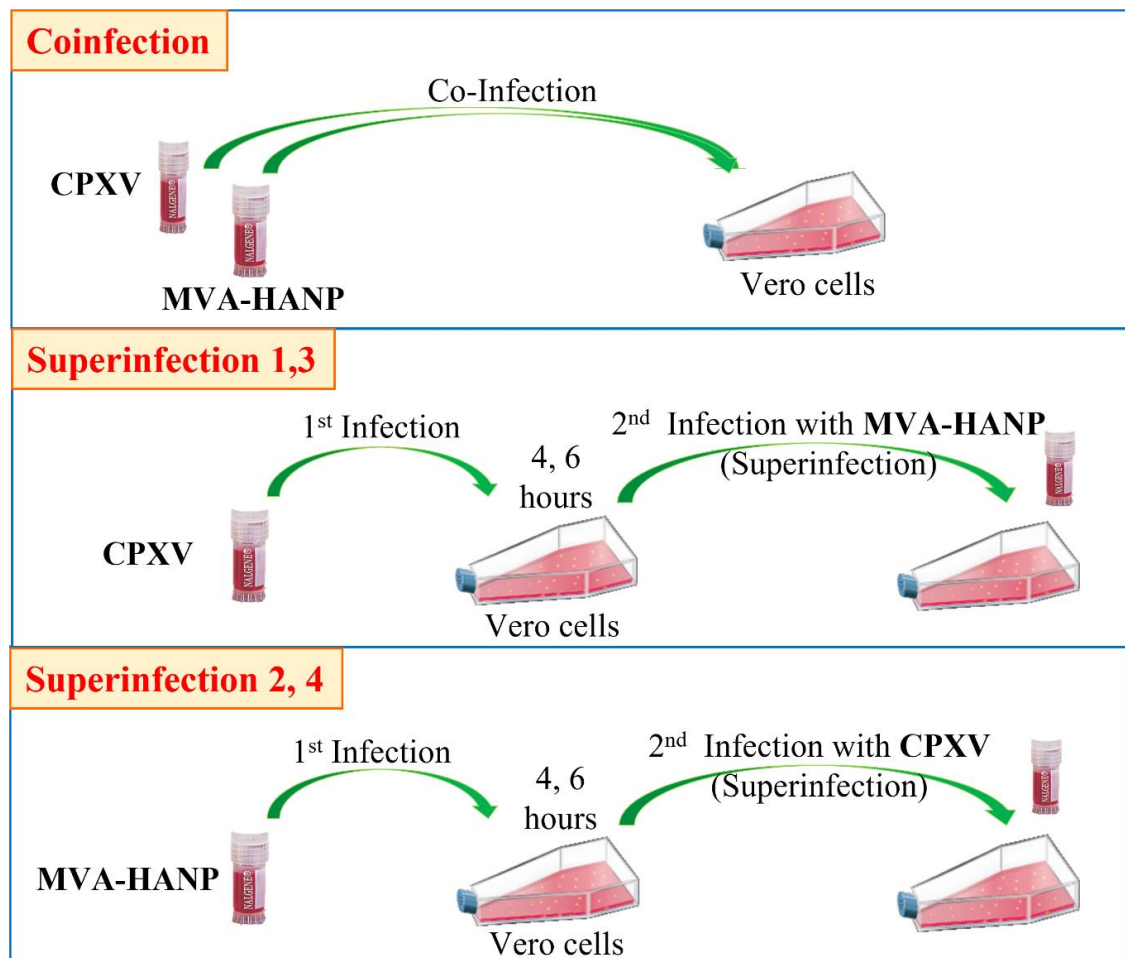


Figure 4. Co-infection and superinfection experiments in Vero cells. Co-infection, Vero cells were co-infected with CPXV-No-F1 and MVA-HANP. Superinfection 1, primary infection with CPXV-No-F1 and secondary infection with MVA-HANP at 4h post primary infection (ppi); Superinfection 2, primary infection with MVA-HANP and secondary infection with CPXV-No-F1 at 4h ppi; Superinfection 3, primary infection with CPXV-No-F1 and secondary infection with MVA-HANP at 6h ppi; Superinfection 4, primary infection with MVA-HANP and secondary infection with CPXV-No-F1 at 6h ppi.

4.2 Viral DNA extraction

The six CPXV isolates were semi-purified by sucrose gradient as previously described²⁰⁹. Viral DNA was extracted from Vero cells infected with the semi-purified virions (**paper I & II**). MVA-HANP was also semi-purified by sucrose gradient, but viral DNA was extracted from infected BKH-21 cells (**paper III**). The progeny viruses from co-infected and superinfected Vero cells were plaque purified and viral DNA was extracted from Vero cells infected with the plaque purified viruses (**paper III**).

The viral DNA extraction was performed following Dabrowski's protocol⁷⁶. In order to release the viral particles, the infected cells were incubated on ice in cold hypertonic buffer (with Triton X-100 and β -mercaptoethanol) to solubilize the plasma membranes. The cell nuclei were removed from cytoplasmic content by centrifugation. Then, the viral particles were isolated from the cytoplasmic content by ultracentrifugation. The viral particles were incubated in cold hypotonic buffer to release viral core. For the following steps, we used a commercial kit for viral DNA extraction (and Qiagen Genomic DNA buffers). These kits have the advantages of extracting high-molecular weight DNA and yielding pure DNA of good quality. Moreover, reproducible DNA yield and quality is achieved.

4.3 Sequencing

Some sequencing technologies can be used for whole genome sequencing. These technologies are second generation sequencing (or next-generation sequencing, NGS) and third generation sequencing (TGS). NGS produces large amounts of short reads (up to a few hundred bp) with low error rate^{339,340}. One disadvantage of NGS is that the short reads are not suitable for assembling genomes with long repeated regions and large structural variants³⁴¹. In contrast to NGS, TGS yields much longer reads (>10 kbp), but with high error rate (~15%)³⁴⁰⁻³⁴². The long reads are useful for *de novo* genome assembly. Both NGS and TGS have advantages and disadvantages; however, one technology overcomes the disadvantages of the other. The hybrid sequencing, that is combination of NGS (short-read sequencing) and TGS (long-read sequencing) platforms, resolves problems such as repetitive regions (e.g. ITR), deletions/insertions and produces genome assemblies with few or no gaps.

Whole genome sequencing of Fennoscandian CPXV isolates (**paper I and II**), MVA-HANP and the progeny viruses from co-infected and superinfected Vero cells (**paper III**) was performed using the hybrid sequencing approach. For this approach, we used Illumina MiSeq platform for short-read sequencing (NGS) and Nanopore platform for long-read sequencing (TGS). Illumina MiSeq is suitable to sequence small genomes (like viral genomes) and generates up to 15 Gb of output and paired-end reads of 300 bp. Nanopore is more cost-effective for generating long reads^{341,342}.

4.4 Genome assembling and annotation

The raw Illumina reads were pre-processed before genome assembling (**paper I, II and III**). The adapters, the low quality reads and short reads were trimmed using Trimmomatic³⁴³. It has been shown that read trimming increases the quality and reliability of downstream analysis and reduces computational requirements and execution time³⁴⁴. After trimming, the reads from contaminants (e.g. Vero cells) were removed using FastQ Screen v0.14.1³⁴⁵ with BWA aligner^{346,347}. The reads were mapped to the possible contaminant genomes (Vero cells) and filtered. FastQ Screen v0.14.1 is a program that maps sequencing reads to one or more reference genomes (e.g. host cell, CPXV and MVA) using an aligner (e.g. BWA) and filters the reads mapping (or not mapping).³⁴⁵ Furthermore, the program allows you to create your own database with the genome of our interest and choose between three aligners. BWA was chosen because it is designed for aligning short and long reads^{346,347}.

The processed reads were used to assemble the viral genomes. The approach used in **paper I, II and III** was hybrid genome assembly (Nanopore and Illumina data) due to the structure of the OPXV genomes. These genomes contain repetitive regions and ITR that hinder the assembly with only Illumina data (short reads). The long reads from Nanopore sequencing overcome this problem. Different assemblers are available for hybrid genome assembly, such as SPAdes³⁴⁸, PBcR³⁴⁹, Unicycler³⁵⁰ and MaSurCa³⁵¹. The viral genomes were assembled using hybridSPAdes. The algorithm first assembles the short reads and then aligns the long reads to generate longer contigs, and generates accurate assemblies³⁴⁸. Unlike PBcR and MaSurCa, it has been designed to assemble small genomes (e.g. bacterial and viral genomes)³⁵².

The assembled genomes were annotated using Genome Annotation Transfer Utility (GATU) (**paper I, II and III**). GATU is a rapid annotation tool with a user-friendly graphical user interface. It transfers annotations from an annotated reference genome to the target genome, which makes the annotation process less time-consuming and less tedious. Additionally, it allows you to review the alignments of putative open reading frames (ORF) with the reference genes³⁵³.

4.5 Gene content comparison

In **paper I**, we compared the gene content of CPXV-No-H2 with other poxvirus genomes. Previously evidence of recombination was detected in CPXV-No-H2⁷¹. First, all predicted CPXV-NoH2 coding sequences (CDS) were translated and compared to the proteins of three OPXV reference genomes (ECTV-Moss, CPXV-BR and VACV-Cop) by BLASTP³⁵⁴. Some regions of the CPXV-No-H2 genome were more similar to either CPXV, ECTV or VACV, but others were less similar to the three OPXV. Hence, in order to detect CPXV-No-H2 genes more similar to other poxvirus genes, all predicted CPXV-NoH2 CDS were translated and compared to poxvirus proteins by BLASTp. The predicted CPXV-No-H2 genes that encode proteins with

the highest amino acid similarity to other OPXV proteins than CPXV proteins were compared to the OPXV genomes by BLASTn.

In **paper II**, we performed the gene content comparison of the five Fennoscandian CPXV with the reference genome CPXV-Br. Similar to procedure of **paper I**, the predicted CDS from five CPXV isolates were extracted, translated into amino acid sequences and compared to the CPXV-Br proteins using BLASTp³⁵⁴.

4.6 Recombination analysis

Since it was suggested that CPXV-No-H2 might originate from a recombination between CPXV-like virus and ECTV-like virus⁷¹, we performed the detection of the possible recombination events in the CPXV-No-H2 genome using RDP4³⁵⁵ and Simplot³⁵⁶ (**paper I**). These programs have been widely used in other studies^{6,71,357,358}. These programs required as input file the alignment of the recombinant sequence with the putative parental sequences. The CPXV-No-H2 genome with other genomes were aligned using Multiple Alignment Fast Fourier Transform (MAFFT). Compared to other aligners, MAFFT is a faster aligner and provides reliable and accurate multiple sequence alignments³⁵⁹.

RDP4 is a recombination detection program that has implemented several methods (RDP³⁶⁰, bootscan³⁶¹, maxchi³⁶², chimaera³⁶³, 3seq³⁶⁴, geneconv³⁶⁵, lard³⁶⁶, and siscan³⁶⁷ to detect potential recombination events in the aligned sequences. It allows to analyse up to 2500 sequences of 10,000 kbp, which makes it suitable for our dataset (genome length < 225 kbp). Furthermore, RDP4 provides the recombination sequences, the sequences that are closely related to the minor and major parental and recombination breakpoints (the beginning and end breakpoints of the potential recombinant sequences)³⁵⁵.

Simplot is another program to detect potential recombination. This software calculates the percent identity (similarity) of the query sequence compared to the other sequences and generates similarity plots (% similarity versus position). The potential recombination breakpoints are easily identified and visualized on the similarity plots.³⁵⁶ Compared to RDP4, Simplot provides fast results, but only allows to analyse up to 10 sequences. Besides the identification of the potential recombinant regions in CPXV-No-H2, we generated phylogenetic trees based on potential CPXV-No-H2 recombinant regions to corroborate the phylogenetic relationship between the putative parental virus (where the recombinant sequence was derived) and CPXV-No-H2. In **paper III**, we conducted recombination analysis of the progeny viruses from co-infected and superinfected Vero cells using the same methodology described above.

4.7 Phylogenetic analysis, patristic and genetic distances

The phylogenetic relationship of Fennoscandian CPXV strains with other CPXV and OPXV was investigated in **paper I and II**. The majority of the OPXV genomes used in this thesis were retrieved from the Viral Orthologous Clusters database (VOCs)³⁶⁸ (**paper I and II**). VOCs is

a repository for large dsDNA viruses, including complete and fully annotated poxvirus genomes ³⁶⁹.

In **paper I and II**, three different alignments were used for the phylogenetic analysis: (1) OPXV core genome (the genomes without ITR), (2) OPXV whole genome (genomic region from the first gene until the last gene), and (3) OPXV orthologous genes. DNA sequences were aligned using MAFFT ³⁷⁰. After aligning, the poorly aligned positions and gaps were removed from the whole and core genome alignments using Gblocks ³⁷¹. It is recommended to remove the problematic alignment regions in long alignments but not in short alignments (as orthologous gene alignment) to generate accurate phylogenetic trees ³⁷¹. The orthologous genes in OPXV genomes were identified using OrthoFinder ³⁷². OrthoFinder is fast, accurate and simple to use. It finds orthogroups, orthologs and gene duplication events and provides comparative genomics statistics ³⁷². The orthologs (present in $\geq 95\%$ of the genomes) were aligned and concatenated.

Two methods of tree reconstruction were used for phylogenetic analysis: maximum likelihood (ML) and Bayesian inference (BI) method. These methods are more efficient than the neighbour joining method in obtaining accurate tree ^{373,374}. Although they are computationally expensive ³⁷⁵. Before generating the phylogenetic trees, the best-fit models of DNA substitution for the datasets were selected because ML and BI methods use an explicit DNA substitution model. The models were selected by modelTest-NG ³⁷⁶. ML analyses were performed using RAxML ³⁷⁷ and BI analyses were performed using MrBayes v.3.2.7 ³⁷⁸.

Recombination events within datasets may cause inconsistencies in the phylogenetic trees and, therefore, erroneous phylogenetic inferences ^{379,380}. In order to assess if recombination in three datasets affects the phylogenetic inferences between CPXV and OPXV in **paper II**, the three datasets were analyzed for recombination events using RDP4 and one additional dataset of 62 non-recombinant OPXV conserved genes was included. OPXV conserved genes were examined for recombination using RDP4 and only conserved genes that did not show recombination were selected. In addition, in **paper II** the phylogenetic signal of the four dataset was assessed by likelihood mapping analysis using IQ-TREE ³⁸¹. It is important to test the presence of phylogenetic signal because the lack of it can affect the reliability of the results ³⁸².

The diversity of CPXV has been reported and it was proposed that CPXV might be more than one species ^{72,73,75,76,307}. Hence, in **paper II**, we used the genetic and patristic distances between and within CPXV clusters to demonstrate the genetic diversity among CPXV isolates. To separate CPXV isolates into sub-species, the genetic and patristic distances between the closest and distinct OPXV species (TATV and CMLV) were used as threshold values. The patristic and genetic distances were estimated using the program Patristic ³⁸³ and p-distances method, respectively.

4.8 Phylodynamic evolutionary analysis of CPXV

The molecular evolution of CPXV was reconstructed using 62 non-recombinant conserved genes of 55 CPXV (**paper II**). Different methods can be used to date the phylogeny: Bayesian³⁸⁴, ML³⁸⁵ or least-squares dating³⁸⁶. We used the Bayesian Markov chain Monte Carlo (MCMC) inference method implemented in *BEAST*³⁸⁷. Before carrying out the phylodynamic evolutionary analysis, we performed some preliminary analyses on the dataset. First, we checked the presence of phylogenetic signal in the dataset by IQtree³⁸¹. Second, the conserved genes were examined for recombination by RPD4³⁵⁵. Only conserved genes that did not show recombination were selected. Third, we assessed the temporal signal in the dataset using TempEst³⁸⁸ because a dataset without temporal signal is not appropriate to calibrate a molecular clock and to infer evolutionary rate and time scale of the virus³⁸². TempEst allows you to detect problematic sequences, for example sequences with assembly errors, annotation errors or incorrect sampling dates³⁸⁸.

5. SUMMARY OF THE MAIN RESULTS

Paper I: “Genomic sequencing and analysis of a novel human *Cowpox virus* with mosaic sequences from North America and Old World orthopoxvirus”

- We presented the whole genome sequence of a human cowpox virus, CPXV-No-H2, from Norway. The length of the CPXV-No-H2 genome was 220,276 bp, containing 217 predicted genes.
- Among 217 predicted genes of CPXV-No-H2, seventeen encoded proteins were most similar to OPXV proteins from the Old World (ECTV and VACV), and North America (AKPV).
- Our analyses revealed that CPXV-No-H2 was a mosaic genome with genes most similar to other OPXV genes.
- The recombination analysis revealed that CPXV-No-H2 may have arisen out of several recombination events between OPXVs.
- One potential recombinant event with parental AKPV contained the *NoH2-210* gene that was most similar to *AKPV-203* and Murmansk gene.
- Within the seven putative recombinant regions in CPXV-No-H2, one was located in the conserved central genomic region.
- The phylogenetic analysis showed that CPXV-No-H2 with two German CPXV isolates (CPXV_GerMygEK938_17 and CPXV_Ger2010_MKY) formed a separate, new CPXV clade, which we named “ECTV-Abatino-like CPXV”.
- CPXV_GerMygEK938_17 and CPXV_Ger2010_MKY shared 96.4% and 96.3% nucleotide identity with CPXV-No-H2, respectively.

Paper II: “Genomic Sequencing and Phylogenomics of *Cowpox Virus*”

- We reported the complete sequence of five Fennoscandian CPXV isolated from cats and humans.
- Their genome size ranged from 220-222 kbp, containing between 215 and 219 predicted CDS.
- The phylogenetic analysis based on the whole genomes, core genomes, orthologous genes and 62 non-recombinant conserved genes of 87 OPXV isolates (including the five Fennoscandian CPXV isolates) confirmed the separation of CPXV isolates into at least five distinct major clusters (CPXV-like 1, CPXV-like 2, VACV-like CPXV, VARV-like CPXV and ECTV-Abatino-like CPXV).
- CPXV strains were closely related to other the Old World OPXV, except for AKMV.
- Based on phylogenetic analysis and the genetic and patristic distances, CPXV isolates can be further divided into eighteen sub-species.
- We reconstructed the evolutionary history of CPXV using Bayesian time-scaled phylogeny of CPXV based on the concatenated 62 non-recombinant conserved genes of 55 CPXV. However, the emergence date of CPXV as well as CPXV clusters could not be accurately estimated.

- The mean evolution rate of CPXV was calculated to be 1.65×10^{-5} subs/site/year, with 95% high posterior density interval (HPD) of $4.36 \times 10^{-7} - 4.32 \times 10^{-5}$ subs/site/year.

Paper III: “Whole genome sequencing of recombinant viruses obtained from co-infection and superinfection of Vero cells with Modified Vaccinia virus Ankara vectored influenza vaccine and naturally occurring *Cowpox virus*”

- Recombination occurred between CPXV and MVA-HANP in co-infected and superinfected Vero cells.
- Some progeny viruses displayed plaque phenotype distinct of that of the parental viruses.
- The distribution of the recombinant events along the progeny virus genomes was random.
- The recombination events were located in both the conserved central region and the variable terminal regions.
- The transgene expression cassette was inserted (recombined) in the same position in the progeny virus genomes.
- The genomes of the recombinant progeny viruses have different lengths.
- Most recombinant progeny virus genomes were a mosaic of the two parental viruses (CPXV-No-F1 and MVA-HANP).
- The percentage of DNA derived from the parental viruses in the recombinant progeny viruses was variable.
- The recombinant viruses, more similar to MVA-HANP (>50%), rescued deleted and/or fragmented genes in MVA and gained new host ranges genes.
- Some recombinant progeny viruses carried the double expression cassette (harboring both influenza virus *HA* and *NP* transgenes) from MVA-HANP.
- The transgene of MVA-HANP was unstable, which led to the partially deletion of the double expression cassette.
- Resulting of the transgene instability of MVA-HANP one non-*HA*-transgene expressing progeny virus contained a fraction of the transgene expression cassette similar to the incomplete MVA-HANP.
- The progeny viruses suffered other genetic changes, such as the large deletion of 16,761 bp in two recombinant progeny viruses.

6. GENERAL DISCUSSION

MVA is a promising vector vaccine candidate. It is in pre-clinical and clinical trial studies for different diseases, including cancer ^{135,140,141,143,389}. However, despite the several studies about MVA and MVA vectored vaccine, there are still knowledge gaps about its potential for recombination with wild type OPXV as well as the distribution, genetic diversity and evolution of naturally circulating OPXV in regions in which MVA or MVA vectored vaccine will be administrated. The occurrence of natural recombination between MVA or MVA vectored vaccine and wild-type OPXV needs favourable scenarios where both viruses are present, that is, in environments where OPXV are circulating and MVA or MVA vectored vaccine is being administrated. Eurasia is a good scenario for recombination of MVA with CPXV since the latter is endemic in this region ³¹⁻³⁷. Several CPXV outbreaks and human CPXV infections have been reported ^{42,45,66,67,69,71,72}. Furthermore, MVA-BN has been approved as a smallpox and Mpox vaccine in Europe. Hence, the genomic characterization of CPXV strains isolated from different geographic locations is important to elucidate the genetic diversity and evolution of CPXV. This information is the baseline for evaluate the potential for recombination of MVA or MVA vectored vaccine with wild type OPXV.

In **paper I & II**, we reported the whole genome sequencing of six Fennoscandian CPXV isolates (CPXV-No-F1, CPXV-No-F2, CPXV-No-H1, CPXV-No-H2, CPXV-Swe-H1 and CPXV-Swe-H2). These isolates were from Norway and Sweden. Among them, there was one atypical CPXV isolate (CPXV-No-H2). It was classified as CPXV based on the presence of ATI, the sequence and phylogenetic analysis of *HA* gene, *cytokine response modifier B (crmB)* gene, and *Chinese hamster ovary host range (CHOhr)* genes ^{70,71}. However, it was an atypical CPXV because of its ATI phenotype (V⁺), presence of the ECTV *atip* gene and atypical CPXV *Hind III* restriction map ^{70,71}.

In **paper I & II**, we studied the phylogenetic relationship of Fennoscandian CPXV with other OPXV. Our phylogenetic analyses revealed that CPXV did not form a monophyletic clade and their isolates were clustered into five major clusters: CPXV-like 1, CPXV-like 2, VARV-like CPXV, VACV-like CPXV and new CPXV clade. CPXV isolates were closely related to all Old World OPXV species, except for AKMV. These findings are in agreement with other phylogenetic studies ^{74,78,307}. The new CPXV clade was composed of CPXV-No-H2 and two German CPXV isolates, CPXV_GerMygEK938_17 and CPXV_Ger2010_MKY. CPXV-No-H2 shared most similarity to CPXV_GerMygEK_938_17. This new CPXV clade was closely related to ECTV and Abatino clade. Thus, we tentatively named this clade as “ECTV-Abatino-like CPXV”. Previously it has been suggested that these two German CPXV isolates formed a new lineage (CPXV-like 3), but their phylogenetic relationship with ECTV and Abatino had a low bootstrap support ⁷⁸. A recently study showed that ECTV-Abatino-like CPXV did not cluster with ECTV and Abatino based on phylogenetic tree of conserved central region (*F11L* - *A23R*) ⁷⁴. In contrast, all our phylogenetic trees showed a closer phylogenetic relationship between ECTV-Abatino-like CPXV and ECTV/Abatino clade, regardless of the dataset used (OPXV whole- and core-genome, OPXV orthologous genes or 62 non-recombinant OPXV

conserved genes) (**paper I and II**). In addition, in our phylogenetic tree construction, we used both ML and BI methods which are more robust and accurate than the NJ method used by Bruneau *et al.* 2023 ⁷⁴.

The Norwegian CPXV isolates grouped in separate CPXV clusters rather than clustering together (**paper I and II**). The Norwegian CPXV-No-H2 belonged to ECTV-Abatino-like CPXV, whereas the other Norwegian CPXV isolates clustered together in CPXV-like 2. Similarly, the Swedish CPXV isolates were grouped together in CPXV-like 2. These Norwegian and Sweden CPXV isolates were closely related to British and Danish isolates, respectively (**paper II**) The phylogenies generated in other studies also showed the close phylogenetic relationship of these Norwegian CPXV isolates with the British CPXV isolates ^{73,75,77}.

Our findings in **paper I and II** revealed the genetic heterogeneity of CPXV isolates. Thus, in **paper II**, we examined the genetic diversity of CPXV using the genetic and patristic distances between and within CPXV clusters as previously reported ^{72,73}. Using the genetic and patristic distances between TATV and CMLV as a threshold value, the five CPXV clusters can be classified as five sub-species and even they can be further divided into 18 sub-species. This is in congruent with our phylogeny (**paper II**). The genetic diversity in CPXV could be attributed to recombination events in CPXV. It has been showed that some CPXV strains were mosaic genomes derived from different CPXV clades ⁷⁷. Even some studies suggested recombination between CPXV and other OPXV ^{6,84,302}. The reported genetic diversity of CPXV in **paper II** could not be a result of recombination events because we used a dataset of 62 non-recombinant OPXV conserved genes and despite the extensive recombination in the other three datasets, the phylogenies and genetic and patristic distances from the datasets with or without evidence of recombination were similar. This was surprisingly because recombination can lead to incongruences in the phylogeny and inaccurate phylogenetic inferences as has been observed in other studies ^{379,380}. Indeed, phylogenetic incongruency was observed when validating the recombinant regions singly in **paper I**. However, it appears that the phylogenetic signals of the recombinant regions were masked by signals from the larger, non-recombinant regions of the genome (**paper II**).

The definition of CPXV has been based on host specificity and two main criteria (ATI bodies and red hemorrhagic pocks on the CAM) ⁷⁹, which allowed that several viruses were classified under the CPXV name. ⁸⁰⁻⁸³. Mauldin *et al.* questioned the classification of CPXV as a single species because CPXV did not meet one of ICTV requirement (monophyly) to be classified as a species ⁷³. Our data presented herein substantiated the genetic diversity between and within CPXV clusters (**paper II**), which has also been noted by other researchers. ^{72,73,75-77,390}. Additionally, we demonstrated that CPXV was a polyphyletic assemblage, and it could be split into 18 sub-species (**paper II**). Earlier studies also suggested the division of CPXV ^{72,73,75}. Therefore, the reclassification of CPXV should be considered.

Within the OPXV, CPXV has the largest genome, broadest host range and contains almost the full set of OPXV genes^{40,84,198,201}. These characteristics have led to the suggestion that a CPXV-like virus was the ancestor of all Old World OPXV (except for AKMV)^{40,198,293,307}. However, the evolution of the CPXV as well as OPXV is not clear. In order to understand the evolution of CPXV, in **paper II** we studied the evolutionary history of CPXV based on the concatenated 62 non-recombinant conserved genes. We calculated CPXV substitution rate and the 95% HPD of our estimate overlapped the reported substitution rate of *Chordopoxvirinae* and OPXV^{292–295}. The emergence and divergence dates of CPXV could not be accurately estimated; the 95% HPD intervals of the emergence dates were quite broad. We presumed that it could be because of (1) the high heterogeneity of CPXV isolates and (2) the low genetic information due to restricted number of isolates in term of location, age and host. However, these findings might support the proposed idea that lineages of CPXV are highly divergent and a reclassification of CPXV is warranted.

As mentioned above, CPXV-No-H2 is an atypical CPXV isolate that contains an ECTV *atip* gene^{70,71}. A previous study of our research group suggested that CPXV-No-H2 could have acquired ECTV-*atip* gene by recombination with ECTV or and ECTV-like virus⁷¹. In order to characterize recombination in CPXV-No-H2, in **paper I** we sequenced the whole genome of CPXV-No-H2. Our analysis revealed that CPXV-No-H2 had a mosaic genome, containing genomic sequences more similar to North America OPXV (i.e., AKPV) and the Old World OPXV (i.e. ECTV and VACV). CPXV-No-H2 contained nine recombinant regions that may be a result of different recombination events between the parentals of AKPV and CPXV, ECTV and CPXV, and VACV and CPXV. Although two potential recombinant events with the parental AKPV overlapped with two potential recombination events with the parental ECTV. Curiously, AKPV may undergo recombination with ECTV in the same position of those overlapped recombinant regions and ECTV may contain AKPV-like sequences⁷. In addition, AKPV contained three genes (*AKPV-203*, *AKPV-204* and *AKPV-205*) that were most similar to Murmansk genes and they may be introduced from/to Murmansk by recombination⁷. One of the recombinant regions between AKPV and CPXV-No-H2 comprised a gene that was most similar to *AKPV-203* and Murmansk gene. Moreover, the phylogenetic analyses based on three recombinant regions between AKPV and CPXV suggested that AKPV-like sequences were introduced to CPXV-No-H2 rather than the other way (**paper I**).

Since CPXV-No-H2 produced atypical V^{+/} ATI⁷¹, we analysed the genes involved in the formation of ATI (**paper I**). Two of the three genes (*p4c* and *A27L*) were most similar to CPXV_GerMygEK_938_17 genes and the third gene (*atip*) was in the two overlapping recombinant regions between CPXV and AKPV, and CPXV and ECTV (**paper I**). Compared to CPXV-No-H2, AKMV and CPXV-Ger 2010 produced wild type V⁺ ATI^{7,77,184}. On the other hand, ECTV_Hampstead displayed V⁺ and V^{+/} ATI and other ECTV strains produced V⁻ ATI^{174,183}. ECTV_Hampstead was the progenitor of the European ECTV outbreaks³⁹¹. The ATI phenotype in CPXV_GerMygEK_938_17 was not reported but we presumed that CPXV_GerMygEK_938_17 produces the wild type V⁺ ATI because its *atip*, *p4c*, and *A27L* genes were similar to CPXV_Ger2010_MKY genes (**paper I**).

It is difficult to reconstruct the evolutionary history of CPXV-NoH2 due to the multiple recombination events. The mosaic genome of CPXV-No-H2 could be explained by symplesiomorphy since most recombinant regions were similar to more than one taxon. However, there was one AKPV-like sequence in CPXV-No-H2 that could not be explained by symplesiomorphy because it was only similar to AKPV. A plausible explanation about the origin of the recombinant regions in CPXV-No-H2 is that it was originated from the recombination of CPXV_GerMygEK_938_17-like virus and AKPV-like virus. Probably both viruses could have circulated in populations of rodents in Europe. Even though the isolation of AKPV was Alaska, its ancestor might circulate in Europe because AKPV contained genes similar to those of Russian *Murmansk virus*^{7,305}. The recombinant progeny virus, CPXV-No-H2-like virus, could have suffered genomic changes linked to the adaptation to mice, resulting in ECTV-like virus. CPXV-like virus has been proposed as ancestor of ECTV⁷⁸. Thus, these findings suggested that recombination between OPXV in nature is more common than we thought (**paper I**).

In **paper I and II**, we demonstrated that CPXV-No-H2 was a natural recombinant CPXV (**paper I**) and the extensive recombination in OPXV and CPXV (**paper II**). Recombination is not a foreign evolutionary mechanism in poxviruses. It has been demonstrated in different poxvirus species, both *in vivo*^{6,7,71,77,302,392} and *in vitro*^{326,393–396}. Hazard characterization of MVA vectored vaccines require the evaluation of potential recombination between the vector and naturally circulating OPXV. In our previous study, we performed co-infection and superinfection experiments of semi-permissive Vero cells with MVA-HANP and CPXV-No-F1 and showed that recombination occurred during *in vitro* co-infection and superinfection of Vero cells¹³³. In **paper III**, we performed whole genome sequencing of these progeny viruses obtained from confection and superinfection of Vero cells. Our results confirmed the recombination with MVA-HANP and CPXV-No-F1 in cells where MVA poorly multiplies (Vero cells). It demonstrated that the recombination occurred in semi-permissive Vero cells, despite they did not form mature particles²⁸⁷. This is not surprising because viral DNA replication is unimpaired in non-permissive cells to MVA infection^{119,286}. Therefore, MVA could undergo recombination in semi- and non-permissive cells because poxviral recombination only requires that the linear DNA molecules share 12 bp of homology³²⁵. On the other hand, the superinfection exclusion did not prevent the superinfection of Vero cells in spite of the superinfection time of 6 hours. It has been reported that 6 hours after primary infection with VACV produced 99% exclusion of superinfecting virus³⁹⁷.

In **paper III**, the genomic characterization of progeny viruses derived from co-infected and superinfected Vero cells revealed that their genomes were a mosaic of the MVA-HANP and CPXV-No-F1 genomes, except for the progeny virus R9. The distribution of the recombination events in the progeny virus genomes was aleatory (**paper III**). Recombination events took place both in conserved central regions (*F4L - A24R*) and variable terminal regions (**paper III**). Similar observations were also made in the natural recombinant CPXV-No-H2 (**paper I**). However, it has been reported that the recombination events in OPXV are more common in the terminal genomic region than the central region^{6,7,77,84,199,300}. Interestingly, there was a genomic

region (*CPXV-Br010* to *CPXV-Br043* gene) in the recombinant progeny viruses where recombination events did not occur (**paper III**). Although two recombinant viruses had suffered a large deletion in this region, from *CPXV-Br016* to *CPXV-Br029* gene (**paper III**).

The proportion of the parental genomes in the progeny virus genomes was not uniform. Most recombinant viruses comprised more CDS from CPXV-No-F1 (**paper III**). This could be because Vero cells were permissive to CPXV-No-F1 infection and the selection of progeny viruses based on visible plaques in Vero cells also biased selection in favor of viruses with more CPXV genomes since CPXV forms plaques in Vero while MVA/MVA-HANP does not. To gain a comprehensive understanding of recombination between MVA vector and naturally circulating CPXV, the limitations of culture-based selection can be overcome by metagenomic sequencing of co-infected and superinfected cells.

Various progeny viruses displayed plaque phenotypes distinct to that of parental viruses and some of them expressed the *HA* transgene (**paper III**). Similar findings were observed in the progeny viruses from co-infected BHK-21 cells and superinfected Vero cells (using 2 hours) ^{133,326}. Our progeny viruses produced different plaque phenotypes, such as non-lytic plaques with comet formation (**paper III**). The plaque morphology of the progeny viruses was affected by the presence or absence of genes involved in the syncytium and plaque formation (*F5L*, *F11L*, *F12L*, *F13L*, *A33R*, *A34R*, *A36R*, *A56R*, *B5R* and *K2L* genes) ^{250,252,253,259,262,263,398–401}. Some of these genes were fragmented (e.g. *F5L* and *F11L* gene) or have suffered small internal deletions (e.g. *A36R*) in MVA ¹²⁰. For instance, a recombinant progeny virus contained the *F5L*, *F11L*, *A36R*, *A33R*, *A34R* and *B5R* genes from MVA-HANP and formed small and non-lytic plaques with comet formation (**paper III**).

Within the progeny viruses, there was a non-recombinant that formed plaques with syncytium formation. The genomic analysis revealed that its *K2L* gene had one non-synonymous single-nucleotide mutation (nsSNM) that caused the truncation of the gene (**paper III**). It has been reported that the lack of the *K2L* gene caused the fusion of infected cells ^{251–253}. Besides nsSNMs, other genetic mutations such as deletion were detected in the progeny viruses. A large deletion (~16 kbp) was found in two recombinant viruses from superinfected Vero cells (**paper III**).

A partial deletion of double expression cassette (harbouring both influenza virus *HA* and *NP* transgenes) was detected in the parental MVA-HANP as well as in one recombinant progeny virus (**paper III**). The instability of the *HA* transgene has been also observed in MVA-HANP and in recombinant progeny viruses from co-infected BHK-21 cells ³²⁷. Other studies also showed the transgene instability in recombinant MVA vectors ^{335–338}. In MVA-HANP, the transgene was inserted in the hybrid genes A51/56, where MVA has suffered a deletion (deletion III) (**paper III**). One study compared the stability of the transgene inserted in different regions of the MVA genome (including deletion II, deletion III, the *CP77* gene locus and the *I8R-GIL* intergenic region) after 35 passages and showed that transgene was most stable in the intergenic region compared to the other regions (including deletion III) ⁴⁰².

We observed that the recombinant progeny viruses, with more DNA derived from MVA (>50%), rescued some deleted and/or fragmented genes from CPXV, including host range genes (**paper III**). One of the main concerns about the recombination of MVA vectored vaccine with a multiplication competent OPXV is the rescue of missing or fragmented host range genes in MVA and, hence, restoring the wild-type phenotype^{133,322}. Another concern is the transfer of the transgene from OPXV vectored vaccine into a multiplication competent OPXV^{133,322}. Our data showed that the recombinant viruses with a genome more similar to CPXV-No-F1 contained the transgenic cassette from MVA-HANP (**paper III**).

The recombination of a wild type OPXV and a poxvirus vaccine has been reported³²⁸. A Russian recombinant virus showed evidence of 27 recombinant events. Their possible parentals were a field LSDV strain and an LSD vaccine³²⁸. In following LSDV outbreaks only vaccine-like LSDV strains have been detected instead of the wild type LSDV strains^{329,330}. However, some researchers suggested the recombinant viruses could be a result of spillover from vaccinated animals³³¹.

7. CONCLUSION AND FUTURE PERSPECTIVES

We have shown that recombination is a common evolutionary mechanism that occurred between OPXV in nature. CPXV-No-H2 was an example of a natural occurring CPXV that might have undergone several recombination events between different OPXV species isolated from different continents. Furthermore, CPXV, which is the potential candidate for recombination with MVA vectored vaccine, had a high genetic diversity and was an assemblage of several sub-species. Among CPXV strains, three CPXV strains (including CPXV-No-H2) were closely related to ECTV and Abatino and formed a new, distinct CPXV clade named “ECTV-Abatino-like CPXV”. With the current genetic information of CPXV strains the evolutionary history of CPXV could not be elucidated. We demonstrated that progeny viruses obtained from co-infection and superinfection *in vitro* of semi-permissive Vero cells with MVA-HANP and CPXV-No-F1 displayed novel biological and genetic characteristics. Furthermore, the rescue of deleted or fragmented MVA genes in recombinant progeny viruses was possible as well the transfer of the transgene to CPXV. Overall, our findings provide relevant data for the hazard characterization of MVA vectored vaccines and, hence, improving the biosafety of MVA vectored vaccines.

The diversity and evolution of CPXV as well as the recombination between OPXV are still not completely elucidated. The diversity of CPXV has awoken debates about the reclassification of CPXV. However, for the re-classification of CPXV, the biological characterization of the CPXV strains is also required. Together, the genetic and biological characterization would provide a better understanding of diversity of CPXV as well as the evolution of CPXV and OPXV. In order to understand the evolution of CPXV, it is necessary to increase surveillance of OPXV (including CPXV) in different species and regions and acquire ancient CPXV strains. The recombination studies reported in this thesis were under *in vitro* conditions, which could differ from *in vivo* conditions. Thus, future studies should examine recombination *in vivo* particularly in immunocompetent and immunocompromised animal models.

8. REFERENCES

1. Moss, B. Poxviridae. in *Fields virology* (eds. Knipe, D. & Howley, P.) 2129–2159 (Lippincott Williams & Wilkins (LWW), 2013).
2. Diven, D. G. An overview of poxviruses. *Journal of the American Academy of Dermatology* **44**, (2001).
3. Silva, N. I. O., de Oliveira, J. S., Kroon, E. G., Trindade, G. de S. & Drumond, B. P. Here, There, and Everywhere: The Wide Host Range and Geographic Distribution of Zoonotic Orthopoxviruses. *Viruses* **13**, (2021).
4. Smithson, C. *et al.* The genomes of three North American orthopoxviruses. *Virus Genes* **53**, 21–34 (2017).
5. Cardeti, G. *et al.* Fatal Outbreak in Tonkean Macaques Caused by Possibly Novel Orthopoxvirus, Italy, January 2015 - Volume 23, Number 12—December 2017 - Emerging Infectious Diseases journal - CDC. *Emerg. Infect. Dis.* **23**, 1941–1949 (2017).
6. Gao, J. *et al.* Genome sequences of Akhmeta virus, an early divergent old world orthopoxvirus. *Viruses* **10**, (2018).
7. Gigante, C. M. *et al.* Genome of Alaskapox Virus, a Novel Orthopoxvirus Isolated from Alaska. *Viruses* **11**, (2019).
8. McFadden, G. Poxvirus tropism. *Nature Reviews Microbiology* **3**, (2005).
9. Behbehani, A. M. The smallpox story: Life and death of an old disease. *Microbiological Reviews* **47**, (1983).
10. Fenner, F., Henderson, D., Arita, I., Jezek, Z. & Ladnyi, D. *Smallpox and its eradication*. (WHO, 1988).
11. Berche, P. Life and death of smallpox. *Press. Medicale* **51**, 104117 (2022).
12. Moore, J. C. *The history of the small pox*. (1815).
13. Farhi, D. & Dupin, N. Origins of syphilis and management in the immunocompetent patient: Facts and controversies. *Clin. Dermatol.* **28**, (2010).
14. Hopkins, D. Ramses V: earliest known victim? 22–26 (1980).
15. Ellner, P. D. Smallpox: Gone but not forgotten. *Infection* **26**, (1998).
16. Deria, A., Jezek, Z., Markvart, K., Carrasco, P. & Weisfeld, J. The world's last endemic case of smallpox: surveillance and containment measures. *Bull. World Health Organ.* **58**, 279 (1980).
17. WHO. *The global eradication of smallpox : final report of the Global Commission for the Certification of Smallpox Eradication, Geneva, December 1979*. (1980).
18. Shchelkunova, G. A. & Shchelkunov, S. N. 40 Years without Smallpox. *Acta Naturae* **9**, (2017).
19. WHO. *A74/43 - Report by the Director-General - Smallpox eradication*. (2021).

20. Barquet, N. & Domingo, P. Smallpox: The triumph over the most terrible of the ministers of death. *Ann. Intern. Med.* **127**, (1997).
21. Jenner, E. The Three Original Publications On Vaccination Against Smallpox. in *The Harvard Classics, Vol. XXXVIII, Part 4* (1909).
22. Jenner, E. An inquiry into the causes and effects of the variolae vaccinae: a disease discovered in some of the western counties of England, particularly Gloucestershire, and known by the name of the cow pox. *Springf. [Mass.] Re-printed Dr. Samuel Cool. by Ashley Brew. 1802* 134 (1802).
23. Willis, N. J. Edward Jenner and the eradication of smallpox. *Scottish Medical Journal* **42**, (1997).
24. Tuells, J. Vaccinology: The name, the concept, the adjectives. *Vaccine* **30**, (2012).
25. Pearson, G. *An Examination of the Report of the Committee of the House of Commons on the Claims of Remuneration for the Vaccine Pock Inoculation.* (1802).
26. Esparza, J., Schrick, L., Damaso, C. R. & Nitsche, A. Equination (inoculation of horsepox): An early alternative to vaccination (inoculation of cowpox) and the potential role of horsepox virus in the origin of the smallpox vaccine. *Vaccine* **35**, 7222–7230 (2017).
27. Damaso, C. R. Revisiting Jenner’s mysteries, the role of the Beaugency lymph in the evolutionary path of ancient smallpox vaccines. *The Lancet Infectious Diseases* **18**, (2018).
28. Brinkmann, A., Souza, A. R. V., Esparza, J., Nitsche, A. & Damaso, C. R. Re-assembly of nineteenth-century smallpox vaccine genomes reveals the contemporaneous use of horsepox and horsepox-related viruses in the USA. *Genome Biology* **21**, (2020).
29. Pead, P. J. Benjamin Jesty: New light in the dawn of vaccination. *Lancet* **362**, (2003).
30. Hammarsten, J. F., Tattersall, W. & Hammarsten, J. E. Who discovered smallpox vaccination? Edward Jenner or Benjamin Jesty? *Transactions of the American Clinical and Climatological Association* **Vol. 90**, (1978).
31. Chantrey, J. *et al.* Cowpox: reservoir hosts and geographic range. *Epidemiol. Infect.* **122**, 455 (1999).
32. Wolfs, T. F. W., Wagenaar, J. A., Niesters, H. G. M. & Osterhaus, A. D. M. E. Rat-to-Human Transmission of Cowpox Infection. *Emerg. Infect. Dis.* **8**, 1495 (2002).
33. Laakkonen, J. *et al.* Serological Survey for Viral Pathogens in Turkish Rodents. *J. Wildl. Dis.* **42**, 672–676 (2006).
34. Vorou, R. M., Papavassiliou, V. G. & Pierrotsakos, I. N. Cowpox virus infection: An emerging health threat. *Curr. Opin. Infect. Dis.* **21**, 153–156 (2008).
35. Popova, A. Y. *et al.* Cowpox in a human, Russia, 2015. *Epidemiol. Infect.* **145**, 755–759 (2017).
36. Diaz, J. H. The Disease Ecology, Epidemiology, Clinical Manifestations, Management, Prevention, and Control of Increasing Human Infections with Animal Orthopoxviruses. *Wilderness Environ. Med.* **32**, 528–536 (2021).
37. Ferrier, A. *et al.* Fatal cowpox virus infection in human fetus, france, 2017. *Emerg. Infect. Dis.*

- 27, 2570–2577 (2021).
38. Oliveira, G. P., Rodrigues, R. A. L., Lima, M. T., Drumond, B. P. & Abrahão, J. S. Poxvirus Host Range Genes and Virus–Host Spectrum: A Critical Review. *Viruses* 2017, Vol. 9, Page 331 **9**, 331 (2017).
 39. Bratke, K. A., McLysaght, A. & Rothenburg, S. A survey of host range genes in poxvirus genomes. *Infect. Genet. Evol.* **14**, 406–425 (2013).
 40. Shchelkunov, S. N. *et al.* The genomic sequence analysis of the left and right species-specific terminal region of a cowpox virus strain reveals unique sequences and a cluster of intact ORFs for immunomodulatory and host range proteins. *Virology* **243**, 432–460 (1998).
 41. Kinnunen, P. M. *et al.* Orthopox Virus Infections in Eurasian Wild Rodents. <https://home.liebertpub.com/vbz> **11**, 1133–1140 (2011).
 42. Prkno, A. *et al.* Epidemiological investigations of four cowpox virus outbreaks in alpaca herds, Germany. *Viruses* **9**, 1–15 (2017).
 43. Girling, S. J., Pizzi, R., Cox, A. & Beard, P. M. Fatal cowpox virus infection in two squirrel monkeys (*Saimiri sciureus*). *Vet. Rec.* **169**, 156–156 (2011).
 44. Smith, K. C., Bennett, M. & Garrett, D. C. Skin lesions caused by orthopoxvirus infection in a dog. *J. Small Anim. Pract.* **40**, 495–497 (1999).
 45. Tryland, M., Myrmel, H., Holtet, L., Haukenes, G. & Traavik, T. Clinical cowpox cases in Norway. *Scand. J. Infect. Dis.* **30**, 301–303 (1998).
 46. Martina, B. E. E. *et al.* Cowpox Virus Transmission from Rats to Monkeys, the Netherlands. *Emerg. Infect. Dis.* **12**, 1005 (2006).
 47. Essbauer, S., Pfeffer, M. & Meyer, H. Zoonotic poxviruses. *Vet. Microbiol.* **140**, 229–236 (2010).
 48. Carletti, F. *et al.* Cat-to-human orthopoxvirus transmission, northeastern Italy. *Emerging Infectious Diseases* **15**, (2009).
 49. Świtaj, K., Kajfasz, P., Kurth, A. & Nitsche, A. Cowpox after a cat scratch – case report from Poland. *Ann. Agric. Environ. Med.* **22**, (2015).
 50. Hemmer, C. J. *et al.* Human cowpox virus infection acquired from a circus elephant in Germany. *Int. J. Infect. Dis.* **14**, (2010).
 51. Kurth, A. *et al.* Cowpox virus outbreak in banded mongooses (*Mungos mungo*) and jaguarundis (*Herpailurus yagouaroundi*) with a time-delayed infection to humans. *PLoS One* **4**, (2009).
 52. Elsendoorn, A. *et al.* Severe ear chondritis due to cowpox virus transmitted by a pet rat. *J. Infect.* **63**, (2011).
 53. Hobi, S. *et al.* Neurogenic inflammation and colliquative lymphadenitis with persistent orthopox virus DNA detection in a human case of cowpox virus infection transmitted by a domestic cat. *Br. J. Dermatol.* **173**, (2015).
 54. Kurth, A. *et al.* Rat-to-Elephant-to-Human Transmission of Cowpox Virus. *Emerg. Infect. Dis.* **14**, 670 (2008).

55. Vogel, S. *et al.* The Munich outbreak of cutaneous cowpox infection: Transmission by infected pet rats. *Acta Derm. Venereol.* **92**, (2012).
56. Becker, C. *et al.* Cowpox Virus Infection in Pet Rat Owners: Not Always Immediately Recognized. *Dtsch. Arztebl. Int.* **106**, 329 (2009).
57. Ducournau, C. *et al.* Concomitant human infections with 2 cowpox virus strains in related cases, France, 2011. *Emerg. Infect. Dis.* **19**, (2013).
58. Favier, A. L. *et al.* Necrotic ulcerated lesion in a young boy caused by cowpox virus infection. *Case Rep. Dermatol.* **3**, (2011).
59. Bonnekoh, B. *et al.* Cowpox infection transmitted from a domestic cat. *JDDG* **6**, (2008).
60. Lawn, R. Risk of cowpox to small animal practitioners. *Veterinary Record* **166**, (2010).
61. Fassbender, P. *et al.* Generalized cowpox virus infection in a patient with HIV, Germany, 2012. *Emerging Infectious Diseases* **22**, (2016).
62. Gazzani, P. *et al.* Fatal disseminated cowpox virus infection in an adolescent renal transplant recipient. *Pediatr. Nephrol.* **32**, (2017).
63. Eis-Hubinger, A. M. *et al.* Fatal cowpox-like virus infection transmitted by cat. *The Lancet* **336**, (1990).
64. Willemsse, A. & Egberink, H. F. Transmission of cowpox virus infection from domestic cat to man. *Lancet (London, England)* **1**, 1515 (1985).
65. Wendt, R. *et al.* Generalized cowpox virus infection in an immunosuppressed patient. *International Journal of Infectious Diseases* **106**, (2021).
66. Stagegaard, J. *et al.* Seasonal recurrence of cowpox virus outbreaks in captive cheetahs (*Acinonyx jubatus*). *PLoS One* **12**, (2017).
67. Antwerpen, M. H. *et al.* Use of next generation sequencing to study two cowpox virus outbreaks. *PeerJ* **2019**, 1–17 (2019).
68. Tryland, M. *et al.* Characteristics of four cowpox virus isolates from Norway and Sweden. *APMIS* **106**, 623–635 (1998).
69. Cronqvist, J., Ekdahl, K., Kjartansdottir, A., Bauer, B. & Klinker, M. [Cowpox--a cat disease in man] . *Lakartidningen* **88**, 2605–2606 (1991).
70. Hansen, H., Okeke, M. I., Nilssen, Ø. & Traavik, T. Comparison and phylogenetic analysis of cowpox viruses isolated from cats and humans in Fennoscandia. *Arch. Virol.* **154**, 1293–1302 (2009).
71. Okeke, M. I., Hansen, H. & Traavik, T. A naturally occurring cowpox virus with an ectromelia virus A-type inclusion protein gene displays atypical A-type inclusions. *Infect. Genet. Evol.* **12**, 160–168 (2012).
72. Okeke, M. I. *et al.* Molecular characterization and phylogenetics of Fennoscandian cowpox virus isolates based on the p4c and atip genes. *Viol. J.* **11**, 1–16 (2014).
73. Mauldin, M. R. *et al.* Cowpox virus: What's in a Name? *Viruses 2017, Vol. 9, Page 101* **9**, 101 (2017).

74. Bruneau, R. C., Tazi, L. & Rothenburg, S. Cowpox Viruses : A Zoo Full of Viral Diversity and Lurking Threats. (2023).
75. Carroll, D. S. *et al.* Chasing Jenner's vaccine: Revisiting Cowpox virus classification. *PLoS One* **6**, 4–9 (2011).
76. Dabrowski, P. W., Radonić, A., Kurth, A. & Nitsche, A. Genome-wide comparison of cowpox viruses reveals a new clade related to variola virus. *PLoS One* **8**, 1–9 (2013).
77. Franke, A. *et al.* Classification of cowpox viruses into several distinct clades and identification of a novel lineage. *Viruses* **9**, 1–14 (2017).
78. Jeske, K. *et al.* Molecular Detection and Characterization of the First Cowpox Virus Isolate Derived from a Bank Vole. *Viruses* **11**, (2019).
79. Downie, A. W. A study of the lesions produced experimentally by cowpox virus. *J. Pathol. Bacteriol.* **48**, (1939).
80. Pilaski, J. & Rösen-Wolff, A. Poxvirus Infection in Zoo-Kept Mammals. in (1988). doi:10.1007/978-1-4613-2091-3_5
81. Zwart, P., Gispén, R. & Peters, J. C. Cowpox in okapis *Okapia johnstoni* at Rotterdam zoo. *Br. Vet. J.* **127**, (1971).
82. Baxby, D. Laboratory Characteristics of British and Dutch Strains of Cowpox Virus. *Zentralblatt für Veterinärmedizin R. B* **22**, (1975).
83. Marennikova, S. S., Maltseva, N. N., Korneeva, V. I. & Garanina, N. M. Outbreak of pox disease among carnivora (Felidae) and edentata. *J. Infect. Dis.* **135**, (1977).
84. Gubser, C., Hué, S., Kellam, P. & Smith, G. L. Poxvirus genomes: A phylogenetic analysis. *J. Gen. Virol.* **85**, 105–117 (2004).
85. Molteni, C., Forni, D., Cagliani, R., Clerici, M. & Sironi, M. Genetic ancestry and population structure of vaccinia virus. *npj Vaccines* **7**, (2022).
86. Esparza, J. & Damaso, C. R. Searching for the origin of the smallpox vaccine: Edward Jenner and his little-known horsepox hypothesis. *Vaccine* **40**, (2022).
87. Singh, R. K., Balamurugan, V., Bhanuprakash, V., Venkatesan, G. & Hosamani, M. Emergence and reemergence of vaccinia-like viruses: Global scenario and perspectives. *Indian Journal of Virology* **23**, (2012).
88. de Oliveira, J. S. *et al.* Vaccinia virus natural infections in Brazil: The good, the bad, and the ugly. *Viruses* **9**, (2017).
89. Eltom, K. H., Samy, A. M., Wahed, A. A. El & Czerny, C. P. Buffalopox virus: An emerging virus in livestock and humans. *Pathogens* **9**, (2020).
90. Miranda, J. B. *et al.* Serologic and Molecular Evidence of Vaccinia Virus Circulation among Small Mammals from Different Biomes, Brazil. *Emerg. Infect. Dis.* **23**, 931 (2017).
91. Baxby, D. & Hill, B. J. Characteristics of a new poxvirus isolated from indian buffaloes. *Arch. Gesamte Virusforsch.* **35**, (1971).
92. Lima, M. T. *et al.* An update on the known host range of the brazilian vaccinia virus: An

- outbreak in Buffalo Calves. *Front. Microbiol.* **10**, (2019).
93. Roy, P. & Chandramohan, A. Buffalopox Disease in Livestock and Milkers, India. *Emerg. Infect. Dis.* **27**, (2021).
 94. MacNeill, A. L. Comparative Pathology of Zoonotic Orthopoxviruses. *Pathogens* **11**, 1–22 (2022).
 95. Zafar, A. *et al.* Nosocomial Buffalopoxvirus Infection, Karachi, Pakistan. *Emerg. Infect. Dis.* **13**, 904 (2007).
 96. Singh, R. K. *et al.* An outbreak of buffalopox in buffalo (*Bubalus bubalis*) dairy herds in Aurangabad, India. *OIE Rev. Sci. Tech.* **25**, (2006).
 97. Franco-Luiz, A. P. M. *et al.* Spread of vaccinia virus to cattle herds, Argentina, 2011. *Emerging Infectious Diseases* **20**, (2014).
 98. Usme-Ciro, J. A. *et al.* Detection and molecular characterization of zoonotic poxviruses circulating in the amazon region of Colombia, 2014. *Emerg. Infect. Dis.* **23**, (2017).
 99. Medaglia, M. L. G., Pessoa, L. C. G. D., Sales, E. R. C., Freitas, T. R. P. & Damaso, C. R. Spread of Cantagalo virus to northern Brazil. *Emerging Infectious Diseases* **15**, (2009).
 100. Trindade, G. S. *et al.* Belo Horizonte virus: A vaccinia-like virus lacking the A-type inclusion body gene isolated from infected mice. *J. Gen. Virol.* **85**, (2004).
 101. Brum, M. C. S. *et al.* An outbreak of orthopoxvirus-associated disease in horses in southern Brazil. *J. Vet. Diagnostic Investig.* **22**, (2010).
 102. Abrahão, J. S. *et al.* Vaccinia virus infection in monkeys, Brazilian Amazon. *Emerg. Infect. Dis.* **16**, (2010).
 103. Damaso, C. R. A., Esposito, J. J., Condit, R. C. & Moussatché, N. An emergent poxvirus from humans and cattle in Rio de Janeiro state: Cantagalo virus may derive from brazilian smallpox vaccine. *Virology* **277**, (2000).
 104. Bhanuprakash, V. *et al.* Zoonotic infections of buffalopox in India. *Zoonoses Public Health* **57**, (2010).
 105. Laiton-Donato, K. *et al.* Progressive vaccinia acquired through zoonotic transmission in a patient with HIV/AIDS, Colombia. *Emerg. Infect. Dis.* **26**, (2020).
 106. Oliveira, G. P. *et al.* Short report: Intrafamilial transmission of Vaccinia virus during a bovine vaccinia outbreak in Brazil: A new insight in viral transmission chain. *Am. J. Trop. Med. Hyg.* **90**, (2014).
 107. Batista, V. H., Scremin, J., Aguiar, L. M. & Schatzmayr, H. G. VULVAR INFECTION AND POSSIBLE HUMAN-TO-HUMAN TRANSMISSION OF BOVINE POXVIRUS DISEASE. *VIRUS Rev. Res.* **14**, (2009).
 108. Jacobs, B. L. *et al.* Vaccinia Virus Vaccines: Past, Present and Future. *Antiviral Res.* **84**, 1 (2009).
 109. Sánchez-Sampedro, L. *et al.* The evolution of poxvirus vaccines. *Viruses* **7**, (2015).
 110. Rosenthal, S. R., Merchlinsky, M., Kleppinger, C. & Goldenthal, K. L. Developing new

- smallpox vaccines. *Emerg. Infect. Dis.* **7**, 920–926 (2001).
111. Qin, L., Liang, M. & Evans, D. H. Genomic analysis of vaccinia virus strain TianTan provides new insights into the evolution and evolutionary relationships between Orthopoxviruses. *Virology* **442**, (2013).
 112. Belongia, E. A. & Naleway, A. L. Smallpox vaccine: the good, the bad, and the ugly. *Clinical medicine & research* **1**, (2003).
 113. Kenner, J., Cameron, F., Empig, C., Jobes, D. V. & Gurwith, M. LC16m8: An attenuated smallpox vaccine. *Vaccine* **24**, 7009–7022 (2006).
 114. Mayr, A., Stickl, H., Müller, H. K., Danner, K. & Singer, H. [The smallpox vaccination strain MVA: marker, genetic structure, experience gained with the parenteral vaccination and behavior in organisms with a debilitated defence mechanism (author's transl)]. *Zentralbl. Bakteriolog. B.* **167**, (1978).
 115. Tartaglia, J. *et al.* NYVAC: a highly attenuated strain of vaccinia virus. *Virology* **188**, 217–232 (1992).
 116. Paran, N. & Sutter, G. Smallpox vaccines: New formulations and revised strategies for vaccination. *Human vaccines* **5**, (2009).
 117. Kennedy, R. B., Ovsyannikova, I. & Poland, G. A. Smallpox vaccines for biodefense. *Vaccine* **27**, (2009).
 118. Smith, G. L. & Moss, B. Infectious poxvirus vectors have capacity for at least 25 000 base pairs of foreign DNA. *Gene* **25**, (1983).
 119. Volz, A. & Sutter, G. Modified Vaccinia Virus Ankara: History, Value in Basic Research, and Current Perspectives for Vaccine Development. in *Advances in Virus Research* **97**, (2017).
 120. Antoine, G., Scheifflinger, F., Dorner, F. & Falkner, F. G. The complete genomic sequence of the modified vaccinia Ankara strain: Comparison with other orthopoxviruses. *Virology* **244**, (1998).
 121. Meyer, H., Sutter, G. & Mayr, A. Mapping of deletions in the genome of the highly attenuated vaccinia virus MVA and their influence on virulence. *J. Gen. Virol.* **72**, (1991).
 122. Meisinger-Henschel, C. *et al.* Genomic sequence of chorioallantois vaccinia virus Ankara, the ancestor of modified vaccinia virus Ankara. *J. Gen. Virol.* **88**, 3249–3259 (2007).
 123. Blanchard, T. J., Alcamí, A., Andrea, P. & Smith, G. L. Modified vaccinia virus Ankara undergoes limited replication in human cells and lacks several immunomodulatory proteins: Implications for use as a human vaccine. *J. Gen. Virol.* **79**, (1998).
 124. Carroll, M. W. & Moss, B. Host range and cytopathogenicity of the highly attenuated MVA strain of vaccinia virus: Propagation and generation of recombinant viruses in a nonhuman mammalian cell line. *Virology* **238**, (1997).
 125. Hornemann, S. *et al.* Replication of Modified Vaccinia Virus Ankara in Primary Chicken Embryo Fibroblasts Requires Expression of the Interferon Resistance Gene E3L. *J. Virol.* **77**, (2003).
 126. Pittman, P. R. *et al.* Phase 3 Efficacy Trial of Modified Vaccinia Ankara as a Vaccine against Smallpox. *N. Engl. J. Med.* **381**, (2019).

127. Mayr, A. Smallpox vaccination and bioterrorism with pox viruses. *Comp. Immunol. Microbiol. Infect. Dis.* **26**, (2003).
128. Mahnel, H. & Mayr, A. Experiences with immunization against orthopox viruses of humans and animals using vaccine strain MVA. *Berl. Munch. Tierarztl. Wochenschr.* **107**, (1994).
129. European Medicines Agency. EMA recommends approval of Imvanex for the prevention of monkeypox disease. (2022). Available at: <https://www.ema.europa.eu/en/news/ema-recommends-approval-imvanex-prevention-monkeypox-disease>. (Accessed: 1st January 2023)
130. U.S. Food and Drugs. Vaccines Licensed for Use in the United States. (2022). Available at: <https://www.fda.gov/vaccines-blood-biologics/vaccines/vaccines-licensed-use-united-states>.
131. Chopra, H. *et al.* FDA approved vaccines for monkeypox: Current eminence. *Int. J. Surg.* **105**, (2022).
132. Suter, M. *et al.* Modified vaccinia Ankara strains with identical coding sequences actually represent complex mixtures of viruses that determine the biological properties of each strain. *Vaccine* **27**, (2009).
133. Okeke, M. I. *et al.* Hazard characterization of modified vaccinia virus ankara vector: What are the knowledge gaps? *Viruses* **9**, (2017).
134. Orlova, O. V., Glazkova, D. V., Bogoslovskaya, E. V., Shipulin, G. A. & Yudin, S. M. Development of Modified Vaccinia Virus Ankara-Based Vaccines: Advantages and Applications. *Vaccines* **10**, (2022).
135. Joachim, A. *et al.* Potent functional antibody responses elicited by HIV-I DNA priming and boosting with heterologous HIV-1 recombinant MVA in healthy tanzanian adults. *PLoS One* **10**, (2015).
136. Nilsson, C. *et al.* Broad and potent cellular and humoral immune responses after a second late HIV-modified vaccinia virus ankara vaccination in HIV-DNA-primed and HIV-modified vaccinia virus ankara-boosted swedish vaccinees. *AIDS Res. Hum. Retroviruses* **30**, (2014).
137. Milligan, I. D. *et al.* Safety and immunogenicity of novel adenovirus type 26-and modified vaccinia Ankara-vectored Ebola vaccines: A randomized clinical trial. *JAMA - J. Am. Med. Assoc.* **315**, (2016).
138. Tapia, M. D. *et al.* Use of ChAd3-EBO-Z Ebola virus vaccine in Malian and US adults, and boosting of Malian adults with MVA-BN-Filo: a phase 1, single-blind, randomised trial, a phase 1b, open-label and double-blind, dose-escalation trial, and a nested, randomised, double-blind, placebo-controlled trial. *Lancet Infect. Dis.* **16**, (2016).
139. Callendret, B. *et al.* A prophylactic multivalent vaccine against different filovirus species is immunogenic and provides protection from lethal infections with Ebolavirus and Marburgvirus species in non-human primates. *PLoS One* **13**, (2018).
140. Fuentes, S., Ravichandran, S., Coyle, E. M., Klenow, L. & Khurana, S. Human Antibody Repertoire following Ebola Virus Infection and Vaccination. *iScience* **23**, (2020).
141. Jordan, E. *et al.* Broad Antibody and Cellular Immune Response from a Phase 2 Clinical Trial with a Novel Multivalent Poxvirus-Based Respiratory Syncytial Virus Vaccine. *J. Infect. Dis.* **223**, (2021).
142. Koch, T. *et al.* Safety and immunogenicity of a modified vaccinia virus Ankara vector vaccine

- candidate for Middle East respiratory syndrome: an open-label, phase 1 trial. *Lancet Infect. Dis.* **20**, (2020).
143. Aldoss, I. *et al.* Poxvirus vectored cytomegalovirus vaccine to prevent cytomegalovirus viremia in transplant recipients: A phase 2, randomized clinical trial. *Ann. Intern. Med.* **172**, (2020).
 144. Kreijtz, J. H. C. M. *et al.* Safety and immunogenicity of a modified-vaccinia-virus-Ankara-based influenza A H5N1 vaccine: A randomised, double-blind phase 1/2a clinical trial. *Lancet Infect. Dis.* **14**, (2014).
 145. Pukhuriwong, S. *et al.* Modified vaccinia Ankara-vectored vaccine expressing nucleoprotein and matrix protein 1 (M1) activates mucosal M1-specific T-Cell immunity and tissue-resident memory T Cells in human nasopharynx-associated lymphoid tissue. *J. Infect. Dis.* **222**, (2020).
 146. Tameris, M. D. *et al.* Safety and efficacy of MVA85A, a new tuberculosis vaccine, in infants previously vaccinated with BCG: A randomised, placebo-controlled phase 2b trial. *Lancet* **381**, (2013).
 147. Hodgson, S. H. *et al.* Evaluation of the efficacy of ChAd63-MVA vectored vaccines expressing circumsporozoite protein and ME-TRAP against controlled human malaria infection in malaria-naive individuals. in *Journal of Infectious Diseases* **211**, (2015).
 148. Biswas, S. *et al.* Assessment of humoral immune responses to blood-stage malaria antigens following ChAd63-MVA immunization, controlled human malaria infection and natural exposure. *PLoS One* **9**, (2014).
 149. Sebastian, S. & Gilbert, S. C. Recombinant modified vaccinia virus Ankara-based malaria vaccines. *Expert Review of Vaccines* **15**, (2016).
 150. Sah, R. *et al.* Monkeypox deaths in 2022 outbreak across the globe : correspondence. *Ann. Med. Surg.* **85(1)**, 57–58 (2023).
 151. Beer, E. M. & Bhargavi Rao, V. A systematic review of the epidemiology of human monkeypox outbreaks and implications for outbreak strategy. *PLoS Negl. Trop. Dis.* **13**, e0007791 (2019).
 152. Mbala, P. K. *et al.* Maternal and Fetal Outcomes among Pregnant Women with Human Monkeypox Infection in the Democratic Republic of Congo. *J. Infect. Dis.* **216**, (2017).
 153. Alakunle, E. & Okeke, M. Monkeypox virus: a neglected zoonotic pathogen spreads globally. *Nat. Rev. Microbiol.* **20**, 507–508 (2022).
 154. Damon, I. K. Status of human monkeypox: Clinical disease, epidemiology and research. *Vaccine* **29**, (2011).
 155. Kmiec, D. & Kirchhoff, F. Monkeypox: A New Threat? *Int. J. Mol. Sci.* **23**, (2022).
 156. WHO. Disease Outbreak News; Multi-country monkeypox outbreak in non-endemic countries. (2022). Available at: <https://www.who.int/emergencies/disease-outbreak-news/item/2022-DON385>. (Accessed: 20th June 2022)
 157. Happi, C. *et al.* Urgent need for a non-discriminatory and non-stigmatizing nomenclature for monkeypox virus. *PLoS Biol.* **20**, 1–6 (2022).
 158. Bunge, E. M. *et al.* The changing epidemiology of human monkeypox—A potential threat? A

- systematic review. *PLoS Negl. Trop. Dis.* **16**, (2022).
159. Magnus, P. von, Andersen, E. K., Petersen, K. B. & Birch-Andersen, A. A POX-LIKE DISEASE IN CYNOMOLGUS MONKEYS. *Acta Pathol. Microbiol. Scand.* **46**, (1959).
 160. Alakunle, E., Moens, U., Nchinda, G. & Okeke, M. I. Monkeypox Virus in Nigeria: Infection Biology, Epidemiology, and Evolution. *Viruses* **12**, (2020).
 161. Ladnyj, I. D., Ziegler, P. & Kima, E. A human infection caused by monkeypox virus in Basankusu Territory, Democratic Republic of the Congo. *Bull. World Health Organ.* **46**, (1972).
 162. Lourie, B. *et al.* Human infection with monkeypox virus: laboratory investigation of six cases in West Africa. *Bull. World Health Organ.* **46**, (1972).
 163. Yinka-Ogunleye, A. *et al.* Reemergence of human monkeypox in Nigeria, 2017. *Emerging Infectious Diseases* **24**, (2018).
 164. Erez, N. *et al.* Diagnosis of Imported Monkeypox, Israel, 2018. *Emerg. Infect. Dis.* **25**, 980 (2019).
 165. Ng, O. T. *et al.* A case of imported Monkeypox in Singapore. *Lancet. Infect. Dis.* **19**, 1166 (2019).
 166. Rao, A. K. *et al.* Monkeypox in a Traveler Returning from Nigeria — Dallas, Texas, July 2021. *Morb. Mortal. Wkly. Rep.* **71**, 509 (2022).
 167. Vaughan, A. *et al.* Two cases of monkeypox imported to the United Kingdom, September 2018. *Eurosurveillance* **23**, (2018).
 168. CDC. Multistate Outbreak of Monkeypox— Illinois, Indiana, and Wisconsin, 2003. *JAMA* **290**(1), 30–31 (2003).
 169. Petersen, E. *et al.* Human Monkeypox: Epidemiologic and Clinical Characteristics, Diagnosis, and Prevention. *Infectious Disease Clinics of North America* **33**, (2019).
 170. WHO. Disease Outbreak News; Monkeypox– United Kingdom of Great Britain and Northern Ireland. (2022).
 171. WHO. 2022-23 Mpox Outbreak: Global Trends. (2023). Available at: https://worldhealthorg.shinyapps.io/mpx_global/.
 172. Buller, R. M. Mousepox: A Small Animal Model for Biodefense Research. *Appl. Biosaf.* **9**, (2004).
 173. Marchal, J. Infectious ectromelia. A hitherto undescribed virus disease of mice. *J. Pathol. Bacteriol.* **33**, (1930).
 174. Mavian, C., López-Bueno, A., Martín, R., Nitsche, A. & Alcamí, A. Comparative pathogenesis, genomics and phylogeography of mousepox. *Viruses* **13**, 1146 (2021).
 175. Mendez-Rios, J. D. *et al.* Genome sequence of erythromelalgia-related poxvirus identifies it as an ectromelia virus strain. *PLoS One* **7**, (2012).
 176. Zheng, Z. M., Specter, S., Zhang, J. H., Friedman, H. & Zhu, W. P. Further characterization of the biological and pathogenic properties of erythromelalgia-related poxviruses. *J. Gen. Virol.*

- 73, (1992).
177. Neubauer, H., Pfeffer, M. & Meyer, H. Specific detection of mousepox virus by polymerase chain reaction. *Lab. Anim.* **31**, (1997).
 178. Trentin, J. J. & Briody, B. A. *An outbreak of mouse-pox (infectious ectromelia) in the United States: II. Definitive diagnosis.* *Science* **117**, (1953).
 179. Spohr de Faundez, I. *et al.* Electron microscopy, plaque assay and preliminary serological characterization of three ectromelia virus strains isolated in Poland in the period 1986-1988. *Arch. Virol.* **114**, (1990).
 180. Lipman, N. S., Nguyen, H. & Perkins, S. Mousepox: A threat to U.S. mouse colonies. *Laboratory Animal Science* **49**, (1999).
 181. Chapman, J. L., Nichols, D. K., Martinez, M. J. & Raymond, J. W. Animal models of orthopoxvirus infection. *Vet. Pathol.* **47**, (2010).
 182. Esteban, D., Parker, S., Schriewer, J., Hartzler, H. & Buller, R. M. Mousepox, a small animal model of smallpox. *Methods Mol. Biol.* **890**, (2012).
 183. Ichihashi, Y. & Matsumoto, S. Studies on the nature of marchal bodies (A-type inclusion) during ectromelia virus infection. *Virology* **29**, 264–275 (1966).
 184. Springer, Y. P. *et al.* Novel Orthopoxvirus Infection in an Alaska Resident. *Clin. Infect. Dis. An Off. Publ. Infect. Dis. Soc. Am.* **64**, 1737 (2017).
 185. Hyun, J. Poxvirus under the eyes of electron microscope. *Appl. Microsc.* **52**, (2022).
 186. Peters, D. Morphology of resting vaccinia virus. *Nature* **178**, (1956).
 187. Dales, S. The uptake and development of vaccinia virus in strain L cells followed with labeled viral deoxyribonucleic acid. *J. Cell Biol.* **18**, (1963).
 188. Resch, W. & Moss, B. The Conserved Poxvirus L3 Virion Protein Is Required for Transcription of Vaccinia Virus Early Genes. *J. Virol.* **79**, (2005).
 189. Peters, D. & Müller, G. The fine structure of the DNA-containing core of vaccinia virus. *Virology* **21**, (1963).
 190. McFadden, B. D. H., Moussatche, N., Kelley, K., Kang, B. H. & Condit, R. C. Vaccinia virions deficient in transcription enzymes lack a nucleocapsid. *Virology* **434**, (2012).
 191. Condit, R. C., Moussatche, N. & Traktman, P. In A Nutshell: Structure and Assembly of the Vaccinia Virion. *Advances in Virus Research* **65**, (2006).
 192. Moussatche, N. & Condit, R. C. Fine structure of the vaccinia virion determined by controlled degradation and immunolocalization. *Virology* **475**, (2015).
 193. Bidgood, S. R. *et al.* Poxviruses package viral redox proteins in lateral bodies and modulate the host oxidative response. *PLoS Pathog.* **18**, (2022).
 194. Cyrklaff, M. *et al.* Cryo-electron tomography of vaccinia virus. *Proc. Natl. Acad. Sci. U. S. A.* **102**, (2005).
 195. Rodrigues, T. C. S. *et al.* Genome characterization of cetaceanpox virus from a managed Indo-

- Pacific bottlenose dolphin (*Tursiops aduncus*). *Virus Res.* **278**, (2020).
196. Tulman, E. R. *et al.* The Genome of Canarypox Virus. *J. Virol.* **78**, (2004).
197. Nakazawa, Y. *et al.* Phylogenetic and ecologic perspectives of a monkeypox outbreak, Southern Sudan, 2005. *Emerg. Infect. Dis.* **19**, (2013).
198. Hendrickson, R. C., Wang, C., Hatcher, E. L. & Lefkowitz, E. J. Orthopoxvirus Genome Evolution: The Role of Gene Loss. *Viruses* **2**, 1933–1967 (2010).
199. Esposito, J. J. *et al.* Genome sequence diversity and clues to the evolution of variola (smallpox) virus. *Science (80-.)*. **313**, (2006).
200. Lefkowitz, E. J., Wang, C. & Upton, C. Poxviruses: Past, present and future. *Virus Res.* **117**, (2006).
201. Senkevich, T. G., Yutin, N., Wolf, Y. I., Koonin, E. V. & Moss, B. Ancient gene capture and recent gene loss shape the evolution of orthopoxvirus-host interaction genes. *MBio* **12**, (2021).
202. Upton, C., Slack, S., Hunter, A. L., Ehlers, A. & Roper, R. L. Poxvirus Orthologous Clusters: toward Defining the Minimum Essential Poxvirus Genome. *J. Virol.* **77**, (2003).
203. Seet, B. T. *et al.* Poxviruses and immune evasion. *Annual Review of Immunology* **21**, (2003).
204. Shchelkunov, S. N. Orthopoxvirus genes that mediate disease virulence and host tropism. *Advances in Virology* **2012**, (2012).
205. Moss, B. Membrane fusion during poxvirus entry. *Seminars in Cell and Developmental Biology* **60**, (2016).
206. Schmidt, F. I., Bleck, C. K. E., Helenius, A. & Mercer, J. Vaccinia extracellular virions enter cells by macropinocytosis and acid-activated membrane rupture. *EMBO J.* **30**, (2011).
207. Schmidt, F. I. *et al.* Vaccinia virus entry is followed by core activation and proteasome-mediated release of the immunomodulatory effector VH1 from lateral bodies. *Cell Rep.* **4**, (2013).
208. Mallardo, M. *et al.* Relationship between Vaccinia Virus Intracellular Cores, Early mRNAs, and DNA Replication Sites. *J. Virol.* **76**, (2002).
209. Pedersen, K. *et al.* Characterization of Vaccinia Virus Intracellular Cores: Implications for Viral Uncoating and Core Structure. *J. Virol.* **74**, (2000).
210. Carter, G. C. *et al.* Vaccinia virus cores are transported on microtubules. *Journal of General Virology* **84**, (2003).
211. Greseth, M. D. & Traktman, P. The Life Cycle of the Vaccinia Virus Genome. *Annu. Rev. Virol.* **9**, 239–259 (2022).
212. Ahn, B. Y. & Moss, B. RNA polymerase-associated transcription specificity factor encoded by vaccinia virus. *Proc. Natl. Acad. Sci. U. S. A.* **89**, (1992).
213. Yang, Z. *et al.* Expression Profiling of the Intermediate and Late Stages of Poxvirus Replication. *J. Virol.* **85**, (2011).
214. Yang, Z. *et al.* Deciphering Poxvirus Gene Expression by RNA Sequencing and Ribosome

- Profiling. *J. Virol.* **89**, (2015).
215. Baldick, C. J. & Moss, B. Characterization and temporal regulation of mRNAs encoded by vaccinia virus intermediate-stage genes. *J. Virol.* **67**, (1993).
 216. Turner, P. C. & Moyer, R. W. The vaccinia virus fusion inhibitor proteins SPI-3 (K2) and HA (A56) expressed by infected cells reduce the entry of superinfecting virus. *Virology* **380**, (2008).
 217. Wagenaar, T. R. & Moss, B. Expression of the A56 and K2 Proteins Is Sufficient To Inhibit Vaccinia Virus Entry and Cell Fusion. *J. Virol.* **83**, (2009).
 218. Laliberte, J. P. & Moss, B. A Novel Mode of Poxvirus Superinfection Exclusion That Prevents Fusion of the Lipid Bilayers of Viral and Cellular Membranes. *J. Virol.* **88**, (2014).
 219. Tolonen, N., Doglio, L., Schleich, S. & Krijnse Locker, J. Vaccinia virus DNA replication occurs in endoplasmic reticulum-enclosed cytoplasmic mini-nuclei. *Mol. Biol. Cell* **12**, (2001).
 220. Cairns, J. The initiation of vaccinia infection. *Virology* **11**, (1960).
 221. Domi, A. & Beaud, G. The punctate sites of accumulation of vaccinia virus early proteins are precursors of sites of viral DNA synthesis. *J. Gen. Virol.* **81**, (2000).
 222. Rochester, S. C. & Traktman, P. Characterization of the Single-Stranded DNA Binding Protein Encoded by the Vaccinia Virus I3 Gene. *J. Virol.* **72**, (1998).
 223. Czarnecki, M. W. & Traktman, P. The vaccinia virus DNA polymerase and its processivity factor. *Virus Research* **234**, (2017).
 224. Bersch, B., Tarbouriech, N., Burmeister, W. P. & Iseni, F. Solution Structure of the C-terminal Domain of A20, the Missing Brick for the Characterization of the Interface between Vaccinia Virus DNA Polymerase and its Processivity Factor. *J. Mol. Biol.* **433**, (2021).
 225. Banham, A. H. & Smith, G. L. Vaccinia virus gene B1R encodes a 34-kDa serine/threonine protein kinase that localizes in cytoplasmic factories and is packaged into virions. *Virology* **191**, (1992).
 226. Murcia-Nicolas, A., Bolbach, G., Blais, J. C. & Beaud, G. Identification by mass spectroscopy of three major early proteins associated with virosomes in vaccinia virus-infected cells. *Virus Res.* **59**, (1999).
 227. Welsch, S., Doglio, L., Schleich, S. & Krijnse Locker, J. The Vaccinia Virus I3L Gene Product Is Localized to a Complex Endoplasmic Reticulum-Associated Structure That Contains the Viral Parental DNA. *J. Virol.* **77**, (2003).
 228. McDonald, W. F., Crozel-Goudot, V. & Traktman, P. Transient expression of the vaccinia virus DNA polymerase is an intrinsic feature of the early phase of infection and is unlinked to DNA replication and late gene expression. *J. Virol.* **66**, (1992).
 229. Boyle, K. A., Arps, L. & Traktman, P. Biochemical and Genetic Analysis of the Vaccinia Virus D5 Protein: Multimerization-Dependent ATPase Activity Is Required To Support Viral DNA Replication. *J. Virol.* **81**, (2007).
 230. Evans, E., Klemperer, N., Ghosh, R. & Traktman, P. The vaccinia virus D5 protein, which is required for DNA replication, is a nucleic acid-independent nucleoside triphosphatase. *J. Virol.* **69**, (1995).

231. McDonald, W. F., Klemperer, N. & Traktman, P. Characterization of a processive form of the vaccinia virus DNA polymerase. *Virology* **234**, (1997).
232. Sèle, C. *et al.* Low-Resolution Structure of Vaccinia Virus DNA Replication Machinery. *J. Virol.* **87**, (2013).
233. Katsafanas, G. C. & Moss, B. Linkage of Transcription and Translation within Cytoplasmic Poxvirus DNA Factories Provides a Mechanism to Coordinate Viral and Usurp Host Functions. *Cell Host Microbe* **2**, (2007).
234. Vos, J. C. & Stunnenberg, H. G. Derepression of a novel class of vaccinia virus genes upon DNA replication. *EMBO J.* **7**, (1988).
235. Keck, J. G., Baldick, C. J. & Moss, B. Role of DNA replication in vaccinia virus gene expression: A naked template is required for transcription of three late trans-activator genes. *Cell* **61**, (1990).
236. Gershon, P. D. & Moss, B. Early transcription factor subunits are encoded by vaccinia virus late genes. *Proc. Natl. Acad. Sci. U. S. A.* **87**, (1990).
237. Yeh, W. W., Moss, B. & Wolffe, E. J. The Vaccinia Virus A9L Gene Encodes a Membrane Protein Required for an Early Step in Virion Morphogenesis. *J. Virol.* **74**, (2000).
238. Roberts, K. L. & Smith, G. L. Vaccinia virus morphogenesis and dissemination. *Trends in Microbiology* **16**, (2008).
239. Smith, G. L., Vanderplassen, A. & Law, M. The formation and function of extracellular enveloped vaccinia virus. *Journal of General Virology* **83**, (2002).
240. Schmelz, M. *et al.* Assembly of vaccinia virus: the second wrapping cisterna is derived from the trans Golgi network. *J. Virol.* **68**, (1994).
241. Tooze, J., Hollinshead, M., Reis, B., Radsak, K. & Kern, H. Progeny vaccinia and human cytomegalovirus particles utilize early endosomal cisternae for their envelopes. *Eur. J. Cell Biol.* **60**, (1993).
242. Weisberg, A. S. *et al.* Enigmatic origin of the poxvirus membrane from the endoplasmic reticulum shown by 3D imaging of vaccinia virus assembly mutants. *Proc. Natl. Acad. Sci. U. S. A.* **114**, (2017).
243. Liu, L., Cooper, T., Howley, P. M. & Hayball, J. D. From crescent to mature virion: Vaccinia virus assembly and maturation. *Viruses* **6**, (2014).
244. Shida, H., Tanabe, K. & Matsumoto, S. Mechanism of virus occlusion into A-type inclusion during poxvirus infection. *Virology* **76**, (1977).
245. Okeke, M. I. *et al.* Comparative sequence analysis of A-type inclusion (ATI) and P4c proteins of orthopoxviruses that produce typical and atypical ATI phenotypes. *Virus Genes* **39**, (2009).
246. Patel, D. D. & Pickup, D. J. Messenger RNAs of a strongly-expressed late gene of cowpox virus contain 5'-terminal poly(A) sequences. *EMBO J.* **6**, 3787 (1987).
247. McKelvey, T. A., Andrews, S. C., Miller, S. E., Ray, C. A. & Pickup, D. J. Identification of the Orthopoxvirus p4c Gene, Which Encodes a Structural Protein That Directs Intracellular Mature Virus Particles into A-Type Inclusions. *J. Virol.* **76**, 11216 (2002).

248. Howard, A. R., Weisberg, A. S. & Moss, B. Congregation of Orthopoxvirus Virions in Cytoplasmic A-Type Inclusions Is Mediated by Interactions of a Bridging Protein (A26p) with a Matrix Protein (ATI_p) and a Virion Membrane-Associated Protein (A27p). *J. Virol.* **84**, 7592 (2010).
249. Firth, C. *et al.* Using Time-Structured Data to Estimate Evolutionary Rates of Double-Stranded DNA Viruses. *Mol. Biol. Evol.* **27**, 2038–2051 (2010).
250. de Haven, B. C., Gupta, K. & Isaacs, S. N. The vaccinia virus A56 protein: A multifunctional transmembrane glycoprotein that anchors two secreted viral proteins. *Journal of General Virology* **92**, (2011).
251. Zhou, J., Sun, X. Y., Fernando, G. J. P. & Frazer, I. H. The vaccinia virus K2L gene encodes a serine protease inhibitor which inhibits cell-cell fusion. *Virology* **189**, (1992).
252. Law, K. M. & Smith, G. L. A vaccinia serine protease inhibitor which prevents virus-induced cell fusion. *J. Gen. Virol.* **73**, (1992).
253. Turner, P. C. & Moyer, R. W. An orthopoxvirus serpinlike gene controls the ability of infected cells to fuse. *J. Virol.* **66**, (1992).
254. Carpentier, D. C. J., Van Loggelenberg, A., Dieckmann, N. M. G. & Smith, G. L. Vaccinia virus egress mediated by virus protein A36 is reliant on the F12 protein. *J. Gen. Virol.* **98**, (2017).
255. Dodding, M. P., Newsome, T. P., Collinson, L. M., Edwards, C. & Way, M. An E2-F12 complex is required for intracellular enveloped virus morphogenesis during vaccinia infection. *Cell. Microbiol.* **11**, (2009).
256. Moss, B. Poxvirus DNA replication. *Cold Spring Harb. Perspect. Biol.* **5**, (2013).
257. Van Eijl, H., Hollinshead, M. & Smith, G. L. The vaccinia virus A36R protein is a type Ib membrane protein present on intracellular but not extracellular enveloped virus particles. *Virology* **271**, (2000).
258. Blasco, R. & Moss, B. Role of cell-associated enveloped vaccinia virus in cell-to-cell spread. *J. Virol.* **66**, (1992).
259. Roper, R. L., Wolffe, E. J., Weisberg, A. & Moss, B. The Envelope Protein Encoded by the A33R Gene Is Required for Formation of Actin-Containing Microvilli and Efficient Cell-to-Cell Spread of Vaccinia Virus. *J. Virol.* **72**, (1998).
260. Wolffe, E. J., Isaacs, S. N. & Moss, B. Deletion of the vaccinia virus B5R gene encoding a 42-kilodalton membrane glycoprotein inhibits extracellular virus envelope formation and dissemination. *J. Virol.* **67**, (1993).
261. Wolffe, E. J., Katz, E., Weisberg, A. & Moss, B. The A34R glycoprotein gene is required for induction of specialized actin-containing microvilli and efficient cell-to-cell transmission of vaccinia virus. *J. Virol.* **71**, (1997).
262. Katz, E., Wolffe, E. & Moss, B. Identification of Second-Site Mutations That Enhance Release and Spread of Vaccinia Virus. *J. Virol.* **76**, (2002).
263. Blasco, R., Sisler, J. R. & Moss, B. Dissociation of progeny vaccinia virus from the cell membrane is regulated by a viral envelope glycoprotein: effect of a point mutation in the lectin homology domain of the A34R gene. *J. Virol.* **67**, (1993).

264. Doceul, V., Hollinshead, M., Van Der Linden, L. & Smith, G. L. Repulsion of superinfecting virions: A mechanism for rapid virus spread. *Science* (80-.). **327**, (2010).
265. McFadden, G., Mohamed, M. R., Rahman, M. M. & Bartee, E. Cytokine determinants of viral tropism. *Nature Reviews Immunology* **9**, (2009).
266. McFadden, G., Pace, W. E., Purres, J. & Dales, S. Biogenesis of poxviruses: Transitory expression of *Molluscum contagiosum* early functions. *Virology* **94**, (1979).
267. Li, Y., Yuan, S. & Moyer, R. W. The non-permissive infection of insect (Gypsy Moth) LD-652 cells by vaccinia virus. *Virology* **248**, (1998).
268. Zhao, Y. *et al.* Non-replicating Vaccinia Virus TianTan Strain (NTV) Translation Arrest of Viral Late Protein Synthesis Associated With Anti-viral Host Factor SAMD9. *Front. Cell. Infect. Microbiol.* **10**, (2020).
269. Bengali, Z. *et al.* *Drosophila* S2 cells are non-permissive for vaccinia virus DNA replication following entry via low pH-dependent endocytosis and early transcription. *PLoS One* **6**, (2011).
270. Johnston, J. B. *et al.* Role of the Serine-Threonine Kinase PAK-1 in Myxoma Virus Replication. *J. Virol.* **77**, (2003).
271. Werden, S. J., Rahman, M. M. & McFadden, G. Chapter 3 Poxvirus Host Range Genes. *Advances in Virus Research* **71**, (2008).
272. Haller, S. L., Peng, C., McFadden, G. & Rothenburg, S. Poxviruses and the evolution of host range and virulence. *Infection, Genetics and Evolution* **21**, (2014).
273. Ramsey-Ewing, A. L. & Moss, B. Complementation of a vaccinia virus host-range K1L gene deletion by the nonhomologous CP77 gene. *Virology* **222**, (1996).
274. Spohner, D., Gillard, S., Drillien, R. & Kirn, A. A cowpox virus gene required for multiplication in Chinese hamster ovary cells. *J. Virol.* **62**, (1988).
275. Drillien, R., Koehren, F. & Kirn, A. Host range deletion mutant of vaccinia virus defective in human cells. *Virology* **111**, (1981).
276. Gillard, S., Spohner, D., Drillien, R. & Kirn, A. Localization and sequence of a vaccinia virus gene required for multiplication in human cells. *Proc. Natl. Acad. Sci. U. S. A.* **83**, (1986).
277. Perkus, M. E. *et al.* Vaccinia virus host range genes. *Virology* **179**, 276–286 (1990).
278. Meng, X., Chao, J. & Xiang, Y. Identification from diverse mammalian poxviruses of host-range regulatory genes functioning equivalently to vaccinia virus C7L. *Virology* **372**, (2008).
279. Beattie, E. *et al.* Host-range restriction of vaccinia virus E3L-specific deletion mutants. *Virus Genes* **12**, (1996).
280. Chang, H. W., Uribe, L. H. & Jacobs, B. L. Rescue of vaccinia virus lacking the E3L gene by mutants of E3L. *J. Virol.* **69**, (1995).
281. Langland, J. O. & Jacobs, B. L. The role of the PKR-inhibitory genes, E3L and K3L, in determining vaccinia virus host range. *Virology* **299**, (2002).
282. Shisler, J. L., Isaacs, S. N. & Moss, B. Vaccinia virus serpin-1 deletion mutant exhibits a host

- range defect characterized by low levels of intermediate and late mRNAs. *Virology* **262**, (1999).
283. Ali, A. N., Brooks, M. A. & Moyer, R. W. The SPI-1 gene of rabbitpox virus determines host range and is required for hemorrhagic pox formation. *Virology* **202**, (1994).
 284. Drexler, I., Heller, K., Wahren, B., Erfle, V. & Sutter, G. Highly attenuated modified vaccinia virus Ankara replicates in baby hamster kidney cells, a potential host for virus propagation, but not in various human transformed and primary cells. *J. Gen. Virol.* **79**, (1998).
 285. Meisinger-Henschel, C. *et al.* Introduction of the Six Major Genomic Deletions of Modified Vaccinia Virus Ankara (MVA) into the Parental Vaccinia Virus Is Not Sufficient To Reproduce an MVA-Like Phenotype in Cell Culture and in Mice. *J. Virol.* **84**, (2010).
 286. Sutter, G. & Moss, B. Nonreplicating vaccinia vector efficiently expresses recombinant genes. *Proc. Natl. Acad. Sci. U. S. A.* **89**, (1992).
 287. Okeke, M. I., Nilssen, Ø. & Traavik, T. Modified vaccinia virus Ankara multiplies in the rat IEC-6 cells and limited production of mature virions occurs in other mammalian cell lines. *J. Gen. Virol.* **87**, (2006).
 288. Jordan, I., Horn, D., Oehmke, S., Leendertz, F. H. & Sandig, V. Cell lines from the Egyptian fruit bat are permissive for modified vaccinia Ankara. *Virus Res.* **145**, (2009).
 289. Meiser, A., Sancho, C. & Krijnse Locker, J. Plasma Membrane Budding as an Alternative Release Mechanism of the Extracellular Enveloped Form of Vaccinia Virus from HeLa Cells. *J. Virol.* **77**, (2003).
 290. Hughes, A. L., Irausquin, S. & Friedman, R. The evolutionary biology of poxviruses. *Infect. Genet. Evol.* **10**, 50–59 (2010).
 291. Brennan, G. *et al.* Molecular Mechanisms of Poxvirus Evolution. *MBio* **14**, (2023).
 292. Babkin, I. V. & Babkina, I. N. A retrospective study of the orthopoxvirus molecular evolution. *Infect. Genet. Evol.* **12**, 1597–1604 (2012).
 293. Zehender, G. *et al.* Bayesian reconstruction of the evolutionary history and cross-species transition of variola virus and orthopoxviruses. *J. Med. Virol.* **90**, 1134–1141 (2018).
 294. Babkin, I. V. & Babkina, I. N. Molecular Dating in the Evolution of Vertebrate Poxviruses. *Intervirology* **54**, 253–260 (2011).
 295. Babkin, I. V. & Shchelkunov, S. N. Molecular evolution of poxviruses. *Russ. J. Genet.* **2008** *44*, 895–908 (2008).
 296. Isidro, J. *et al.* Phylogenomic characterization and signs of microevolution in the 2022 multi-country outbreak of monkeypox virus. *Nat. Med.* **28**, 1569–1572 (2022).
 297. Elde, N. C. *et al.* Poxviruses deploy genomic accordions to adapt rapidly against host antiviral defenses. *Cell* **150**, (2012).
 298. Grossegeisse, M., Doellinger, J., Tyshaieva, A., Schaade, L. & Nitsche, A. Combined proteomics/genomics approach reveals proteomic changes of mature virions as a novel poxvirus adaptation mechanism. *Viruses* **9**, (2017).
 299. Brennan, G., Kitzman, J. O., Rothenburg, S., Shendure, J. & Geballe, A. P. Adaptive Gene

- Amplification As an Intermediate Step in the Expansion of Virus Host Range. *PLoS Pathog.* **10**, (2014).
300. Coulson, D. & Upton, C. Characterization of indels in poxvirus genomes. *Virus Genes* **42**, 171–177 (2011).
 301. Smithson, C., Purdy, A., Verster, A. J. & Upton, C. Prediction of Steps in the Evolution of Variola Virus Host Range. *PLoS One* **9**, e91520 (2014).
 302. Doty, J. B. *et al.* Isolation and Characterization of Akhmeta Virus from Wild-Caught Rodents (*Apodemus* spp.) in Georgia . *J. Virol.* **93**, (2019).
 303. Qin, L., Favis, N., Famulski, J. & Evans, D. H. Evolution of and Evolutionary Relationships between Extant Vaccinia Virus Strains. *J. Virol.* **89**, 1809 (2015).
 304. Qin, L., Upton, C., Hazes, B. & Evans, D. H. Genomic Analysis of the Vaccinia Virus Strain Variants Found in Dryvax Vaccine. *J. Virol.* **85**, 13049 (2011).
 305. Smithson, C. *et al.* Two novel poxviruses with unusual genome rearrangements: NY_014 and Murmansk. *Virus Genes* **53**, 883–897 (2017).
 306. Qin, L. & Evans, D. H. Genome Scale Patterns of Recombination between Coinfecting Vaccinia Viruses. *J. Virol.* **88**, 5277–5286 (2014).
 307. Babkin, I. V., Babkina, I. N. & Tikunova, N. V. An Update of Orthopoxvirus Molecular Evolution. *Viruses* 2022, Vol. 14, Page 388 **14**, 388 (2022).
 308. Hoffmann, D. *et al.* Out of the Reservoir: Phenotypic and Genotypic Characterization of a Novel Cowpox Virus Isolated from a Common Vole. *J. Virol.* **89**, (2015).
 309. Gruber, C. E. M. *et al.* Whole genome characterization of orthopoxvirus (Opv) abatino, a zoonotic virus representing a putative novel clade of old world orthopoxviruses. *Viruses* **10**, 1. – 12 of 12 (2018).
 310. Guan, H. *et al.* Emergence, phylogeography, and adaptive evolution of mpox virus. *New Microbes New Infect.* **52**, 101102 (2023).
 311. Forni, D., Molteni, C., Cagliani, R., Clerici, M. & Sironi, M. Analysis of variola virus molecular evolution suggests an old origin of the virus consistent with historical records. *Microb. Genomics* **9**, 1–7 (2023).
 312. European Parliament and Council. Directive 2001/18/EC of the European Parliament and of the Council of 12 March on the deliberate release into the environment of genetically modified organisms and repealing Council Directive 90/220/EEC. 1–39 (2001).
 313. Wyatt, L. S. *et al.* Marker rescue of the host range restriction defects of modified vaccinia virus Ankara. *Virology* **251**, (1998).
 314. Liu, R. *et al.* SPI-1 is a missing host-range factor required for replication of the attenuated modified vaccinia ankara (MVA) vaccine vector in human cells. *PLoS Pathog.* **15**, (2019).
 315. Zwilling, J., Sliva, K., Schwantes, A., Schnierle, B. & Sutter, G. Functional F11L and K1L genes in modified vaccinia virus Ankara restore virus-induced cell motility but not growth in human and murine cells. *Virology* **404**, (2010).
 316. Peng, C. & Moss, B. Repair of a previously uncharacterized second host-range gene

- contributes to full replication of modified vaccinia virus Ankara (MVA) in human cells. *Proc. Natl. Acad. Sci. U. S. A.* **117**, (2020).
317. Sutter, G. A vital gene for modified vaccinia virus Ankara replication in human cells. *Proceedings of the National Academy of Sciences of the United States of America* **117**, (2020).
 318. Erez, N., Wyatt, L. S., Americo, J. L., Xiao, W. & Moss, B. Spontaneous and Targeted Mutations in the Decapping Enzyme Enhance Replication of Modified Vaccinia Virus Ankara (MVA) in Monkey Cells. *J. Virol.* **95**, (2021).
 319. Reynolds, M. G., Guagliardo, S. A. J., Nakazawa, Y. J., Doty, J. B. & Mauldin, M. R. Understanding orthopoxvirus host range and evolution: from the enigmatic to the usual suspects. *Curr. Opin. Virol.* **28**, 108–115 (2018).
 320. Brochier, B. M. *et al.* Use of recombinant vaccinia-rabies virus for oral vaccination of fox cubs (*Vulpes vulpes*, L) against rabies. *Vet. Microbiol.* **18**, (1988).
 321. Freuling, C. M. *et al.* The elimination of fox rabies from Europe: Determinants of success and lessons for the future. *Philos. Trans. R. Soc. B Biol. Sci.* **368**, (2013).
 322. Verheust, C., Goossens, M., Pauwels, K. & Breyer, D. Biosafety aspects of modified vaccinia virus Ankara (MVA)-based vectors used for gene therapy or vaccination. *Vaccine* **30**, (2012).
 323. Goossens, M., Pauwels, K., Willemarck, N. & Breyer, D. Environmental Risk Assessment of Clinical Trials Involving Modified Vaccinia Virus Ankara (MVA)-Based Vectors. *Curr. Gene Ther.* **13**, (2014).
 324. Nitsche, A., Kurth, A. & Pauli, G. Viremia in human Cowpox virus infection. *J. Clin. Virol.* **40**, (2007).
 325. Willer, D. O., Yao, X. D., Mann, M. J. & Evans, D. H. In vitro concatemer formation catalyzed by vaccinia virus DNA polymerase. *Virology* **278**, (2000).
 326. Hansen, H., Okeke, M. I., Nilssen, Ø. & Traavik, T. Recombinant viruses obtained from co-infection in vitro with a live vaccinia-vectored influenza vaccine and a naturally occurring cowpox virus display different plaque phenotypes and loss of the transgene. *Vaccine* **23**, 499–506 (2004).
 327. Okeke, M. I., Nilssen, I., Moens, U., Tryland, M. & Traavik, T. In vitro host range, multiplication and virion forms of recombinant viruses obtained from co-infection in vitro with a vaccinia-vectored influenza vaccine and a naturally occurring cowpox virus isolate. *Virol. J.* **6**, (2009).
 328. Sprygin, A. *et al.* Analysis and insights into recombination signals in lumpy skin disease virus recovered in the field. *PLoS One* **13**, (2018).
 329. Sprygin, A. *et al.* Evidence of recombination of vaccine strains of lumpy skin disease virus with field strains, causing disease. *PLoS One* **15**, (2020).
 330. Shumilova, I. *et al.* Overwintering of recombinant lumpy skin disease virus in northern latitudes, Russia. *Transbound. Emerg. Dis.* **69**, (2022).
 331. Vandenbussche, F. *et al.* Recombinant LSDV Strains in Asia: Vaccine Spillover or Natural Emergence? *Viruses* **14**, (2022).
 332. Mayr, A., Hochstein-Mintzel, V. & Stickl, H. Abstammung, Eigenschaften und Verwendung

- des attenuierten Vaccinia-Stammes MVA. *Infection* **3**, (1975).
333. Cottingham, M. G. & Carroll, M. W. Recombinant MVA vaccines: Dispelling the myths. *Vaccine* **31**, (2013).
334. Jordan, I., Horn, D., John, K. & Sandig, V. A genotype of modified vaccinia Ankara (MVA) that facilitates replication in suspension cultures in chemically defined medium. *Viruses* **5**, (2013).
335. Burgers, W. A. *et al.* Construction, characterization, and immunogenicity of a multigene modified vaccinia Ankara (MVA) vaccine based on HIV Type 1 subtype C. *AIDS Res. Hum. Retroviruses* **24**, (2008).
336. Wyatt, L. S., Belyakov, I. M., Earl, P. L., Berzofsky, J. A. & Moss, B. Enhanced cell surface expression, immunogenicity and genetic stability resulting from a spontaneous truncation of HIV Env expressed by a recombinant MVA. *Virology* **372**, (2008).
337. Wang, Z. *et al.* Modified H5 promoter improves stability of insert genes while maintaining immunogenicity during extended passage of genetically engineered MVA vaccines. *Vaccine* **28**, (2010).
338. Wyatt, L. S. *et al.* Elucidating and Minimizing the Loss by Recombinant Vaccinia Virus of Human Immunodeficiency Virus Gene Expression Resulting from Spontaneous Mutations and Positive Selection. *J. Virol.* **83**, (2009).
339. Stoler, N. & Nekrutenko, A. Sequencing error profiles of Illumina sequencing instruments. *NAR Genomics Bioinforma.* **3**, (2021).
340. Heather, J. M. & Chain, B. The sequence of sequencers: The history of sequencing DNA. *Genomics* **107**, (2016).
341. Van Dijk, E. L., Jaszczyszyn, Y., Naquin, D. & Thermes, C. The Third Revolution in Sequencing Technology. *Trends Genet.* **34**, (2018).
342. Cui, J. *et al.* Analysis and comprehensive comparison of PacBio and nanopore-based RNA sequencing of the Arabidopsis transcriptome. *Plant Methods* **16**, (2020).
343. Bolger, A. M., Lohse, M. & Usadel, B. Trimmomatic: a flexible trimmer for Illumina sequence data. *Bioinformatics* **30**, 2114–2020 (2014).
344. Del Fabbro, C., Scalabrin, S., Morgante, M. & Giorgi, F. M. An extensive evaluation of read trimming effects on illumina NGS data analysis. *PLoS One* **8**, (2013).
345. Wingett, S. W. & Andrews, S. FastQ Screen: A tool for multi-genome mapping and quality control. *F1000Research* **7**, 1338 (2018).
346. Li, H. & Durbin, R. Fast and accurate short read alignment with Burrows–Wheeler transform. *Bioinformatics* **25**, 1754–1760 (2009).
347. Li, H. & Durbin, R. Fast and accurate long-read alignment with Burrows-Wheeler transform. *Bioinformatics* **26**, (2010).
348. Antipov, D., Korobeynikov, A., McLean, J. S. & Pevzner, P. A. HybridSPAdes: An algorithm for hybrid assembly of short and long reads. *Bioinformatics* **32**, (2016).
349. Koren, S. *et al.* Hybrid error correction and de novo assembly of single-molecule sequencing

- reads. *Nat. Biotechnol.* **30**, (2012).
350. Wick, R. R., Judd, L. M., Gorrie, C. L. & Holt, K. E. Unicycler: Resolving bacterial genome assemblies from short and long sequencing reads. *PLoS Comput. Biol.* **13**, (2017).
 351. Zimin, A. V. *et al.* The MaSuRCA genome assembler. *Bioinformatics* **29**, (2013).
 352. Haghshenas, E., Asghari, H., Stoye, J., Chauve, C. & Hach, F. HASLR: Fast Hybrid Assembly of Long Reads. *iScience* **23**, (2020).
 353. Tcherepanov, V., Ehlers, A. & Upton, C. Genome Annotation Transfer Utility (GATU): rapid annotation of viral genomes using a closely related reference genome. *BMC Genomics* **7**, 150 (2006).
 354. Camacho, C. *et al.* BLAST+: architecture and applications. *BMC Bioinformatics* **10**, 421 (2009).
 355. Martin, D. P., Murrell, B., Golden, M., Khoosal, A. & Muhire, B. RDP4: Detection and analysis of recombination patterns in virus genomes. *Virus Evolution* **1**, (2015).
 356. Lole, K. S. *et al.* Full-Length Human Immunodeficiency Virus Type 1 Genomes from Subtype C-Infected Seroconverters in India, with Evidence of Intersubtype Recombination. *Journal of Virology* **73**, 160 (1999).
 357. Mühlemann, B. *et al.* Diverse variola virus (smallpox) strains were widespread in northern Europe in the Viking Age. *Science (80-.)*. **369**, (2020).
 358. Gyuranecz, M. *et al.* Worldwide Phylogenetic Relationship of Avian Poxviruses. *J. Virol.* **87**, (2013).
 359. Pais, F. S. M., Ruy, P. de C., Oliveira, G. & Coimbra, R. S. Assessing the efficiency of multiple sequence alignment programs. *Algorithms Mol. Biol.* **9**, (2014).
 360. Martin, D. & Rybicki, E. RDP: detection of recombination amongst aligned sequences. *Bioinformatics* **16**, 562–563 (2000).
 361. Salminen, M. O., Carr, J. K., Burke, D. S. & Mccutchan, F. E. Identification of Breakpoints in Intergenotypic Recombinants of HIV Type 1 by Bootscanning. *AIDS Res. Hum. Retroviruses* **11**, (1995).
 362. Smith, J. M. Analyzing the mosaic structure of genes. *Journal of Molecular Evolution* 1992 **34:2** **34**, 126–129 (1992).
 363. Posada, D. & Crandall, K. A. Evaluation of methods for detecting recombination from DNA sequences: Computer simulations. *Proceedings of the National Academy of Sciences* **98**, 13757–13762 (2001).
 364. Boni, M. F., Posada, D. & Feldman, M. W. An Exact Nonparametric Method for Inferring Mosaic Structure in Sequence Triplets. *Genetics* **176**, 1035–1047 (2007).
 365. Padidam, M., Sawyer, S. & Fauquet, C. M. Possible Emergence of New Geminiviruses by Frequent Recombination. *Virology* **265**, 218–225 (1999).
 366. Holmes, E. C., Worobey, M. & Rambaut, A. Phylogenetic evidence for recombination in dengue virus. *Mol. Biol. Evol.* **16**, (1999).

367. Gibbs, M. J., Armstrong, J. S. & Gibbs, A. J. Sister-Scanning: a Monte Carlo procedure for assessing signals in recombinant sequences. *Bioinformatics* **16**, 573–582 (2000).
368. Ehlers, A., Osborne, J., Slack, S., Roper, R. L. & Upton, C. Poxvirus Orthologous Clusters (POCs). *Bioinformatics* **18**, 1544–1545 (2002).
369. McLeod, K. & Upton, C. Virus Databases. in *Reference Module in Biomedical Sciences* (2017). doi:10.1016/b978-0-12-801238-3.95728-3
370. Katoh, K. & Standley, D. M. MAFFT Multiple Sequence Alignment Software Version 7: Improvements in Performance and Usability. *Molecular Biology and Evolution* **30**, 772–780 (2013).
371. Talavera, G. & Castresana, J. Improvement of Phylogenies after Removing Divergent and Ambiguously Aligned Blocks from Protein Sequence Alignments. *Systematic Biology* **56**, 564–577 (2007).
372. Emms, D. M. & Kelly, S. OrthoFinder: solving fundamental biases in whole genome comparisons dramatically improves orthogroup inference accuracy. *Genome Biology* **16**, (2015).
373. Ogden, T. H. & Rosenberg, M. S. Multiple sequence alignment accuracy and phylogenetic inference. *Syst. Biol.* **55**, (2006).
374. Hall, B. G. Comparison of the accuracies of several phylogenetic methods using protein and DNA sequences. *Mol. Biol. Evol.* **22**, (2005).
375. Holder, M. & Lewis, P. O. Phylogeny estimation: Traditional and Bayesian approaches. *Nature Reviews Genetics* **4**, (2003).
376. Darriba, Di. *et al.* ModelTest-NG: A New and Scalable Tool for the Selection of DNA and Protein Evolutionary Models. *Molecular Biology and Evolution* **37**, 294 (2020).
377. Stamatakis, A., Hoover, P. & Rougemont, J. A Rapid Bootstrap Algorithm for the RAxML Web Servers. *Syst. Biol.* **57**, 758–771 (2008).
378. Ronquist, F. *et al.* MrBayes 3.2: Efficient Bayesian Phylogenetic Inference and Model Choice Across a Large Model Space. *Systematic Biology* **61**, 539–542 (2012).
379. Smithson, C., Kampman, S., Hetman, B. M. & Upton, C. Incongruencies in vaccinia virus phylogenetic trees. *Computation* **2**, (2014).
380. Rousseau, C. M. *et al.* Extensive Intrasubtype Recombination in South African Human Immunodeficiency Virus Type 1 Subtype C Infections. *J. Virol.* **81**, (2007).
381. Minh, B. Q. *et al.* IQ-TREE 2: New Models and Efficient Methods for Phylogenetic Inference in the Genomic Era. *Mol. Biol. Evol.* **37**, 1530–1534 (2020).
382. Mavian, C., Marini, S., Prospero, M. & Salemi, M. A snapshot of SARS-CoV-2 genome availability up to April 2020 and its implications: Data analysis. *JMIR Public Heal. Surveill.* **6**, (2020).
383. Fourment, M. & Gibbs, M. J. PATRISTIC: a program for calculating patristic distances and graphically comparing the components of genetic change. *BMC Evolutionary Biology* **6**, 1 (2006).

384. Drummond, A. J. & Rambaut, A. BEAST: Bayesian evolutionary analysis by sampling trees. *BMC Evol. Biol.* **7**, (2007).
385. Sagulenko, P., Puller, V. & Neher, R. A. TreeTime: Maximum-likelihood phylodynamic analysis. *Virus Evol.* **4**, (2018).
386. To, T. H., Jung, M., Lycett, S. & Gascuel, O. Fast Dating Using Least-Squares Criteria and Algorithms. *Syst. Biol.* **65**, (2016).
387. Suchard, M. A. *et al.* Bayesian phylogenetic and phylodynamic data integration using BEAST 1.10. *Virus Evol.* **4**, (2018).
388. Rambaut, A., Lam, T. T., Carvalho, L. M. & Pybus, O. G. Exploring the temporal structure of heterochronous sequences using TempEst (formerly Path-O-Gen). *Virus Evol.* **2**, (2016).
389. Demaria, P. J. *et al.* Phase 1 open-label trial of intravenous administration of MVA-BN-brachyury-TRICOM vaccine in patients with advanced cancer. *J. Immunother. Cancer* **9**, (2021).
390. Kaysser, P., von Bomhard, W., Dobrzykowski, L. & Meyer, H. Genetic diversity of feline cowpox virus, Germany 2000-2008. *Vet. Microbiol.* **141**, (2010).
391. Mavian, C. *et al.* The genome sequence of ectromelia virus Naval and Cornell isolates from outbreaks in North America. *Virology* **462–463**, 218–226 (2014).
392. Gershon, P. D., Kitching, R. P., Hammond, J. M. & Black, D. N. Poxvirus genetic recombination during natural virus transmission. *J. Gen. Virol.* **70**, (1989).
393. Lin, Y.-C. J. & Evans, D. H. Vaccinia Virus Particles Mix Inefficiently, and in a Way That Would Restrict Viral Recombination, in Coinfected Cells. *J. Virol.* **84**, 2432–2443 (2010).
394. Chernos, V. I., Antonova, T. P. & Senkevich, T. G. Recombinants between vaccinia and ectromelia viruses bearing the specific pathogenicity markers on both parents. *J. Gen. Virol.* **66**, (1985).
395. Ball, L. A. High-frequency homologous recombination in vaccinia virus DNA. *J. Virol.* **61**, (1987).
396. Fathi, Z., Dyster, L. M., Seto, J., Condit, R. C. & Niles, E. G. Intragenic and intergenic recombination between temperature-sensitive mutants of vaccinia virus. *J. Gen. Virol.* **72**, (1991).
397. Christen, L., Seto, J. & Niles, E. G. Superinfection exclusion of vaccinia virus in virus-infected cell cultures. *Virology* **174**, (1990).
398. Dobson, B. M. *et al.* Vaccinia virus F5 is required for normal plaque morphology in multiple cell lines but not replication in culture or virulence in mice. *Virology* **456–457**, (2014).
399. Dobson, B. M. & Tschärke, D. C. Truncation of gene F5L partially masks rescue of vaccinia virus strain MVA growth on mammalian cells by restricting plaque size. *J. Gen. Virol.* **95**, (2014).
400. Morales, I. *et al.* The vaccinia virus F11L gene product facilitates cell detachment and promotes migration. *Traffic* **9**, (2008).
401. Zhang, W.-H., Wilcock, D. & Smith, G. L. Vaccinia Virus F12L Protein Is Required for Actin

Tail Formation, Normal Plaque Size, and Virulence. *J. Virol.* **74**, (2000).

402. Atukorale, V. N., Weir, J. P. & Meseda, C. A. Stability of the hsv-2 us-6 gene in the del ii, del iii, cp77, and i8r-g11 sites in modified vaccinia virus ankara after serial passage of recombinant vectors in cells. *Vaccines* **8**, (2020).

Paper I



Genomic Sequencing and Analysis of a Novel Human Cowpox Virus With Mosaic Sequences From North America and Old World Orthopoxvirus

Diana Díaz-Cánova¹, Ugo L. Moens^{1*}, Annika Brinkmann², Andreas Nitsche² and Malachy Ifeanyi Okeke^{3*}

¹ Molecular Inflammation Research Group, Department of Medical Biology, UiT - The Arctic University of Norway, Tromsø, Norway, ² Highly Pathogenic Viruses, Centre for Biological Threats and Special Pathogens, WHO Reference Laboratory for SARS-CoV-2 and WHO Collaborating Centre for Emerging Infections and Biological Threats, Robert Koch Institute, Berlin, Germany, ³ Section of Biomedical Sciences, Department of Natural and Environmental Sciences, School of Arts and Sciences, American University of Nigeria, Yola, Nigeria

OPEN ACCESS

Edited by:

Vladimir N. Uversky,
University of South Florida,
United States

Reviewed by:

David Hugh Evans,
University of Alberta, Canada
Sergei Shchelkunov,
State Research Center of Virology
and Biotechnology VECTOR (ISTC),
Russia

*Correspondence:

Ugo L. Moens
ugo.moens@uit.no
Malachy Ifeanyi Okeke
malachy.okeke@aun.edu.ng

Specialty section:

This article was submitted to
Virology,
a section of the journal
Frontiers in Microbiology

Received: 03 February 2022

Accepted: 24 February 2022

Published: 03 May 2022

Citation:

Díaz-Cánova D, Moens UL,
Brinkmann A, Nitsche A and
Okeke MI (2022) Genomic
Sequencing and Analysis of a Novel
Human Cowpox Virus With Mosaic
Sequences From North America
and Old World Orthopoxvirus.
Front. Microbiol. 13:868887.
doi: 10.3389/fmicb.2022.868887

Orthopoxviruses (OPXVs) not only infect their natural hosts, but some OPXVs can also cause disease in humans. Previously, we partially characterized an OPXV isolated from an 18-year-old male living in Northern Norway. Restriction enzyme analysis and partial genome sequencing characterized this virus as an atypical cowpox virus (CPXV), which we named CPXV-No-H2. In this study, we determined the complete genome sequence of CPXV-No-H2 using Illumina and Nanopore sequencing. Our results showed that the whole CPXV-No-H2 genome is 220,276 base pairs (bp) in length, with inverted terminal repeat regions of approximately 7 kbp, containing 217 predicted genes. Seventeen predicted CPXV-No-H2 proteins were most similar to OPXV proteins from the Old World, including *Ectromelia virus* (ECTV) and *Vaccinia virus*, and North America, *Alaskapox virus* (AKPV). CPXV-No-H2 has a mosaic genome with genes most similar to other OPXV genes, and seven potential recombination events were identified. The phylogenetic analysis showed that CPXV-No-H2 formed a separate clade with the German CPXV isolates CPXV_GerMygEK938_17 and CPXV_Ger2010_MKY, sharing 96.4 and 96.3% nucleotide identity, respectively, and this clade clustered closely with the ECTV-OPXV Abatino clade. CPXV-No-H2 is a mosaic virus that may have arisen out of several recombination events between OPXVs, and its phylogenetic clustering suggests that ECTV-Abatino-like cowpox viruses form a distinct, new clade of cowpox viruses.

Keywords: poxvirus, phylogenetics, Fennoscandian, Norway, recombination

INTRODUCTION

Poxvirus is a family of double-stranded DNA viruses that can infect a broad range of hosts, including mammals, birds, reptiles, and insects (International Committee on Taxonomy of Viruses, ICTV¹). Based on the host, *Poxviridae* is divided into two subfamilies: *Chordopoxvirinae* (poxviruses that infect vertebrates) and *Entomopoxvirinae* (poxviruses that infect insects)

¹<https://talk.ictvonline.org/taxonomy/>

(MacLachlan and Dubovi, 2017). Within the subfamily *Chordopoxvirinae*, there is the genus *Orthopoxvirus* (OPXV). They are viruses with large, linear, double-stranded DNA genomes ranging in size from 170 to 250 kbp (Hendrickson et al., 2010).

One of the best-known species among OPXV is *Variola virus* (VARV), the causative agent of smallpox. It was one of the deadliest viruses in human history and was declared to be successfully eradicated in 1980 after a worldwide smallpox vaccination campaign (Strassburg, 1982). Other members of the OPXV genus also cause human diseases, such as *Cowpox virus* (CPXV), *Monkeypox virus* (MPXV), and vaccinia-like virus (Vora et al., 2015; Reynolds et al., 2018; Diaz, 2021; Silva et al., 2021), but those are zoonotic OPXVs. *Variola virus* is the only OPXV that exclusively infected humans in nature. Among the most studied members of OPXVs, *Vaccinia virus* (VACV) is the prototype species. Several VACV strains were used as smallpox vaccines during the world vaccination campaign (Jacobs et al., 2009).

OPXVs can be further divided into New World and Old World OPXVs according to their endemism. The Old World or African-Eurasian OPXV group contains seven species: VARV, VACV, MPXV, CPXV, *Camelpox virus* (CMLV), *Ectromelia virus* (ECTV), and *Taterapox virus* (TATV). The New World OPXV group comprises three species that are endemic to North America: *Raccoonpox virus* (RCNV), *Volepox virus* (VPXV), and *Skunkpox virus* (SKPV) (Smithson et al., 2017b).

In recent times, the increased number of reported OPXV infections as well as the emergence of new OPXVs or re-emergence of existing OPXVs has been reported in several countries across the world (Abrahão et al., 2015; Kalthan et al., 2018). Three novel OPXV species have recently been discovered: *Abatino macacapox virus* (OPXV Abatino) in Italy (Cardeti et al., 2017), *Ahkmata virus* (AKMV) in Georgia (Gao et al., 2018), and *Alaskapox virus* (AKPV) in the United States (Gigante et al., 2019).

The increasing number of OPXV infections in humans could be due to low population immunity against smallpox after the cessation of smallpox vaccination. The vaccinia-like virus infections were reported in different places and host species (Dumbell and Richardson, 1993; Abrahão et al., 2015; Miranda et al., 2017), including humans (Damaso et al., 2007; Megid et al., 2012). In different countries in Africa, human cases of MPXV infections have been reported (Nakoune et al., 2017; Durski et al., 2018; Yinka-Ogunleye et al., 2019; Alakunle et al., 2020); imported MPXV cases were as well reported in Israel, the United Kingdom and Singapore (Vaughan et al., 2018; Erez et al., 2019; Ng et al., 2019). In Europe, cases of cowpox were reported (Tryland et al., 1998; Kalthoff et al., 2014; Ferrier et al., 2021). The distribution of CPXV is in Eurasia (Chantrey et al., 1999; Wolfs et al., 2002; Laakkonen et al., 2006; Vorou et al., 2008; Popova et al., 2017; Diaz, 2021; Ferrier et al., 2021). The natural reservoirs of CPXV are wild rodents (Chantrey et al., 1999; Kinnunen et al., 2011). CPXV has a wide host spectrum, including humans, monkeys, cats, dogs, horses, and farmed llamas (Tryland et al., 1998; Smith et al., 1999; Girling et al., 2011; Prkno et al., 2017; Diaz, 2021). CPXV's broad range is associated with its large genome, which is the largest

genome among OPXVs (Gubser et al., 2004; Carroll et al., 2011). CPXV is polyphyletic (Carroll et al., 2011; Okeke et al., 2014; Franke et al., 2017; Mauldin et al., 2017), and their strains cluster in at least five clades (Mauldin et al., 2017; Jeske et al., 2019). Among them, some clades are more genetically similar to VACV (VACV-like virus) and VARV (VARV-like virus), whereas other CPXV strains appear as single branches and have a mosaic genome that contains genomic parts from different clades (Franke et al., 2017). The genetic heterogeneity inside CPXV could partially be due to recombination processes with other OPXV species or between CPXV clades (Okeke et al., 2012, 2014; Franke et al., 2017).

A poxvirus was isolated from an 18-year-old man living in the county Nordland, Norway (Hansen et al., 2009). Based on the detection of A-type inclusion (ATI) bodies, the sequence and phylogenetic analysis of hemagglutinin (*HA*) gene, cytokine response modifier B (*crmB*) gene, and Chinese hamster ovary host range (*CHOhr*) genes as well as *Hind III* restriction map, this virus was classified as a CPXV and was tentatively named CPXV-No-H2 (Hansen et al., 2009; Okeke et al., 2012). This isolate produces an atypical ATI phenotype, $V^{+/-}$, in which the virions are encrusted only in the periphery of ATI (Okeke et al., 2012). The sequencing of two of the three genes (*atip*, *p4c*, and *A27L*) involved in the production of ATI with virions embedded into ATI (V^{+}) (Patel and Pickup, 1987; McKelvey et al., 2002; Howard et al., 2010) showed that it has intact *atip* and *p4c* genes. Furthermore, interestingly, the *atip* gene of CPXV-No-H2 closely related to that of ECTV with a bootstrap support of 100%, whereas the *p4c* gene was more diverse compared to the orthologs in other OPXVs (Okeke et al., 2012, 2014).

In this study, we report the whole sequence and genomic characterization of a Norwegian human CPXV isolate, CPXV-No-H2. We annotated the open reading frames, performed recombination analysis, and determined phylogenetic relationships with other OPXV genomes.

MATERIALS AND METHODS

Cell, Virus Culture, and DNA Isolation

The Fennoscandian CPXV No-H2 strain was isolated in 2001 from a human patient from Northern Norway (Hansen et al., 2009; Okeke et al., 2012). CPXV-No-H2 was cultured on a monolayer of Vero cells (ATCC No. CCL-81) in 175-cm² flasks (NUNC Sweden) as previously described (Okeke et al., 2012). Viral DNA was extracted from semi-purified virions using QIAGEN Genomic-tip 100/G and QIAGEN Genomic DNA Buffer Set, following the manufacturer's instructions (Qiagen, Hilden, Germany). DNA concentration was measured using NanoDrop 2000 spectrophotometer (Thermo Fischer ScientificTM, Waltham, MA, United States).

Whole-Genome Sequencing

The genome of CPXV-No-H2 was sequenced using Illumina and Oxford Nanopore Technologies (ONT; Oxford, United Kingdom), respectively. The preparation of sequencing libraries and next-generation sequencing with Illumina was

performed at the Norwegian Sequencing Centre, Oslo. ThruPLEX DNA-Seq kit with an input DNA of 50 ng was used for the library preparation. Whole-genome sequencing was performed on an Illumina MiSeq instrument (Illumina Inc., San Diego, CA, United States) using MiSeq Reagent v3 (600 cycles), producing 2×300-bp paired-end reads. For nanopore sequencing, sequencing libraries were prepared using the Ligation Sequencing Kit SQK-LSK109 (ONT, Oxford, United Kingdom) and native barcoding expansion kit EXP-NBD104 and EXP-NBD114 (ONT). Up to 14 samples were multiplexed on R9.4 flow cells (FLO-MIN106). The run was performed on GridION X5 (Oxford, United Kingdom) using MinKNOW v20.10.6. Library preparation and nanopore sequencing were performed at the Genomics Support Centre Tromsø at UiT-The Arctic University of Norway.

Genome Assembly

Raw sequencing data from Illumina MiSeq were evaluated for their quality using FastQC software v0.11.8 (Andrews, 2010). Adapter removal and quality filtering were conducted using Trimmomatic v0.39 (Parameters: ILLUMINACLIP:TruSeq3-PE-2.fa:2:30:10 LEADING:3 TRAILING:3 SLIDINGWINDOW:4:20 MINLEN:36) (Bolger et al., 2014). In order to remove reads corresponding to host cells, filtered reads were mapped against *Chlorocebus sabaeus* (GCF_000409795.2) using FastQ Screen v0.14.1 (Wingett and Andrews, 2018) with BWA v.0.7.17 (Li and Durbin, 2009). The remaining reads were used in the genome assembly. Raw nanopore data (fast5 files) were base called using Guppy 4.2.3 in MinKNOW 20.10.6, with a qscore of 7 as filter, to produce Fastq formatted sequence files. Fastq sequences were demultiplexed using Guppy 4.2.3—likewise with barcode removal. Host sequences were filtered out using FastQ Screen v0.14.1 (Wingett and Andrews, 2018) with BWA v.0.7.17 (Li and Durbin, 2009) as described above. SPAdes v3.15.3 (Bankevich et al., 2012) was used to combine the ONT long reads and the Illumina reads to produce a hybrid assembly (with nanopore option and default parameters). Contigs were screened using BLAST² to remove host contamination. In order to assemble the complete genome, the Illumina reads were mapped to the contigs using Geneious mapper implemented in Geneious Prime 2020.2.4 (Biomatters, Inc., Newark, NJ, United States). Then, the extended contigs were merged into one by Geneious assembler in Geneious Prime 2020.2.4.

Genome Annotation

The assembled genome was annotated using Genome Annotation Transfer Utility (GATU) software from the Viral Bioinformatics Resource Centre (Tcherepanov et al., 2006). ECTV Moscow strain (ECTV_Mos), CPXV Brighton Red strain (CPXV_Br), and VACV Copenhagen strain (VACV_Cop) were used as reference genomes. These reference sequences were retrieved from the Viral Orthologous Clusters (VOCs) database (Ehlers et al., 2002). The GATU parameters included open reading frames (ORFs) longer than 30 amino acids, with a maximum overlap of 25%.

²<https://blast.ncbi.nlm.nih.gov/Blast.cgi>

Gene annotations from the reference genomes were transferred to the CPXV-No-H2 genome when the level of similarity was ≥80%. The putative coding sequences (CDS) with low similarity to the reference genes were subjected to a BLASTp analysis against the proteins belonging to the *Poxviridae* family from the NCBI database. Putative CDS with high similarity to other poxviruses were annotated. Similarly, the unassigned ORFs were investigated using BLASTp searches to find orthologous genes. In cases where more than one CDS were found in the same genomic region, the CDS with the highest similarity was selected. Geneious Prime 2020.2.4 was used to visualize, edit, and correct the annotations, if needed.

Phylogenetic Analysis

For phylogenetic analysis, 75 OPXV genomes were retrieved from the VOCs database (Ehlers et al., 2002), except for CPXV_GerMygEK938_17, which was retrieved from GenBank. The OPXV genomes used in this study are listed in **Supplementary Table 1**. The alignments of (1) the genomes, excluding the inverted terminal repeats (ITRs; called core genome), (2) the genomic region from the first gene until the last gene (referred to as the whole genome), and (3) the orthologous genes of the 76 OPXVs (including CPXV-No-H2) were performed using MAFFT v1.4.0 (with default parameters; Katoh and Standley, 2013) implemented in Geneious Prime 2020.2.4. The poorly aligned positions were removed from the alignments (1 and 2) with Gblocks 0.91b using default parameters (Talavera and Castresana, 2007). The orthologous genes were identified using OrthoFinder v2.5.2 (Emms and Kelly, 2015). The orthologs (present in ≥95% of the genomes) were aligned as described above and concatenated in Geneious Prime 2020.2.4.

The phylogenetic relationship among these OPXVs was inferred by the maximum likelihood (ML) and Bayesian inference (BI) methods. ML trees were constructed in RAxML v.8.2.12 (Stamatakis, 2014) using the best-fitting nucleotide substitution model and 1,000 bootstrap replicates. The best-fit nucleotide substitution model for the alignment data was selected using the modelTest-NG v.0.1.6 (Darriba et al., 2020). BI analyses were performed using MrBayes v.3.2.7 (Ronquist et al., 2012) under the best-fitting substitution model with the following parameters: 2 million generations, nchains = 4, samplefreq = 500, and burninfrac = 0.25. The phylogenetic trees were visualized using FigTree v1.4.4 (Rambaut, 2018).

Gene Content Comparison

Predicted CDS from isolate CPXV-No-H2 were extracted, translated into amino acid sequences, and compared to the CPXV_Br, ECTV_Mos, or VACV_Cop proteins using BLASTp (ncbi-blast+ v2.11.0) (Camacho et al., 2009). To find the closest annotated proteins for all predicted CPXV-No-H2 CDS, every translated CPXV-No-H2 CDS was analyzed by BLASTp search against proteins of the *Poxviridae* family. A BLASTn identity analysis was performed on predicted CPXV-No-H2 CDS that encode proteins with a higher identity to other OPXV proteins than CPXV proteins. When the first hit in BLASTp or BLASTn was CPXV-No-H2 protein or genome, the second hit was used.

Investigation of Potential Recombination Events

The genome sequence of CPXV-No-H2 was examined for potential recombination events using recombination detection program 4 (RPD4) (Martin et al., 2015) and SimPlot v3.5.1 (Lole et al., 1999). A putative recombinant event was taken into account if it was identified by RDP4 and/or Simplot analysis and the sequence was most similar to the possible minor parental. The whole genome of CPXV-No-H2 was aligned to other OPXV genomes used as putative parentals (AKPV, CPXV_Gri, CPXV_GerMygEK938_17, ECTV_Mos, MPXV_Zaire, and VACV_LC16m8), with MAFFT v1.4.0 (Katoh and Standley, 2013) implemented in Geneious Prime 2020.2.4. Gaps were not removed from the multiple alignments. Similarity plots were performed on the multiple alignments using the SimPlot program (Lole et al., 1999) with default settings. Putative recombination breakpoints were determined by maximization of χ^2 analysis (Lole et al., 1999; Lim et al., 2011). For recombination analysis with RPD4, seven methods [RDP (Martin and Rybicki, 2000), GENECONV (Padidam et al., 1999), Bootscan (Martin et al., 2005), MaxChi (Smith, 1992), Chimaera (Posada and Crandall, 2001), SiScan (Gibbs et al., 2000), and 3Seq (Boni et al., 2007)] were used to detect potential recombination events. RDP4 was used with the default parameters, except for the option “require topological evidence.” The recombination events that were identified by 6 of 7 methods with significant *p*-values ($p \leq 0.01$) were considered potential recombinant events. The beginning and end of the breakpoints of these events suggested by RPD4 were used to identify the potential recombinant sequence. When the breakpoints were not identified by RDP4, the range of positions of the breakpoints obtained by Simplot analysis was used. Those potential recombinant sequences were utilized to build an ML tree using RAxML v.8.2.12 (Stamatakis, 2014). Phylogenetic tree incongruence was further used to map potential recombination sequences. Furthermore, a BLASTn identity analysis was performed on those potential recombinant sequences.

RESULTS

Genome Assembly and Genome Annotation

Two large contigs (>1000 bp) were obtained with the hybrid assembly and after removing the host contamination. The average coverage of the major and minor contig was 1502X and 735X, respectively. The mean genomic coverage of CPXV-No-H2 was 1370X. The assembled whole-genome length of CPXV-No-H2 was 220,276 bp. The ITR regions were approximately 7 kbp, and the central region was 206,204 bp. The A+T content of the CPXV-No-H2 genome was 66.6%. Genome annotation predicted 217 potential genes in the CPXV-No-H2 genome (Figure 1 and Supplementary Table 2). The overlapping genes were excluded from the annotation process. However, there were 20 predicted overlapping genes (Supplementary Table 3). Some of them were homologs of CPXV_Br genes (CPXV004,

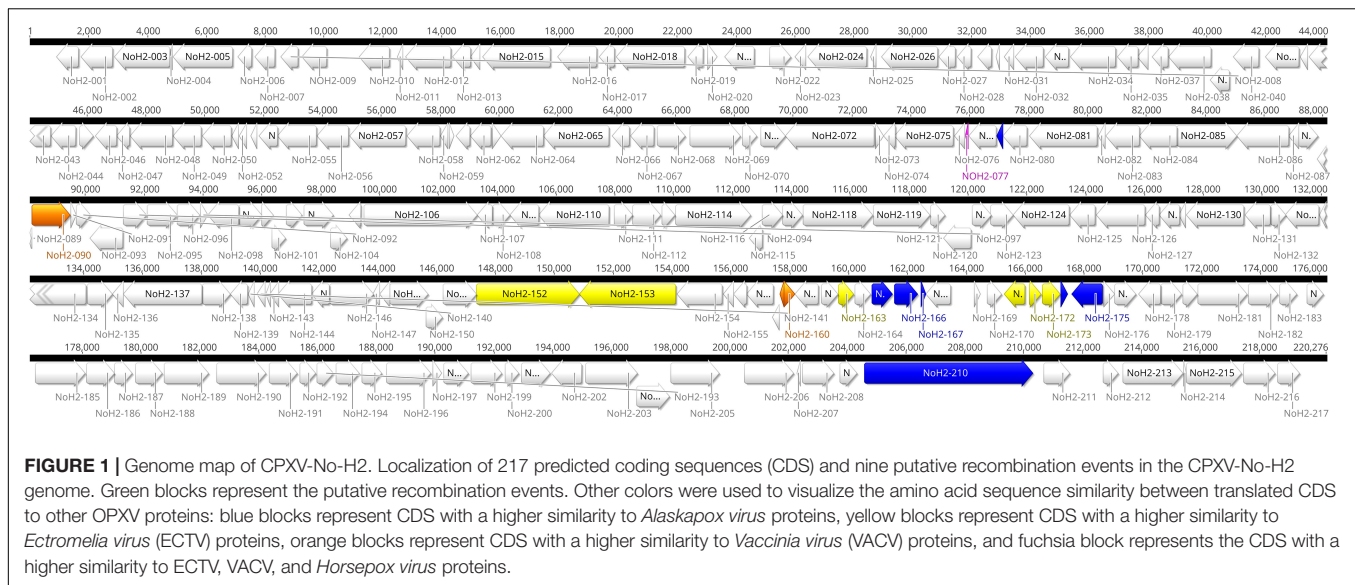
CPXV47, CPXV51A, CPXV058, CPXV078A, CPXV096, CPXV116, CPXV119A, CPXV130, CPXV152A, CPXV160, CPXV170, and CPXV214). The whole genome sequence is deposited in GenBank with accession number OM460002.

Phylogenetic Analysis

The phylogenetic analysis showed that the ML tree topologies were similar to the phylogenetic trees generated by the BI method, regardless of the alignments used. The BI phylogenetic trees had strong posterior probabilities in most nodes (≥ 0.95) (Figures 2–4). Unlike the BI trees, the ML trees had low clade support ($< 70\%$) in some of the nodes (Supplementary Figures 2–4). The BI phylogenetic trees of 76 OPXV whole genomes, 76 OPXV core genomes, and 134 OPXV orthologous genes are shown in Figures 2–4, respectively. The Old World and New World OPXV were separated into two groups in the phylogenetic trees generated from 76 OPXV whole genomes (Figure 2), 76 OPXV core genomes (Figure 3), and 134 OPXV orthologous genes (Figure 4). Within the Old World OPXV, the strains from the same OPXV species were grouped into clusters, except for CPXV strains that formed more than one cluster. CPXV was divided into clusters: CPXV-like 1, CPXV-like 2, VARV-like, VACV-like, and new clade (Franke et al., 2017). Although the strains of VACV-like did not form a proper cluster, they were closely related VACV (Figures 2–4).

The new clade comprised CPXV-No-H2 and two German CPXV isolates: CPXV_GerMygEK938_17 and CPXV_Ger2010_MKY (posterior probabilities of 1.0 and bootstrap values of 100%) (Figures 2–4 and Supplementary Figures 2–4). The CPXV-No-H2 genome was most similar to the CPXV_GerMygEK_938_17 genome (96.38% identical), and the second most similar virus was CPXV_Ger2010_MKY (96.26% identical), based on the alignment of 76 OPXV whole genomes. The new clade was closely related to the ECTV/Abatino clade. Both clades formed a major clade together (posterior probabilities of 1.0 and bootstrap values $> 89\%$) (Figures 2–4 and Supplementary Figures 2–4). In this study, the new clade (CPXV-No-H2/CPXV_GerMygEK938_17/ CPXV_Ger2010_MKY) was tentatively named “ECTV-Abatino-like.”

In phylogenetic trees derived from the 134 OPXV orthologous genes, the ECTV-Abatino-like/ECTV/OPXV Abatino clade clustered with CPXV_Ger1998/CPXV-like 2 clade with a strong posterior probability (1.0), but with a low bootstrap support value (46%) (Figure 4 and Supplementary Figure 4), whereas the phylogeny of the 76 OPXV whole and core genomes showed that the ECTV-Abatino-like/ECTV/OPXV Abatino clade was separated from the other Old World OPXV, which formed a major polyphyletic clade (posterior probability of 1.0 and bootstrap values $> 81\%$) (Figures 2, 3 and Supplementary Figures 2, 3). This major polyphyletic clade was further resolved in two groups: the CPXV_Ger1998/CPXV-like 2 clade (posterior probability of 1.0 and bootstrap values of 100%) and a larger group containing CPXV-like 1, VARV-like, VARV-TATV-CMLV, CPXV_HumLit08, VACV-like, MPXV, RPXV, and VACV clades (posterior probabilities of 1.0 and bootstrap values of 100%) (Figures 2, 3 and Supplementary Figures 2, 3). The clustering



within this monophyletic group apparently differs between the tree based on 76 OPXV whole genomes and the trees built from 76 OPXV core genomes and 134 OPXV orthologous genes (Figures 2–4 and Supplementary Figures 2–4). In the former, CPXV-like 1 branches separated from other members of the large polyphyletic group (Figure 2 and Supplementary Figure 2). These members formed a cluster and were further split into two clusters: the VARV-like/TATV/CMLV/VARV cluster and the CPXV_HumLit08/VACV-like/MPXV/RPXV/VACV cluster. Both clusters were supported by strong posterior probabilities (1.0) and bootstrap values (100%) (Figure 2 and Supplementary Figure 2), while 76 OPXV core genomes and 134 OPXV orthologous gene phylogenies grouped CPXV-like 1 into the same cluster with VARV-like/TATV/CMLV/VARV, with posterior probabilities of 0.99 and 1.0 and bootstrap values of 51 and 99%, respectively (Figures 3, 4 and Supplementary Figures 3, 4). Additionally, CPXV_HumLit08, VACV-like, MPXV, RPXV, and VACV were grouped into the same cluster, with posterior probabilities of 1.0 and bootstrap values of 100%.

However irrespective of the aforementioned differences between the whole genome tree on one hand and the core genome and the concatenated 134 orthologous genes on the other, the following topologies were consistent in all the trees generated from the three distinct datasets: (i) ECTV-Abatino-like CPXV clustered closely with ECTV-OPXV Abatino clade, (ii) VACV-like CPXV grouped together with VACV, (iii) VARV-like CPXV clustered closely with VARV-TATV-CMLV clade, (iv) CPXV-like 1 clade is sister to VACV-like clade, and (vi) AKPV/AKMV are intermediate between Old World and New World OPXV.

Gene Content Comparison

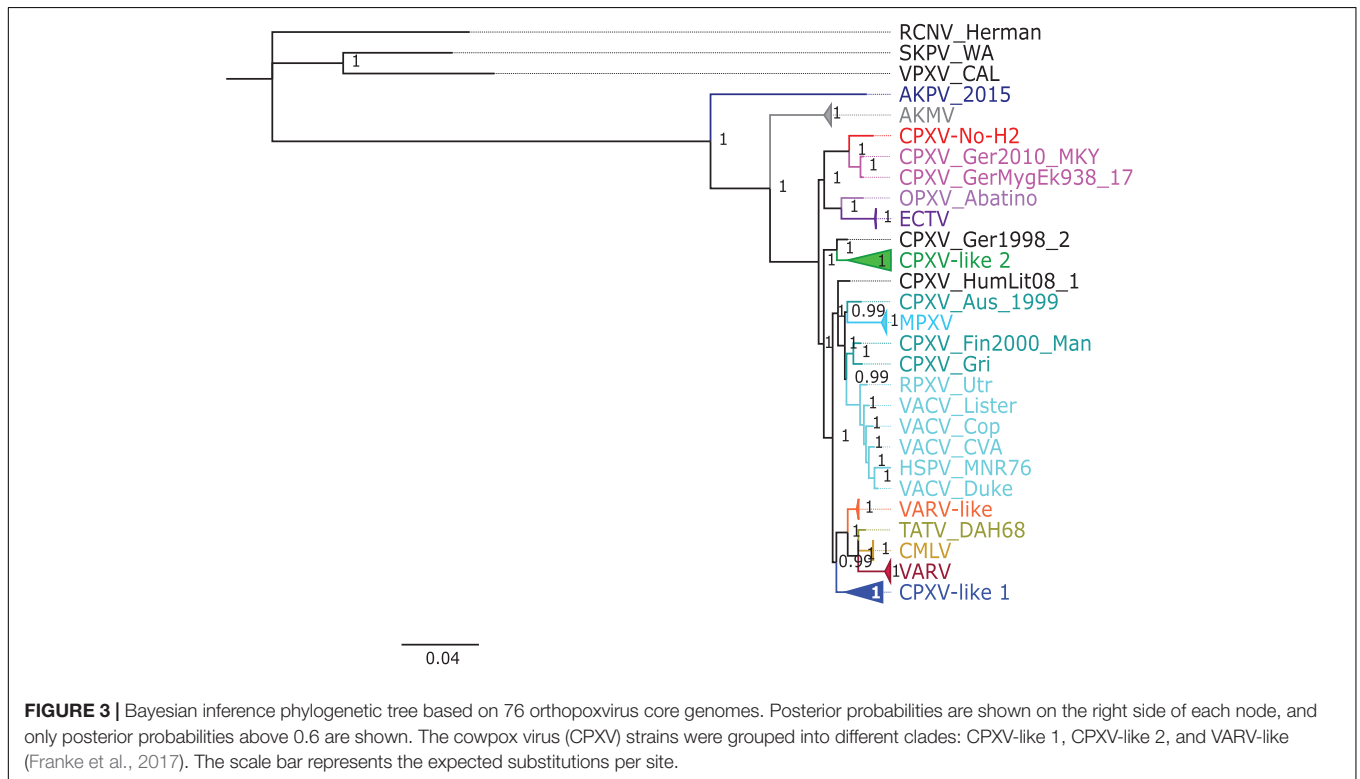
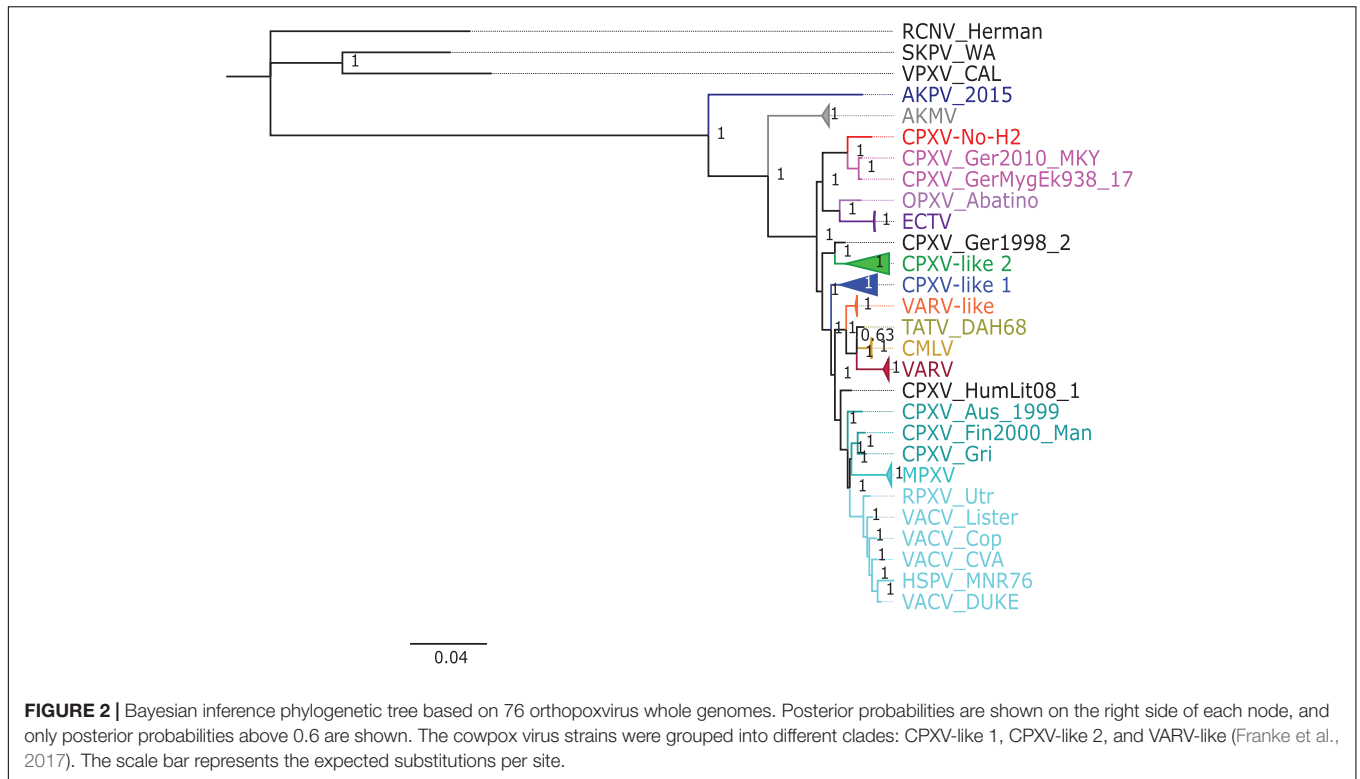
The gene content and organization of the CPXV-No-H2 genome were similar to that of the CPXV_Br and ECTV_Mos genomes. All CPXV_Br genes (excluding ITR genes) were found in the CPXV-No-H2 genome, except for *CPXV221* (encodes CrmD protein) and *CPXV192* (encodes CPXV192 protein).

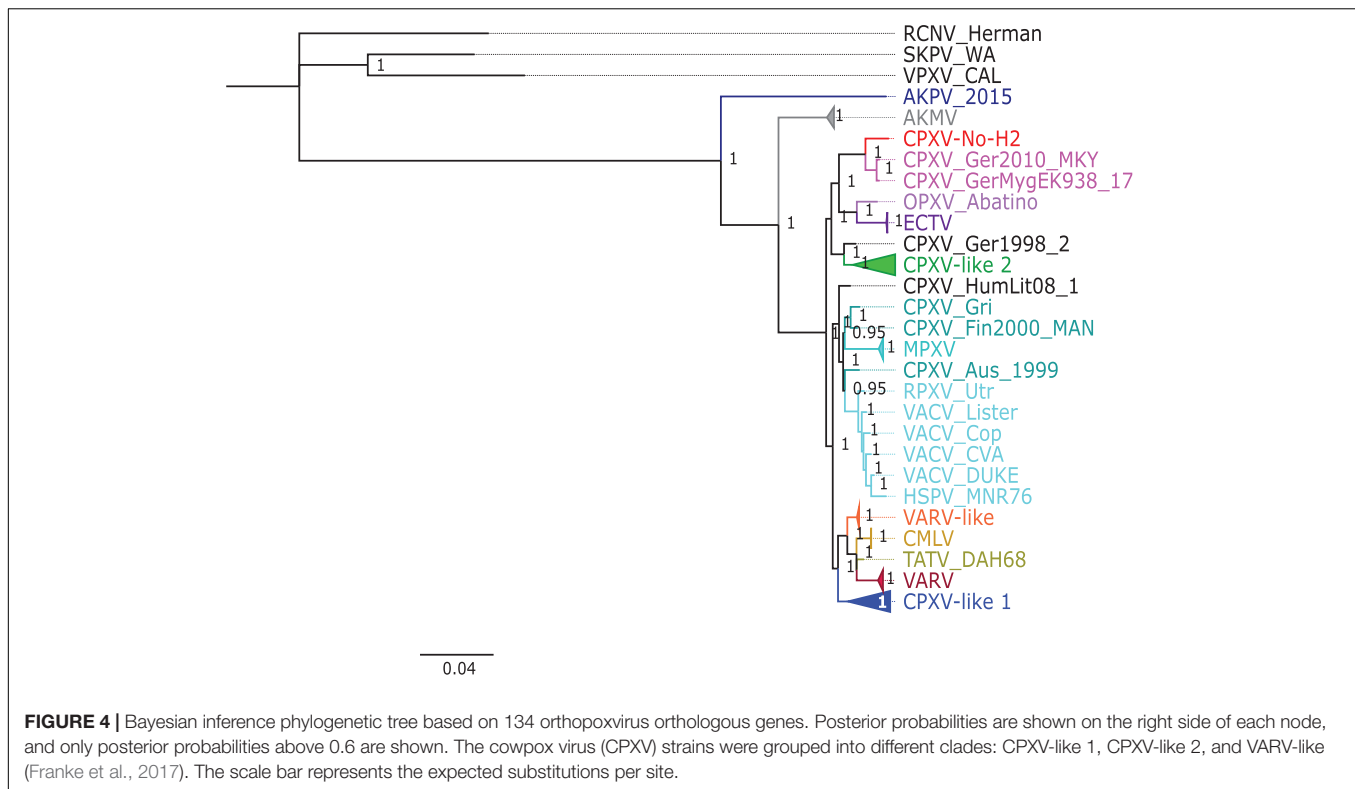
The last gene is truncated in CPXV-No-H2 and overlapped to a major predicted gene. Similarly, comparing CPXV-No-H2 and ECTV_Mos, it was shown that *EVM003/170* (homolog to *CPXV221*) was missing in the CPXV-No-H2 genome. Additionally, the *EVM006* gene (encodes C-type lectin) was absent in the CPXV-No-H2 genome.

The predicted gene *NoH2-154* encodes an intact *p4c* protein compared to CPXV_Br, whose *p4c* gene is disrupted in two fragments (*CPXV159* and *CPXV161*). Similarly, this gene is fragmented in ECTV_Mos (Chen et al., 2003). The BLASTp analysis for NoH2-154 revealed that the best hit was an inclusion protein III from *Buffalopox virus*, with 87.7% identity. This protein (501 aa) was smaller than the *p4c* protein from CPXV-No-H2 (512 aa). The next best BLASTp hits were longer proteins of 527 aa from CPXV_Ger2010_MKY and 523 aa from CPXV_GerMygEK938_17, which shared 88.6 and 89.12% identity with *p4c* protein from CPXV-No-H2, respectively. BLASTn showed that the CPXV-No-H2 *p4c* gene was most similar to the *p4c* gene from CPXV_GerMygEK938_17.

Within ITRs of CPXV-No-H2, five of eight duplicate CPXV_Br genes were found (*CPXV003/227*, *CPXV005/226*, *CPXV006/225*, *CPXV007/224*, and *CPXV008/223*). The terminal *CPXV004* gene was also found in both ITRs of CPXV-No-H2 (*NoH2-A* and *NoH2-T*) (Supplementary Table 3), but they overlapped two major predicted genes (*NoH2-002* and *NoH2-216*). Interestingly, *NoH2-006*, the ortholog of *CPXV009/222*, was found as a single copy downstream of the left ITR of the CPXV-No-H2 genome (Figure 1).

All predicted genes in CPXV-No-H2 were found to have homologs in either CPXV_Br, ECTV_Mos, or VACV_Cop, except for *NoH2-008* and *NoH2-212*. The translated *NoH2-008* CDS shared 100% amino acid identity with the hypothetical protein CPXV0285 of CPXV_FM2292 (CRL86746.1) and CPXV_Ger2007_Vole (SBN49117.1). The predicted gene *NoH2-212* was a homolog of *CPXV-GRI-K3R* (encodes CrmE protein). The BLASTp analysis of this translated CDS showed





that it shared the highest amino acid identity (95.2%) with a CPXV_GerMygEK938_17 protein (hypothetical protein pCPXV003 CAB5514210.1). The *NoH2-212* gene was located upstream of the right ITR of CPXV-No-H2 (**Figure 1**).

Of the 217 predicted genes of CPXV-No-H2, 17 coded for proteins that were most similar to other OPXV proteins than CPXV proteins. Seven of them shared high similarity to North American OPXV proteins, AKPV, and 10 genes were most similar to Old World OPXV proteins, including ECTV and VACV (**Supplementary Table 4**). The seven predicted CPXV-No-H2 proteins were most similar (i.e., >92% amino acid identity) to AKPV proteins, including NoH2-079, NoH2-165, NoH2-166, NoH2-167, NoH2-174, NoH2-175, and NoH2-210. The BLASTn analysis of their seven predicted CPXV-No-H2 genes revealed that *NoH2-079*, *NoH2-165*, *NoH2-166*, *NoH2-167*, *NoH2-174*, and *NoH2-210* shared the highest similarity (i.e., > 97% nucleotide identity) with AKPV-076, AKPV-162, AKPV-163, AKPV-164, AKPV-171, and AKPV-203, respectively, whereas *NoH2-175* shared the highest nucleotide similarity with CPXV_GerMygEK938_17/CPXV_Ger2010_MKY. However, the BLASTn analysis of *NoH2-175* with the intergenic region between *NoH2-174* and *NoH2-175* revealed the highest similarity with AKPV (93.98% nucleotide identity).

The six predicted proteins most identical (i.e., > 94% amino acid identity) to ECTV proteins were NoH2-152, NoH2-153, NoH2-163, NoH2-171, NoH2-172, and NoH2-173. At the nucleotide level, *NoH2-152*, *NoH2-153*, *NoH2-171*, *NoH2-172*, and *NoH2-173* had > 95% identity with the

corresponding ECTV *EVM127*, *EVM128*, *EVM140*, *EVM141*, and *EVM142* genes. The *NoH2-163* gene, however, was most similar to CPXV169 from CPXV_GerMygEK938_17 and CPXV_Ger2010_MKY (98.6% identity), whereas the next best BLASTn hit was an ECTV gene with 98.4% identity. The difference between their percent identities was due to one identical nucleotide (**Supplementary Figure 1**).

The three CPXV-No-H2 predicted proteins most similar to VACV proteins included NoH2-090, NoH2-159, and NoH2-160. The BLASTn search of these predicted genes revealed that *NoH2-159* shared 100% nucleotide identity with VACV, BPXV, and CPXV genomes, and *NoH2-160* was 98.4% identical to VACV LC16m8 (*m8197R*) and VACV LC16mO genes (*mO197R*). The predicted protein of the gene *NoH2-077* was 100% identical to ECTV, HSPV, and VACV proteins. However, the BLASTn of this predicted gene showed that it was 100% identical to CPXV_GerMygEK938_17 genome, but this region was not annotated.

Overlapping genes were excluded from the annotation process. There were 20 overlapping predicted genes (**Supplementary Table 3**). Fourteen of them were homologs of CPXV_Br (*CPXV004*, *CXPV47*, *CPXV51A*, *CPXV058*, *CPXV078A*, *CPXV096*, *CPXV116*, *CPXV119A*, *CPXV130*, *CPXV152A*, *CPXV160*, *CPXV170*, and *CPXV214*). Another six overlapping genes did not correspond to any annotated CPXV gene. The BLASTp analysis of the protein encoded by the six overlapping genes revealed that five shared the highest similarity (> 83% amino acid identity) to CMLV_0408151v (NoH2-B), OPXV Abatino (NoH2-H), VACV_CEvY1

(NoH2-G and NoH2-N), or VACV_Lister (NoH2-R) proteins (**Supplementary Table 3**).

Recombination Analysis

Previous studies by our group had identified a putative crossover event downstream of the *atip* gene (Okeke et al., 2012). Consequently, the complete CPXV-No-H2 genome was examined for recombination because it contained genomic regions with predicted genes similar to AKPV, ECTV, or VACV genomes. Nine putative recombination events were predicted by RDP4 and Simplot analysis for the CPXV-No-H2 genome (**Table 1** and **Figure 1**). Six potential recombination regions were a result of recombination events between the parents of AKPV and CPXV (putative recombination events 1–6), two originated from recombination events between the parental ECTV and CPXV (putative recombination events 7 and 8), and one was a product of a recombination event between the parental VACV and CPXV (putative recombination event 9) (**Table 1**). Within the nine putative recombinant regions in CPXV-No-H2, only one recombinant region (putative recombination event 6) was close to terminal regions, whereas the other eight recombinant regions were located in the central region of the genome.

The first potential recombinant region in the CPXV-No-H2 genome (putative recombination event 1) comprised the *NoH2-079* gene and started from position 76,946 bp in the CPXV-No-H2. The ending breaking could be between positions 77,201 and 77,208 bp in the CPXV-No-H2 genome based on Simplot analysis. The next potential recombinant region (putative recombination event 2) was almost 500 bp downstream of the first one. It was located between 77,741 and 78,243 bp in the CPXV-No-H2 genome and contained parts of *NoH2-080* and *NoH2-081*. These two putative recombinant regions shared the highest similarity to the AKPV genome (>98% identical) (**Supplementary Table 5**).

The third potential recombinant region (putative recombination event 3) spanned approximately 4,500 bp, from position 150,156 to 154,530 bp in the CPXV-No-H2 genome. However, it overlapped with the predicted recombinant region between the parental ECTV and CPXV (putative recombination event 7), located between 150,119 and 153,968 bp in the CPXV-No-H2 genome. The latter encompassed only two genes, *NoH2-152* and *No-153*, compared to the former that also contained part of the *NoH2-154* gene. The BLASTn analysis of the third potential recombinant region revealed the highest similarity with the AKPV genome (96.89% identical), whereas the putative recombinant region between the parental ECTV and CPXV was most similar to the ECTV genomes, with 97.93% nucleotide identity (**Supplementary Table 5**).

The fourth potential recombinant region in the CPXV-No-H2 genome (putative recombination event 4) included the genes *NoH2-165*, *NoH2-166*, and *NoH2-167* and part of *NoH2-168*. The Simplot analysis revealed that the beginning and ending breakpoints were located between 160,774 and 160,878 bp and between 162,909 and 162,948 bp in the CPXV-No-H2 genome, respectively. This genomic region was most similar to the AKPV genome, sharing 97.66% nucleotide identity (**Supplementary Table 5**). The fifth potential recombinant region

(putative recombination event 5) started from 165,874 to 168,063 bp in the CPXV-No-H2 genome. It overlapped with another putative recombinant region between the parental ECTV and CPXV (putative recombination event 8), which was located between 165,847 and 167,892 bp in the CPXV-No-H2 genome. Both regions contained part of *NoH2-171*, *NoH2-172*, *NoH2-173*, and *NoH2-174* and part of *NoH2-175*. The BLASTn analysis of these two putative recombination regions revealed that the first hit was the AKPV genome, with > 97% nucleotide identity (**Supplementary Table 5**).

A sixth potential recombinant event between the parental AKPV and CPXV (putative recombination event 6) was detected only by Simplot analysis. The cross-over points lay between 204,960 and 204,977 bp and between 209,488 and 209,901 bp in the CPXV-No-H2 genome. It contained a major part of the *NoH2-210* gene, which was most similar to AKPV-203 (97.15% identical) and also shared similarity with the Murmansk-007 gene (91.44% identical). Furthermore, this putative recombinant sequence showed its highest identity with the AKPV genome (98.4% identical), followed by the *Murmansk microtus pox virus* genome (91.44% identical).

One putative recombination event between the parental VACV and CPXV (putative recombination event 9) was detected. The breakpoints were undetermined by RDP4, but the Simplot analysis revealed that the putative recombinant sequence started from position 164,400–164,525 bp and ended at position 164,756–164,768 bp in the CPXV-No-H2 genome. This region contained a small part of *NoH2-169* and a major part of *NoH2-170*. The latter gene shared 94.44% identity with the genes of CPXV and RPXV and the VACV strains, such as Lister, Cantagalo, CVA, and NYCBH.

The phylogenetic analysis of the six putative recombinant regions between the parental AKPV and CPXV showed that CPXV-No-H2 clustered with AKPV with a bootstrap support of > 91%, except for the phylogenetic tree based on the fifth putative recombinant region (165,874–168,063 bp in the CPXV-No-H2 genome), where CPXV-No-H2 clustered with ECTV with a low bootstrap support (55%), and they were grouped with AKPV (bootstrap value of 100%) (**Supplementary Figures 5–10**). CPXV-No-H2 likewise clustered with ECTV in the phylogenetic tree generated from the potential recombinant region between the parental ECTV and CPXV (165,847–167,892 bp in the CPXV-No-H2 genome) that overlapped the fifth putative recombinant region (**Supplementary Figure 12**). Unlike the previous phylogenetic tree, the bootstrap support for this clade was higher (93%) though.

Based on the phylogenetic analysis of the putative recombinant sequence between the parental ECTV and CPXV (150,119–153,968 bp in the CPXV-No-H2 genome), CPXV-No-H2 formed a cluster with ECTV (**Supplementary Figure 11**). This cluster was most closely related to AKPV and formed a major clade, with AKPV and AKMV, separating them from other Old World OPXV. However, the phylogenetic tree of the recombinant region between the parental AKPV and CPXV (150,156–154,530 bp in the CPXV-No-H2 genome), which overlapped that recombinant region, clustered CPXV-No-H2 with AKPV, and both isolates were closely related to ECTV

TABLE 1 | Predicted recombination events in the CPXV-No-H2 genome using recombination detection program 4 (RPD4) and Simplot analysis.

Putative parental strains	Major parental	Minor parental	Recombinant virus	Recombination event	RPD4		Recombination detection programs	Simplot	
					Breakpoint in CPXV-No-H2			Breakpoint interval in CPXV-No-H2	
					Begin (bp)	End (bp)		Begin (bp)	End (bp)
AKPV, CPXV_GerMygEK938_17, CPXV_Gri, CPXV-No-H2	CPXV_GerMygEK938_17	AKPV	CPXV-No-H2	1	76,946	77,244*	RPD, GENECONV, Bootscan, MaxChi, Chimaera, 3Seq	76,679–76,957	77,201–77,208
	CPXV_GerMygEK938_17	AKPV	CPXV-No-H2	2	77,741	78,243	RPD, GENECONV, Bootscan, MaxChi, Chimaera, 3Seq	77,717–77,765	78,237–78,399
	CPXV_GerMygEK938_17	AKPV	CPXV-No-H2	3	150,156	154,530	GENECONV, Bootscan, MaxChi, Chimaera, SiScan, 3Seq	150041–150158	154,524–154,570
	CPXV_GerMygEK938_17	AKPV	CPXV-No-H2	4	160,988*	162,917*	RPD, GENECONV, Bootscan, MaxChi, Chimaera, SiScan, 3Seq	160,774–160,878	162,909–162,948
	CPXV_GerMygEK938_17	AKPV	CPXV-No-H2	5	165,874	168,063	RPD, GENECONV, Bootscan, MaxChi, Chimaera, SiScan, 3Seq	165,828–165,878	168,042–168,066
ECTV_Mos, CPXV_GerMygEK938_17, CPXV_Gri, CPXV-No-H2	CPXV_GerMygEK938_17	AKPV	CPXV-No-H2	6	-	-	-	204,960–204,977	209,498–209,901
	CPXV_GerMygEK938_17	ECTV_Mos	CPXV-No-H2	7	150,119	153,968	GENECONV, Bootscan, MaxChi, Chimaera, SiScan, 3Seq	149,993–150,158	153,952–154,180
	CPXV_GerMygEK938_17	ECTV_Mos	CPXV-No-H2	8	165,847	167,892	RPD, GENECONV, Bootscan, MaxChi, Chimaera, SiScan, 3Seq	165,678–165,855	167,879–167,943
VACV_LC16m8, CPXV_GerMygEK938_17, CPXV_Gri, CPXV-No-H2	CPXV_GerMygEK938_17	VACV_LC16m8	CPXV-No-H2	9	164,419*	165,036*	RPD, Bootscan, MaxChi, Chimaera, SiScan, 3Seq	164,399–164,525	164,756–164,768

The breakpoint that was undetermined is marked with an asterisk. AKPV, Alakapox virus; CPXV, Cowpox virus; ECTV, Ectromelia virus; VACV, Vaccinia virus. The breakpoint that was undetermined is marked with an asterisk.

(**Supplementary Figure 7**). The phylogenetic tree based on the putative recombinant sequence between the parental VACV and CPXV placed CPXV-No-H2 inside the VACV cluster (**Supplementary Figure 13**).

DISCUSSION

CPXV-No-H2 is an isolate from a human in Northern Norway that was classified as an atypical CPXV based on ATI phenotype, sequence of the *atip* and *p4c* genes, and Hind III restriction map (Hansen et al., 2009; Okeke et al., 2012). Our phylogeny analysis indicated that CPXV-No-H2 is most closely related to the German CPXV isolates CPXV_GerMygEK938_17 and CPXV_Ger2010_MKY (**Figures 2–4**). Similarly, phylogenetic analysis based on the *HA* gene also resolved CPXV_Ger2010_MKY and CPXV-No-H2 in the same cluster (Kalthoff et al., 2014). The three CPXV isolates (CPXV_GerMygEK938_17, CPXV_Ger2010_MKY, and CPXV-No-H2) may be part of a novel CPXV lineage separated from the other CPXV strains. It was previously suggested that CPXV_Ger2010_MKY and CPXV_GerMygEK938_17 were part of a new cluster provisionally called CPXV-like 3 (Franke et al., 2017; Jeske et al., 2019). However, this cluster was supported by a low bootstrap value (Jeske et al., 2019). The phylogenetic analysis reported in our study indicated that the new clade (CPXV-No-H2/CPXV_GerMygEK938_17/CPXV_Ger2010_MKY) was more closely related to ECTV and OPXV Abatino than other OPXVs, with strong posterior probabilities and bootstrap values (**Figures 2–4** and **Supplementary Figures 2–4**). Thus, we tentatively named this clade as “ECTV-Abatino-like.”

The ECTV-Abatino-like/ECTV/OPXV Abatino clade was separated from the Old World OPXV in 76 OPXV whole- and core-genome phylogenetic trees, while a phylogenetic tree based on 134 OPXV orthologous genes showed that this clade clustered closely with CPXV_Ger1998/CPXV-like 2 but with poor bootstrap support (46%). We suggest that the separation of ECTV-Abatino-like/ECTV/OPXV Abatino from the other Old World OPXV may be due to the presence of some genes (or genomic regions) located in the core genome, which are not included within the 134 OPXV orthologous genes. A previous study showed that CPXV_GerMygEK938_17/CPXV_Ger2010_MKY/ECTV/OPXV Abatino clustered with CPXV-like 2 but with low bootstrap support (< 70%) (Jeske et al., 2019), although AKPV was not included in their phylogenetic analysis compared to our study that included AKPV and more OPXV strains. When AKPV was excluded from the construction of our phylogenetic trees, the ECTV-Abatino-like/ECTV/OPXV Abatino clade clustered with CPXV_Ger1998/CPXV-like 2 in 75 OPXV whole- and core-genome phylogenetic trees but with low bootstrap support (**Supplementary Figures 14–17**). In contrast, the bootstrap value in the node that clustered these clades increased from 46 to 82% in the phylogenetic tree based on 134 OPXV orthologous genes (**Supplementary Figures 18, 19**). We suspect that the genes or genomic regions that separated those clades have homologs in AKPV—for instance, homologs

of *NoH2-166*, *NoH2-167*, *NoH2-174*, and *NoH2-210* genes, which were most similar to the AKPV genes, were not included in the construction of the phylogenetic tree based on 134 OPXV orthologous genes.

In fact, CPXV-No-H2 has a mosaic genome with genes most similar to the OPXV genes from the Old World, including ECTV and VACV, and the North America, AKPV. Previously, we have shown that the *atip* gene from CPXV-No-H2 displayed the highest similarity to the corresponding ECTV gene, and the insertion of the ECTV *atip* gene may be a result of the recombination between CPXV and ECTV or an ECTV-like virus (Okeke et al., 2012). Our present study suggested similar findings and indicated that CPXV-No-H2 has also undergone recombination events between AKPV and VACV. A recombination between OPXVs has been reported by others (Gubser et al., 2004; Coulson and Upton, 2011; Qin et al., 2011, 2015; Okeke et al., 2012; Smithson et al., 2014, 2017a; Franke et al., 2017; Gao et al., 2018; Gigante et al., 2019).

CPXV-No-H2 displays recombination events with OPXVs that were isolated from different places and species. CPXV-No-H2 is a strain from Northern Norway (Okeke et al., 2012). Its closest relatives CPXV_GerMygEK938_17 and CPXV_Ger2010_MKY were isolated in Germany, but they were isolated from different species: bank vole and cotton-top tamarin, respectively (Kalthoff et al., 2014; Jeske et al., 2019). It was suggested that the infection of cotton-top tamarin was mediated by bank vole infected with CPXV (Jeske et al., 2019; Weber et al., 2020). In contrast, AKPV was isolated from a human patient in North America (Alaska, the United States). The patient's infection source is unknown, but it is presumable that she was infected by a small mammal (Springer et al., 2017; Gigante et al., 2019). VACV and ECTV have been reported around the world (Dumbell and Richardson, 1993; Miranda et al., 2017; Mavian et al., 2021). ECTV infects laboratory mice worldwide (Trentin and Briody, 1953; Mavian et al., 2021; Wang et al., 2021). The first discovered ECTV strain, ECTV_Hampstead, was isolated in the United Kingdom and was the progenitor of the European outbreaks. Only one ECTV strain (ECTV_MouKre) was isolated from a wild mouse in Germany (Mavian et al., 2021). The worldwide presence of ECTV in animals suggests their presence also in Norwegian fauna and hence the possibility to recombine with CPXV.

Among the nine potential recombination events in the CPXV-No-H2 genome, two potential recombination events with the parental AKPV (putative recombination events 3 and 5) overlap with two potential recombination events with the parental ECTV (putative recombination events 6 and 7). Interestingly, in the same position of these recombinant regions, AKPV has undergone a potential recombination with ECTV, and it was suggested that ECTV contains an AKPV-like sequence (Gigante et al., 2019).

These recombinant regions (putative recombination events 5 and 8) contain the *atip* gene, which is one of the three genes (*atip*, *p4c*, and *A27L*) required for the formation of the V⁺ ATI phenotype (Patel and Pickup, 1987; McKelvey et al., 2002; Howard et al., 2010). CPXV-No-H2 contains an intact ECTV-like *atip*, *p4c*, and *A27L* genes. Those latter genes

were most similar to CPXV_GerMygEK938_17 genes. CPXV-No-H2 produces mainly virions encrusted on the surface of ATI ($V^{+/}$) similar to ECTV_Hampstead, which produces both V^+ and $V^{+/}$ ATI phenotype (Ichihashi and Matsumoto, 1966; Okeke et al., 2012; Mavian et al., 2021). ECTV_Hampstead encodes a full-length *p4c* protein compared to other ECTV isolates with V^- ATI phenotype. Besides this, it contains the *atip* and *A27L* genes (Mavian et al., 2021). AKPV and CPXV_Ger2010_MKY also comprise these three genes and produce the V^+ ATI phenotype (Franke et al., 2017; Springer et al., 2017; Gigante et al., 2019). There is no report of the production of ATI bodies in CPXV_GerMygEK938_17; however, its *atip*, *p4c*, and *A27L* genes are most similar to those of CPXV_Ger2010_MKY.

The potential recombination event between the parental AKPV and CPXV (putative recombinant event 6) located close to the terminal region contains part of the *NoH2-210* gene that shared similarity with *AKPV-203* and the Murmansk gene. *AKPV-203* is one of the three AKPV genes that may be introduced from/to Murmansk poxvirus by recombination (Gigante et al., 2019). Murmansk is a non-OPXV that belongs to the genus *Centapoxvirus* that was isolated in Murmansk, Russia (Smithson et al., 2017a). In three of the six recombination events with the parental AKPV (putative recombination events 1, 4, and 6), it seems that CPXV-No-H2 contains AKPV-like sequences rather than AKPV containing CPXV-No-H2-like sequences because the phylogenetic trees showed that CPXV-No-H2 is not part of the ECTV-Abatino-like clade and was placed next to AKPV (**Supplementary Figures 5, 8, 10**). In contrast, the overlapping recombinant regions seem to be CPXV-No-H2-like sequences that were introduced to AKPV based on the phylogenetic tree and the sequence similarity (**Supplementary Figures 7, 9, 11, 12**).

Reconstructing the evolutionary history of CPXV-No-H2 is difficult since it displays several potential recombination events with different OPXVs, especially when it is suspected that recombination events occurred between these OPXVs (such as AKPV and ECTV) (Gigante et al., 2019). Additionally, these OPXVs were isolated from different continents (Springer et al., 2017; Mavian et al., 2021). One plausible hypothesis about the mosaic genome of CPXV-No-H2 is that the CPXV_GerMygEK938_17-like virus was probably circulating in a population of rodents in Europe, and it underwent recombination with the AKPV-like virus. The resultant virus, CPXV-No-H2-like virus, could have suffered genomic changes and adapted to mice, which could be the possible ancestor of ECTV. The origin of ECTV from the CPXV-like ancestor was previously proposed (Jeske et al., 2019) since ECTV has a shorter genome (ranging from 204 to 208 kbp) and reduced number of genes compared to CPXV that has the largest genome among OPXVs, about 220 kbp (Chen et al., 2003; Hendrickson et al., 2010; Carroll et al., 2011; Dabrowski et al., 2013; Mavian et al., 2014, 2021). Our results suggest that CPXV-No-H2 could be derived from a CPXV_GerMygEK938_17-like virus because (1) CPXV_GerMygEK938_17 shares the highest similarity with CPXV-No-H2, (2) it did not show any significant recombination event (Kalthoff et al., 2014; Jeske et al., 2019), (3) none of the

seven recombination regions in CPXV-No-H2 was highly similar to either CPXV_GerMygEK938_17 or CPXV_Ger2010_MKY, (4) there is high similarity between their *p4c* and *A27L* genes, (5) its place of isolation was also in Europe, and (6) we speculated that it has V^+ ATI phenotype similar to CPXV_Ger2010_MKY due to the similarity between their *atip*, *p4c*, and *A27L* genes.

The recombination may have occurred between CPXV_GerMygEK938_17-like virus and AKPV-like virus rather than ECTV-like virus because, aside from two recombination events with the parental AKPV that overlapped a recombination event with the parental ECTV, there are other four recombinant events with the parental AKPV which cannot be viewed as a simple coincidence. In addition, the two suspected recombination regions in the ECTV genome (Gigante et al., 2019) were more similar to CPXV-No-H2 than AKPV (data not shown). Furthermore, hypothetically, CPXV_GerMygEK938_17 may produce V^+ ATI similar to AKPV, while CPXV-No-H2 and ECTV_Hampstead produce both V^+ and $V^{+/}$ ATI phenotypes (Ichihashi and Matsumoto, 1966; Okeke et al., 2012; Mavian et al., 2021). It seems that the putative progeny virus, CPXV-No-H2-like virus, may have reduced its ability to embed virions into ATI bodies. This was also observed in the derivatives of ECTV_Hampstead that produces the V^- ATI phenotype (Mavian et al., 2021). We speculated that the recombination between CPXV_GerMygEK938_17-like virus and AKPV-like virus could take place in a rodent in Europe because AKPV contains genes from a Russian poxvirus, Murmansk, which was isolated from a root vole (Smithson et al., 2017a; Gigante et al., 2019), and CPXV_GerMygEK938_17 was isolated from bank vole in Europe (Jeske et al., 2019). Furthermore, CPXV-No-H2 was isolated in Europe, likewise with CPXV_Ger2010_MKY and ECTV_Hampstead (the source of the European outbreaks) (Hansen et al., 2009; Okeke et al., 2012; Kalthoff et al., 2014; Mavian et al., 2021).

However, it is pertinent to note that recombination detection programs predict hypothetical recombination events across genomes, and the outputs are sensitive to input parameter settings, particularly the sliding window size. To increase the likelihood of putative recombination events being real, we recommend the following: (i) use of these programs at default settings, (ii) identification of the exact recombination event by at least two different programs and algorithms, (iii) discountenance of recombination events without very high statistical support, (iv) confirmation of recombination breakpoints by manual inspection of similarity plots, and (v) incongruence of phylogenetic trees.

Another explanation for the presence of the OPXV-like genomic regions in CPXV-No-H2 could be symplesiomorphy because most genomic regions were similar to more than one taxon—for instance, the two CPXV-No-H2 genomic regions that were similar to ECTV and AKPV may be inherited from a common ancestral virus, likewise with the AKPV-like genomic region that contains part of the *NoH2-210* similar to AKPV and Murmansk. However, symplesiomorphy does not explain the presence of the AKPV-like genomic region of 2,150 bp in CPXV-No-H2, which did not share high similarity with

other taxa. The only plausible explanation is that CPXV-No-H2 may have obtained this sequence from an AKPV-like virus by recombination.

Overall, the genetic analysis of the atypical CPXV-No-H2 suggested that it contains sequences similar to other OPXVs, and one of the plausible explanations for their presence was recombination events with other OPXVs. In addition, CPXV-No-H2 is part of a new CPXV clade that was more phylogenetically related to ECTV and OPXV Abatino than other CPXV strains. Our findings provide some insight into the evolutionary history of CPXV and strongly support the genetic heterogeneity of the species CPXV. The discovery of new CPXV isolates and their phylogenetic relationship with OPXVs as well their genomic characterization will contribute to the further elucidation of the complex evolutionary history of CPXV.

DATA AVAILABILITY STATEMENT

The original contributions presented in the study are publicly available. This data can be found here: <https://www.ncbi.nlm.nih.gov/genbank/OM460002>.

AUTHOR CONTRIBUTIONS

DD-C conducted the experiments, analyzed the data, and wrote the manuscript. MO and UM conceptualized the study,

supervised the design and execution of the project, and wrote the manuscript. AB and AN contributed to data interpretation and revision of the manuscript for improved intellectual content. All authors contributed to the article and approved the submitted version.

FUNDING

This study was supported by the University of Tromsø, the Arctic University of Norway (project A212100108) and the National Graduate School in Infection Biology and Antimicrobials (grant no. 249062). Article processing charge was paid UiT - The Arctic University of Norway.

ACKNOWLEDGMENTS

We thank Jessin Janice and Juan Daniel Montenegro Cabrera for their assistance during the bioinformatics analysis.

SUPPLEMENTARY MATERIAL

The Supplementary Material for this article can be found online at: <https://www.frontiersin.org/articles/10.3389/fmicb.2022.868887/full#supplementary-material>

REFERENCES

- Abrahão, J. S., Campos, R. K., De Souza Trindade, G., Da Fonseca, F. G., Ferreira, P. C. P., and Kroon, E. G. (2015). Outbreak of Severe Zoonotic Vaccinia Virus Infection, Southeastern Brazil. *Emerg. Infect. Dis.* 21:695. doi: 10.3201/EID2104.140351
- Alakunle, E., Moens, U., Nchinda, G., and Okeke, M. I. (2020). Monkeypox Virus in Nigeria: infection Biology, Epidemiology, and Evolution. *Viruses* 12:1211157. doi: 10.3390/V12111257
- Andrews, S. (2010). *A Quality Control tool for High Throughput Sequence Data*. Available online at: <https://www.bioinformatics.babraham.ac.uk/projects/fastqc/> (accessed October 16, 2020).
- Bankevich, A., Nurk, S., Antipov, D., Gurevich, A. A., Dvorkin, M., Kulikov, A. S., et al. (2012). SPAdes: a New Genome Assembly Algorithm and Its Applications to Single-Cell Sequencing. *J. Comput. Biol.* 19:477. doi: 10.1089/CMB.2012.0021
- Bolger, A. M., Lohse, M., and Usadel, B. (2014). Trimmomatic: a flexible trimmer for Illumina sequence data. *Bioinformatics* 30, 2114–2020. doi: 10.1093/BIOINFORMATICS/BTU170
- Boni, M. F., Posada, D., and Feldman, M. W. (2007). An Exact Nonparametric Method for Inferring Mosaic Structure in Sequence Triplets. *Genetics* 176, 1035–1047. doi: 10.1534/GENETICS.106.068874
- Camacho, C., Coulouris, G., Avagyan, V., Ma, N., Papadopoulos, J., Bealer, K., et al. (2009). BLAST+: architecture and applications. *BMC Bioinform.* 10:421. doi: 10.1186/1471-2105-10-421
- Cardeti, G., Gruber, C. E. M., Eleni, C., Carletti, F., Castilletti, C., Manna, G., et al. (2017). Fatal Outbreak in Tonkean Macaques Caused by Possibly Novel Orthopoxvirus, Italy, January 2015 - Volume 23, Number 12—December 2017 - Emerging Infectious Diseases journal - CDC. *Emerg. Infect. Dis.* 23, 1941–1949. doi: 10.3201/EID2312.162098
- Carroll, D. S., Emerson, G. L., Li, Y., Sammons, S., Olson, V., Frace, M., et al. (2011). Chasing Jenner's vaccine: Revisiting Cowpox virus classification. *PLoS One* 6, 4–9. doi: 10.1371/journal.pone.0023086
- Chantrey, J., Meyer, H., Baxby, D., Begon, M., Bown, K. J., Hazel, S. M., et al. (1999). Cowpox: reservoir hosts and geographic range. *Epidemiol. Infect.* 122:455. doi: 10.1017/S0950268899002423
- Chen, N., Danila, M. I., Feng, Z., Buller, R. M. L., Wang, C., Han, X., et al. (2003). The genomic sequence of ectromelia virus, the causative agent of mousepox. *Virology* 317, 165–186. doi: 10.1016/S0042-6822(03)00520-8
- Coulson, D., and Upton, C. (2011). Characterization of indels in poxvirus genomes. *Virus Genes* 42, 171–177. doi: 10.1007/S11262-010-0560-X/FIGURES/4
- Dabrowski, P. W., Radonić, A., Kurth, A., and Nitsche, A. (2013). Genome-wide comparison of cowpox viruses reveals a new clade related to variola virus. *PLoS One* 8, 1–9. doi: 10.1371/journal.pone.0079953
- Damaso, C. R. A., Reis, S. A., Jesus, D. M., Lima, P. S. F., and Moussatché, N. (2007). A PCR-based assay for detection of emerging vaccinia-like viruses isolated in Brazil. *Diagn. Microbiol. Infect. Dis.* 57, 39–46. doi: 10.1016/J.DIAGMICROBIO.2006.07.012
- Darriba, D., Posada, D., Kozlov, A. M., Stamatakis, A., Morel, B., and Flouri, T. (2020). ModelTest-NG: A New and Scalable Tool for the Selection of DNA and Protein Evolutionary Models. *Mol. Biol. Evol.* 37:294. doi: 10.1093/MOLBEV/MSZ189
- Diaz, J. H. (2021). The Disease Ecology, Epidemiology, Clinical Manifestations, Management, Prevention, and Control of Increasing Human Infections with Animal Orthopoxviruses. *Wilderness Environ. Med.* 32, 528–536. doi: 10.1016/J.WEM.2021.08.003
- Dumbell, K., and Richardson, M. (1993). Virological investigations of specimens from buffaloes affected by buffalopox in Maharashtra State, India between 1985 and 1987. *Arch. Virol.* 128, 257–267. doi: 10.1007/BF01309438
- Durski, K. N., McCollum, A. M., Nakazawa, Y., Petersen, B. W., Reynolds, M. G., Briand, S., et al. (2018). Emergence of Monkeypox — West and Central

- Africa, 1970–2017. *Morb. Mortal. Wkly. Rep.* 67:310. doi: 10.15585/MMWR.MM6710A5
- Ehlers, A., Osborne, J., Slack, S., Roper, R. L., and Upton, C. (2002). Poxvirus Orthologous Clusters (POCs). *Bioinformatics* 18, 1544–1545. doi: 10.1093/BIOINFORMATICS/18.11.1544
- Emms, D. M., and Kelly, S. (2015). OrthoFinder: solving fundamental biases in whole genome comparisons dramatically improves orthogroup inference accuracy. *Genome Biol.* 16:2. doi: 10.1186/S13059-015-0721-2
- Erez, N., Achdout, H., Milrot, E., Schwartz, Y., Wiener-Well, Y., Paran, N., et al. (2019). Diagnosis of Imported Monkeypox, Israel, 2018. *Emerg. Infect. Dis.* 25:980. doi: 10.3201/EID2505.190076
- Ferrier, A., Frenois-Veyrat, G., Schvoerer, E., Henard, S., Jarjaval, F., Drouet, I., et al. (2021). Fatal cowpox virus infection in human fetus, France, 2017. *Emerg. Infect. Dis.* 27, 2570–2577. doi: 10.3201/eid2710.204818
- Franke, A., Pfaff, F., Jenckel, M., Hoffmann, B., Höper, D., Antwerpen, M., et al. (2017). Classification of cowpox viruses into several distinct clades and identification of a novel lineage. *Viruses* 9, 1–14. doi: 10.3390/v9060142
- Gao, J., Gigante, C., Khmaladze, E., Liu, P., Tang, S., Wilkins, K., et al. (2018). Genome sequences of Akhmeta virus, an early divergent old world orthopoxvirus. *Viruses* 10:50252. doi: 10.3390/v10050252
- Gibbs, M. J., Armstrong, J. S., and Gibbs, A. J. (2000). Sister-Scanning: a Monte Carlo procedure for assessing signals in recombinant sequences. *Bioinformatics* 16, 573–582. doi: 10.1093/BIOINFORMATICS/16.7.573
- Gigante, C. M., Gao, J., Tang, S., McCollum, A. M., Wilkins, K., Reynolds, M. G., et al. (2019). Genome of Alaskapox Virus, a Novel Orthopoxvirus Isolated from Alaska. *Viruses* 11:1080708. doi: 10.3390/V111080708
- Girling, S. J., Pizzi, R., Cox, A., and Beard, P. M. (2011). Fatal cowpox virus infection in two squirrel monkeys (*Saimiri sciureus*). *Vet. Rec.* 169, 156–156. doi: 10.1136/VR.D4005
- Gubser, C., Hué, S., Kellam, P., and Smith, G. L. (2004). Poxvirus genomes: A phylogenetic analysis. *J. Gen. Virol.* 85, 105–117. doi: 10.1099/VIR.0.19565-0/CITE/REFWORKS
- Hansen, H., Okeke, M. I., Nilssen, O., and Traavik, T. (2009). Comparison and phylogenetic analysis of cowpox viruses isolated from cats and humans in Fennoscandia. *Arch. Virol.* 154, 1293–1302. doi: 10.1007/S00705-009-0442-5/FIGURES/3
- Hendrickson, R. C., Wang, C., Hatcher, E. L., and Lefkowitz, E. J. (2010). Orthopoxvirus Genome Evolution: the Role of Gene Loss. *Viruses* 2, 1933–1967. doi: 10.3390/V2091933
- Howard, A. R., Weisberg, A. S., and Moss, B. (2010). Congregation of Orthopoxvirus Virions in Cytoplasmic A-Type Inclusions Is Mediated by Interactions of a Bridging Protein (A26p) with a Matrix Protein (AT1p) and a Virion Membrane-Associated Protein (A27p). *J. Virol.* 84:7592. doi: 10.1128/JVI.00704-10
- Ichihashi, Y., and Matsumoto, S. (1966). Studies on the nature of marchal bodies (A-type inclusion) during ectromelia virus infection. *Virology* 29, 264–275. doi: 10.1016/0042-6822(66)90033-X
- Jacobs, B. L., Langland, J. O., Kibler, K. V., Denzler, K. L., White, S. D., Holechek, S. A., et al. (2009). Vaccinia virus vaccines: past, present and future. *Antiviral Res.* 84, 1–13. doi: 10.1016/J.ANTIVIRAL.2009.06.006
- Jeske, K., Weber, S., Pfaff, F., Imholt, C., Jacob, J., Beer, M., et al. (2019). Molecular Detection and Characterization of the First Cowpox Virus Isolate Derived from a Bank Vole. *Viruses* 11:1111075. doi: 10.3390/V11111075
- Kalthan, E., Tenguere, J., Ndjapou, S. G., Koyazengbe, T. A., Mbomba, J., Marada, R. M., et al. (2018). Investigation of an outbreak of monkeypox in an area occupied by armed groups, Central African Republic. *Méd. Mal. Infect.* 48, 263–268. doi: 10.1016/J.MEDMAL.2018.02.010
- Kalthoff, D., Bock, W. I., Hühn, F., Beer, M., and Hoffmann, B. (2014). Fatal cowpox virus infection in cotton-top tamarins (*Saguinus oedipus*) in Germany. *Vector-Borne Zoonotic Dis.* 14, 303–305. doi: 10.1089/VBZ.2013.1442
- Katoh, K., and Standley, D. M. (2013). MAFFT Multiple Sequence Alignment Software Version 7: improvements in Performance and Usability. *Mol. Biol. Evol.* 30, 772–780. doi: 10.1093/MOLBEV/MST010
- Kinnunen, P. M., Henttonen, H., Hoffmann, B., Kallio, E. R., Korhase, C., Laakkonen, J., et al. (2011). Orthopox Virus Infections in Eurasian Wild Rodents. *Vector Borne Zoonotic Dis.* 11, 1133–1140. doi: 10.1089/VBZ.2010.0170
- Laakkonen, J., Kallio-Kokko, H., Öktem, M. A., Blasdel, K., Plyusnina, A., Niemimaa, J., et al. (2006). Serological Survey for Viral Pathogens in Turkish Rodents. *J. Wildl. Dis.* 42, 672–676. doi: 10.7589/0090-3558-42.3.672
- Li, H., and Durbin, R. (2009). Fast and accurate short read alignment with Burrows–Wheeler transform. *Bioinformatics* 25, 1754–1760. doi: 10.1093/BIOINFORMATICS/BTP324
- Lim, T. H., Lee, H. J., Lee, D. H., Lee, Y. N., Park, J. K., Youn, H. N., et al. (2011). An emerging recombinant cluster of nephropathogenic strains of avian infectious bronchitis virus in Korea. *Infect. Genet. Evol.* 11, 678–685. doi: 10.1016/J.MEEGID.2011.01.007
- Lole, K. S., Bollinger, R. C., Paranjape, R. S., Gadkari, D., Kulkarni, S. S., Novak, N. G., et al. (1999). Full-Length Human Immunodeficiency Virus Type 1 Genomes from Subtype C-Infected Seroconverters in India, with Evidence of Intersubtype Recombination. *J. Virol.* 73:160. doi: 10.1128/jvi.73.1.152-160.1999
- MacLachlan, N. J., and Dubovi, E. J. (eds) (2017). “Poxviridae,” in *Fenner’s Veterinary Virology*, (Boston: Academic Press), 157–174. doi: 10.1016/B978-0-12-800946-8.00007-6
- Martin, D. P., Murrell, B., Golden, M., Khoosal, A., and Muhire, B. (2015). RDP4: Detection and analysis of recombination patterns in virus genomes. *Virus Evol.* 1:3. doi: 10.1093/VE/VEV003
- Martin, D. P., Posada, D., Crandall, K. A., and Williamson, C. (2005). A Modified Bootscan Algorithm for Automated Identification of Recombinant Sequences and Recombination Breakpoints. *AIDS Res. Hum. Retrovir.* 21, 98–102. doi: 10.1089/AID.2005.21.98
- Martin, D., and Rybicki, E. (2000). RDP: detection of recombination amongst aligned sequences. *Bioinformatics* 16, 562–563. doi: 10.1093/BIOINFORMATICS/16.6.562
- Mauldin, M. R., Antwerpen, M., Emerson, G. L., Li, Y., Zoeller, G., Carroll, D. S., et al. (2017). Cowpox virus: What’s in a Name? *Viruses* 2017:101. doi: 10.3390/V9050101
- Mavian, C., López-Bueno, A., Bryant, N. A., Seeger, K., Quail, M. A., Harris, D., et al. (2014). The genome sequence of ectromelia virus Naval and Cornell isolates from outbreaks in North America. *Virology* 462–463, 218–226. doi: 10.1016/j.virol.2014.06.010
- Mavian, C., López-Bueno, A., Martin, R., Nitsche, A., and Alcamí, A. (2021). Comparative pathogenesis, genomics and phylogeography of mousepox. *Viruses* 13:13061146. doi: 10.3390/v13061146
- McKelvey, T. A., Andrews, S. C., Miller, S. E., Ray, C. A., and Pickup, D. J. (2002). Identification of the Orthopoxvirus p4c Gene, Which Encodes a Structural Protein That Directs Intracellular Mature Virus Particles into A-Type Inclusions. *J. Virol.* 76:11216. doi: 10.1128/JVI.76.22.11216-11225.2002
- Megid, J., Borges, I. A., Abrahão, J. S., Trindade, G. S., Appolinário, C. M., Ribeiro, M. G., et al. (2012). Vaccinia Virus Zoonotic Infection, São Paulo State, Brazil. *Emerg. Infect. Dis.* 18:189. doi: 10.3201/EID1801.110692
- Miranda, J. B., Borges, I. A., Campos, S. P. S., Vieira, F. N., De Ázara, T. M. F., Marques, F. A., et al. (2017). Serologic and Molecular Evidence of Vaccinia Virus Circulation among Small Mammals from Different Biomes, Brazil. *Emerg. Infect. Dis.* 23:931. doi: 10.3201/EID2306.161643
- Nakoune, E., Lampaert, E., Ndjapou, S. G., Janssens, C., Zuniga, I., Van Herp, M., et al. (2017). A Nosocomial Outbreak of Human Monkeypox in the Central African Republic. *Open Forum Infect. Dis.* 4:168. doi: 10.1093/OFID/OFX168
- Ng, O. T., Lee, V., Marimuthu, K., Vasoo, S., Chan, G., Lin, R. T. P., et al. (2019). A case of imported Monkeypox in Singapore. *Lancet. Infect. Dis.* 19:1166. doi: 10.1016/S1473-3099(19)30537-7
- Okeke, M. I., Hansen, H., and Traavik, T. (2012). A naturally occurring cowpox virus with an ectromelia virus A-type inclusion protein gene displays atypical A-type inclusions. *Infect. Genet. Evol.* 12, 160–168. doi: 10.1016/J.MEEGID.2011.09.017
- Okeke, M. I., Okoli, A. S., Nilssen, O., Moens, U., Tryland, M., Bøhn, T., et al. (2014). Molecular characterization and phylogenetics of Fennoscandian cowpox virus isolates based on the p4c and atip genes. *Virol. J.* 11, 1–16. doi: 10.1186/1743-422X-11-119/TABLES/5
- Padidam, M., Sawyer, S., and Fauquet, C. M. (1999). Possible Emergence of New Geminiviruses by Frequent Recombination. *Virology* 265, 218–225. doi: 10.1006/VIRO.1999.0056

- Patel, D. D., and Pickup, D. J. (1987). Messenger RNAs of a strongly-expressed late gene of cowpox virus contain 5'-terminal poly(A) sequences. *EMBO J.* 6:3787. doi: 10.1002/J.1460-2075.1987.TB02714.X
- Popova, A. Y., Maksyutov, R. A., Taranov, O. S., Tregubchak, T. V., Zaikovskaya, A. V., Sergeev, A. A., et al. (2017). Cowpox in a human, Russia, 2015. *Epidemiol. Infect.* 145, 755–759. doi: 10.1017/S0950268816002922
- Posada, D., and Crandall, K. A. (2001). Evaluation of methods for detecting recombination from DNA sequences: Computer simulations. *Proc. Natl. Acad. Sci.* 98, 13757–13762. doi: 10.1073/PNAS.241370698
- Prkno, A., Hoffmann, D., Goerigk, D., Kaiser, M., van Maanen, A. C. F., Jeske, K., et al. (2017). Epidemiological investigations of four cowpox virus outbreaks in alpaca herds, Germany. *Viruses* 9, 1–15. doi: 10.3390/v9110344
- Qin, L., Favis, N., Famulski, J., and Evans, D. H. (2015). Evolution of and Evolutionary Relationships between Extant Vaccinia Virus Strains. *J. Virol.* 89:1809. doi: 10.1128/JVI.02797-14
- Qin, L., Upton, C., Hazes, B., and Evans, D. H. (2011). Genomic Analysis of the Vaccinia Virus Strain Variants Found in Dryvax Vaccine. *J. Virol.* 85:13049. doi: 10.1128/JVI.05779-11
- Rambaut, A. (2018). *FigTree*. Available online at: <http://tree.bio.ed.ac.uk/software/figtree/> [accessed February 19, 2021]
- Reynolds, M. G., Guagliardo, S. A. J., Nakazawa, Y. J., Doty, J. B., and Mauldin, M. R. (2018). Understanding orthopoxvirus host range and evolution: from the enigmatic to the usual suspects. *Curr. Opin. Virol.* 28, 108–115. doi: 10.1016/j.COVIRO.2017.11.012
- Ronquist, F., Teslenko, M., Van Der Mark, P., Ayres, D. L., Darling, A., Höhna, S., et al. (2012). MrBayes 3.2: Efficient Bayesian Phylogenetic Inference and Model Choice Across a Large Model Space. *Syst. Biol.* 61, 539–542. doi: 10.1093/SYSBIO/SYS029
- Silva, N. I. O., de Oliveira, J. S., Kroon, E. G., Trindade, G., de, S., and Drummond, B. P. (2021). Here, There, and Everywhere: The Wide Host Range and Geographic Distribution of Zoonotic Orthopoxviruses. *Viruses* 2021:13. doi: 10.3390/V13010043
- Smith, J. M. (1992). Analyzing the mosaic structure of genes. *J. Mol. Evol.* 34, 126–129. doi: 10.1007/BF00182389
- Smith, K. C., Bennett, M., and Garrett, D. C. (1999). Skin lesions caused by orthopoxvirus infection in a dog. *J. Small Anim. Pract.* 40, 495–497. doi: 10.1111/J.1748-5827.1999.TB03003.X
- Smithson, C., Tang, N., Sammons, S., Frace, M., Batra, D., Li, Y., et al. (2017b). The genomes of three North American orthopoxviruses. *Virus Genes* 53, 21–34. doi: 10.1007/S11262-016-1388-9/TABLES/2
- Smithson, C., Meyer, H., Gigante, C. M., Gao, J., Zhao, H., Batra, D., et al. (2017a). Two novel poxviruses with unusual genome rearrangements: NY_014 and Murmansk. *Virus Genes* 53, 883–897. doi: 10.1007/S11262-017-1501-8/FIGURES/5
- Smithson, C., Purdy, A., Verster, A. J., and Upton, C. (2014). Prediction of Steps in the Evolution of Variola Virus Host Range. *PLoS One* 9:e91520. doi: 10.1371/JOURNAL.PONE.0091520
- Springer, Y. P., Hsu, C. H., Werle, Z. R., Olson, L. E., Cooper, M. P., Castrodale, L. J., et al. (2017). Novel Orthopoxvirus Infection in an Alaska Resident. *Clin. Infect. Dis. An Off. Publ. Infect. Dis. Soc. Am.* 64:1737. doi: 10.1093/CID/CIX219
- Stamatakis, A. (2014). RAXML version 8: a tool for phylogenetic analysis and post-analysis of large phylogenies. *Bioinformatics* 30:1313. doi: 10.1093/BIOINFORMATICS/BTU033
- Strassburg, M. A. (1982). The global eradication of smallpox. *Am. J. Infect. Control* 10, 53–59. doi: 10.1016/0196-6553(82)90003-7
- Talavera, G., and Castresana, J. (2007). Improvement of Phylogenies after Removing Divergent and Ambiguously Aligned Blocks from Protein Sequence Alignments. *Syst. Biol.* 56, 564–577. doi: 10.1080/10635150701472164
- Therapepanov, V., Ehlers, A., and Upton, C. (2006). Genome Annotation Transfer Utility (GATU): rapid annotation of viral genomes using a closely related reference genome. *BMC Gen.* 7:150. doi: 10.1186/1471-2164-7-150
- Trentin, J. J., and Briody, B. A. (1953). An outbreak of mouse-pox (infectious ectromelia) in the United States: II. *Definit. Diag.* 1953, 227. doi: 10.1126/science.117.3035.227
- Tryland, M., Myrmet, H., Holtet, L., Haukenes, G., and Traavik, T. (1998). Clinical cowpox cases in Norway. *Scand. J. Infect. Dis.* 30, 301–303. doi: 10.1080/00365549850160972
- Vaughan, A., Aarons, E., Astbury, J., Balasegaram, S., Beadsworth, M., Beck, C. R., et al. (2018). Two cases of monkeypox imported to the United Kingdom, September 2018. *Eurosurveillance* 23:1800509. doi: 10.2807/1560-7917.ES.2018.23.38.1800509
- Vora, N. M., Li, Y., Geleishvili, M., Emerson, G. L., Khmaladze, E., Maghlakelidze, G., et al. (2015). Human Infection with a Zoonotic Orthopoxvirus in the Country of Georgia. *N. Engl. J. Med.* 372:1223. doi: 10.1056/NEJM0A1407647
- Vorou, R. M., Papavassiliou, V. G., and Pierroutsakos, I. N. (2008). Cowpox virus infection: An emerging health threat. *Curr. Opin. Infect. Dis.* 21, 153–156. doi: 10.1097/QCO.0B013E3282F44C74
- Wang, J., Liu, X., Zhu, Q., Wu, Q., Tang, S., Zhang, L., et al. (2021). Identification, Isolation, and Characterization of an Ectromelia Virus New Strain from an Experimental Mouse. *Virol. Sin.* 36, 155–158. doi: 10.1007/s12250-020-00263-w
- Weber, S., Jeske, K., Ulrich, R. G., Imholt, C., Jacob, J., Beer, M., et al. (2020). In vivo characterization of a bank vole-derived cowpox virus isolate in natural hosts and the rat model. *Viruses* 12:12020237. doi: 10.3390/v12020237
- Wingett, S. W., and Andrews, S. (2018). FastQ Screen: a tool for multi-genome mapping and quality control. *F1000Research* 7:1338. doi: 10.12688/F1000RESEARCH.15931.2
- Wolfs, T. F. W., Wagenaar, J. A., Niesters, H. G. M., and Osterhaus, A. D. M. E. (2002). Rat-to-Human Transmission of Cowpox Infection. *Emerg. Infect. Dis.* 8:1495. doi: 10.3201/EID0812.020089
- Yinka-Ogunleye, A., Aruna, O., Dalhat, M., Ogoina, D., McCollum, A., Disu, Y., et al. (2019). Outbreak of human monkeypox in Nigeria in 2017–18: a clinical and epidemiological report. *Lancet Infect. Dis.* 19, 872–879. doi: 10.1016/S1473-3099(19)30294-4

Conflict of Interest: The authors declare that the research was conducted in the absence of any commercial or financial relationships that could be construed as a potential conflict of interest.

Publisher's Note: All claims expressed in this article are solely those of the authors and do not necessarily represent those of their affiliated organizations, or those of the publisher, the editors and the reviewers. Any product that may be evaluated in this article, or claim that may be made by its manufacturer, is not guaranteed or endorsed by the publisher.

Copyright © 2022 Diaz-Cánova, Moens, Brinkmann, Nitsche and Okeke. This is an open-access article distributed under the terms of the Creative Commons Attribution License (CC BY). The use, distribution or reproduction in other forums is permitted, provided the original author(s) and the copyright owner(s) are credited and that the original publication in this journal is cited, in accordance with accepted academic practice. No use, distribution or reproduction is permitted which does not comply with these terms.

Supplementary Material

1 Supplementary Figures

Supplementary Figure S1. Schematic diagram of alignment of CPXV-No-H2, CPXV_GerMygEK938_17, CPXV_Ger2010_MKY and ECTV_Mos showing the *NoH2-163* gene and their homologs, using Geneious software 2021.2.2. Grey regions indicate conserved bases while colors (red, blue, yellow, green) indicate differences (A, C, G, T, respectively) from CPXV-No-H2.

Supplementary Figure S2. Maximum-Likelihood phylogenetic tree based on 76 orthopoxvirus whole genomes. Bootstrap values were determined from 1000 replica sampling. *Cowpox virus* (CPXV) strains were grouped into different clades: CPXV-like 1, CPXV-like 2, and VARV-like (Franke et al., 2017). The scale bar represents expected substitutions per site.

Supplementary Figure S3. Maximum-Likelihood phylogenetic tree on 76 orthopoxvirus core genomes. Bootstrap values were determined from 1000 replica sampling. *Cowpox virus* (CPXV) strains were grouped into different clades: CPXV-like 1, CPXV-like 2, and VARV-like (Franke et al., 2017). The scale bar represents expected substitutions per site.

Supplementary Figure S4. Maximum-Likelihood phylogenetic tree of 134 orthopoxvirus orthologous genes. Bootstrap values were determined from 1000 replica sampling. *Cowpox virus* (CPXV) strains were grouped into different clades: CPXV-like 1, CPXV-like 2, and VARV-like (Franke et al., 2017). The scale bar represents expected substitutions per site.

Supplementary Figure S5. Maximum-Likelihood phylogenetic tree based on the putative recombinant region 1 between the parental AKPV and CPXV (potential recombinant event 1). Bootstrap values were determined from 1000 replica sampling. Clades are identified with colors.

Supplementary Figure S6. Maximum-Likelihood phylogenetic tree based on the putative recombinant region 2 between the parental AKPV and CPXV (potential recombinant event 2). Bootstrap values were determined from 1000 replica sampling. Clades are identified with colors.

Supplementary Figure S7. Maximum-Likelihood phylogenetic tree based on the putative recombinant region 3 between the parental AKPV and CPXV (potential recombinant event 3). Bootstrap values were determined from 1000 replica sampling. Clades are identified with colors.

Supplementary Figure S8. Maximum-Likelihood phylogenetic tree based on the putative recombinant region 4 between the parental AKPV and CPXV (potential recombinant event 4). Bootstrap values were determined from 1000 replica sampling. Clades are identified with colors.

Supplementary Figure S9. Maximum-Likelihood phylogenetic tree based on the putative recombinant region 5 between the parental AKPV and CPXV (potential recombinant event 5). Bootstrap values were determined from 1000 replica sampling. Clades are identified with colors.

Supplementary Figure S10. Maximum-Likelihood phylogenetic tree based on the putative recombinant region 6 between the parental AKPV and CPXV (potential recombinant event 6). Bootstrap values were determined from 1000 replica sampling. Clades are identified with colors.

Supplementary Figure S11. Maximum-Likelihood phylogenetic tree based on the putative recombinant region 1 between the parental ECTV and CPXV (potential recombinant event 7). Bootstrap values were determined from 1000 replica sampling. Clades are identified with colors.

Supplementary Figure S12. Maximum-Likelihood phylogenetic tree based on the putative recombinant region 2 between the parental ECTV and CPXV (potential recombinant event 8). Bootstrap values were determined from 1000 replica sampling. Clades are identified with colors.

Supplementary Figure S13. Maximum-Likelihood phylogenetic tree based on the putative recombinant region between the parental VACV and CPXV (potential recombinant event 9). Bootstrap values were determined from 1000 replica sampling. Clades are identified with colors.

Supplementary Figure S14. Maximum-Likelihood phylogenetic tree based on 75 OPXV whole genomes. Bootstrap values were determined from 1000 replica sampling. Clades are identified with colors.

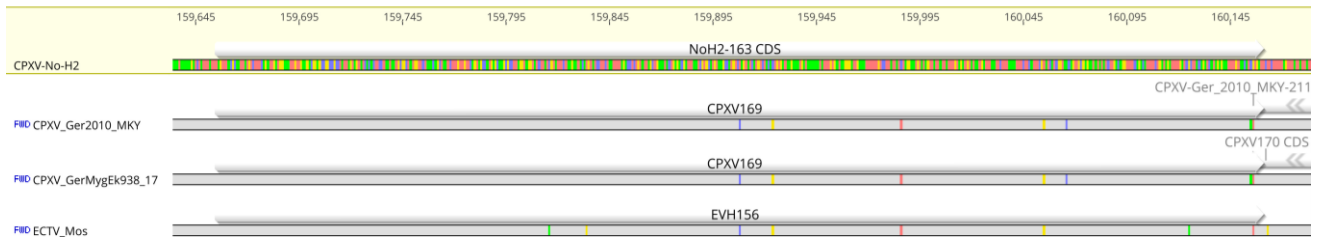
Supplementary Figure S15. Bayesian Inference phylogenetic tree based on 75 OPXV whole genomes. Clades are identified with colors.

Supplementary Figure S16. Maximum-Likelihood phylogenetic tree based on 75 OPXV core genomes. Bootstrap values were determined from 1000 replica sampling. Clades are identified with colors.

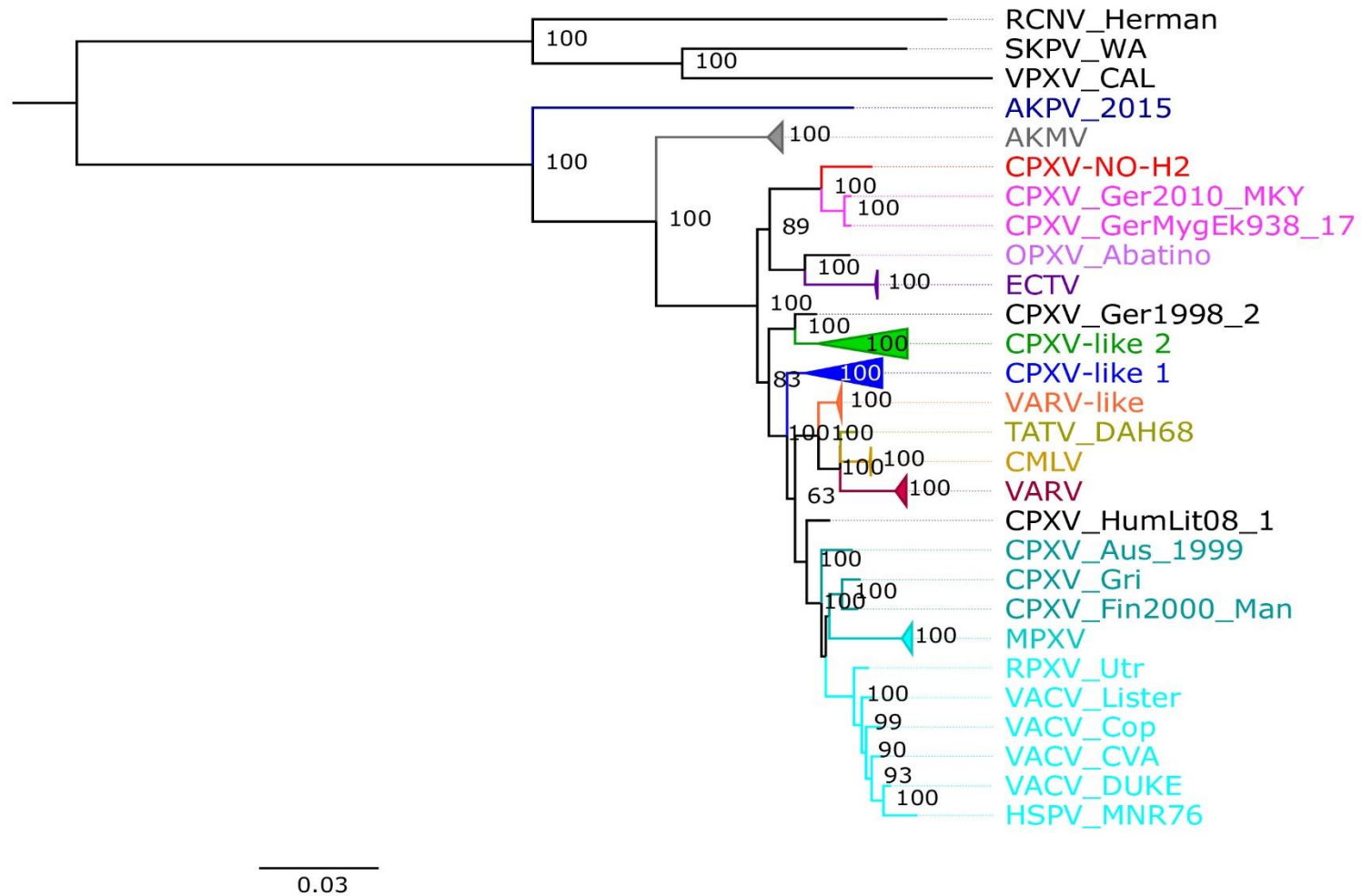
Supplementary Figure S17. Bayesian Inference phylogenetic tree based on 75 OPXV core genomes. Clades are identified with colors.

Supplementary Figure S18. Maximum-Likelihood phylogenetic tree based on 134 orthologous genes from 75 OPXV genomes. Bootstrap values were determined from 1000 replica sampling. Clades are identified with colors.

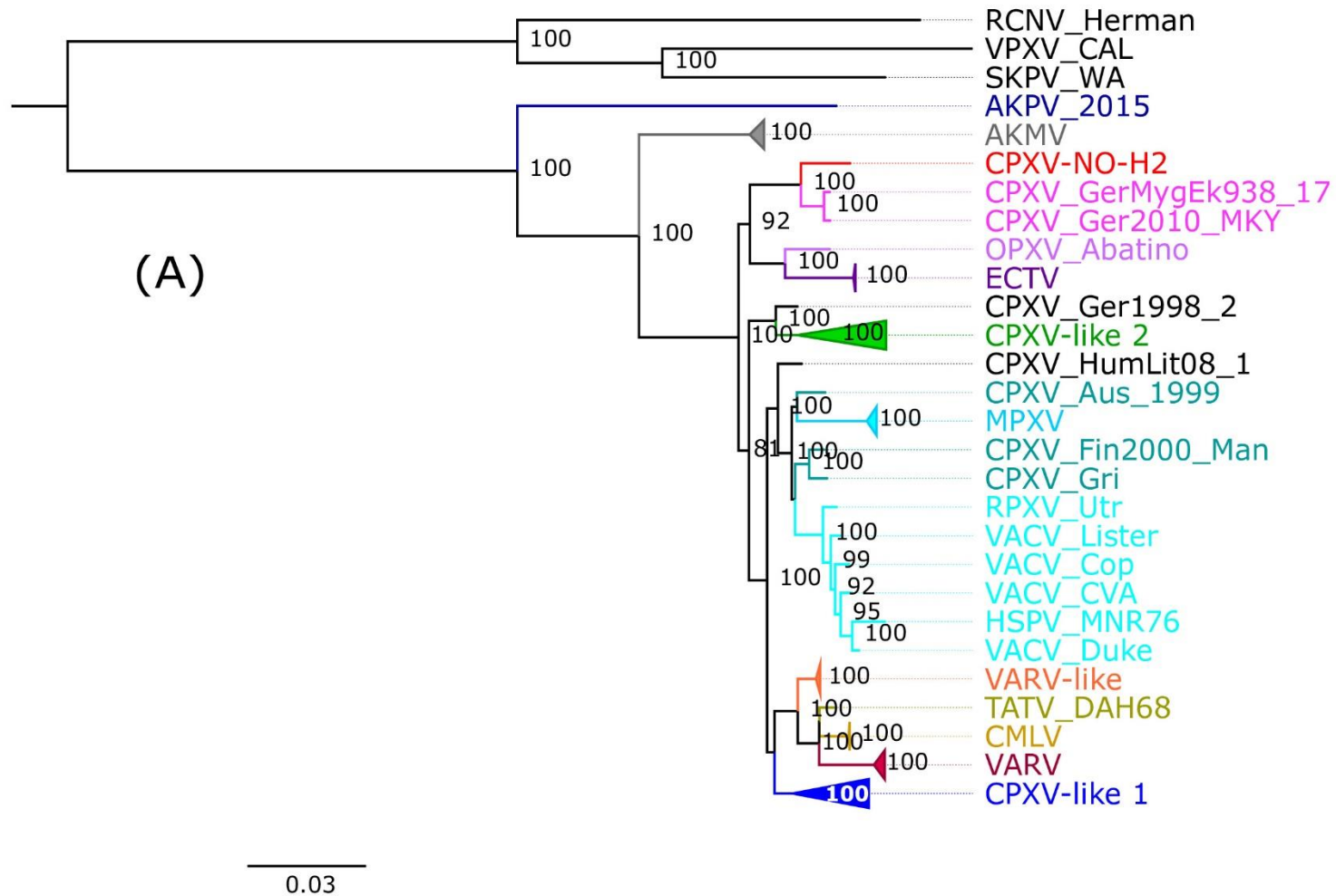
Supplementary Figure S19. Bayesian Inference phylogenetic tree based on 134 orthologous genes from 75 OPXV genomes. Clades are identified with colors.



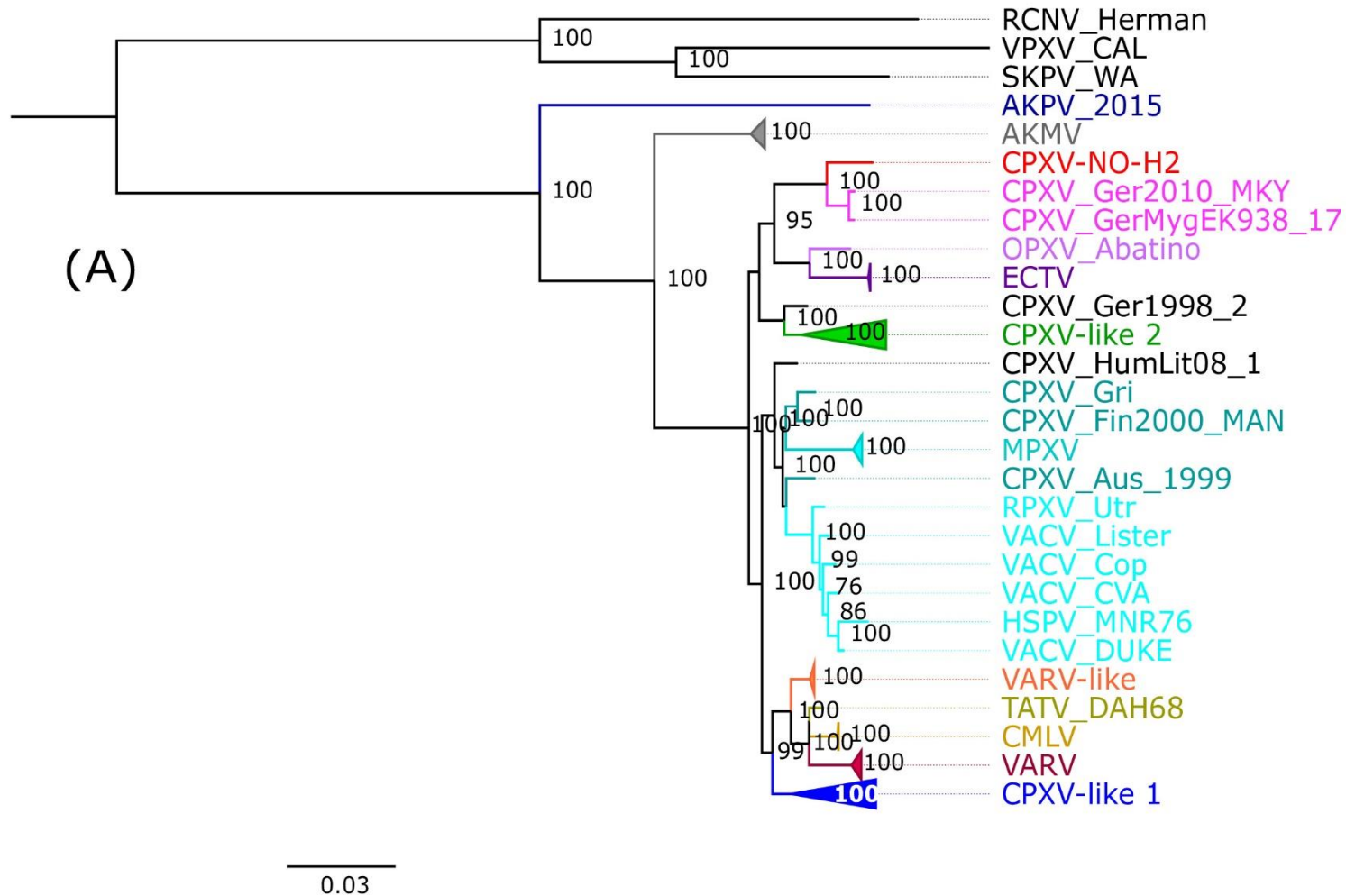
Supplementary Figure S1. Schematic diagram of alignment of CPXV-No-H2, CPXV_GerMygEK938_17, CPXV_Ger2010_MKY and ECTV_Mos showing the *NoH2-163* gene and their homologs, using Geneious software 2021.2.2. Grey regions indicate conserved bases while colors (red, blue, yellow, green) indicate differences (A, C, G, T, respectively) from CPXV-No-H2.



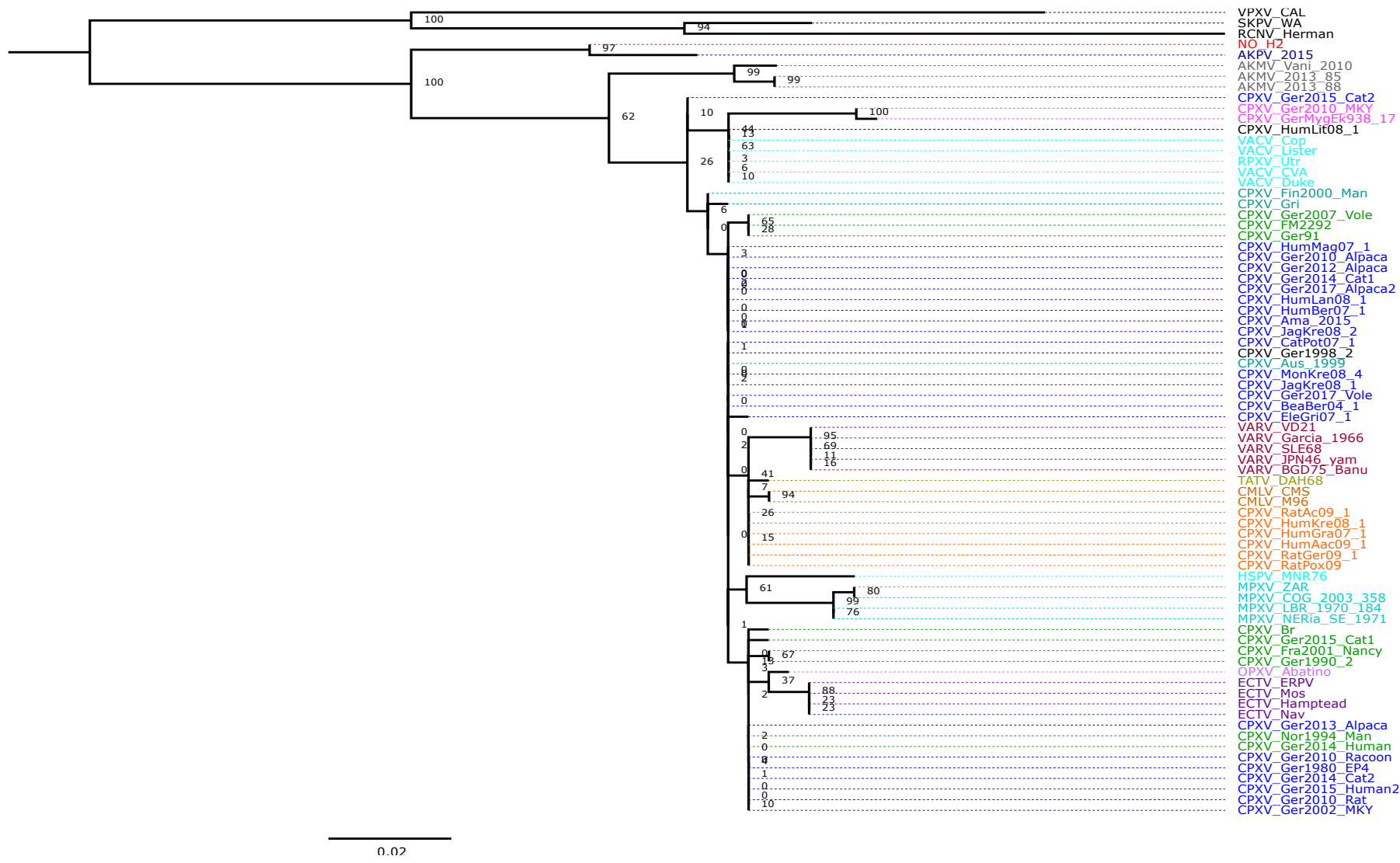
Supplementary Figure S2. Maximum-Likelihood phylogenetic tree based on 76 orthopoxvirus whole genomes. Bootstrap values were determined from 1000 replica sampling. *Cowpox virus* (CPXV) strains were grouped into different clades: CPXV-like 1, CPXV-like 2, and VARV-like (Franke et al., 2017). The scale bar represents expected substitutions per site.



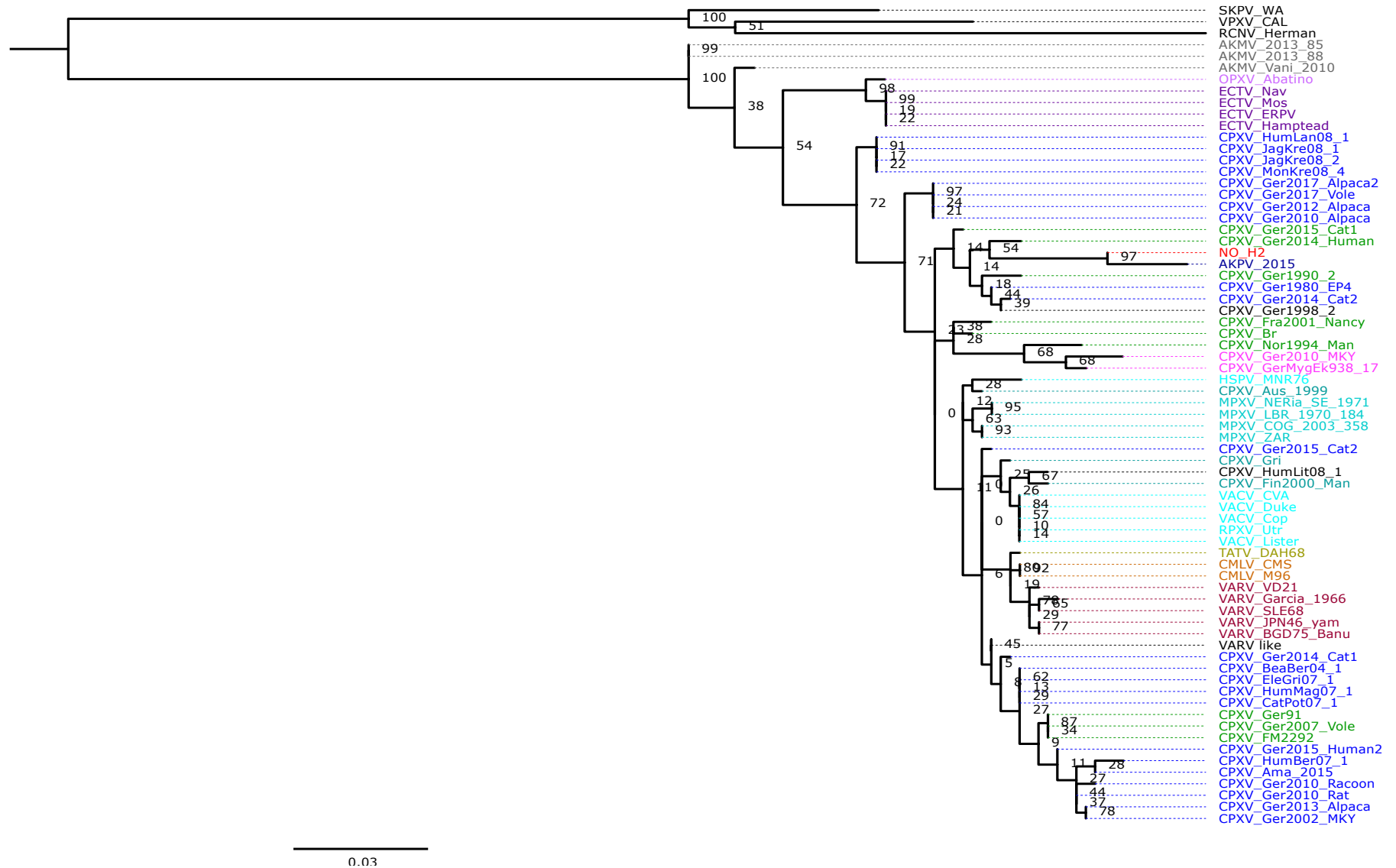
Supplementary Figure S3. Maximum-Likelihood phylogenetic tree on 76 orthopoxvirus core genomes. Bootstrap values were determined from 1000 replica sampling. *Cowpox virus* (CPXV) strains were grouped into different clades: CPXV-like 1, CPXV-like 2, and VARV-like (Franke et al., 2017). The scale bar represents expected substitutions per site.



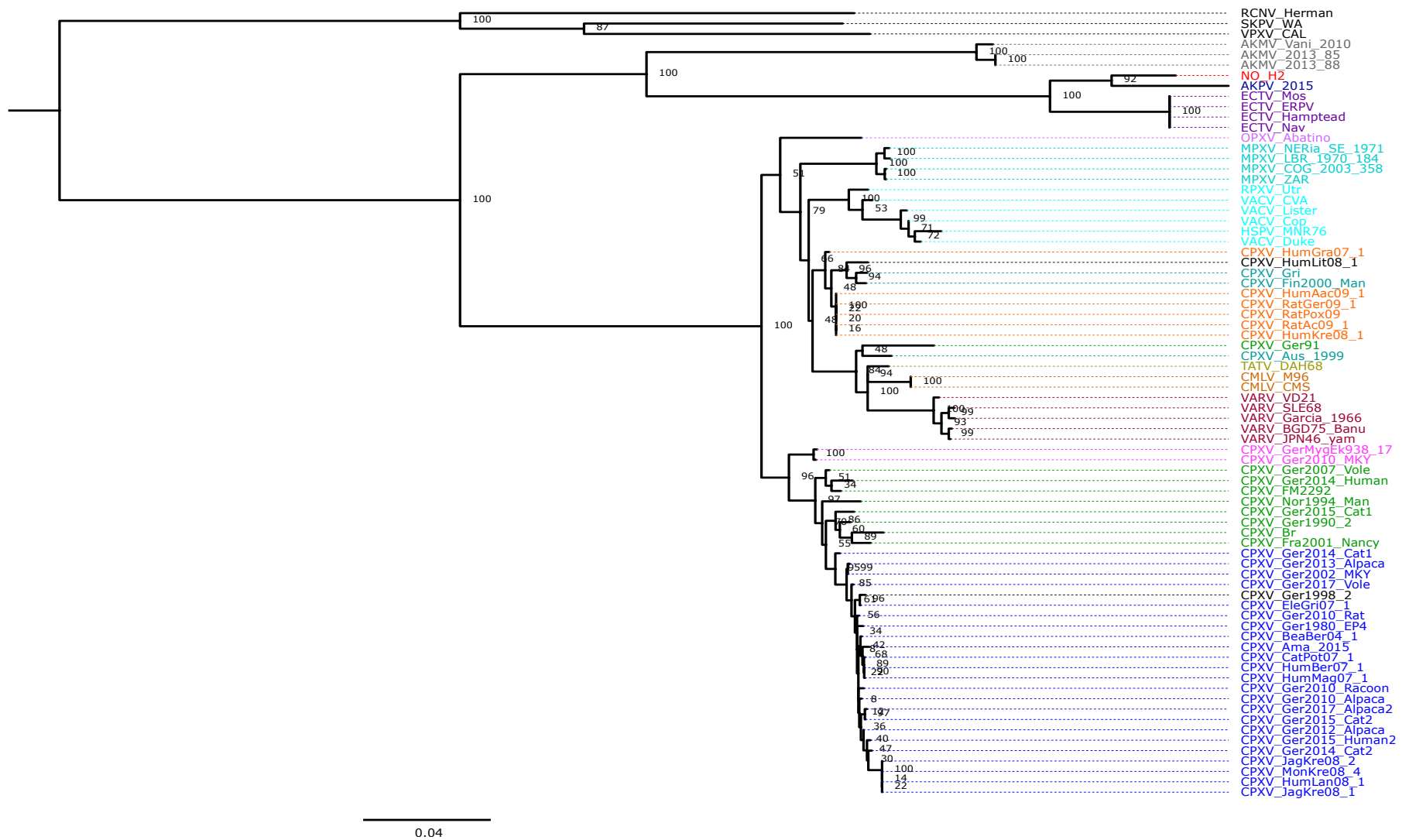
Supplementary Figure S4. Maximum-Likelihood phylogenetic tree of 134 orthopoxvirus orthologous genes. Bootstrap values were determined from 1000 replica sampling. *Cowpox virus* (CPXV) strains were grouped into different clades: CPXV-like 1, CPXV-like 2, and VARV-like (Franke et al., 2017). The scale bar represents expected substitutions per site.



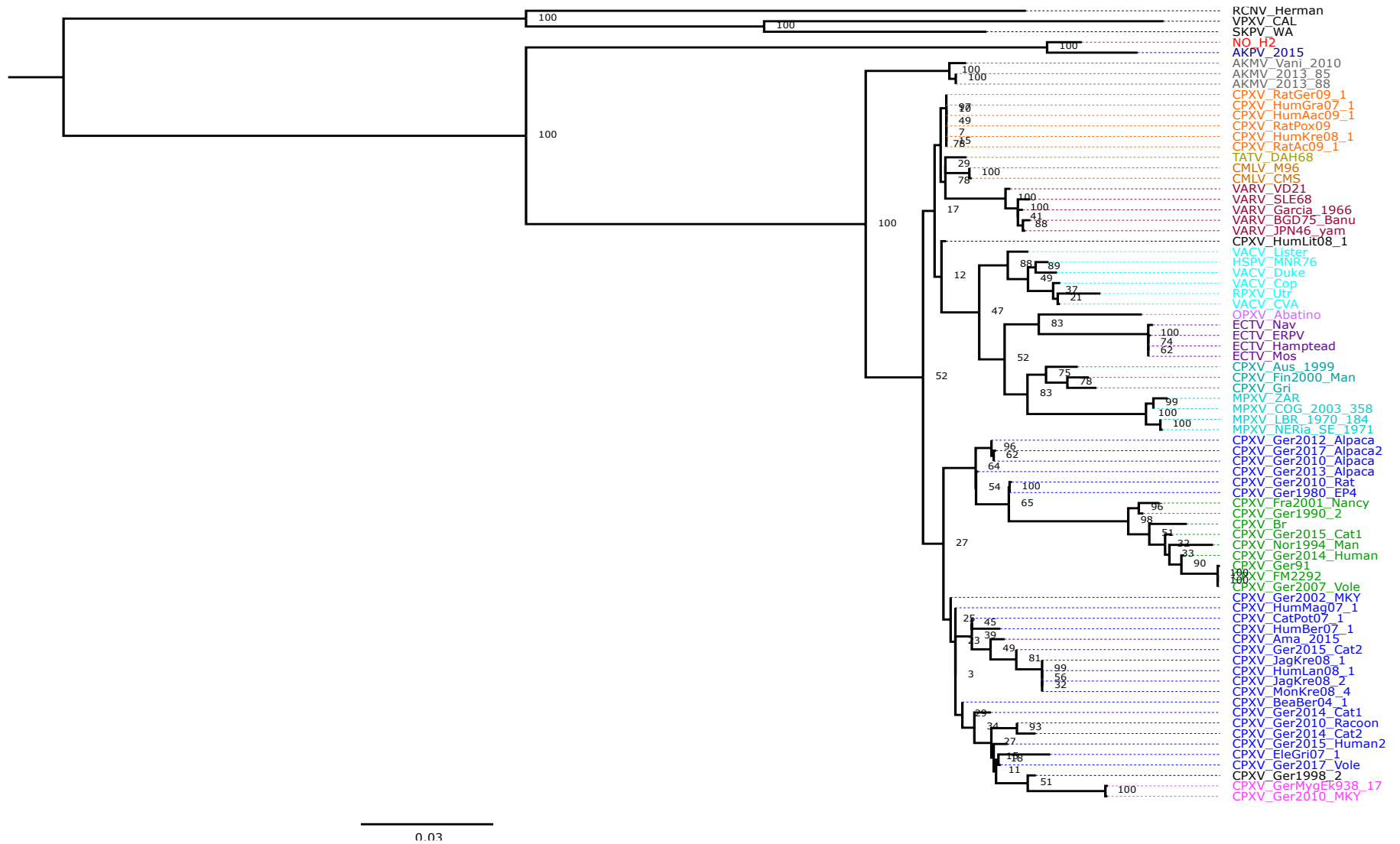
Supplementary Figure S5. Maximum-Likelihood phylogenetic tree based on the putative recombinant region 1 between the parental AKPV and CPXV (potential recombinant event 1). Bootstrap values were determined from 1000 replica sampling. Clades are identified with colors.



Supplementary Figure S6. Maximum-Likelihood phylogenetic tree based on the putative recombinant region 2 between the parental AKPV and CPXV (potential recombinant event 2). Bootstrap values were determined from 1000 replica sampling. Clades are identified with colors.



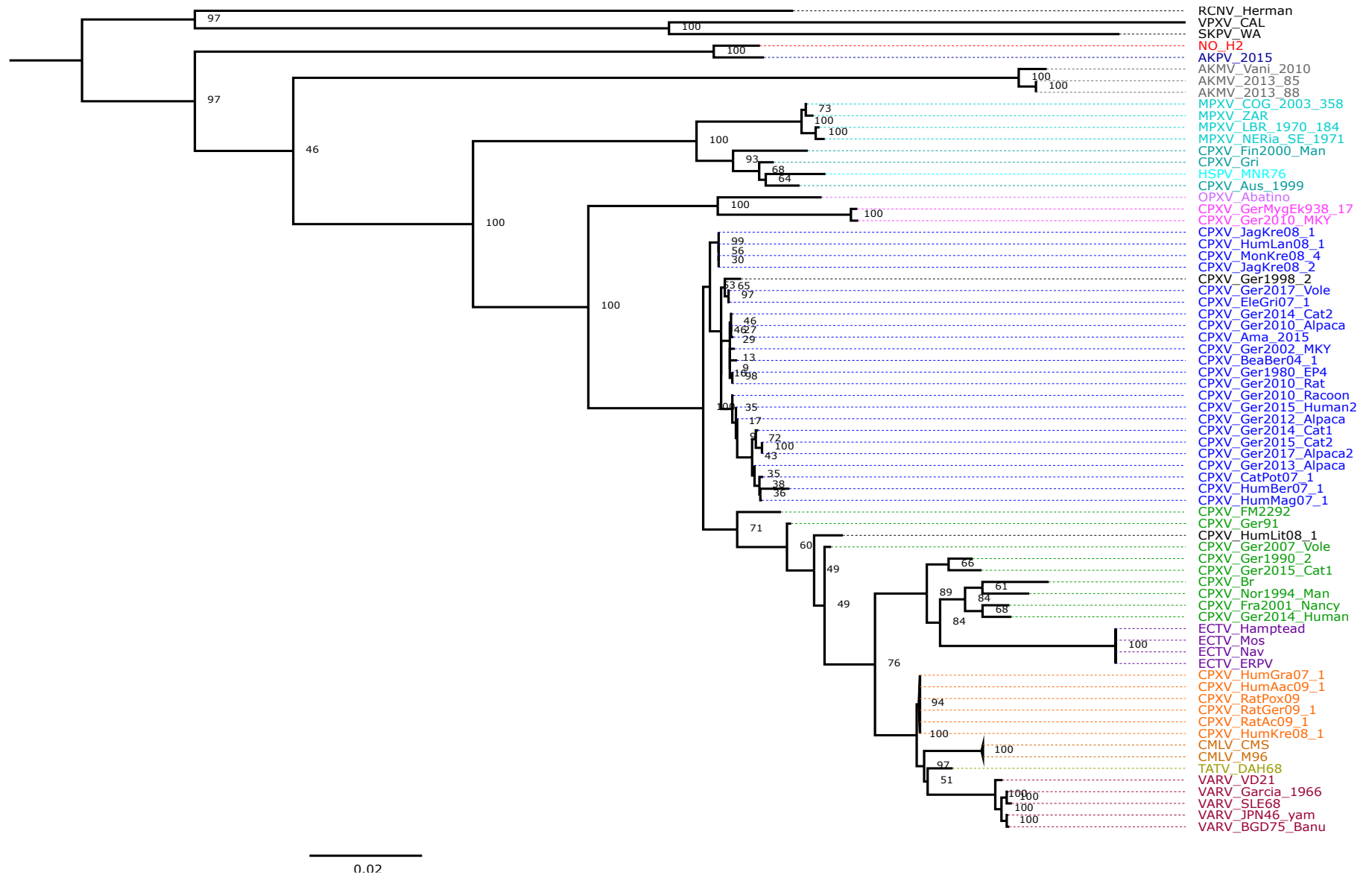
Supplementary Figure S7. Maximum-Likelihood phylogenetic tree based on the putative recombinant region 3 between the parental AKPV and CPXV (potential recombinant event 3). Bootstrap values were determined from 1000 replica sampling. Clades are identified with colors.



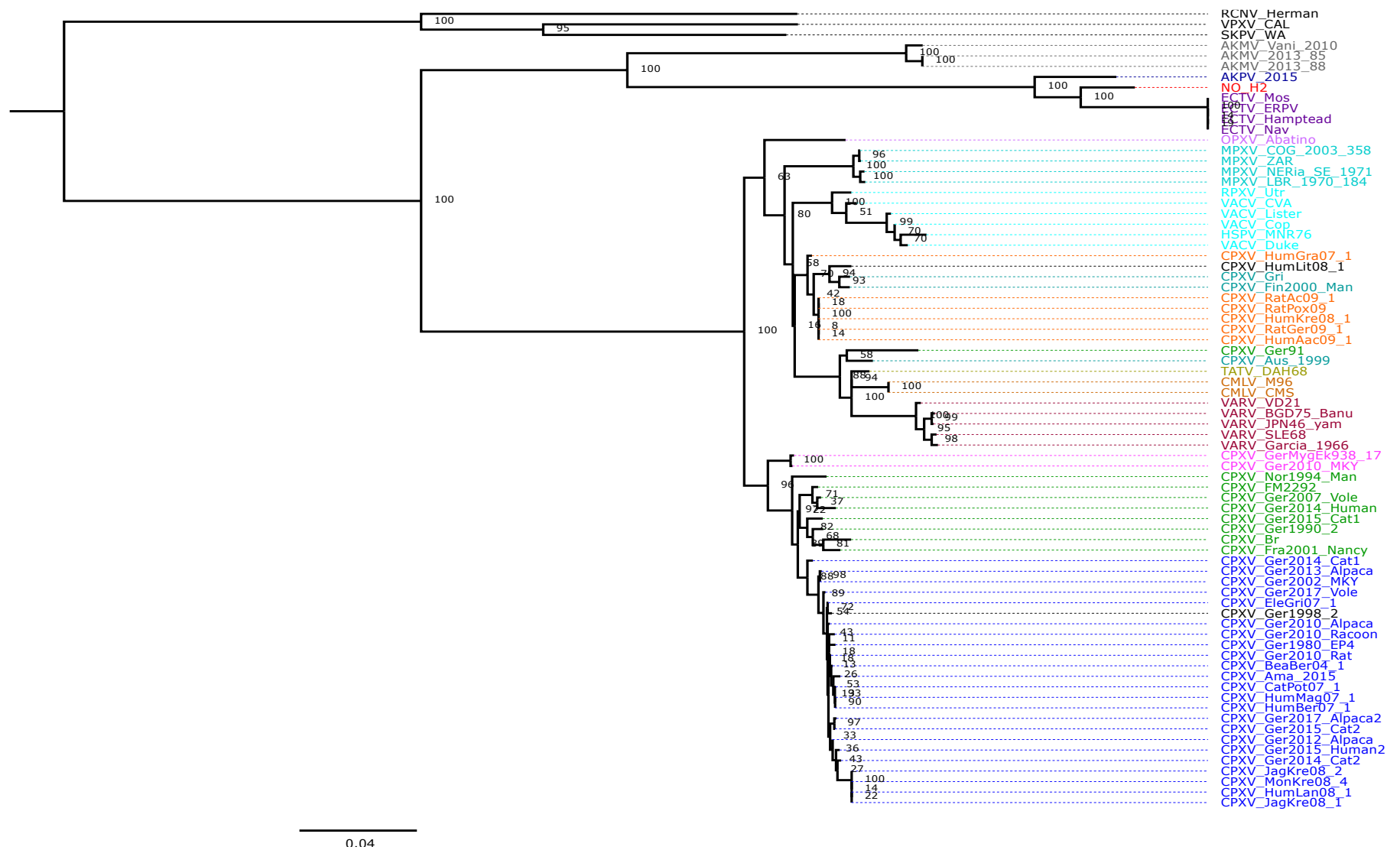
Supplementary Figure S8. Maximum-Likelihood phylogenetic tree based on the putative recombinant region 4 between the parental AKPV and CPXV (potential recombinant event 4). Bootstrap values were determined from 1000 replica sampling. Clades are identified with colors.



Supplementary Figure S9. Maximum-Likelihood phylogenetic tree based on the putative recombinant region 5 between the parental AKPV and CPXV (potential recombinant event 5). Bootstrap values were determined from 1000 replica sampling. Clades are identified with colors.



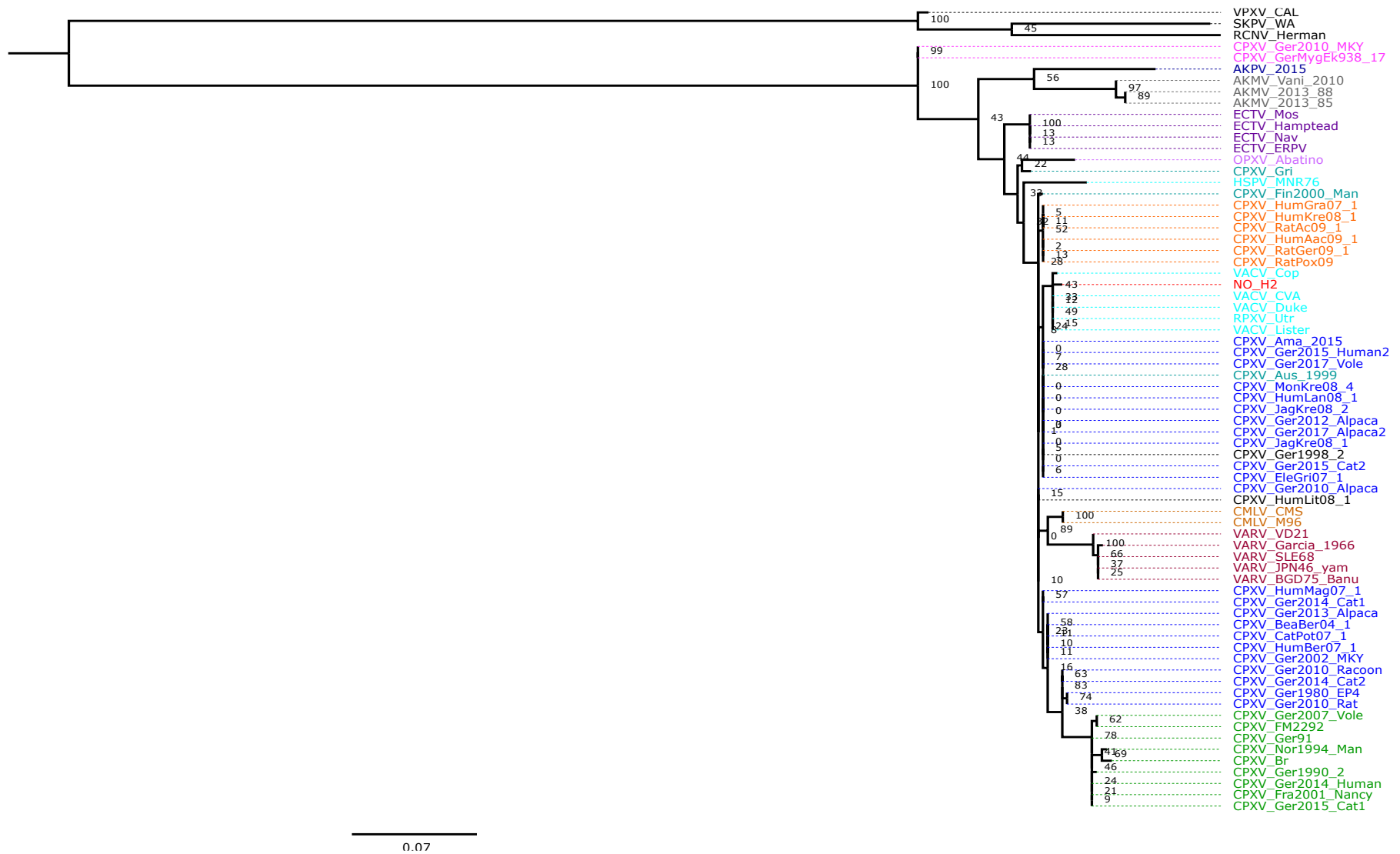
Supplementary Figure S10. Maximum-Likelihood phylogenetic tree based on the putative recombinant region 6 between the parental AKPV and CPXV (potential recombinant event 6). Bootstrap values were determined from 1000 replica sampling. Clades are identified with colors.



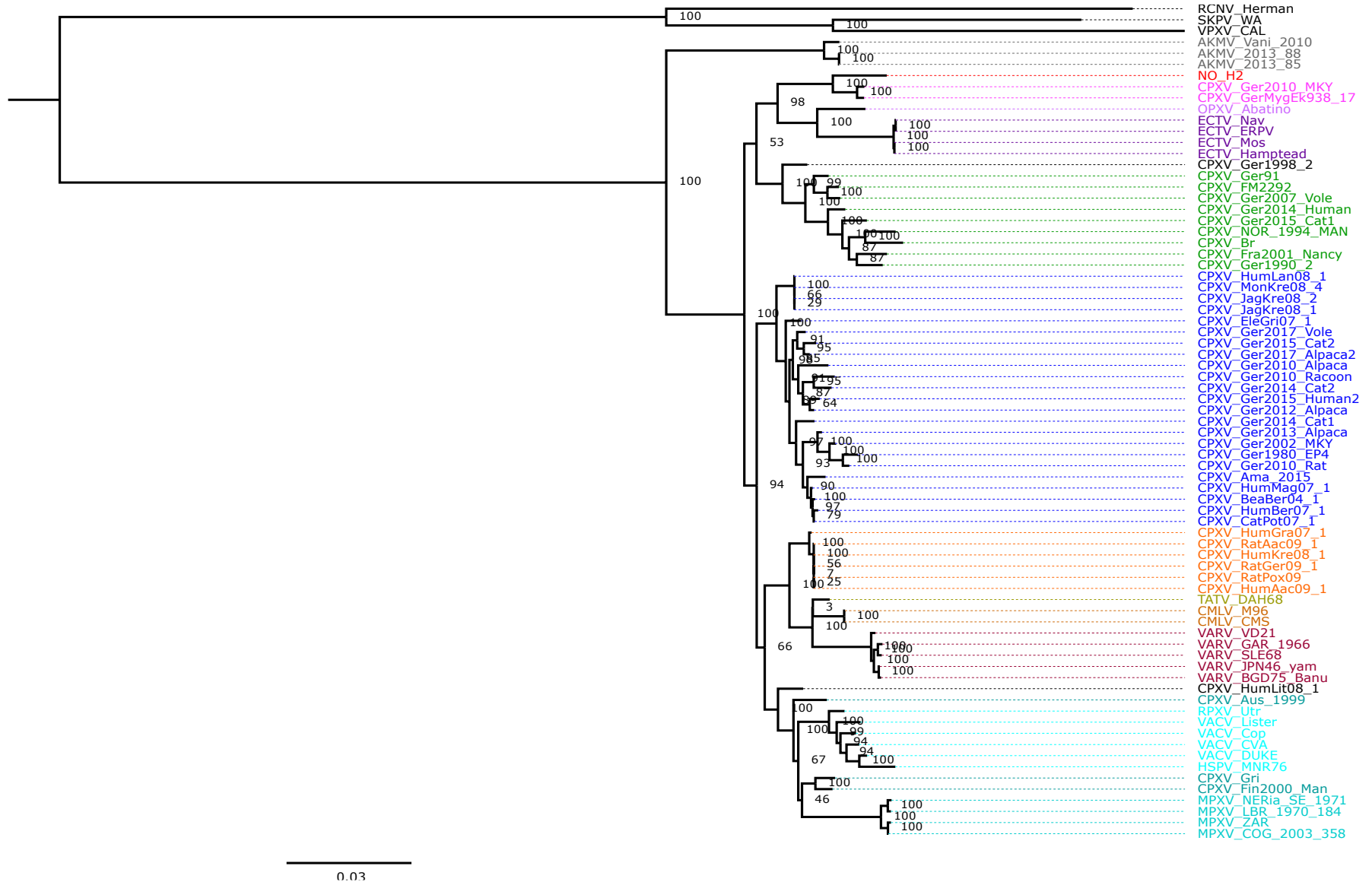
Supplementary Figure S11. Maximum-Likelihood phylogenetic tree based on the putative recombinant region 1 between the parental ECTV and CPXV (potential recombinant event 7). Bootstrap values were determined from 1000 replica sampling. Clades are identified with colors.



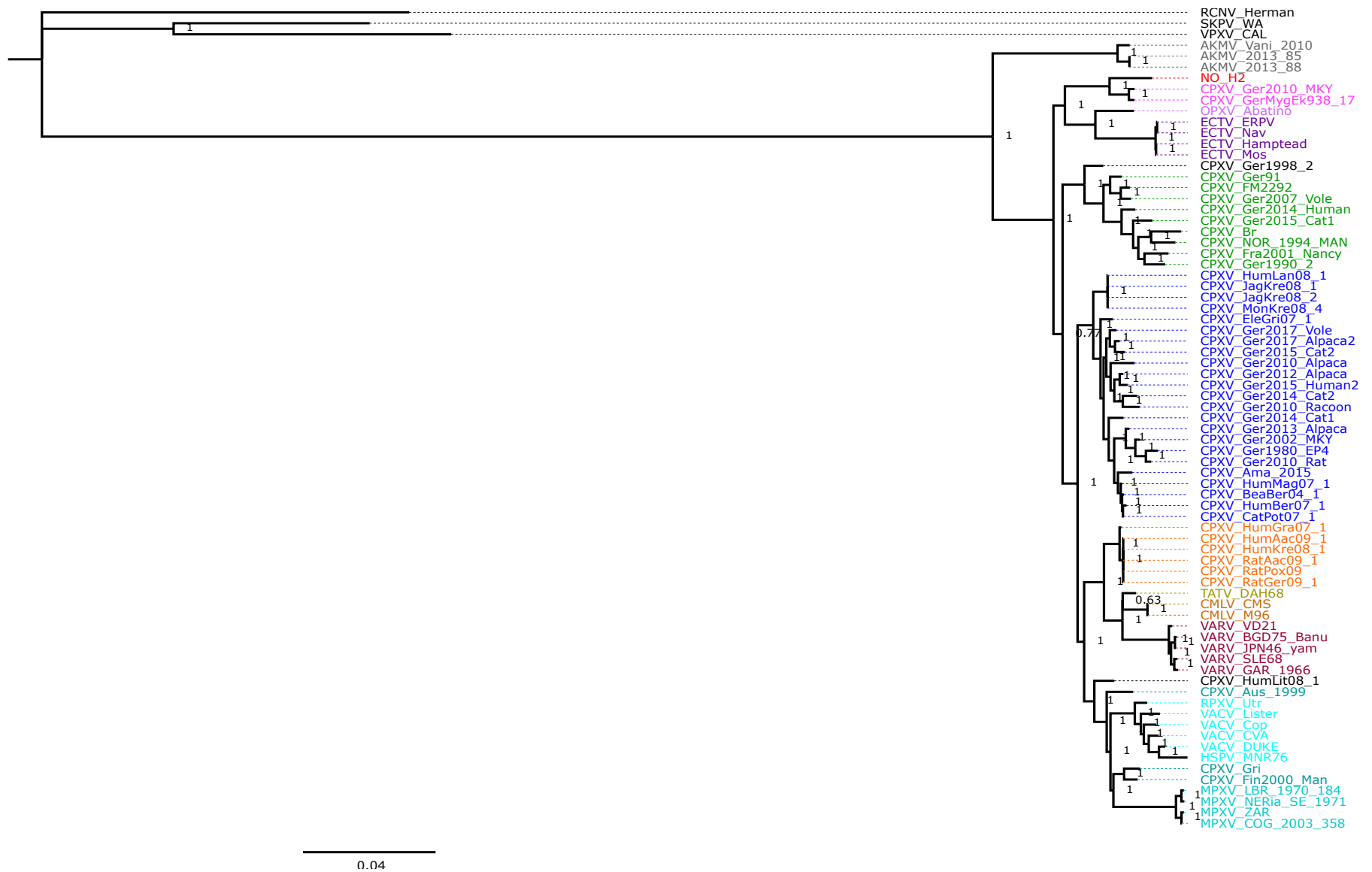
Supplementary Figure S12. Maximum-Likelihood phylogenetic tree based on the putative recombinant region 2 between the parental ECTV and CPXV (potential recombinant event 8). Bootstrap values were determined from 1000 replica sampling. Clades are identified with colors.



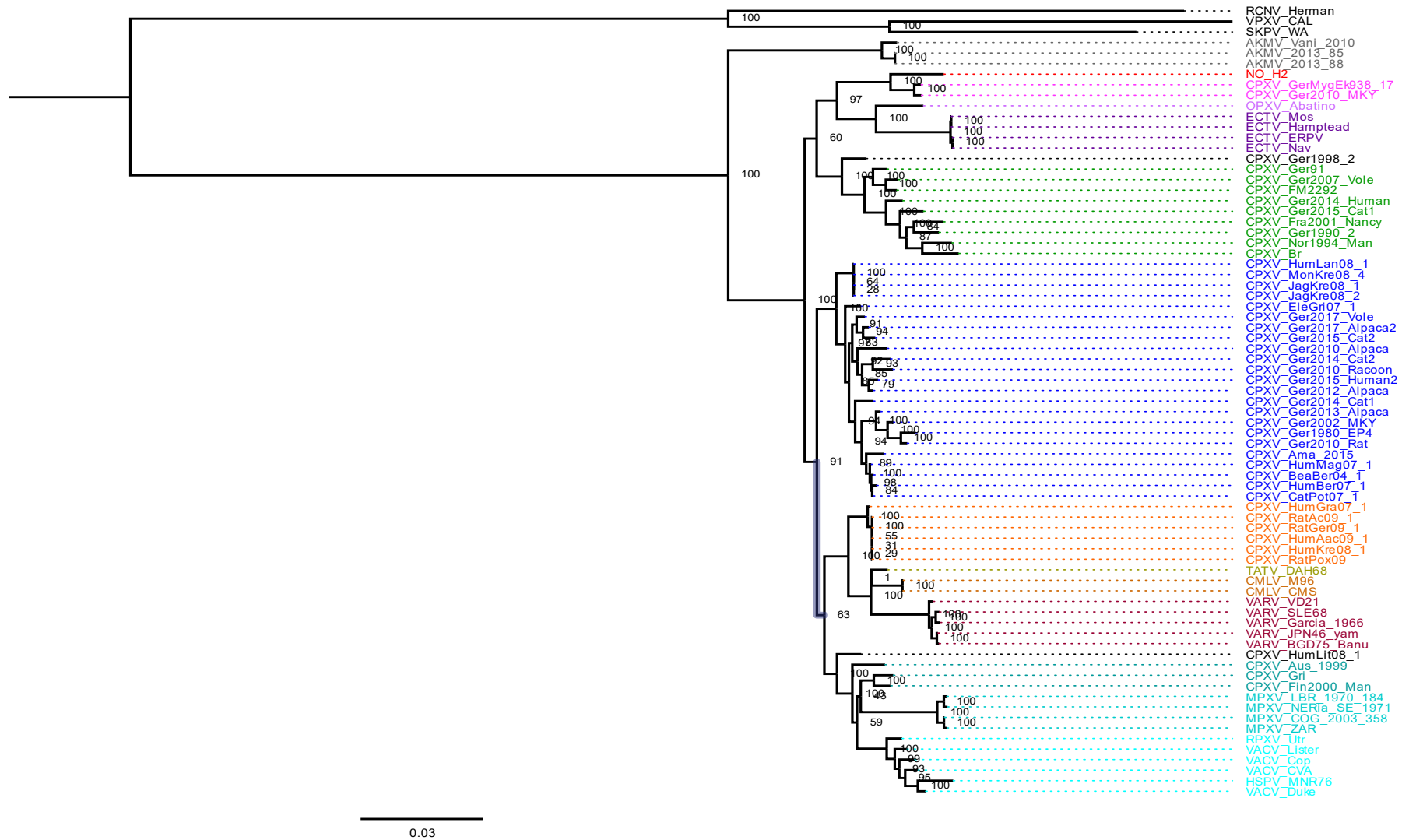
Supplementary Figure S13. Maximum-Likelihood phylogenetic tree based on the putative recombinant region between the parental VACV and CPXV (potential recombinant event 9). Bootstrap values were determined from 1000 replica sampling. Clades are identified with colors.



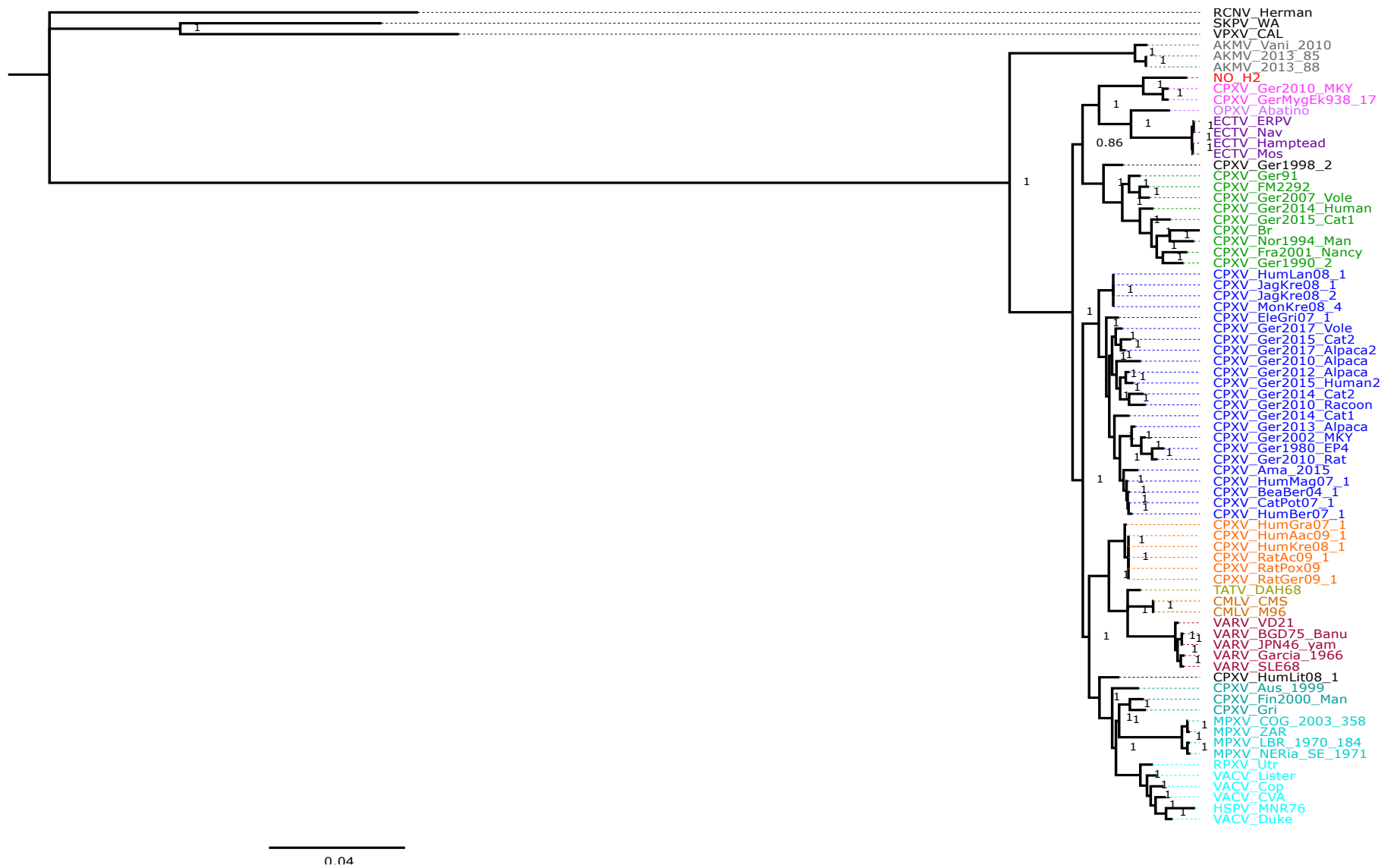
Supplementary Figure S14. Maximum-Likelihood phylogenetic tree based on 75 OPXV whole genomes. Bootstrap values were determined from 1000 replica sampling. Clades are identified with colors.



Supplementary Figure S15. Bayesian Inference phylogenetic tree based on 75 OPXV whole genomes. Clades are identified with colors.



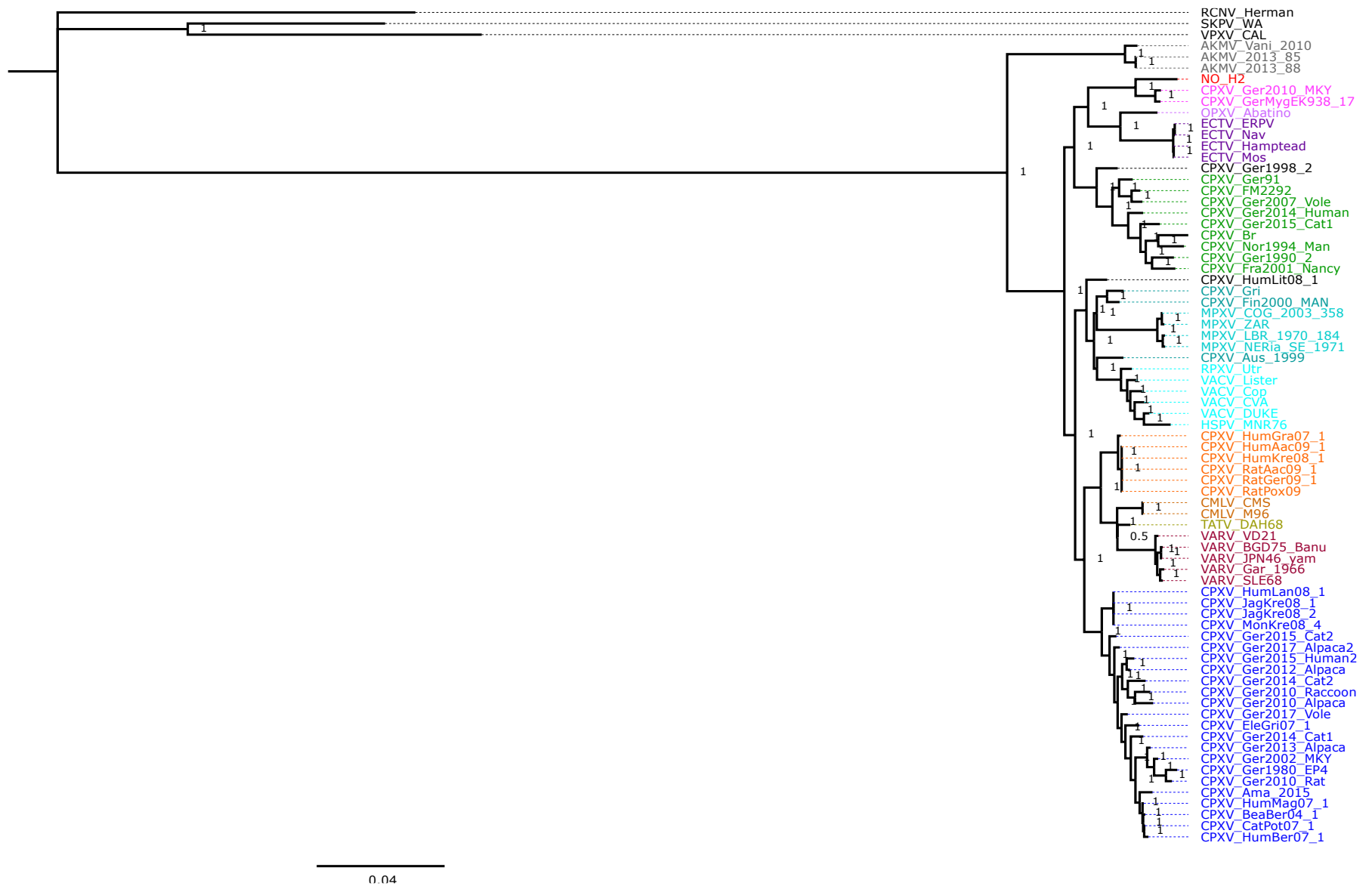
Supplementary Figure S16. Maximum-Likelihood phylogenetic tree based on 75 OPXV core genomes. Bootstrap values were determined from 1000 replica sampling. Clades are identified with colors.



Supplementary Figure S17. Bayesian Inference phylogenetic tree based on 75 OPXV core genomes. Clades are identified with colors.



Supplementary Figure S18. Maximum-Likelihood phylogenetic tree based on 134 orthologous genes from 75 OPXV genomes. Bootstrap values were determined from 1000 replica sampling. Clades are identified with colors.



Supplementary Figure S19. Bayesian Inference phylogenetic tree based on 134 orthologous genes from 75 OPXV genomes. Clades are identified with colors.

Supplementary Table S1. List of strains used in this study.

Virus species	Strain	GenBank number accession	Abbreviation	
<i>Akhmeta virus</i>	2013-85	MH607142	AKMV_2013_85	
	2013-88	MH607141	AKMV_2013_88	
	Vani_2010	MH607143	AKMV_Vani_2010	
<i>Alaskapox virus</i>	2015	MN240300	AKPV_2015	
<i>Camelpox virus</i>	CMS	AY009089	CMLV_CMS	
	M96	NC_003391	CMLV_M96	
<i>Cowpox virus</i>	Amadeus 2015	LN879483	CPXV_AMA_2015	
	Austria 1999	HQ407377	CPXV_AUS_1999	
	BeaBer04/1	KC813491.1	CPXV_BeaBer04_1	
	Brighton Red	NC_003663	CPXV_BR	
	CatPot07/1	KC813506.1	CPXV_CatPot07/1	
	EkGri07/1	KC813507	CPXV_EkGRI07/1	
	Finland 2000 MAN	HQ420893	CPXV_FIN_2000_MAN	
	FM2292	LN864566	CPXV_FM2292	
	France 2001 Nancy	HQ420894	CPXV_FRA_2001_Nancy	
	Germany 91-3	DQ437593	CPXV_Ger91	
	Germany 1980 EP4	HQ420895	CPXV_Ger1980_EP4	
	Germany 1990 2	HQ420896	CPXV_Ger1990_2	
	Germany 1998 2	HQ420897	CPXV_Ger1998_2	
	Germany 2002 MKY	HQ420898	CPXV_Ger2002_MKY	
	Ger/2007/Vole	LT896722	CPXV_Ger2007_Vole	
	Ger/2010/Alpaca	LT896718	CPXV_Ger2010_Alpaca	
	Ger/2010/MKY	LT896721	CPXV_Ger2010_MKY	
	Ger/2010/Raccoon	LT896730	CPXV_Ger2010_Raccoon	
	Ger/2010/Rat	LT896728	CPXV_Ger2010_Rat	
	Ger/2012/Alpaca	LT896726	CPXV_Ger2012_Alpaca	
	Ger/2013/Alpaca	LT896719	CPXV_Ger2013_Alpaca	
	Ger/2014/Cat1	LT896723	CPXV_Ger2014_Cat1	
	Ger/2014/Cat2	LT896725	CPXV_Ger2014_Cat2	
	Ger/2014/Human	LT993226	CPXV_Ger2014_Human	
	Ger/2015/Cat1	LT896724	CPXV_Ger2015_Cat1	
	Ger/2015/Cat2	LT896727	CPXV_Ger2015_Cat2	
	Ger/2015/Human2	LT993232	CPXV_Ger2015_Human2	
	Ger/2017/Alpaca2	LT896732	CPXV_Ger2017_Alpaca2	
	Ger/2017/CommonvoleFMEimka	LT993228	CPXV_Ger2017_Vole	
	GerMygEK938/17	LR812035	CPXV_GerMygEk93_17	
	GRI-90	X94355	CPXV_GRI	
	HumAac09/1	KC813508.1	CPXV_HumAac09_1	
	HumBer07/1	KC813509.1	CPXV_HumBer07_1	
	HumGra07/1	KC813510.1	CPXV_HumGra07_1	
	HumKre08/1	KC813512.1	CPXV_HumKre08_1	
	HumLan08/1	KC813492.1	CPXV_HumLan08_1	
	HumLit08/1	KC813493.1	CPXV_HumLit08_1	
	HumMag07/1	KC813495.1	CPXV_HumMag07_1	
	JagKre08/1	KC813497.1	CPXV_JagKre08_1	
	JagKre08/2	KC813498.1	CPXV_JagKre08_2	
	MonKre08/4	KC813500.1	CPXV_MonKre08_4	
	Norway1994MAN	HQ420899	CPXV_NOR_1994_MAN	
	RatAac09/1	KC813501.1	CPXV_RatAac09_1	
	RatGer09/1	KC813503.1	CPXV_RatGer09_1	
	Ratpox09	LN864565	CPXV_RatPox09	
	<i>Ectromelia virus</i>	ERPV culture-collection ATCC:VR-1431	JQ410350	ECTV_ERPV
		Hampstead	KY554976	ECTV_Hampstead
Moscow		NC_004105	ECTV_Mos	
Naval		KJ563295	ECTV_Nav	
<i>Horsepox virus</i>	MNR-76	DQ792504	HSPV_MNR76	
<i>Monkeypox virus</i>	Congo_2003_358	DQ011154	MPXV_COG_2003_358	
	Liberia_1970_184	DQ011156	MPXV_LBR_1970_184	
	Nigeria-SE-1971	KJ642617	MPXV_NERia_SE_1971	
	Zaire	NC_003310	MPXV_ZAR	
<i>Abatino macacapox virus</i>	-	MH816996	OPXV_Abatino	
<i>Raccoonpox virus</i>	Herman	KP143769	RCNV_Herman	
<i>Rabbüppox virus</i>	Utrecht	AY484669	RPXV_Utr	
<i>Skunkpox virus</i>	WA	NC_031038.1	SKPV_WA	
<i>Taterapox virus</i>	Dahomey 1968	NC_008291	TATV_DAH68	
<i>Vaccinia virus</i>	Copenhagen	M35027	VACV_Cop	
	Chorioallantois Ankara (CVA)	AM501482	VACV_CVA	
	DUKE	DQ439815	VACV_DUKE	
	Lister	AY678276	VACV_Lister	
<i>Variola virus</i>	Bangladesh 1975 v75-550 Banu	DQ437581	VARV_BGD75_Banu	
	Garcia 1966	Y16780	VARV_GARV_1966	
	Japan 1946 (Yamada MS-2(A) Tokyo)	DQ441429	VARV_JPN46_yam	
	Sierra Leone 1969 (V68-258)	DQ441437	VARV_SLE68	
	VD21	KY358055	VARV_VD21	
<i>Volepox virus</i>	CA	NC_031033.1	VPXV_CAL	

Supplementary Table S3. Predicted overlapping genes in CPXV-No-H2 and BLAST analysis.

CDS	Start	Stop	CPXV_Br	Identity (%)	BLASTp		BLASTn	
					OPXV Genome with Highest Identity	Aminoacid identity (%)	OPXV Genome with Highest Identity	Nucleotide identity (%)
NoH2-A	1636	1845	CPXV004	74.65	CPXV	76.1	CPXV GerMygEK938/17	98.1
NoH2-B	38093	38188	-	-	CMLV 0408151v	83.3	CPXV GerMygEK938/17	99.0
NoH2-C	45836	46030	-	-	CPXV GerMygEK938/17, CPXVGer2010MKY	100.0	CPXV GerMygEK938/17, CPXVGer2010MKY	100.0
NoH2-D	46234	46413	CPXV047	83.05	CPXV Ger 2010 MKY	94.9	CPXV Ger 2010 MKY	98.3
NoH2-E	49188	49424	CPXV051A	97.44	CPXV GerMygEK938/17, CPXVGer2010MKY	100.0	CPXV GerMygEK938/17, CPXVGer2010MKY	99.2
NoH2-F	53895	54017	CPXV058	97.5	CPXV, VACV	97.5	ECTV	100.0
NoH2-G	54768	54890	-	-	VACV CEyV1	87.5	CPXV	99.2
NoH2-H	58313	58462	-	-	OPXV Abatino	98.0	CPXV GerMygEK938/17, CPXVGer2010MKY	100.0
NoH2-I	75455	75643	CPXV078A	96.77	CPXV GerMygEK938/17, CPXVGer2010MKY	98.4	CPXV GerMygEK938/17, CPXVGer2010MKY	99.5
NoH2-J	91226	91435	CPXV096	100	AKMV, CMLV, CPXV, VACV	100.0	CPXV, VACV	100.0
NoH2-K	109530	109703	CPXV116	94.12	CPXV, VACV	96.1	CPXV	98.3
NoH2-L	112614	112856	CPXV119A	100	CPXV	100.0	CPXV, OPXVA	99.2
NoH2-M	124280	124498	CPXV130	100	CPXV	100.0	CPXV	99.5
NoH2-N	139869	139985	-	-	VACV CEyV1	94.7	CPXV, VACV	100.0
NoH2-O	144031	144159	CPXV152A	95.24	CPXV	97.6	CPXV, TATV, VARV	100.0
NoH2-P	154705	154911	CPXV160	88.24	CPXV Ger2010MKY	97.1	CPXV Ger2010MKY	98.6
NoH2-Q	160152	160364	CPXV170	94.34	CPXV	100.0	CPXV	99.4
NoH2-R	179029	179130	-	-	VACV Lister	97.0	VACV_VK01	99.0
NoH2-S	200439	200600	CPXV214	84	CPXV Ger2010MKY	94.0	CPXV Ger2010MKY	97.5
NoH2-T	218432	218641	CPXV004	74.65	CPXV	76.1	CPXV GerMygEK938/17	98.1

Supplementary Table S4. BLASTn analysis of predicted genes in CPXV-No-H2 that encode proteins with highest aminoacid similarity to other OPXV proteins than CPXV proteins.

CDS	Start	Stop	Length (bp)	BLASTp		BLASTn	
				OPV Genome with Highest Identity	Aminoacid identity (%)	OPV Genome with Highest Identity	Nucleotide identity (%)
NoH2-077	75843	75950	108	ECTV, HSPV, VACV	100.0	CPXV GerMygEK938/17	100.0
NoH2-079	76910	77128	219	AKPV	98.592	AKPV	98.2
NoH2-090	88183	89487	1305	VACV WAU86/88-1	99.5	CPXV GerMygEK938/17	99.2
NoH2-152	147351	150845	3495	ECTV	99.828	ECTV	98.9
NoH2-153	150838	154107	3270	ECTV*	94.82	ECTV	98.3
NoH2-159	157663	157791	129	VACV	100	BPXV, CPXV , VACV	100
NoH2-160	157790	158170	381	VACV	98.425	VACV LC16m8, VACV LC16mO	98.4
NoH2-163	159655	160161	507	ECTV	97.6	CPXV Ger2010MKY, CPXV GerMygEK938/17	98.6
NoH2-165	160801	161481	681	AKPV	92.92	AKPV	95.2
NoH2-166	161546	162340	795	AKPV	98.485	AKPV	99.1
NoH2-167	162451	162630	180	AKPV	98.305	AKPV	99.4
NoH2-171	165294	165971	678	ECTV	95.556	ECTV_Mill-Hill, ECTV_Hampstead-Egg	95.9
NoH2-172	166133	166537	405	ECTV	100	ECTV	99.8
NoH2-173	166577	167188	612	ECTV	99.507	ECTV	99.7
NoH2-174	167207	167431	225	AKPV	97.297	AKPV	98.7
NoH2-175	167586	168626	1041	AKPV	95.1	CPXV GerMygEK938/17, CPXV Ger2010MKY	94.4
NoH2-210	204592	210315	5724	AKPV	94.905	AKPV	97.2

Supplementary Table S5. Position of the putative recombinant regions in the CPXV-No-H2 genome and BLASTn analysis

Putative recombination event	CPXV-No-H2 genome		BLASTn	
	Start	End	OPXV Genome with Highest Identity	Identity (%)
1	76946	77205	AKPV	98.33
2	77741	78243	AKPV	98.21
3	150156	154530	AKPV	96.89
4	160786	162936	AKPV	97.66
5	165874	168063	AKPV	97.37
6	204966	209636	AKPV	98.42
7	150119	153968	ECTV	97.93
8	165847	167892	AKPV	97.29
9	164405	164766	VACV	99.44

Paper II

Article

Genomic Sequencing and Phylogenomics of Cowpox Virus

Diana Diaz-Cánova ¹, Carla Mavian ², Annika Brinkmann ³, Andreas Nitsche ³, Ugo Moens ^{1,*}
and Malachy Ifeanyi Okeke ^{4,*}

¹ Molecular Inflammation Research Group, Department of Medical Biology, UiT—The Arctic University of Norway, N-9037 Tromsø, Norway

² Emerging Pathogens Institute, Department of Pathology, College of Medicine, University of Florida, Gainesville, FL 32610, USA

³ Highly Pathogenic Viruses, Centre for Biological Threats and Special Pathogens, WHO Reference Laboratory for SARS-CoV-2 and WHO Collaborating Centre for Emerging Infections and Biological Threats, Robert Koch Institute, 1335 Berlin, Germany

⁴ Section of Biomedical Sciences, Department of Natural and Environmental Sciences, School of Arts and Sciences, American University of Nigeria, Yola PMB 2250, Nigeria

* Correspondence: ugo.moens@uit.no (U.M.); malachy.okeke@aun.edu.ng (M.I.O.)

Abstract: Cowpox virus (CPXV; genus *Orthopoxvirus*; family *Poxviridae*) is the causative agent of cowpox, a self-limiting zoonotic infection. CPXV is endemic in Eurasia, and human CPXV infections are associated with exposure to infected animals. In the Fennoscandian region, five CPXVs isolated from cats and humans were collected and used in this study. We report the complete sequence of their genomes, which ranged in size from 220–222 kbp, containing between 215 and 219 open reading frames. The phylogenetic analysis of 87 orthopoxvirus strains, including the Fennoscandian CPXV isolates, confirmed the division of CPXV strains into at least five distinct major clusters (CPXV-like 1, CPXV-like 2, VACV-like, VARV-like and ECTV-Abatino-like) and can be further divided into eighteen sub-species based on the genetic and patristic distances. Bayesian time-scaled evolutionary history of CPXV was reconstructed employing concatenated 62 non-recombinant conserved genes of 55 CPXV. The CPXV evolution rate was calculated to be 1.65×10^{-5} substitution/site/year. Our findings confirmed that CPXV is not a single species but a polyphyletic assemblage of several species and thus, a reclassification is warranted.

Keywords: phylogenetic; orthopoxvirus; poxviridae; molecular clock; Fennoscandian; phylodynamics; cowpox virus



Citation: Diaz-Cánova, D.; Mavian, C.; Brinkmann, A.; Nitsche, A.; Moens, U.; Okeke, M.I. Genomic Sequencing and Phylogenomics of Cowpox Virus. *Viruses* **2022**, *14*, 2134. <https://doi.org/10.3390/v14102134>

Academic Editor: Stefan Rothenburg

Received: 17 August 2022

Accepted: 24 September 2022

Published: 28 September 2022

Publisher's Note: MDPI stays neutral with regard to jurisdictional claims in published maps and institutional affiliations.



Copyright: © 2022 by the authors. Licensee MDPI, Basel, Switzerland. This article is an open access article distributed under the terms and conditions of the Creative Commons Attribution (CC BY) license (<https://creativecommons.org/licenses/by/4.0/>).

1. Introduction

Cowpox virus (CPXV) is an orthopoxvirus species, belonging to the subfamily *Chordopoxvirinae* of the family *Poxviridae* [1]. Orthopoxvirus (OPXV) comprises several species from the New World and Old World. The most representative species from the New World are raccoonpox virus (RCNV), volepox virus (VPXV) and skunkpox virus (SKPV) [2]. Within Old World OPXV, there are several species: ectromelia virus (ECTV), vaccinia virus (VACV), monkeypox virus (MPXV), variola virus (VARV), taterapox virus (TATV), camelpox virus (CMLV) and CPXV [3–5]. In the last decade, new OPXV species were discovered in the United States (alaskapox virus, AKPV), Italy (abatino macacapox virus, Abatino) and Georgia (akhmeta virus, AKMV) [6–8].

The most notable member of OPXV genus is VARV, the etiologic agent of smallpox. However, after a large, massive vaccination campaign, smallpox was eradicated in 1980 [9]. The last natural cases of smallpox in humans were in Somalia in 1977 [10]. OPXV species, such as CPXV and MPXV, can cause zoonotic diseases [11–14]. MPXV and CPXV are the causative agents of monkeypox and cowpox, respectively, and have a wide host range [13,15]. Recently, a multi-country human monkeypox outbreak in 50 countries has been reported [16]. Compared to MPXV that occurs in Central and Western Africa [17],

CPXV is endemic of Eurasia, mainly present in Europe [12,18–23]. The natural reservoirs of CPXV are wild rodents [18,24]. Nevertheless, CPXV is also able to infect felines, monkeys, dogs, alpacas, rats, horses and humans [12,25–29]. The first zoonotic case was reported in the Netherlands in 1985, where CPXV was transmitted from a domestic cat to a woman [30]. In Fennoscandia, human cases of CPXV infections have been reported (CPXV-No-H1, CPXV-No-H2, CPXV-Swe-H1 and CPXV-Swe-H2) as well as feline cases (CPXV-No-F1 and CPXV-No-F2) [27,31–35]. CPXV has been classified as a single species; however, it has been proposed that CPXV should be considered as a polyphyletic species [33,35–40]. Based on phylogenetic studies, CPXV was divided into at least five clades: CPXV-like 1, CPXV-like 2, ECTV-Abatino-like, VACV-like and VARV-like [38,40–42]. Among OPXV, CPXV has the largest genome [43] and contains the highest number of orthopoxviral genes [42,44]. It was suggested that CPXV-like virus was the ancestor of Old World OPXV, except for AKPV and AKMV [39,44,45]. Until now, the evolutionary history of CPXV is still unclear. Most studies have focused on the molecular evolution of VARV, but few studies were focused on OPXV and, specially, on CPXV [39,45–49].

In this study, we present the whole genome sequence of five Fennoscandian CPXV isolates. We determined the phylogenetic relationship of CPXV, including the Fennoscandian isolates, with other OPXV and studied the evolutionary history of CPXV based on the concatenated 62 non-recombinant conserved genes of several representatives CPXV isolates from the different CPXV clades. Furthermore, we propose a new classification of CPXV.

2. Materials and Methods

2.1. Cell, Virus Culture and DNA Isolation

Five Fennoscandian isolates were used in this study: CPXV-No-H1, CPXV-No-F1, CPXV-No-F2, CPXV-Swe-H1 and CPXV-Swe-H2. The isolates were cultured on a monolayer of Vero cells (ATCC No. CCL-81), and the viral DNA was extracted from semi-purified virions, as previously described [34,40]. The origin of the five CPXV isolates has been described elsewhere [27,31–34].

2.2. Whole Genome Sequencing, Genome Assembly and Genome Annotation

The genomes of the five Fennoscandian isolates (CPXV-No-H1, CPXV-No-F1, CPXV-No-F2, CPXV-Swe-H1 and CPXV-Swe-H2) were sequenced using Oxford Nanopore Technology GridION (ONT; Oxford, UK) and Illumina MiSeq using reagent kit v3 with 2×300 bp paired-end reads, as previously described [40]. Illumina sequencing was performed at the Norwegian Sequencing Centre, Oslo, and Nanopore sequencing was performed at the Genomics Support Centre Tromsø at UiT—The Arctic University of Norway. The genomes were assembled using SPAdes v3.15.3 [50] and annotated with Genome Annotation Transfer Utility (GATU) [51], as previously reported [40].

2.3. Gene Content Comparison

The five Fennoscandian CPXV genomes were compared to CPXV-Br genome. Predicted CDS from five CPXV isolates were extracted, translated into amino acid sequences and compared to the CPXV-Br proteins using BLASTp (ncbi-blast+ v2.11.0) [52].

2.4. Phylogenetic Analysis, Patristic and Genetic Distances

A total of 87 OPXV genomes, including the five Fennoscandian genomes, were used in this study (Table S1). Eighty-two OPXV genomes were retrieved from the Viral Orthologous Clusters (VOCs) database [53], with the exception of CPXV_GerMygEK938_17 (retrieved from GenBank). The genes and genomes were aligned using MAFFT v7.450 (with default parameters) [54], as implemented in Geneious Prime 2022.0.2. Four different alignments were used to build the phylogenetic trees: (1) 87 OPXV whole genome alignment, (2) 87 OPXV core genome alignment, (3) OPXV orthologous gene alignment (Table S2) and (4) 62 conserved genes alignment (Table S3), as previously described [40].

Recombination detection program 4 (RDP4) [55] was used to detect genome-wide recombination in the datasets. Recombination events identified by 5 of 7 methods (RDP [56], GENECONV [57], Bootscan [58], MaxChi [59], Chimaera [60], SiScan [61] and 3Seq [62]) with significant p -values ($p \leq 0.01$) were considered credible evidences of recombination. Whole genome, core genome and orthologous gene alignments were generated without removing the putative recombinant regions.

The conserved gene alignment was generated by examining the 90 Chordopoxvirus (ChPV) conserved genes for recombination using RDP4 [55], as described above. The 62 conserved genes identified as non-recombinant were aligned singly and the 62 single gene alignments were concatenated to generate the conserved gene dataset.

Gblocks 0.91b was used to remove poorly aligned positions from 87 OPXV whole and core genome alignments [63]. The presence of phylogenetic signal of the datasets was assessed by likelihood mapping analysis with the evaluation of 2000 random quartets using IQ-TREE v.2.0.3. [64] (Figure S1). The best-fit nucleotide substitution model for the alignment data was selected using the modelTest-NG v.0.1.6 [65]. Two inference methods, maximum likelihood (ML) and Bayesian inference (BI), were conducted with RAxML v8.2.12 [66] using a rapid bootstrap algorithm [67] and MrBayes v3.2.7 [68], respectively, as previously described [40]. The Markov Chain Monte Carlo (MCMC) analysis was run until reaching convergence. The phylogenetic trees were visualized applying FigTree v1.4.4 (<http://tree.bio.ed.ac.uk/software/figtree/>, accessed on 19 February 2021). The BI phylogenetic tree based on the OPXV orthologous genes was not built because MCMC analysis did not reach convergence after 50,000,000 generations.

Patristic distances between different groups were calculated from the ML/BI trees of concatenated 62 conserved non-recombinant genes using the program Patristic version 1.0 [69]. The genetic distances between the different groups were estimated by p -distances, as implemented in MEGA version 11 [70]. For patristic and genetic distances, the distances were averaged across taxa to produce a single value. The genetic and patristic distances between TATV and CMLV were used as threshold values since they are closest and distinct OPXV species. These threshold values were used to compare the distance between CPXV clusters and OPXV species and separate them in different sub-species if they were equal or greater than TATV-CMLV threshold values.

2.5. *Phylogenetic Evolutionary Analysis of CPXV*

A Bayesian MCMC inference method implemented in BEAST 1.10.4 [71] was used to estimate evolutionary rates and the divergence times. Evolutionary analysis was carried out on alignment of concatenated 62 conserved non-recombinant genes of 55 CPXV strains (listed in Table S4). The temporal signal was assessed from the ML tree of 62 conserved genes of 55 CPXV by regression of genetic divergence (root-to-tip genetic distance) and the sampling date using TempEst v.1.5.3 [72] (Figure S2). In the analysis, we did not include other OPXV species because the dataset did not contain temporal signal (correlation coefficient = -0.15 , value of $R^2 = 0.02$). The presence of phylogenetic signal of the dataset was evaluated using IQ-TREE v.2.0.3. [64], as described above (Figure S2).

The Bayesian phylogenetic analysis was calibrated using the following parameters: log-normal relaxed clock, coalescent Bayesian skyline population, HKY substitution model and four gamma categories. MCMC chain was run for 1 billion generations. The effective sampling size (ESS) values were checked in Tracer v1.7.2 [73]. Only the Effective Sampling Size (ESS) values > 200 (after burn-in) were accepted. The maximum clade credibility (MCC) tree was generated using TreeAnnotator v1.10.4, visualized using FigTree v1.4.4 and edited graphically using the ggtree package available in R [74].

3. Results

3.1. *Genome Assembly, Genome Annotation and Gene Content*

The whole genomes of five Fennoscandian CPXV isolates (CPXV-No-H1, CPXV-No-F1, CPXV-No-F2, CPXV-Swe-H1 and CPXV-Swe-H2) were assembled, and the coverage of the

assembled genomes varied from 300X to 2400X, as shown in Table 1. The genome size of the Fennoscandian CPXV isolates ranges from 220,808 to 222,178 bp and the length of inverted terminal repeats (ITRs) were approximately 8 kbp (Table 1). The whole genome sequences of these isolates are available in GenBank, with Accession Number: OP125537, OP125538, OP125539, OP125540, OP125541.

Table 1. Genome size, number of predicted coding sequences (CDS) and genome coverage of the Fennoscandian CPXV isolates sequenced in this study.

Name	Genome Size (bp)	CDS	Genome Coverage	
			Illumina	Nanopore
CPXV-No-H1	221,926	215	300X	600X
CPXV-No-F1	221,334	217	820X	1519X
CPXV-No-F2	222,178	217	940X	1480X
CPXV-Swe-H1	220,981	217	700X	2500X
CPXV-Swe-H2	220,808	217	990X	2400X

Gene annotation of the five Fennoscandian CPXV genomes (CPXV-No-H1, CPXV-No-F1, CPXV-No-F2, CPXV-Swe-H1 and CPXV-Swe-H2) revealed 212, 219, 217, 217 and 217 predicted coding sequences (CDS), respectively. A comparison of the predicted CDS of the five Fennoscandian CPXV isolates with the CPXV-Br genome is shown in Table S5. The genome content of the five Fennoscandian CPXV isolates was similar to CPXV-Br genome. The majority of predicted CDS of the five CPXV strains were found to have homologs in CPXV-Br, except for few predicted CDS. *NoF1-009*, *NoF2-009* and *NoH1-008*, present in the Norwegian isolates, were homologs of *EVM004* that encodes a BTB Kelch-domain containing protein. The Swedish isolates contain a CDS (*SweH1-210* and *SweH2-210*) that was homolog of *CPXV-GRI-K3R* (codes for CrmE protein). The five Fennoscandian isolates contain a homolog of *VACV-Cop O3L*, encoding a virus entry/fusion complex component.

The five Fennoscandian CPXV strains lacked homologs of *CPXV001* and *CPXV216*. Furthermore, *CPXV002* and *CPXV191* (*CrmC*) were absent in CPXV-No-H1 and CPXV-No-F1 genomes, respectively.

3.2. Phylogenetic Analysis

The recombination analysis evidenced the extensive recombination in OPXV core genomes (Figure S3) as well as in the datasets of OPXV whole genomes and orthologous genes (data not shown). Recombination regions were not removed from the alignments used to generate the phylogenetic trees for the whole genome, core genome and orthologous genes. To examine if the recombinant regions in the three datasets biased the phylogenetic signal, we generated some fourth data, in which 62 OPXV conserved genes without any evidence of recombination were used in phylogenetic reconstruction, as described in methods. The ML and BI phylogenetic trees built from concatenated 62 conserved genes without recombination is shown in Figure 1 and Figure S4, respectively.

The topology of the phylogenetic trees based on 87 OPXV core genomes (Figure 2 and Figure S5) was identical to that of trees generated from 87 OPXV whole genomes (Figures S6 and S7) and similar to that of the phylogenetic tree built based on OPXV orthologous genes (Figure S8). Whereas the topology of phylogenetic trees based on 62 conserved genes (Figure 1 and Figure S4) slightly differed from that of the phylogenetic trees generated from 87 OPXV core genomes (Figure 2 and Figure S5).

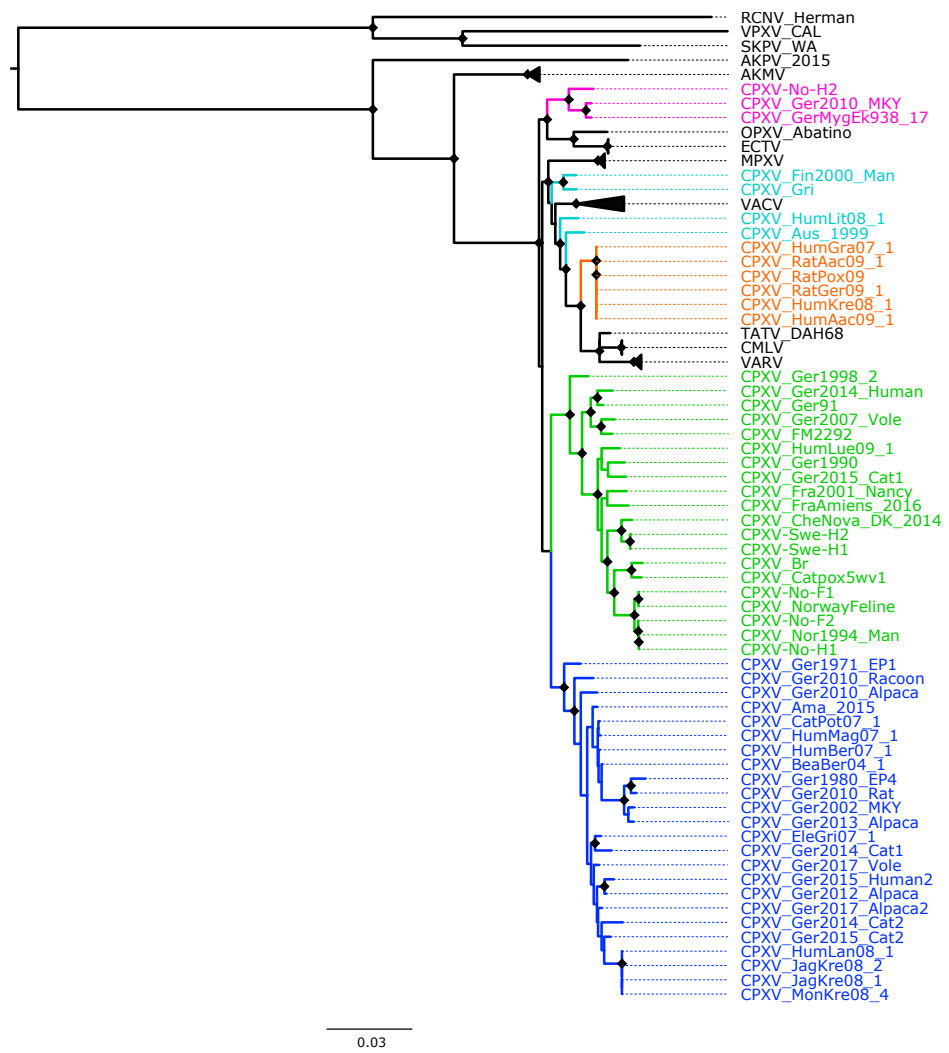


Figure 1. Maximum likelihood phylogenetic tree of 62 conserved genes from 87 orthopoxviruses. Bootstrap values were inferred from 1000 rapid bootstrap replicates. Diamonds at the nodes indicate bootstrap values > 80%. The scale indicates substitution per site. The main five cowpox virus (CPXV) clusters were highlighted in different colors: pink (Ectromelia-Abatino-like CPXV), blue (CPXV-like 1), green (CPXV-like 2), turquoise blue (Vaccinia-like CPXV) and orange (Variola-like CPXV).

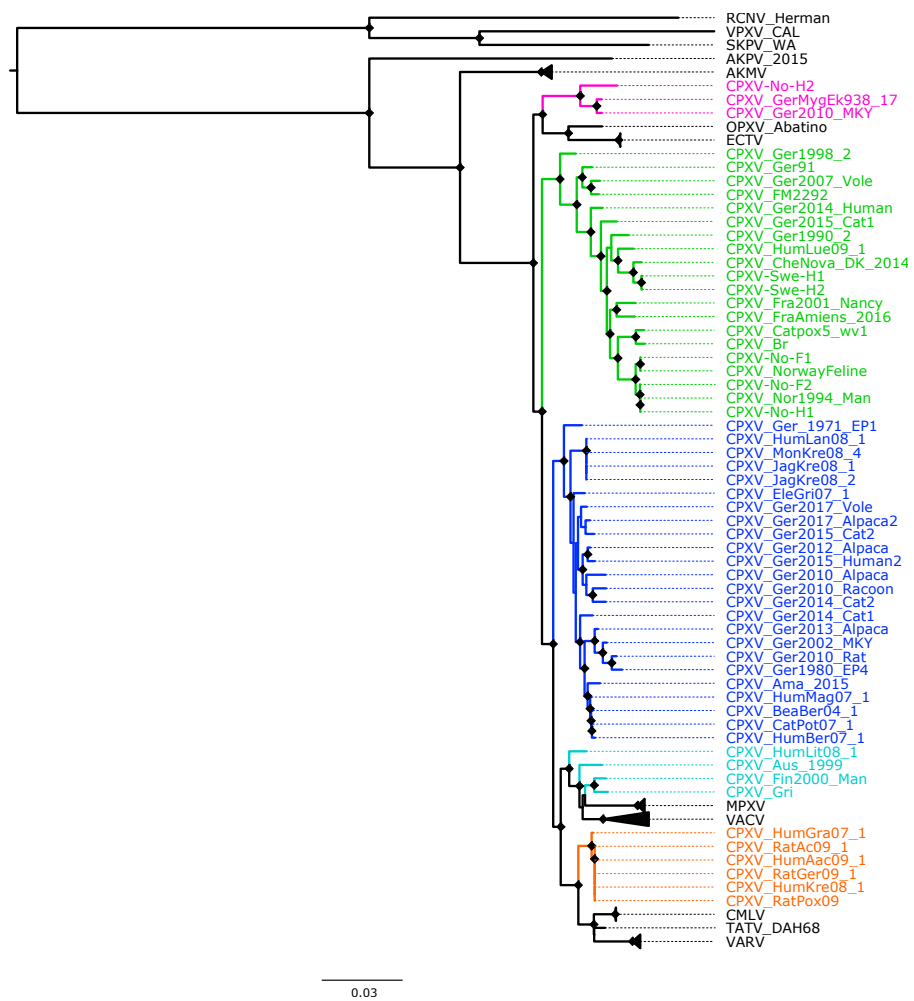


Figure 2. Maximum likelihood phylogenetic tree of 87 orthopoxvirus core genome. Bootstrap values were inferred from 1000 rapid bootstrap replicates. Diamonds at the nodes indicate bootstrap values > 80%. The scale indicates substitution per site. The main five cowpox virus (CPXV) clusters were highlighted in different colors: pink (Ectromelia-Abatino-like CPXV), blue (CPXV-like 1), green (CPXV-like 2), turquoise blue (Vaccinia-like CPXV) and orange (Variola-like CPXV).

As expected, in all phylogenetic trees, the New World and Old World OPXV were separated and AKPV and AKMV clades were placed between them (Figure 1, Figure 2 and Figures S4–S8). Within the Old OPXV, the strains from the same species formed distinct clades, except for CPXV strains. They formed separated clusters with different OPXV species such as VACV, VARV, ECTV and Abatino. CPXV isolates were separated in five clusters: ECTV-Abatino-like CPXV, CPXV-like 1, CPXV-like 2, VACV-like CPXV and VARV-like CPXV. Even though CPXV strains from VACV-like did not form a cluster, they were closely related to VACV clade. ECTV/Abatino group was clustered with ECTV-Abatino-like clade, which includes one Fennoscandian isolate (CXPV-No-H2) and two German isolates. ECTV/Abatino/ECTV-Abatino-like CPXV clade clustered with a major clade that contains: CPXV-like 2, CPXV-like 1, VACV-like, VACV, MPXV, VARV-like, VARV, TATV and CMLV clusters (PP = 1.0 and bootstrap values = 100%). In the phylogenetic trees based on 87 OPXV core genomes (Figure 2 and Figure S5), CPXV-like 2 was separated from the other CPXV clusters and OPXV. Furthermore, CPXV-like 1 clade was sister to a major clade that comprised VACV-like, VACV, MPXV, VARV-like, TATV, CMLV and VARV (PP = 1.0 and bootstrap values = 100%). Within this major clade VACV-like/VACV/MPXV cluster was separated from VARV-like, TATV, CMLV and VARV. Whereas the phylogenetic trees generated from 62 conserved genes (Figure 2 and Figure S6) showed that CPXV-like 1 and

CPXV-like 2 were sister clades (PP = 1 and bootstrap values = 70%) and these clustered together with a clade that contains VACV-like, VACV, MPXV, VARV-like, VARV, TATV and CMLV, but with low bootstrap support (48%) and PP of 0.93. In comparison to a phylogenetic tree built from 87 OPXV core genomes, VACV-like/VACV/MPXV did not form separate from VARV-like.

All Fennoscandian CPXV isolates except CPXV-No-H2 were grouped into CPXV-like 2 clade (Figure 1, Figure 2 and Figures S4–S8). This clade also contains CPXV strains from Germany, Denmark, Russia, The United Kingdom (UK) and France. Within CPXV-like 2, CPXV-Ger1998_2 formed a deeper single branch and the remaining CPXV isolates were divided in two main sub-clusters. In the phylogenetic trees built from 87 OPXV core genomes (Figure 2 and Figure S5), the sub-cluster one contained three German isolates (CPXV_Ger91, CPXV_Ger2007_Vole and CPXV_FM2292) and sub-cluster two comprised 16 CPXV isolates, including the five Fennoscandian CPXV isolates reported in this study (CPXV_Ger2014_Human, CPXV_Ger2015_cat1, CPXV_Ger1990_2, CPXV_HumLue09_1, CPXV_CheNova_DK_2014, CPXV-Swe-H1, CPXV-Swe-H2, CPXV-Fra2001-Nancy, CPXV-FraAmiens_2016, CPXV-Catpox5-wv1, CPXV-Br, CPXV-No-F1, CPXV-Norwayfeline, CPXV-No-F2, CPXV-No-H1 and CPXV-Nor1994_Man). Whereas sub-cluster one of the phylogenetic tree based on 62 conserved genes contained an additional CPXV strain, CPXV_Ger0214_Human (Figure 1 and Figure S4). In all phylogenetic trees, the Norwegian isolates were closely related to the UK isolates (CPXV-Br and CPXV-Catpox5_wv1), while Swedish isolates were closer to the Danish isolate. CPXV-like 1 clade was the largest CPXV clade and comprises only German CPXV isolates as well as VARV-like clade. This clade was sister group of VARV/CMLV/TATV. VACV-like contains CPXV strains from Austria, Russia, Finland and Lithuania. These strains were closely related to VACV and MPXV. Compared to VACV-like, VARV-like and ECTV-Abatino-like, CPXV-like 1 and CPXV-like 2 did not cluster together with other OPXV species (Figure 1, Figure 2 and Figures S4–S8). Overall, all phylogenetic trees (based on 87 OPXV whole genomes, core genomes, orthologous genes and conserved genes) showed the five major CPXV clusters and the clustering of the CPXV-like 2 strains were similar. Thus, although recombination among CPXV is extensive, tree topology from datasets with recombinant regions and datasets without evidence of recombination were very similar.

3.3. Patristic and Genetic Distances

Based on the genetic and patristic distances, CPXV strains can be classified into 18 sub-species (Figure 3). The genetic and patristic distances between CPXV clusters and OPXV species were higher than the TATV-CMLV genetic and patristic distance threshold (Tables S6 and S7). Furthermore, the genetic and patristic distances within some CPXV clusters, such as CPXV-like 2, were higher than the threshold values (Table S8). According to the genetic and patristic distances between CPXV-like 2 strains, CPXV-like 2 was further divided into ten sub-species: group one (CPXV-Ger1998_2), group two (CPXV_Ger2014_Human, CPXV_Ger91, CPXV_Ger2007_Vole and CPXV_FM2292), group three (CPXV_HumLue09_1), group four (CPXV_Ger1990_2), group five (CPXV_Ger2015_cat1), group six (CPXV-Fra2001-Nancy), group seven (CPXV-FraAmiens_2016), group eight (CPXV_CheNova_DK_2014, CPXV-Swe-H1 and CPXV-Swe-H2), group nine (CPXV-Catpox5-wv1 and CPXV-Br) and group ten (CPXV-No-F1, CPXV-Norwayfeline, CPXV-No-F2, CPXV-No-H1 and CPXV-Nor1994_Man) (Tables S9 and S10). The isolates were grouped together according to their origin, except for the German and French isolates that were separated into five and two distinct sub-species, respectively.



Figure 3. New classification of cowpox virus (CPXV) based on phylogenetic tree inference from 62 conserved genes without evidence of recombination, patristic and genetic distances. Diamonds at the nodes indicate bootstrap values > 80%. The main five CPXV clusters were highlighted in different colors: pink (Ectromelia-Abatino-like CPXV), blue (CPXV-like 1), green (CPXV-like 2), turquoise blue (Vaccinia-like CPXV) and orange (Variola-like CPXV).

Similarly, in the ECTV-Abatino-like clade, the genetic and patristic distances between the Norwegian human isolate, CPXV-No-H2, and the German isolates (CPXV_GerMygEk938_17 and CPXV_Ger201_MKY) exceeded the distances between TATV and CMLV (Table S11). Within VACV-like, the distances between the CPXV strains were higher than the threshold values, except for the distances between CXPV-Gri and CPXV-Fin2000-Man (Tables S12 and S13). VACV-like strains were divided into three different sub-species: sub-species one, CPXV_HumLit08_1;

sub-species two, CPXV_Aus_1999; sub-species three, CPXV_Gri and CPXV_Fin2000_Man (Figure 3). In CPXV-like 1, CPXV_Ger_1971_EP1 was classified as one sub-species and the remaining CPXV-like 1 strains as another sub-species, according to the genetic and patristic distances (Table S14). However, the patristic distances between CPXV_Ger2010_Alpa and other CPXV-like 1 strains were higher than the threshold value, but some genetic distances were lower than the threshold values (Tables S15 and S16). VARV-like strains remained together as one sub-species based on the genetic and patristic distances and phylogeny. Curiously, these strains contain a genomic region of approximately 5860 bp that was also identified in some CPXV-like 2 strains (CPXV_Ger91, CPXV_2007_vole, CPXV_FM2291 and CPXV_Fra2001_Nancy), VARV and CMLV.

3.4. Evolutionary Analysis of CPXV

The phylodynamic analysis was performed based on the 62 conserved genes of CPXV genomes. The dataset exhibited a positive correlation between the genetic divergence and the sampling time, which indicates the presence of temporal signal in the sequence dataset (correlation efficient = 0.48; $R^2 = 0.23$). The mean evolution rate of CPXV was estimated to be 1.65×10^{-5} substitutions per site per year (subs/site/year), with 95% high posterior density interval (HPD) of $4.36 \times 10^{-7} - 4.32 \times 10^{-5}$ subs/site/year.

The MCC tree showed that CPXV strains were divided into two main clusters (Figure S9). The minor cluster contained CPXV-like 2 clade (PP = 0.88) and the major cluster comprised ECTV-Abatino-like, VACV-like, VARV-like and CXPV-like 1 clades (PP = 0.89) (Figure S9). However, the emergence date of CPXV as well as major CPXV clusters could not be accurately estimated since the 95% HPD intervals were wide, especially in the deepest nodes. As compared to the 95% HPD intervals tMRCA for recent nodes, tMRCA for deeper internal nodes were quite broad and showed some degree of overlap.

4. Discussion

CPXV strains examined in this study were isolated from different countries in Eurasia, with most of CPXV isolates from Germany. We included five CPXV isolates collected from Fennoscandian as well as our previously published CPXV isolate, CPXV-No-H2 [40]. These five Fennoscandian isolates were previously classified as CPXV based on Hind III restriction map of virus DNA, phylogenetic analysis of multiple conserved genes and the possession of two copies of the intact *cytokine response modifier B (CrmB)* gene [33–35].

CPXV is classified as one species, but this has been debated in many studies due to its genetic heterogeneity and polyphyletic character [33,35–40]. The genetic heterogeneity among CPXV strains could be due to recombination processes [34,35,41] since it is part of the evolution of OPXV [8,34,40,41,43,75–79]. It has been suggested that recombination can affect the accuracy of the phylogenetic inferences [80]. Since the extensive recombination in OPXV genomes has been reported by others [41], we included in our study a dataset of 62 non-recombinant conserved genes to avoid inaccuracy of phylogenetic estimation due the presence of recombination in 87 OPXV whole genomes, core genomes and orthologous genes.

Our phylogenetic analysis using different datasets always showed that CPXV isolates were divided into at least five clusters: CPXV-like 1, CPXV-like 2, VACV-like CPXV, VARV-like CPXV and ECTV-Abatino-like CPXV (Figure 1, Figure 2 and Figures S3–S7). Similar phylogenetic clustering of CPXV has been reported in other studies [40,81]. Three of the five CPXV clusters were closely related to other OPXV species, such as ECTV, Abatino, VARV and VACV. Previous studies have also showed this phylogenetic relationship of CPXV with other OPXV [35,37,38,40,41,43,81].

The German isolates were present in all CPXV clusters, except for VACV-like, while the Fennoscandian CPXV isolates clustered into CPXV-like 2 and grouped into separate clusters according to their country of origin (Norway, Sweden and Denmark), except for CPXV-No-H2. These results are in agreement with the phylogenetic analysis based on single genes (*atip*, *p4c*, *CrmB*, *HA*, complete *CHOhr* or partial *CHOhr*) reported in our previous studies [33,35]. However, not all Fennoscandian isolates were closely related. The

Norwegian isolates were closely related to the UK strains, whereas the Swedish CPXV isolates were closer to the Danish CPXV isolate. The phylogenetic relationship of the Norwegian and UK isolates has been previously reported [38,41]. In our previous studies the relationship of the Fennoscandian isolates with other CPXV isolates varied depending on the single gene used in the phylogenetic analysis [33,35]. However, in the present study, the phylogenetic relationship between the Norwegian and UK isolates as well as the Swedish and Danish isolates were consistent, regardless of the alignment used (87 OPXV whole genomes, core genomes, orthologous genes or 62 conserved genes).

Genetic and patristic distances have been previously used to examine the diversity of CPXV [35,36,38]. We used the genetic and patristic distances between TATV and CMLV to classify OPXV into the same or different species because they are the closest and recognized OPXV species. Our examination of the genetic and patristic distances between and within CPXV clusters revealed that the five CPXV clusters can be considered distinct CPXV sub-species and that even the CPXV strains can be separated into 18 sub-species (Figure 3). The heterogeneity of CPXV was not only demonstrated between CPXV clusters, but it was also present within some clusters. Among them, CPXV-like 2 was the most heterogeneous. Their isolates were classified into ten sub-species based on the genetic and patristic distances. This clade comprised isolates of diverse geographic origins (Norway, Sweden, Denmark, UK, Germany and France) and its classification followed their geographical origin. Only German and French isolates were separated into more than one sub-species.

Large genetic variation was also found within VACV-like strains, which were closely related to VACV and MPXV, as previously described [38,40,41]. These strains split into three different sub-species based on the genetic and patristic distances. This division is in agreement with phylogenetic work reported in other previous studies [38,40,41]. Among VACV-like strains, it has been reported that CPXV-HumLit08/1 is a recombinant virus that contains genomic regions related to VACV, VACV-like and VARV-like [41]. However, our findings based on 62 non-recombinant conserved genes evidenced that CPXV-HumLit08/1 can be considered as one sub-species. Similarly, within ECTV-Abatino-like clade, CPXV-No-H2 has undergone recombination with other OPXV [40] and our data supported the separation of CPXV-No-H2 and the other ECTV-Abatino-like strains into different sub-species.

The most genetically homogeneous CPXV cluster was the VARV-like group. The origin of these strains was associated with infected pet rats, probably imported from the Czech Republic [37,82]. Overall, our findings are in concordance with the results of Mauldin et al. [38]. They reported that CPXV-like 1 strains were split into more than one cluster (referred in the study as E1, E2, E3, E4 and E5), VACV-like strains were divided into three groups (referred in the study as A, B and C) and VARV-like strains were clustered into a single group.

Despite the evidence of recombination in the datasets of 87 OPXV whole genomes, core genomes and orthologous genes, their phylogeny, genetic and patristic distances agreed with and are very similar to the phylogeny, patristic and genetic distances reconstructed from the dataset of 62 conserved genes without evidence of recombination. All four datasets suggested that CPXV strains can be divided into at least 18 sub-species (Figure 3, Figure S10 and Tables S6–S16). However, biological characterization of CPXV is required to accurately infer the taxonomic level to which these 18 sub-species of CPXV belong. Furthermore, our phylogenetic analysis evidenced that recombination did not change the phylogenetic relationship between CPXV strains and OPXV despite the extensive recombination between OPXV genomes. Taking into cognizance the extensive recombination present in CPXV genomes, it is rather surprising that recombination appears not to alter the clustering pattern in OPXV phylogeny. Plausible reasons may be that recombination among CPXVs occurred very early in CPXV/OPXV evolution, recombination regions occurred in small batch sizes compared to the whole genomes and the phylogenetic signals from recombinant regions were small and was diluted out by larger phylogenetic signals from other parts of the genome.

We estimated the evolution rate of CPXV based on 62 conserved genes of 55 CPXV to be 1.65×10^{-5} substitution/site/year (95% HPD, 4.36×10^{-7} – 4.32×10^{-5} subs/site/year). The 95% HPD of our estimate overlapped the reported substitution rates of *Chordopoxvirinae*, 0.5 – 8.8×10^{-6} substitutions/site/year, and OPXV, 1.7 – 6.5×10^{-6} substitutions/site/year [45–47,49]. The divergence times of CPXV could not be accurately estimated using 62 conserved genes of 55 CPXV genomes (Figure S9), even using conserved central region (F4L-A24L) of CPXV genomes (data not shown), since the broad 95% HPD intervals of the divergence time were quite broad. It could be due to the high heterogeneity of CPXV strains and the limited number of samples in terms of location, host and sample age. The majority of CPXV strains were isolated in Germany and from infections in humans. Furthermore, most CPXV strains were isolated in the last decades, there were no ancient CPXV isolates. Therefore, the low genetic information and the high genetic distances between the current CPXV strains increase the uncertainty of the node ages. In our opinion, our result strengthens the proposed idea that lineages of CPXV are highly divergent and a reclassification is needed, rather than showing a lack of a good calibration (tempest indicated presence of temporal signal). It has been proposed that the CPXV-like virus was the ancestor of Old World OPXV, excluding AKPV and AKMV, [39,44,45,83] due to its large genome, broadest host range and the presence of the most orthopoxviral genes [42,43,83,84]. Thus, despite the exclusion of other OPXV in our analysis due to the lack of temporal signal in the dataset, the evolutionary analysis of only CPXV may reflect the genomic history of all OPXV taking into account the high genetic heterogeneity among CPXV, the suggestion that CPXV or cowpox-like virus may be the ancestor to Old World OPXV species and the phylogenetic evidence of CPXV being the only OPXV that clusters with all Old World OPXV. However, the phylodynamic analysis of only CPXV has limitations because of oversampling of CPXV strains from Germany, from human zoonotic events and lack of ancient isolates. To improve the reconstruction of the evolutionary history of CPXV, increased genomic surveillance of CPXV across different regions of Eurasia and in multiple species or by the acquisition of ancient CPXV strains are required. These will result in a more accurate estimation of the time-scale of CPXV evolution.

5. Conclusions

In conclusion, the present study demonstrated the high genetic heterogeneity among CPXV isolates and the polyphyletic character of CPXV. Furthermore, our findings confirmed that CPXV was not a single species but a polyphyletic assemblage of several (up to 18) sub-species. Therefore, the current classification of CPXV as one single species should be re-evaluated. We also provided the first reconstruction of the evolutionary history of only CPXV. Overall, this study has shed significant insight on the evolution, phylogeny and classification of CPXV.

Supplementary Materials: The following supporting information can be downloaded at: <https://www.mdpi.com/article/10.3390/v14102134/s1>, Figure S1. Presence of phylogenetic signal was evaluated by likelihood mapping checking for alternative topologies (tips), unresolved quartets (center) and partly resolved quartets (edges) for 87 OPXV whole genomes (a), core genomes (b), OPXV orthologous genes (c) and 62 conserved genes. Figure S2. Phylogenetic and temporal signal analyses. (a) Presence of phylogenetic signal was evaluated by likelihood mapping checking for alternative topologies (tips), unresolved quartets (center) and partly resolved quartets (edges) for 62 conserved genes of 55 CPXV strains. (b) Linear regression of root-to-tip genetic distance in a maximum likelihood phylogeny against sampling time for 62 conserved genes of 55 CPXV strains. Figure S3. Recombination analysis of 87 orthopoxvirus (OPXV) core genomes with RPD4. Schematic sequence display depicting color-coded representations of the analyzed sequences and the locations of detected recombination events in the 87 OPXV core genomes. The detected recombination events were detected for at least 5 of 7 methods (RDP, GENECONV, Bootscan, MaxChi, Chimaera, SiScan and 3Seq) with significant p -values ($p \leq 0.01$). Figure S4. Bayesian inference phylogenetic tree of 62 conserved genes from 87 orthopoxviruses. Diamonds at the nodes indicate posterior probabilities > 0.9 . The scale bar represents expected substitutions per site. The main five cowpox virus (CPXV) clus-

ters were highlighted in different colors: pink (Ectromelia-Abatino-like CPXV), blue (CPXV-like 1), green (CPXV-like 2), turquoise blue (Vaccinia-like CPXV) and orange (Variola-like CPXV). Figure S5. Bayesian inference phylogenetic tree of 87 OPXV core genomes. Posterior probabilities are shown on the right side of each node and only posterior probabilities above 0.9 are shown. The scale bar represents expected substitutions per site. The main five cowpox virus (CPXV) clusters were highlighted in different colors: pink (Ectromelia-Abatino-like CPXV), blue (CPXV-like 1), green (CPXV-like 2), turquoise blue (Vaccinia-like CPXV) and orange (Variola-like CPXV). Figure S6. Maximum likelihood phylogenetic tree of 87 orthopoxvirus whole genome. Bootstrap values were inferred from 1000 rapid bootstrap replicates. Diamonds at the nodes indicate bootstrap values > 80%. The scale bar indicates substitution per site. The main five cowpox virus (CPXV) clusters were highlighted in different colors: pink (Ectromelia-Abatino-like CPXV), blue (CPXV-like 1), green (CPXV-like 2), turquoise blue (Vaccinia-like CPXV) and orange (Variola-like CPXV). Figure S7. Bayesian inference phylogenetic tree of 87 OPXV whole genomes. Diamonds at the nodes indicate posterior probabilities > 0.9. The scale bar represents expected substitutions per site. The main five cowpox virus (CPXV) clusters were highlighted in different colors: pink (Ectromelia-Abatino-like CPXV), blue (CPXV-like 1), green (CPXV-like 2), turquoise blue (Vaccinia-like CPXV) and orange (Variola-like CPXV). Figure S8. Maximum likelihood phylogenetic tree based on orthopoxvirus orthologous genes. Bootstrap values were inferred from 1000 rapid bootstrap replicates. Diamonds at the nodes indicate bootstrap values > 80%. The scale indicates substitution per site. The main five cowpox virus (CPXV) clusters were highlighted in different colors: pink (Ectromelia-Abatino-like CPXV), blue (CPXV-like 1), green (CPXV-like 2), turquoise blue (Vaccinia-like CPXV) and orange (Variola-like CPXV). Figure S9. Bayesian maximum clade credibility (MCC) tree of 62 non-recombinant conserved genes of 55 CPXV genomes. The MCC tree was generated using BEAST 1, using a log-normal relaxed clock, coalescent Bayesian skyline population, HKY substitution model and four gamma categories. The numbers on the nodes indicate the time of the most recent common ancestor of the clades. Diamonds at the nodes indicate posterior probability values > 0.9. The main five CPXV clusters were highlighted in different colors: pink (Ectromelia-Abatino-like CPXV), blue (CPXV-like 1), green (CPXV-like 2), turquoise blue (Vaccinia-like CPXV) and orange (Variola-like CPXV). Figure S10. New classification of Cowpox virus (CPXV) based on phylogenetic inference (from 87 OPXV whole genomes, core genomes and orthologous genes), patristic and genetic distances. Diamonds at the nodes indicate bootstrap values > 80%. The main five CPXV clusters were highlighted in different colors: pink (Ectromelia-Abatino-like CPXV), blue (CPXV-like 1), green (CPXV-like 2), turquoise blue (Vaccinia-like CPXV) and orange (Variola-like CPXV). Table S1: List of strains used in the phylogenetic analysis. Table S2: List of orthologous genes from 87 orthopoxviruses used in this study. Table S3: List of 62 conserved genes from 87 orthopoxviruses used in this study. Table S4: List of strains used in the evolution molecular analysis. Table S5. Predicted genes in CPXV-No-F1, CPXV-No-F2, CPXV-No-H1, CPXV-Swe-H1 and CPXV-Swe-H2 compared to reference genomes CPXV-Brighton (CPXV_BR). Table S6. Patristic distances between CPXV clusters and OPXV species calculated from the Maximum likelihood (ML) and Bayesian inference (BI) trees of 62 conserved genes, 87 OPXV whole genomes, core genomes and orthologous genes. Table S7. Genetic distances between CPXV clusters and OPXV species estimated by p-distances from the alignment of 62 conserved genes (A), 87 OPXV whole genomes (B), core genomes (C) and orthologous genes (D). Table S8. Patristic and genetic distances within CPXV clusters calculated from the Maximum likelihood (ML) and Bayesian inference (BI) trees of 62 conserved genes, 87 OPXV core genomes, whole genomes and orthologous genes and their alignments, respectively. Table S9. Patristic distances within CPXV-like 2 calculated from the Maximum likelihood (ML) and Bayesian inference (BI) trees of 62 conserved genes, 87 OPXV whole genomes, core genomes and orthologous genes. Table S10. Genetic distances within CPXV-like 2 estimated by p-distances from the alignment of 62 conserved genes (A), 87 OPXV whole genomes (B), core genomes (C) and orthologous genes (D). Table S11. Patristic and genetic distances within ECTV-Abatino-like calculated from the Maximum likelihood (ML) and Bayesian inference (BI) trees of 62 conserved genes, 87 OPXV whole genomes, core genomes and orthologous genes and their alignments, respectively. Table S12. Patristic distances within VACV-like calculated from the Maximum likelihood (ML) and Bayesian inference (BI) trees of 62 conserved genes, 87 OPXV whole genomes, core genomes and orthologous genes. Table S13. Genetic distances within VACV-like clade estimated by p-distances from the alignment of 62 conserved genes (A), 87 OPXV whole genomes (B), core genomes (C) and orthologous genes (D). Table S14. Patristic and genetic distances within CPXV-like 1 calculated from the Maximum likelihood (ML) and Bayesian inference (BI) trees of 87 OPXV whole genomes, core

genomes and orthologous genes and their alignments, respectively. Table S15. Patristic distances within CPXV-like 1 calculated from the Maximum likelihood (ML) and Bayesian inference (BI) trees of 62 conserved genes, 87 OPXV whole genomes, core genomes and orthologous genes. Table S16. Genetic distances within CPXV-like 1 estimated by p-distances from the alignment of 62 conserved genes (A), 87 OPXV whole genomes (B), core genomes (C) and orthologous genes (D).

Author Contributions: Conceptualization, D.D.-C., U.M. and M.I.O.; Methodology, D.D.-C., C.M., U.M. and M.I.O.; Supervision, U.M. and M.I.O.; Writing—original draft, D.D.-C., C.M., U.M. and M.I.O.; Writing—review and editing, D.D.-C., C.M., A.N., A.B., U.M. and M.I.O. All authors have read and agreed to the published version of the manuscript.

Funding: This research was funded by UiT—The Arctic University of Norway, grant number A212100108 and the National Graduate School in Infection Biology and Antimicrobials, grant number 249062. The APC was funded by UiT—The Arctic University of Norway.

Institutional Review Board Statement: Not applicable.

Informed Consent Statement: Not applicable.

Data Availability Statement: The original contributions presented in the study are publicly available. These data can be found here: <https://www.ncbi.nlm.nih.gov/genbank/> (accessed on 2 August 2022), OP125537, OP125538, OP125539, OP125540, OP125541.

Conflicts of Interest: The authors declare no conflict of interest.

References

- MacLachlan, N.J.; Dubovi, E.J. (Eds.) Poxviridae. In *Fenner's Veterinary Virology*; Academic Press: Boston, MA, USA, 2017; pp. 157–174. ISBN 9780128009468.
- Smithson, C.; Tang, N.; Sammons, S.; Frace, M.; Batra, D.; Li, Y.; Emerson, G.L.; Carroll, D.S.; Upton, C. The Genomes of Three North American Orthopoxviruses. *Virus Genes* **2017**, *53*, 21–34. [[CrossRef](#)]
- International Committee on Taxonomy of Viruses (ICTV). Available online: <https://talk.ictvonline.org/taxonomy/> (accessed on 16 July 2022).
- Gubser, C.; Smith, G.L. The Sequence of Camelpox Virus Shows It Is Most Closely Related to Variola Virus, the Cause of Smallpox. *J. Gen. Virol.* **2002**, *83*, 855–872. [[CrossRef](#)] [[PubMed](#)]
- Mavian, C.; López-Bueno, A.; Martín, R.; Nitsche, A.; Alcamí, A. Comparative Pathogenesis, Genomics and Phylogeography of Mousepox. *Viruses* **2021**, *13*, 1146. [[CrossRef](#)] [[PubMed](#)]
- Cardeti, G.; Gruber, C.E.M.; Eleni, C.; Carletti, F.; Castilletti, C.; Manna, G.; Rosone, F.; Giombini, E.; Selleri, M.; Lapa, D.; et al. Fatal Outbreak in Tonkean Macaques Caused by Possibly Novel Orthopoxvirus, Italy, January 2015. *Emerg. Infect. Dis. J.* **2017**, *23*, 1941–1949. [[CrossRef](#)] [[PubMed](#)]
- Springer, Y.P.; Hsu, C.H.; Werle, Z.R.; Olson, L.E.; Cooper, M.P.; Castrodale, L.J.; Fowler, N.; Mccollum, A.M.; Goldsmith, C.S.; Emerson, G.L.; et al. Novel Orthopoxvirus Infection in an Alaska Resident. *Clin. Infect. Dis.* **2017**, *64*, 1737. [[CrossRef](#)] [[PubMed](#)]
- Gao, J.; Gigante, C.; Khmaladze, E.; Liu, P.; Tang, S.; Wilkins, K.; Zhao, K.; Davidson, W.; Nakazawa, Y.; Maghlakelidze, G.; et al. Genome Sequences of Akhmeta Virus, an Early Divergent Old World Orthopoxvirus. *Viruses* **2018**, *10*, 252. [[CrossRef](#)] [[PubMed](#)]
- Strassburg, M.A. The Global Eradication of Smallpox. *Am. J. Infect. Control* **1982**, *10*, 53–59. [[CrossRef](#)]
- Deria, A.; Jezek, Z.; Markvart, K.; Carrasco, P.; Weisfeld, J. The World's Last Endemic Case of Smallpox: Surveillance and Containment Measures. *Bull. World Health Organ.* **1980**, *58*, 279.
- Vora, N.M.; Li, Y.; Geleishvili, M.; Emerson, G.L.; Khmaladze, E.; Maghlakelidze, G.; Navdarashvili, A.; Zakhshvili, K.; Kokhraidze, M.; Endeladze, M.; et al. Human Infection with a Zoonotic Orthopoxvirus in the Country of Georgia. *N. Engl. J. Med.* **2015**, *372*, 1223. [[CrossRef](#)] [[PubMed](#)]
- Diaz, J.H. The Disease Ecology, Epidemiology, Clinical Manifestations, Management, Prevention, and Control of Increasing Human Infections with Animal Orthopoxviruses. *Wilderness Environ. Med.* **2021**, *32*, 528–536. [[CrossRef](#)]
- Silva, N.I.O.; de Oliveira, J.S.; Kroon, E.G.; de Souza Trindade, G.; Drumond, B.P. Here, There, and Everywhere: The Wide Host Range and Geographic Distribution of Zoonotic Orthopoxviruses. *Viruses* **2021**, *13*, 43. [[CrossRef](#)] [[PubMed](#)]
- Alakunle, E.; Moens, U.; Nchinda, G.; Okeke, M.I. Monkeypox Virus in Nigeria: Infection Biology, Epidemiology, and Evolution. *Viruses* **2020**, *12*, 1257. [[CrossRef](#)] [[PubMed](#)]
- Reynolds, M.G.; Guagliardo, S.A.J.; Nakazawa, Y.J.; Doty, J.B.; Mauldin, M.R. Understanding Orthopoxvirus Host Range and Evolution: From the Enigmatic to the Usual Suspects. *Curr. Opin. Virol.* **2018**, *28*, 108–115. [[CrossRef](#)] [[PubMed](#)]
- WHO. Disease Outbreak News; Multi-Country Monkeypox Outbreak: Situation Update. Available online: <https://www.who.int/emergencies/disease-outbreak-news/item/2022-DON396> (accessed on 9 July 2022).
- WHO. Disease Outbreak News; Multi-Country Monkeypox Outbreak in Non-Endemic Countries. Available online: <https://www.who.int/emergencies/disease-outbreak-news/item/2022-DON385> (accessed on 20 June 2022).

18. Chantrey, J.; Meyer, H.; Baxby, D.; Begon, M.; Bown, K.J.; Hazel, S.M.; Jones, T.; Montgomery, W.I.; Bennett, M. Cowpox: Reservoir Hosts and Geographic Range. *Epidemiol. Infect.* **1999**, *122*, 455. [[CrossRef](#)] [[PubMed](#)]
19. Wolfs, T.F.W.; Wagenaar, J.A.; Niesters, H.G.M.; Osterhaus, A.D.M.E. Rat-to-Human Transmission of Cowpox Infection. *Emerg. Infect. Dis.* **2002**, *8*, 1495. [[CrossRef](#)]
20. Laakkonen, J.; Kallio-Kokko, H.; Öktem, M.A.; Blasdel, K.; Plyusnina, A.; Niemimaa, J.; Karataş, A.; Plyusnin, A.; Vaheri, A.; Henttonen, H. Serological Survey for Viral Pathogens in Turkish Rodents. *J. Wildl. Dis.* **2006**, *42*, 672–676. [[CrossRef](#)]
21. Vorou, R.M.; Papavassiliou, V.G.; Pierroutsakos, I.N. Cowpox Virus Infection: An Emerging Health Threat. *Curr. Opin. Infect. Dis.* **2008**, *21*, 153–156. [[CrossRef](#)]
22. Popova, A.Y.; Maksyutov, R.A.; Taranov, O.S.; Tregubchak, T.V.; Zaikovskaya, A.V.; Sergeev, A.A.; Vlashchenko, I.V.; Bodnev, S.A.; Ternovoi, V.A.; Alexandrova, N.S. Cowpox in a Human, Russia, 2015. *Epidemiol. Infect.* **2017**, *145*, 755–759. [[CrossRef](#)]
23. Ferrier, A.; Frenois-Veyrat, G.; Schvoerer, E.; Henard, S.; Jarjavall, F.; Drouet, I.; Timera, H.; Boutin, L.; Mosca, E.; Peyrefitte, C.; et al. Fatal Cowpox Virus Infection in Human Fetus, France, 2017. *Emerg. Infect. Dis.* **2021**, *27*, 2570–2577. [[CrossRef](#)]
24. Kinnunen, P.M.; Henttonen, H.; Hoffmann, B.; Kallio, E.R.; Korthase, C.; Laakkonen, J.; Niemimaa, J.; Palva, A.; Schlegel, M.; Ali, H.S.; et al. Orthopox Virus Infections in Eurasian Wild Rodents. *Vector-Borne Zoonotic Dis.* **2011**, *11*, 1133–1140. [[CrossRef](#)]
25. Girling, S.J.; Pizzi, R.; Cox, A.; Beard, P.M. Fatal Cowpox Virus Infection in Two Squirrel Monkeys (*Saimiri sciureus*). *Vet. Rec.* **2011**, *169*, 156. [[CrossRef](#)] [[PubMed](#)]
26. Smith, K.C.; Bennett, M.; Garrett, D.C. Skin Lesions Caused by Orthopoxvirus Infection in a Dog. *J. Small Anim. Pract.* **1999**, *40*, 495–497. [[CrossRef](#)] [[PubMed](#)]
27. Tryland, M.; Myrnel, H.; Holtet, L.; Haukenes, G.; Traavik, T. Clinical Cowpox Cases in Norway. *Scand. J. Infect. Dis.* **1998**, *30*, 301–303. [[CrossRef](#)] [[PubMed](#)]
28. Martina, B.E.E.; Van Doornum, G.; Dorrestein, G.M.; Niesters, H.G.M.; Stittelaar, K.J.; Wolters, M.A.B.I.; Van Bolhuis, H.G.H.; Osterhaus, A.D.M.E. Cowpox Virus Transmission from Rats to Monkeys, the Netherlands. *Emerg. Infect. Dis.* **2006**, *12*, 1005. [[CrossRef](#)]
29. Prkno, A.; Hoffmann, D.; Goerigk, D.; Kaiser, M.; van Maanen, A.C.F.; Jeske, K.; Jenckel, M.; Pfaff, F.; Vahlenkamp, T.W.; Beer, M.; et al. Epidemiological Investigations of Four Cowpox Virus Outbreaks in Alpaca Herds, Germany. *Viruses* **2017**, *9*, 344. [[CrossRef](#)]
30. Willemsse, A.; Egberink, H.F. Transmission of Cowpox Virus Infection from Domestic Cat to Man. *Lancet* **1985**, *1*, 1515. [[CrossRef](#)]
31. Tryland, M.; Sandvik, T.; Hansen, H.; Haukenes, G.; Holtet, L.; Bennett, M.; Mehl, R.; Moens, U.; Olsvik, T.; Traavik, T. Characteristics of Four Cowpox Virus Isolates from Norway and Sweden. *APMIS* **1998**, *106*, 623–635. [[CrossRef](#)]
32. Cronqvist, J.; Ekdahl, K.; Kjartansdottir, A.; Bauer, B.; Klinker, M. Cowpox—A Cat Disease in Man. *Lakartidningen* **1991**, *88*, 2605–2606.
33. Hansen, H.; Okeke, M.I.; Nilssen, Ø.; Traavik, T. Comparison and Phylogenetic Analysis of Cowpox Viruses Isolated from Cats and Humans in Fennoscandia. *Arch. Virol.* **2009**, *154*, 1293–1302. [[CrossRef](#)]
34. Okeke, M.I.; Hansen, H.; Traavik, T. A Naturally Occurring Cowpox Virus with an Ectromelia Virus A-Type Inclusion Protein Gene Displays Atypical A-Type Inclusions. *Infect. Genet. Evol.* **2012**, *12*, 160–168. [[CrossRef](#)]
35. Okeke, M.I.; Okoli, A.S.; Nilssen, Ø.; Moens, U.; Tryland, M.; Bøhn, T.; Traavik, T. Molecular Characterization and Phylogenetics of Fennoscandian Cowpox Virus Isolates Based on the P4c and Atip Genes. *Virol. J.* **2014**, *11*, 119. [[CrossRef](#)]
36. Carroll, D.S.; Emerson, G.L.; Li, Y.; Sammons, S.; Olson, V.; Frace, M.; Nakazawa, Y.; Czerny, C.P.; Tryland, M.; Kolodziejek, J.; et al. Chasing Jenner’s Vaccine: Revisiting Cowpox Virus Classification. *PLoS ONE* **2011**, *6*, 4–9. [[CrossRef](#)]
37. Dabrowski, P.W.; Radonić, A.; Kurth, A.; Nitsche, A. Genome-Wide Comparison of Cowpox Viruses Reveals a New Clade Related to Variola Virus. *PLoS ONE* **2013**, *8*, e79953. [[CrossRef](#)] [[PubMed](#)]
38. Mauldin, M.R.; Antwerpen, M.; Emerson, G.L.; Li, Y.; Zoeller, G.; Carroll, D.S.; Meyer, H. Cowpox Virus: What’s in a Name? *Viruses* **2017**, *9*, 101. [[CrossRef](#)]
39. Babkin, I.V.; Babkina, I.N.; Tikunova, N.V. An Update of Orthopoxvirus Molecular Evolution. *Viruses* **2022**, *14*, 388. [[CrossRef](#)]
40. Diaz-Cánova, D.; Moens, U.L.; Brinkmann, A.; Nitsche, A.; Okeke, M.I. Genomic Sequencing and Analysis of a Novel Human Cowpox Virus With Mosaic Sequences From North America and Old World Orthopoxvirus. *Front. Microbiol.* **2022**, *13*, 868887. [[CrossRef](#)]
41. Franke, A.; Pfaff, F.; Jenckel, M.; Hoffmann, B.; Höper, D.; Antwerpen, M.; Meyer, H.; Beer, M.; Hoffmann, D. Classification of Cowpox Viruses into Several Distinct Clades and Identification of a Novel Lineage. *Viruses* **2017**, *9*, 142. [[CrossRef](#)] [[PubMed](#)]
42. Senkevich, T.G.; Yutin, N.; Wolf, Y.I.; Koonin, E.V.; Moss, B. Ancient Gene Capture and Recent Gene Loss Shape the Evolution of Orthopoxvirus-Host Interaction Genes. *mBio* **2021**, *12*, e01495-21. [[CrossRef](#)] [[PubMed](#)]
43. Gubser, C.; Hué, S.; Kellam, P.; Smith, G.L. Poxvirus Genomes: A Phylogenetic Analysis. *J. Gen. Virol.* **2004**, *85*, 105–117. [[CrossRef](#)] [[PubMed](#)]
44. Hendrickson, R.C.; Wang, C.; Hatcher, E.L.; Lefkowitz, E.J. Orthopoxvirus Genome Evolution: The Role of Gene Loss. *Viruses* **2010**, *2*, 1933–1967. [[CrossRef](#)] [[PubMed](#)]
45. Zehender, G.; Lai, A.; Veo, C.; Bergna, A.; Ciccozzi, M.; Galli, M. Bayesian Reconstruction of the Evolutionary History and Cross-Species Transition of Variola Virus and Orthopoxviruses. *J. Med. Virol.* **2018**, *90*, 1134–1141. [[CrossRef](#)]
46. Babkin, I.V.; Babkina, I.N. A Retrospective Study of the Orthopoxvirus Molecular Evolution. *Infect. Genet. Evol.* **2012**, *12*, 1597–1604. [[CrossRef](#)]
47. Babkin, I.V.; Shchelkunov, S.N. Molecular Evolution of Poxviruses. *Russ. J. Genet.* **2008**, *44*, 895–908. [[CrossRef](#)]

48. Babkin, I.V.; Shchelkunov, S.N. Time Scale of Poxvirus Evolution. *Mol. Biol.* **2006**, *40*, 16–19. [[CrossRef](#)]
49. Babkin, I.V.; Babkina, I.N. Molecular Dating in the Evolution of Vertebrate Poxviruses. *Intervirology* **2011**, *54*, 253–260. [[CrossRef](#)] [[PubMed](#)]
50. Bankevich, A.; Nurk, S.; Antipov, D.; Gurevich, A.A.; Dvorkin, M.; Kulikov, A.S.; Lesin, V.M.; Nikolenko, S.I.; Pham, S.; Prjibelski, A.D.; et al. SPAdes: A New Genome Assembly Algorithm and Its Applications to Single-Cell Sequencing. *J. Comput. Biol.* **2012**, *19*, 477. [[CrossRef](#)]
51. Tcherepanov, V.; Ehlers, A.; Upton, C. Genome Annotation Transfer Utility (GATU): Rapid Annotation of Viral Genomes Using a Closely Related Reference Genome. *BMC Genom.* **2006**, *7*, 150. [[CrossRef](#)]
52. Camacho, C.; Coulouris, G.; Avagyan, V.; Ma, N.; Papadopoulos, J.; Bealer, K.; Madden, T.L. BLAST+: Architecture and Applications. *BMC Bioinform.* **2009**, *10*, 421. [[CrossRef](#)] [[PubMed](#)]
53. Ehlers, A.; Osborne, J.; Slack, S.; Roper, R.L.; Upton, C. Poxvirus Orthologous Clusters (POCs). *Bioinformatics* **2002**, *18*, 1544–1545. [[CrossRef](#)] [[PubMed](#)]
54. Katoh, K.; Standley, D.M. MAFFT Multiple Sequence Alignment Software Version 7: Improvements in Performance and Usability. *Mol. Biol. Evol.* **2013**, *30*, 772–780. [[CrossRef](#)]
55. Martin, D.P.; Murrell, B.; Golden, M.; Khoosal, A.; Muhire, B. RDP4: Detection and Analysis of Recombination Patterns in Virus Genomes. *Virus Evol.* **2015**, *1*, vev003. [[CrossRef](#)]
56. Martin, D.; Rybicki, E. RDP: Detection of Recombination amongst Aligned Sequences. *Bioinformatics* **2000**, *16*, 562–563. [[CrossRef](#)]
57. Padidam, M.; Sawyer, S.; Fauquet, C.M. Possible Emergence of New Geminiviruses by Frequent Recombination. *Virology* **1999**, *265*, 218–225. [[CrossRef](#)]
58. Martin, D.P.; Posada, D.; Crandall, K.A.; Williamson, C. A Modified Bootscan Algorithm for Automated Identification of Recombinant Sequences and Recombination Breakpoints. *AIDS Res. Hum. Retrovir.* **2005**, *21*, 98–102. [[CrossRef](#)] [[PubMed](#)]
59. Smith, J.M. Analyzing the Mosaic Structure of Genes. *J. Mol. Evol.* **1992**, *34*, 126–129. [[CrossRef](#)]
60. Posada, D.; Crandall, K.A. Evaluation of Methods for Detecting Recombination from DNA Sequences: Computer Simulations. *Proc. Natl. Acad. Sci. USA* **2001**, *98*, 13757–13762. [[CrossRef](#)] [[PubMed](#)]
61. Gibbs, M.J.; Armstrong, J.S.; Gibbs, A.J. Sister-Scanning: A Monte Carlo Procedure for Assessing Signals in Recombinant Sequences. *Bioinformatics* **2000**, *16*, 573–582. [[CrossRef](#)] [[PubMed](#)]
62. Boni, M.F.; Posada, D.; Feldman, M.W. An Exact Nonparametric Method for Inferring Mosaic Structure in Sequence Triplets. *Genetics* **2007**, *176*, 1035–1047. [[CrossRef](#)] [[PubMed](#)]
63. Talavera, G.; Castresana, J. Improvement of Phylogenies after Removing Divergent and Ambiguously Aligned Blocks from Protein Sequence Alignments. *Syst. Biol.* **2007**, *56*, 564–577. [[CrossRef](#)] [[PubMed](#)]
64. Minh, B.Q.; Schmidt, H.A.; Chernomor, O.; Schrempf, D.; Woodhams, M.D.; Von Haeseler, A.; Lanfear, R.; Teeling, E. IQ-TREE 2: New Models and Efficient Methods for Phylogenetic Inference in the Genomic Era. *Mol. Biol. Evol.* **2020**, *37*, 1530–1534. [[CrossRef](#)]
65. Darriba, D.; Posada, D.; Kozlov, A.M.; Stamatakis, A.; Morel, B.; Flouri, T. ModelTest-NG: A New and Scalable Tool for the Selection of DNA and Protein Evolutionary Models. *Mol. Biol. Evol.* **2020**, *37*, 294. [[CrossRef](#)] [[PubMed](#)]
66. Stamatakis, A. RAxML Version 8: A Tool for Phylogenetic Analysis and Post-Analysis of Large Phylogenies. *Bioinformatics* **2014**, *30*, 1313. [[CrossRef](#)] [[PubMed](#)]
67. Stamatakis, A.; Hoover, P.; Rougemont, J. A Rapid Bootstrap Algorithm for the RAxML Web Servers. *Syst. Biol.* **2008**, *57*, 758–771. [[CrossRef](#)]
68. Ronquist, F.; Teslenko, M.; Van Der Mark, P.; Ayres, D.L.; Darling, A.; Höhna, S.; Larget, B.; Liu, L.; Suchard, M.A.; Huelsenbeck, J.P. MrBayes 3.2: Efficient Bayesian Phylogenetic Inference and Model Choice Across a Large Model Space. *Syst. Biol.* **2012**, *61*, 539–542. [[CrossRef](#)]
69. Fourment, M.; Gibbs, M.J. PATRISTIC: A Program for Calculating Patristic Distances and Graphically Comparing the Components of Genetic Change. *BMC Evol. Biol.* **2006**, *6*, 1. [[CrossRef](#)] [[PubMed](#)]
70. Tamura, K.; Stecher, G.; Kumar, S. MEGA11: Molecular Evolutionary Genetics Analysis Version 11. *Mol. Biol. Evol.* **2021**, *38*, 3022–3027. [[CrossRef](#)]
71. Suchard, M.A.; Lemey, P.; Baele, G.; Ayres, D.L.; Drummond, A.J.; Rambaut, A. Bayesian Phylogenetic and Phylodynamic Data Integration Using BEAST 1.10. *Virus Evol.* **2018**, *4*, vey016. [[CrossRef](#)] [[PubMed](#)]
72. Rambaut, A.; Lam, T.T.; Carvalho, L.M.; Pybus, O.G. Exploring the Temporal Structure of Heterochronous Sequences Using TempEst (Formerly Path-O-Gen). *Virus Evol.* **2016**, *2*, vew007. [[CrossRef](#)]
73. Rambaut, A.; Drummond, A.J.; Xie, D.; Baele, G.; Suchard, M.A. Posterior Summarization in Bayesian Phylogenetics Using Tracer 1.7. *Syst. Biol.* **2018**, *67*, 901. [[CrossRef](#)]
74. Yu, G.; Smith, D.K.; Zhu, H.; Guan, Y.; Lam, T.T.Y. Ggtree: An R Package for Visualization and Annotation of Phylogenetic Trees with Their Covariates and Other Associated Data. *Methods Ecol. Evol.* **2017**, *8*, 28–36. [[CrossRef](#)]
75. Coulson, D.; Upton, C. Characterization of Indels in Poxvirus Genomes. *Virus Genes* **2011**, *42*, 171–177. [[CrossRef](#)]
76. Qin, L.; Upton, C.; Hazes, B.; Evans, D.H. Genomic Analysis of the Vaccinia Virus Strain Variants Found in Dryvax Vaccine. *J. Virol.* **2011**, *85*, 13049. [[CrossRef](#)] [[PubMed](#)]
77. Qin, L.; Favis, N.; Famulski, J.; Evans, D.H. Evolution of and Evolutionary Relationships between Extant Vaccinia Virus Strains. *J. Virol.* **2015**, *89*, 1809. [[CrossRef](#)] [[PubMed](#)]

78. Smithson, C.; Purdy, A.; Verster, A.J.; Upton, C. Prediction of Steps in the Evolution of Variola Virus Host Range. *PLoS ONE* **2014**, *9*, e91520. [[CrossRef](#)] [[PubMed](#)]
79. Smithson, C.; Meyer, H.; Gigante, C.M.; Gao, J.; Zhao, H.; Batra, D.; Damon, I.; Upton, C.; Li, Y. Two Novel Poxviruses with Unusual Genome Rearrangements: NY_014 and Murmansk. *Virus Genes* **2017**, *53*, 883–897. [[CrossRef](#)]
80. Smithson, C.; Kampman, S.; Hetman, B.M.; Upton, C. Incongruencies in Vaccinia Virus Phylogenetic Trees. *Computation* **2014**, *2*, 182–198. [[CrossRef](#)]
81. Jeske, K.; Weber, S.; Pfaff, F.; Imholt, C.; Jacob, J.; Beer, M.; Ulrich, R.G.; Hoffmann, D. Molecular Detection and Characterization of the First Cowpox Virus Isolate Derived from a Bank Vole. *Viruses* **2019**, *11*, 1075. [[CrossRef](#)]
82. Becker, C.; Kurth, A.; Hessler, F.; Kramp, H.; Gokel, M.; Hoffmann, R.; Kuczka, A.; Nitsche, A. Cowpox Virus Infection in Pet Rat Owners: Not Always Immediately Recognized. *Dtsch. Ärzteblatt Int.* **2009**, *106*, 329. [[CrossRef](#)]
83. Shchelkunov, S.N.; Safronov, P.F.; Totmenin, A.V.; Petrov, N.A.; Ryazankina, O.I.; Gutorov, V.V.; Kotwal, G.J. The Genomic Sequence Analysis of the Left and Right Species-Specific Terminal Region of a Cowpox Virus Strain Reveals Unique Sequences and a Cluster of Intact ORFs for Immunomodulatory and Host Range Proteins. *Virology* **1998**, *243*, 432–460. [[CrossRef](#)]
84. Hendrickson, R.C.; Wang, C.; Hatcher, E.L.; Lefkowitz, E.J. Orthopoxvirus Genome Evolution: The Role of Gene Loss. *Viruses* **2010**, *2*, 1933. [[CrossRef](#)]

Supplementary information

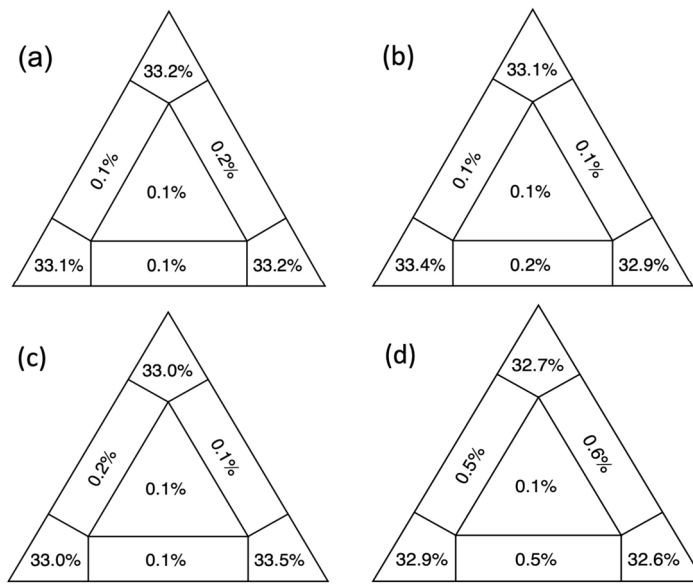


Figure S1. Presence of phylogenetic signal was evaluated by likelihood mapping checking for alternative topologies (tips), unresolved quartets (center) and partly resolved quartets (edges) for 87 OPXV whole genome (a), core genome (b), OPXV orthologous genes (c) and 62 conserved genes.

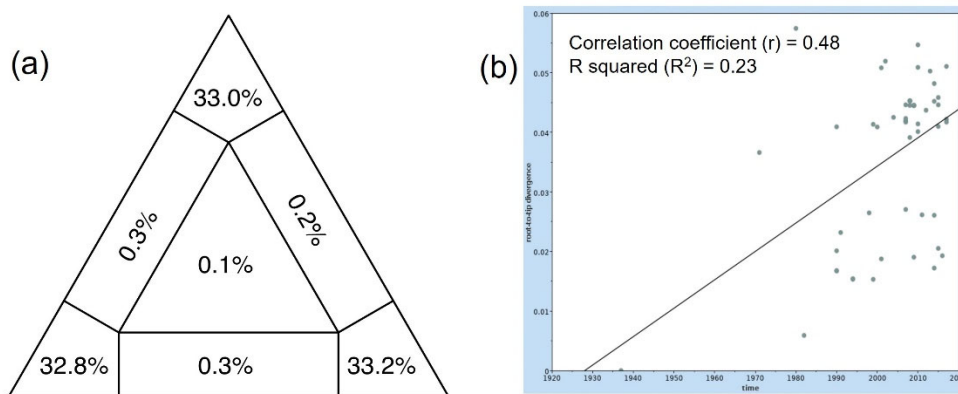
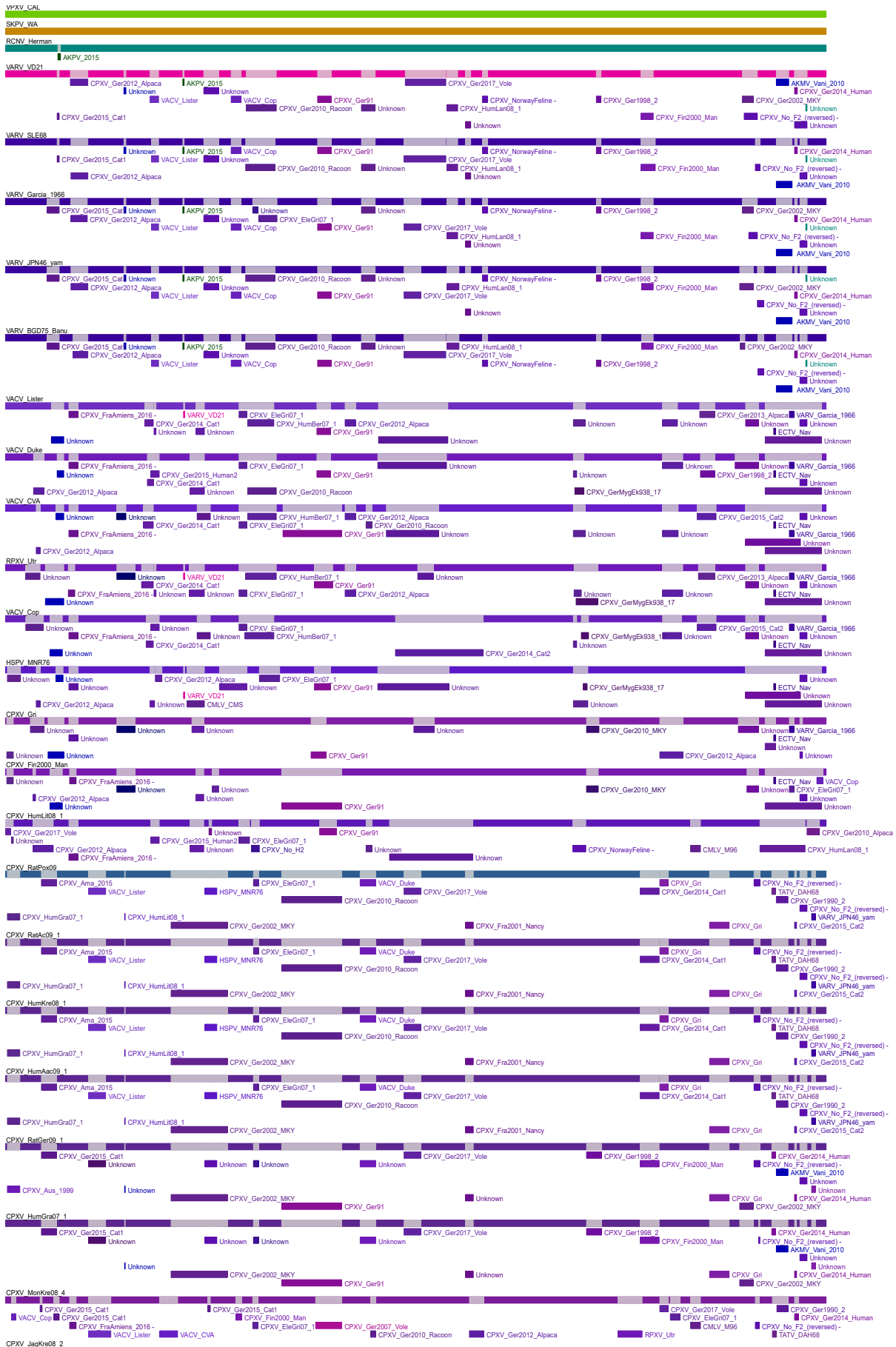
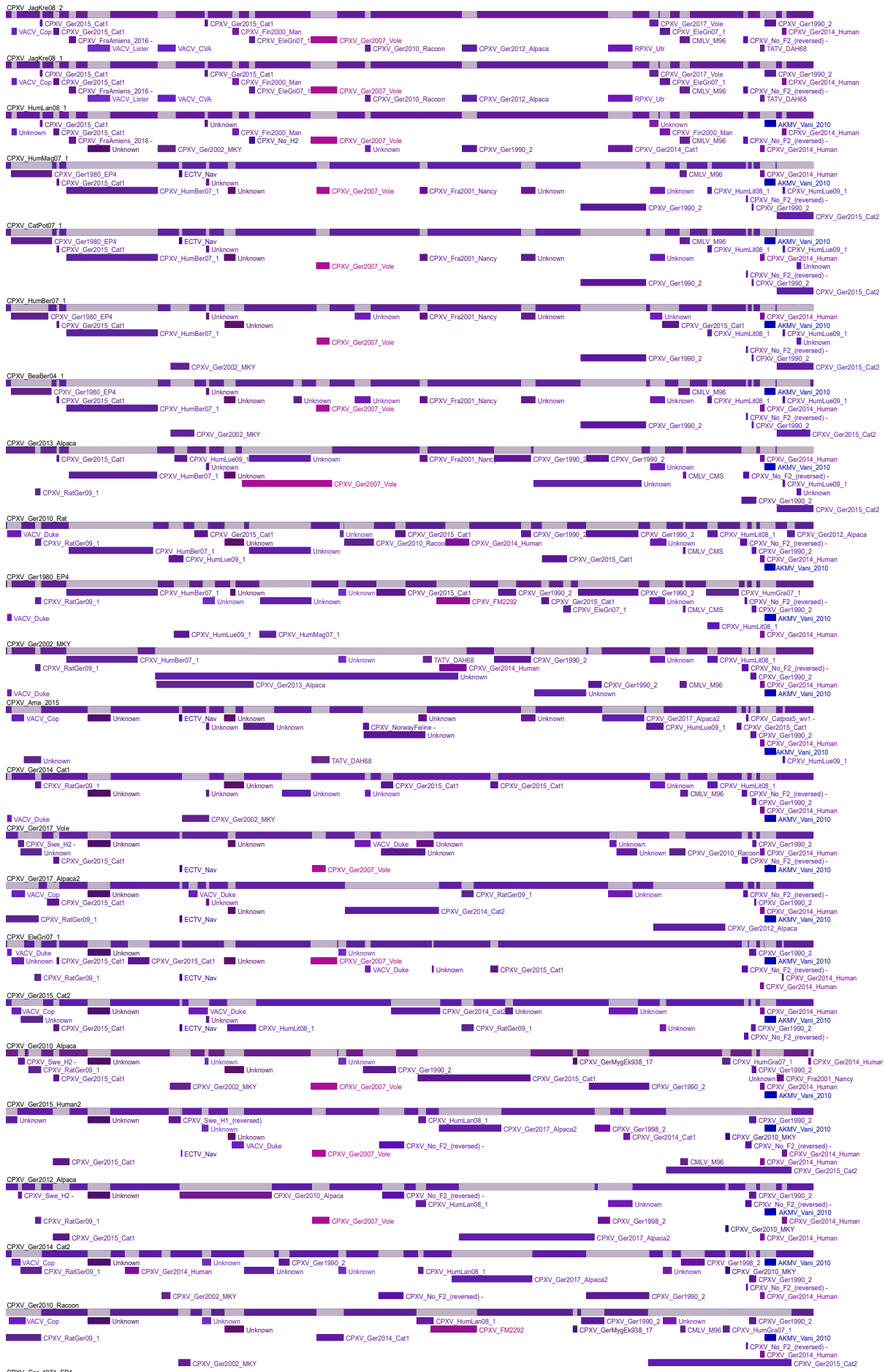
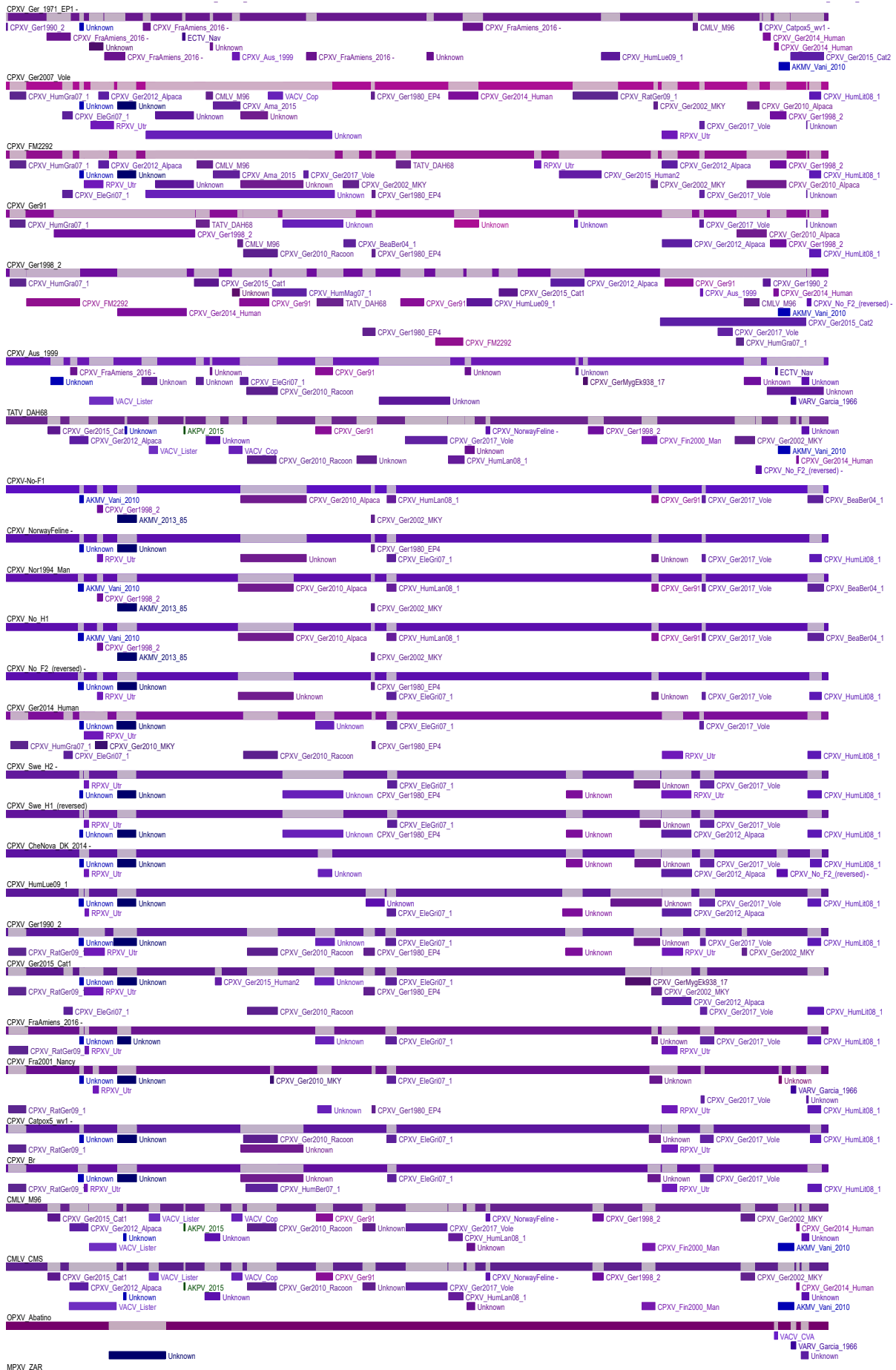


Figure S2. Phylogenetic and temporal signal analyses. (a) Presence of phylogenetic signal was evaluated by likelihood mapping checking for alternative topologies (tips), unresolved quartets (centre) and partly resolved quartets (edges) for 62 conserved genes of 55 CPXV strains. (b) Linear regression of root-to-tip genetic distance in a maximum likelihood phylogeny against sampling time for 62 conserved genes of 55 CPXV strains.







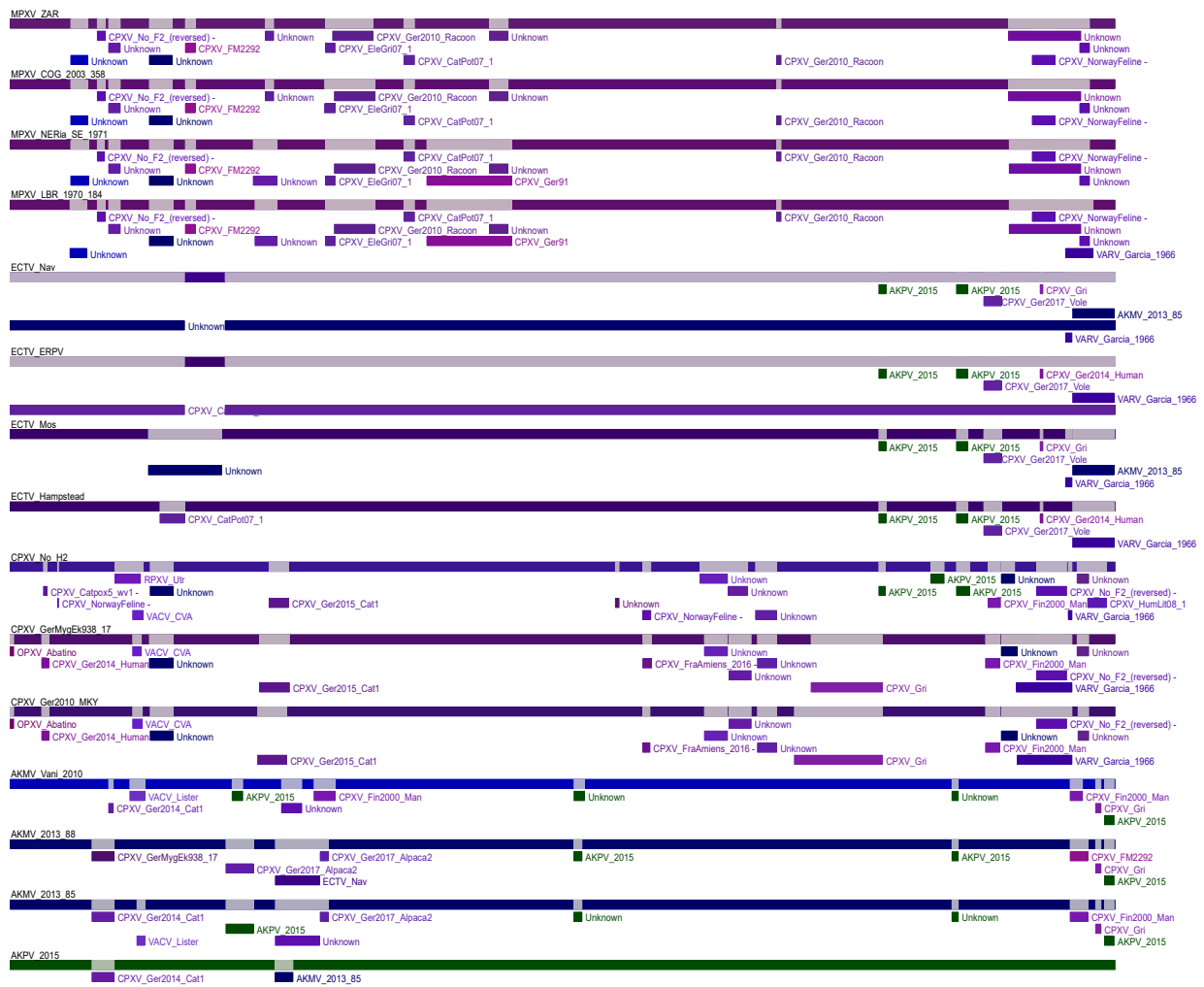
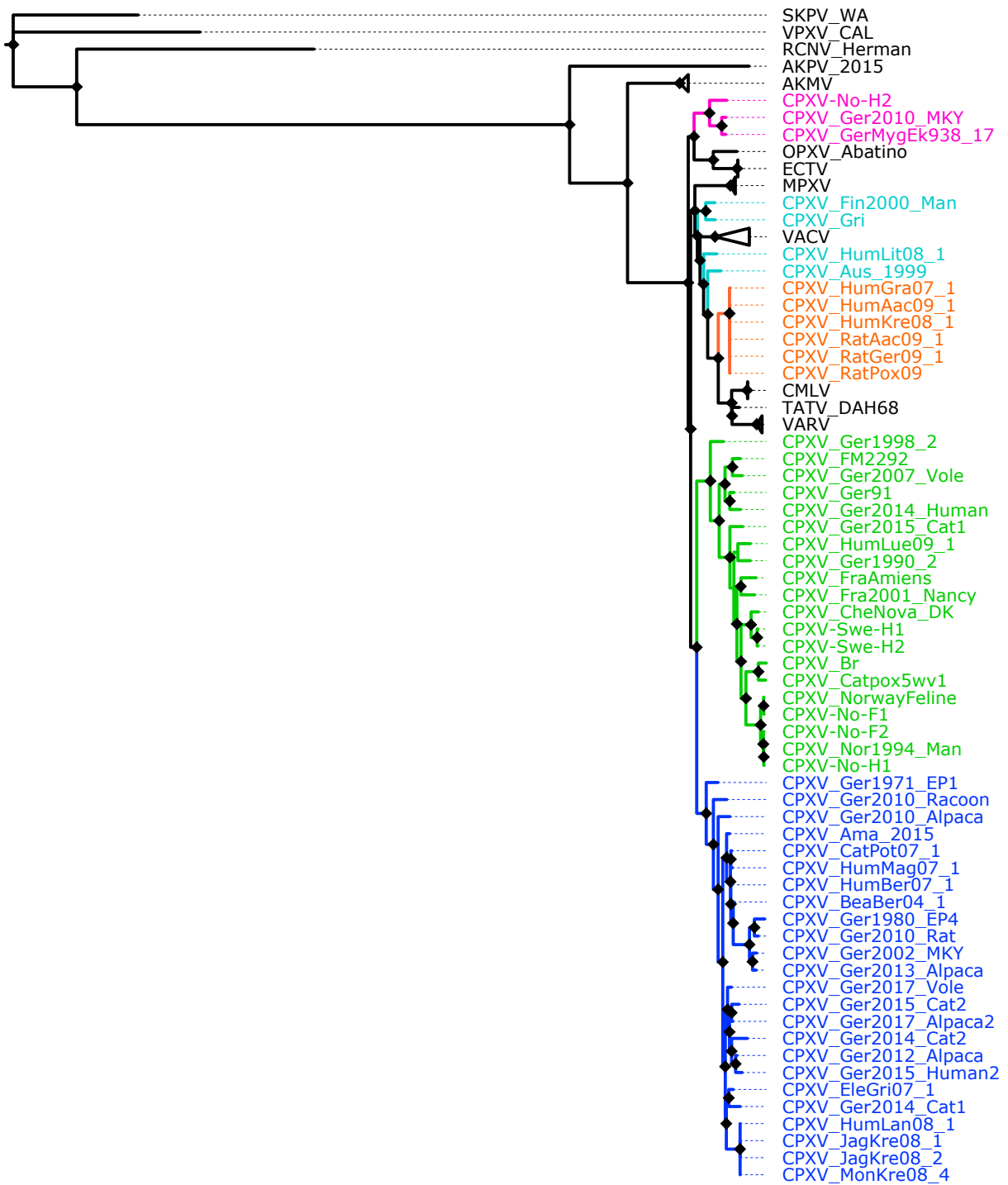


Figure S3. Recombination analysis of 87 orthopoxvirus (OPXV) core genomes with RPD4. Schematic sequence display depicting colour-coded representations of the analyzed sequences and the locations of detected recombination events in the 87 OPXV core genomes. The detected recombination events were detected for at least 5 of 7 methods (RDP, GENECONV, Bootscan, MaxChi, Chimaera, SiScan, and 3Seq) with significant p-values ($p \leq 0.01$).



0.04

Figure S4. Bayesian inference phylogenetic tree of 62 conserved genes from 87 orthopoxviruses. Diamonds at the nodes indicate posterior probabilities >0.9. The scale bar represents expected substitutions per site. The main five cowpox virus (CPXV) clusters were highlighted in different colors: pink (Ectromelia-Abatino-like CPXV), blue (CPXV-like 1), green (CPXV-like 2), turquoise blue (Vaccinia-like CPXV) and orange (Variola-like CPXV).



Figure S5. Bayesian inference phylogenetic tree of 87 OPXV core genomes. Posterior probabilities are shown on the right side of each node and only posterior probabilities above 0.9. are shown. The scale bar represents expected substitutions per site. The main five cowpox virus (CPXV) clusters were highlighted in different colors: pink (Ectromelia-Abatino-like CPXV), blue (CPXV-like 1), green (CPXV-like 2), turquoise blue (Vaccinia-like CPXV) and orange (Variola-like CPXV).

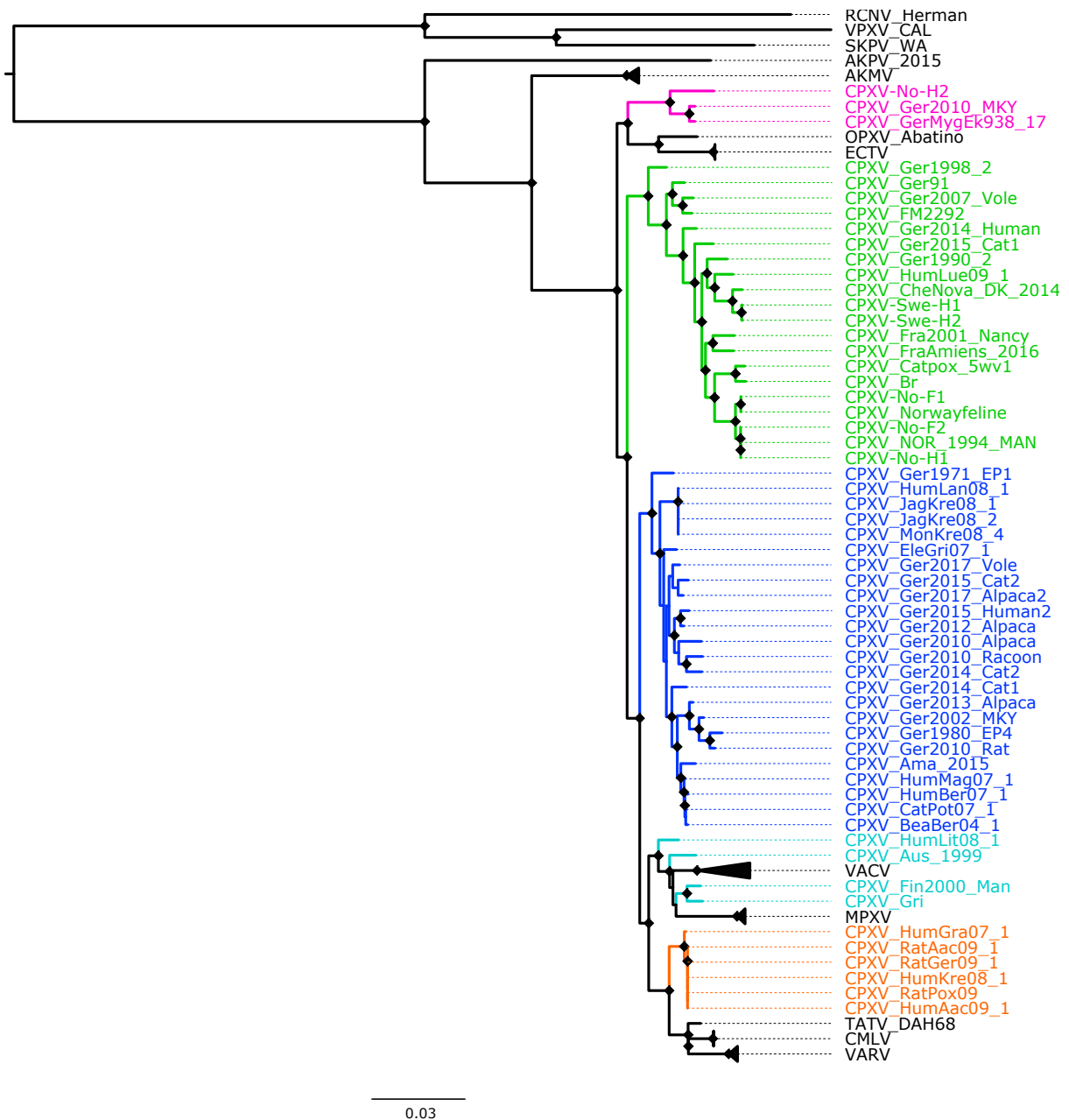
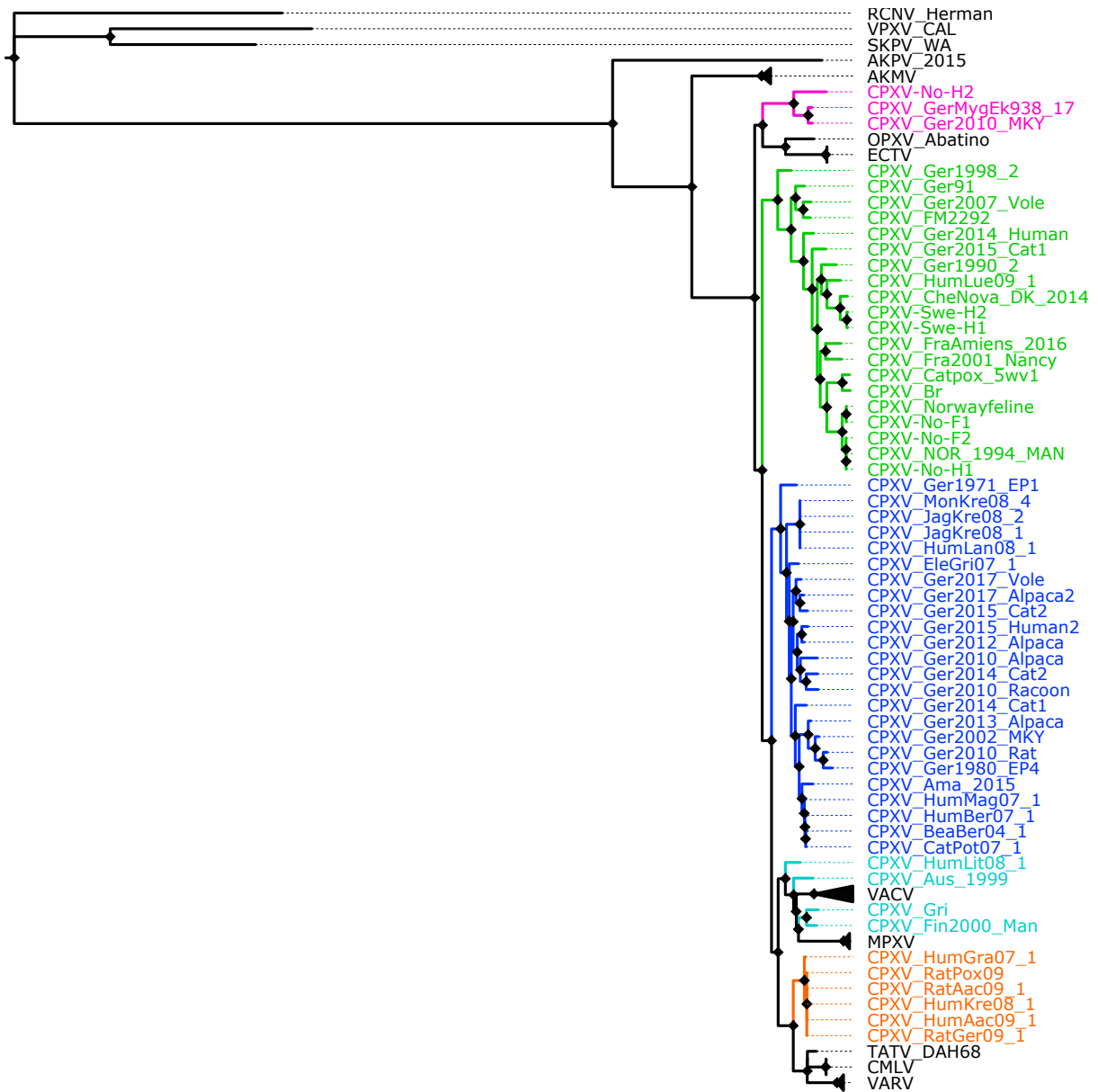


Figure S6. Maximum Likelihood phylogenetic tree of 87 orthopoxvirus whole genomes. Bootstrap values were inferred from 1000 rapid bootstrap replicates. Diamonds at the nodes indicate bootstrap values >80%. The scale bar indicates substitution per site. The main five cowpox virus (CPXV) clusters were highlighted in different colors: pink (Ectromelia-Abatino-like CPXV), blue (CPXV-like 1), green (CPXV-like 2), turquoise blue (Vaccinia-like CPXV) and orange (Variola-like CPXV).



0.04

Figure S7. Bayesian inference phylogenetic tree of 87 OPXV whole genomes. Diamonds at the nodes indicate posterior probabilities > 0.9. The scale bar represents expected substitutions per site. The main five cowpox virus (CPXV) clusters were highlighted in different colors: pink (Ectromelia-Abatino-like CPXV), blue (CPXV-like 1), green (CPXV-like 2), turquoise blue (Vaccinia-like CPXV) and orange (Variola-like CPXV).

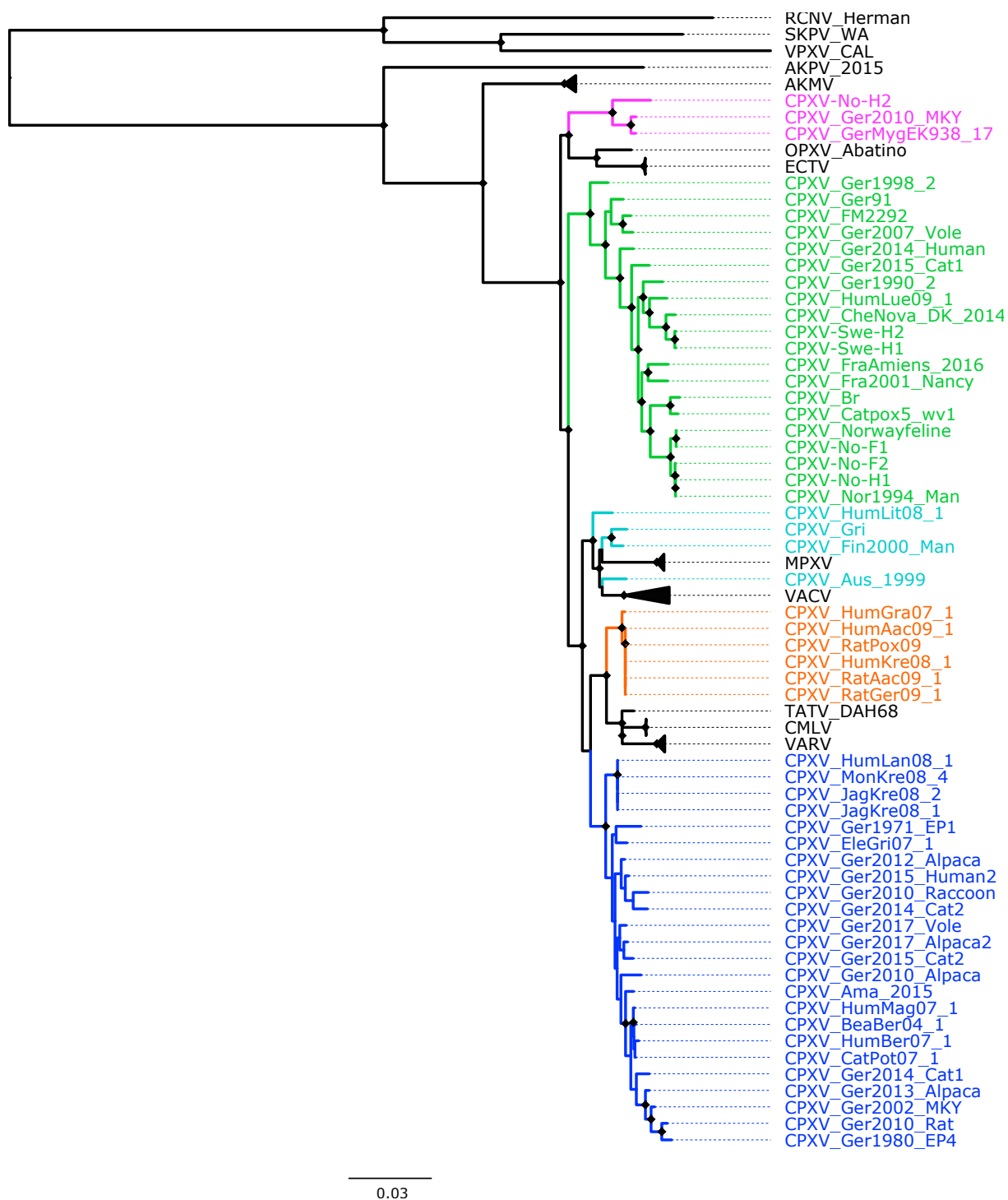


Figure S8. Maximum Likelihood phylogenetic tree based on orthopoxvirus orthologous genes. Bootstrap values were inferred from 1000 rapid bootstrap replicates. Diamonds at the nodes indicate bootstrap values >80%. The scale indicates substitution per site. The main five cowpox virus (CPXV) clusters were highlighted in different colors: pink (Ectromelia-Abatino-like CPXV), blue (CPXV-like 1), green (CPXV-like 2), turquoise blue (Vaccinia-like CPXV) and orange (Variola-like CPXV).

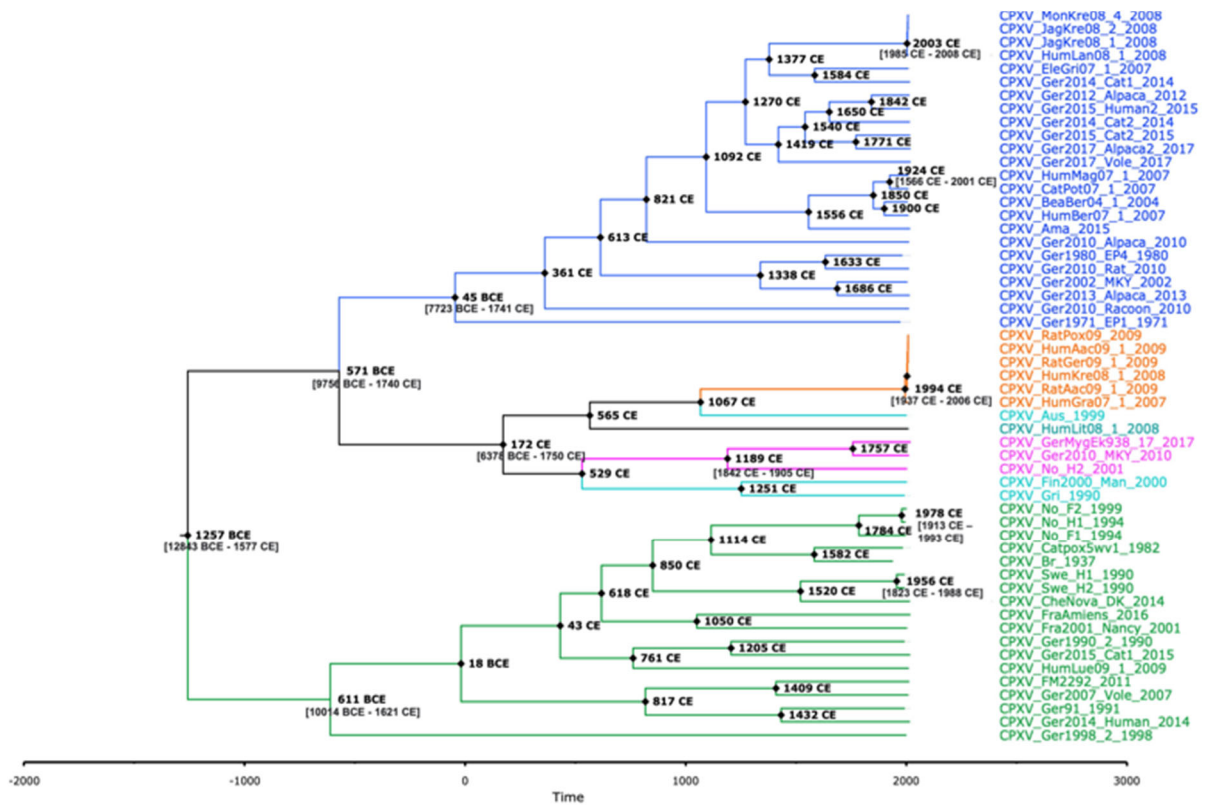


Figure S9. Bayesian maximum clade credibility (MCC) tree of 62 non-recombinant conserved genes of 55 CPXV genomes. The MCC tree was generated using BEAST 1, using a log-normal relaxed clock, coalescent Bayesian skyline population, HKY substitution model and four gamma categories. The numbers on the nodes indicate the time of the most recent common ancestor of the clades. Diamonds at the nodes indicate posterior probability values >0.9. The main five CPXV clusters were highlighted in different colors: pink (Ectromelia-Abatino-like CPXV), blue (CPXV-like 1), green (CPXV-like 2), turquoise blue (Vaccinia-like CPXV) and orange (Variola-like CPXV).



Figure S10. New classification of cowpox virus (CPXV) based on phylogenetic inference (from 87 OPXV whole genomes, core genomes and orthologous genes), patristic and genetic distances. Diamonds at the nodes indicate bootstrap values >80%. The main five CPXV clusters were highlighted in different colors: pink (Ectromelia-Abatino-like CPXV), blue (CPXV-like 1), green (CPXV-like 2), turquoise blue (Vaccinia-like CPXV) and orange (Variola-like CPXV).

Table S1. List of strains used in the phylogenetic analysis

GenBank number accession	Virus species	Strain
MH816996	<i>Abatino macacapox virus</i>	-
MH607142	<i>Akhmeta virus</i>	2013-85
MH607141	<i>Akhmeta virus</i>	2013-88
MH607143	<i>Akhmeta virus</i>	Vani_2010
MN240300	<i>Alaskapox virus</i>	2015
AY009089	<i>Camelpox virus</i>	CMS
NC_003391	<i>Camelpox virus</i>	M-96
LN879483	<i>Cowpox virus</i>	Amadeus 2015
HQ407377	<i>Cowpox virus</i>	Austria 1999
KC813491	<i>Cowpox virus</i>	BeaBer04/1
NC_003663	<i>Cowpox virus</i>	Brighton Red
KC813506	<i>Cowpox virus</i>	CatPot07/1
KY549144	<i>Cowpox virus</i>	CatPox5_wv1
KY569019	<i>Cowpox virus</i>	CheNova_DK_2014
KC813507	<i>Cowpox virus</i>	EkGr07/1
HQ420893	<i>Cowpox virus</i>	Finland_2000_MAN
LN864566	<i>Cowpox virus</i>	FM2292
HQ420894	<i>Cowpox virus</i>	France_2001_Nancy
LT883663	<i>Cowpox virus</i>	France Amiens 2016
DQ437593	<i>Cowpox virus</i>	Germany 91-3
HQ420895	<i>Cowpox virus</i>	Germany_1980_EP4
HQ420896	<i>Cowpox virus</i>	Germany_1990_2
HQ420897	<i>Cowpox virus</i>	Germany_1998_2
HQ420898	<i>Cowpox virus</i>	Germany_2002_MKY
LT896722	<i>Cowpox virus</i>	Ger/2007/Vole
LT896718	<i>Cowpox virus</i>	Ger/2010/Alpaca
LT896721	<i>Cowpox virus</i>	Ger 2010 MKY
LT896730	<i>Cowpox virus</i>	Ger/2010/Raccoon
LT896728	<i>Cowpox virus</i>	Ger/2010/Rat
LT896726	<i>Cowpox virus</i>	Ger/2012/Alpaca
LT896719	<i>Cowpox virus</i>	Ger/2013/Alpaca
LT896723	<i>Cowpox virus</i>	Ger/2014/Cat1
LT896725	<i>Cowpox virus</i>	Ger/2014/Cat2
LT993226	<i>Cowpox virus</i>	Ger/2014/Human
LT896724	<i>Cowpox virus</i>	Ger/2015/Cat1
LT896727	<i>Cowpox virus</i>	Ger/2015/Cat2
LT993232	<i>Cowpox virus</i>	Ger/2015/Human2
LT896732	<i>Cowpox virus</i>	Ger/2017/Alpaca2
LT993228	<i>Cowpox virus</i>	Ger/2017/common vole FMEinka
KY463519	<i>Cowpox virus</i>	Ger/1971_EP1
LR812035	<i>Cowpox virus</i>	GerMygEK 938/17
X94355	<i>Cowpox virus</i>	GR1-90
KC813508	<i>Cowpox virus</i>	HumAac09/1
KC813509	<i>Cowpox virus</i>	HumBer07/1
KC813510	<i>Cowpox virus</i>	HumGra07/1
KC813512	<i>Cowpox virus</i>	HumKre08/1
KC813492	<i>Cowpox virus</i>	HumLan08/1
KC813493	<i>Cowpox virus</i>	HumLat08/1
KC813494	<i>Cowpox virus</i>	HumLae09/1
KC813495	<i>Cowpox virus</i>	HumMag07/1
KC813497	<i>Cowpox virus</i>	JagKre08/1
KC813498	<i>Cowpox virus</i>	JagKre08/2
KC813500	<i>Cowpox virus</i>	MonKre08/4
HQ420899	<i>Cowpox virus</i>	Norway_1994_MAN
KY549151	<i>Cowpox virus</i>	NorwayFeline
KC813501	<i>Cowpox virus</i>	RatAac09/1
KC813503	<i>Cowpox virus</i>	RatGer09/1
LN864565	<i>Cowpox virus</i>	RatPox09
OP125541	<i>Cowpox virus</i>	No-F1
OP125540	<i>Cowpox virus</i>	No-F2
OP125539	<i>Cowpox virus</i>	No-H1
OM460002	<i>Cowpox virus</i>	No-H2
OP125538	<i>Cowpox virus</i>	Swe-H1
OP125537	<i>Cowpox virus</i>	Swe-H2
KY554976	<i>Ectromelia virus</i>	Hampstead
NC_004105	<i>Ectromelia virus</i>	Moscow
JQ410350	<i>Ectromelia virus</i>	ERPV
KJ563295	<i>Ectromelia virus</i>	Naval
DQ011154	<i>Monkeypox virus</i>	Congo_2003_358
DQ011156	<i>Monkeypox virus</i>	Liberia_1970_184
KJ642617	<i>Monkeypox virus</i>	Nigeria-SE-1971
NC_003310	<i>Monkeypox virus</i>	Zaire-96-I-16
NC_008291	<i>Taterapox virus</i>	Dahomey 1968
AY484669	<i>Vaccinia virus</i>	Rabbitpox virus Utrecht
DQ792504	<i>Vaccinia virus</i>	MNR-76
M35027	<i>Vaccinia virus</i>	Copenhagen
AM501482	<i>Vaccinia virus</i>	chorioallantois vaccinia virus Ankara (CVA)
DQ439815	<i>Vaccinia virus</i>	Duke
AY678276	<i>Vaccinia virus</i>	Lister
Y16780	<i>Variola virus</i>	Garcia-1966
DQ437581	<i>Variola virus</i>	Bangladesh 1975 v75-550 Banu
DQ441429	<i>Variola virus</i>	Japan 1946 (Yamada MS-2(A) Tokyo)
DQ441437	<i>Variola virus</i>	Sierra Leone 1969 (V68-258)
KY358055	<i>Variola virus</i>	VD21
NC_031033.1	<i>Volepox virus</i>	CA
KP143769	<i>Raccoonpox virus</i>	Herman
NC_031038	<i>Skunkpox virus</i>	WA

Table S3. List of 62 conserved genes from 87 orthopoxviruses used in this study

	VACV_Cop
1	A11R
2	A16L
3	A18R
4	A1L
5	A21L
6	A22R
7	A23R
8	A28L
9	A29L
10	A2L
11	A5R
12	A7L
13	D10R
14	D12L
15	D7R
16	E10R
17	E6R
18	F10L
19	F9L
20	G5R
21	G9R
22	H2R
23	H3L
24	H6R
25	J3R
26	J5L
27	L1R
28	L4R
29	L5R
30	A12L
31	A13L
32	A14L
33	A15L
34	A19L
35	A20E
36	A34R
37	A6L
38	A8R
39	D3R
40	D9R
41	E4L
42	E8R
43	F12L
44	F13L
45	F15L
46	F17R
47	G2R
48	G4L
49	G5.5.R
50	G7L
51	G8R
52	H1L
53	H7R
54	I1L
55	I2L
56	I3L
57	I5L
58	I6L
59	A2.5L
60	G6R
61	H5R
62	J1R

Table S4. List of strains used in the evolution molecular analysis.

GenBank number accession	Virus species	Strain	Country	Year
LN879483	<i>Cowpox virus</i>	Amadeus 2015	Germany	2015
HQ407377	<i>Cowpox virus</i>	Austria 1999	Austria	1999
KC813491	<i>Cowpox virus</i>	BeaBer04/1	Germany	2004
NC_003663	<i>Cowpox virus</i>	Brighton Red	UK	1937
KC813506	<i>Cowpox virus</i>	CatPot07/1	Germany	2007
KY549144	<i>Cowpox virus</i>	CatPox5_wv1	UK	1982
KY569019	<i>Cowpox virus</i>	CheNova_DK_2014	Denmark	2014
KC813507	<i>Cowpox virus</i>	EleGri07/1	Germany	2007
HQ420893	<i>Cowpox virus</i>	Finland_2000_MAN	Finland	2000
LN864566	<i>Cowpox virus</i>	FM2292	Germany	2011
HQ420894	<i>Cowpox virus</i>	France_2001_Nancy	France	2001
LT883663	<i>Cowpox virus</i>	France Amiens 2016	France	2016
DQ437593	<i>Cowpox virus</i>	Germany 91-3	Germany	1991
HQ420895	<i>Cowpox virus</i>	Germany_1980_EP4	Germany	1980
HQ420896	<i>Cowpox virus</i>	Germany_1990_2	Germany	1990
HQ420897	<i>Cowpox virus</i>	Germany_1998_2	Germany	1998
HQ420898	<i>Cowpox virus</i>	Germany_2002_MKY	Germany	2002
LT896722	<i>Cowpox virus</i>	Ger/2007/Vole	Germany	2007
LT896718	<i>Cowpox virus</i>	Ger/2010/Alpaca	Germany	2010
LT896721	<i>Cowpox virus</i>	Ger 2010 MKY	Germany	2010
LT896730	<i>Cowpox virus</i>	Ger/2010/Racoon	Germany	2010
LT896728	<i>Cowpox virus</i>	Ger/2010/Rat	Germany	2010
LT896726	<i>Cowpox virus</i>	Ger/2012/Alpaca	Germany	2012
LT896719	<i>Cowpox virus</i>	Ger/2013/Alpaca	Germany	2013
LT896723	<i>Cowpox virus</i>	Ger/2014/Cat1	Germany	2014
LT896725	<i>Cowpox virus</i>	Ger/2014/Cat2	Germany	2014
LT993226	<i>Cowpox virus</i>	Ger/2014/Human	Germany	2014
LT896724	<i>Cowpox virus</i>	Ger/2015/Cat1	Germany	2015
LT896727	<i>Cowpox virus</i>	Ger/2015/Cat2	Germany	2015
LT993232	<i>Cowpox virus</i>	Ger/2015/Human2	Germany	2015
LT896732	<i>Cowpox virus</i>	Ger/2017/Alpaca2	Germany	2017
LT993228	<i>Cowpox virus</i>	Ger/2017/common vole FMEimka	Germany	2017
KY463519	<i>Cowpox virus</i>	Ger/1971_EP1	Germany	1971
LR812035	<i>Cowpox virus</i>	GerMygEK 938/17	Germany	2017
X94355	<i>Cowpox virus</i>	GRI-90	Russia	1990
KC813508	<i>Cowpox virus</i>	HumAac09/1	Germany	2009
KC813509	<i>Cowpox virus</i>	HumBer07/1	Germany	2007
KC813510	<i>Cowpox virus</i>	HumGra07/1	Germany	2007
KC813512	<i>Cowpox virus</i>	HumKre08/1	Germany	2008
KC813492	<i>Cowpox virus</i>	HumLan08/1	Germany	2008
KC813493	<i>Cowpox virus</i>	HumLit08/1	Lithuania	2008
KC813494	<i>Cowpox virus</i>	HumLue09/1	Germany	2009
KC813495	<i>Cowpox virus</i>	HumMag07/1	Germany	2007
KC813497	<i>Cowpox virus</i>	JagKre08/1	Germany	2008
KC813498	<i>Cowpox virus</i>	JagKre08/2	Germany	2008
KC813500	<i>Cowpox virus</i>	MonKre08/4	Germany	2008
HQ420899	<i>Cowpox virus</i>	Norway_1994_MAN	Norway	1994
KY549151	<i>Cowpox virus</i>	NorwayFeline	Norway	1994
KC813501	<i>Cowpox virus</i>	RatAac09/1	Germany	2009
KC813503	<i>Cowpox virus</i>	RatGer09/1	Germany	2009
LN864565	<i>Cowpox virus</i>	RatPox09	Germany	2009
OP125541	<i>Cowpox virus</i>	No-F1	Norway	1994
OP125540	<i>Cowpox virus</i>	No-F2	Norway	1999
OP125539	<i>Cowpox virus</i>	No-H1	Norway	1994
OM460002	<i>Cowpox virus</i>	No-H2	Norway	2001
OP125538	<i>Cowpox virus</i>	Swe-H1	Sweden	1990
OP125537	<i>Cowpox virus</i>	Swe-H2	Sweden	1990

Table S6. Patristic distances between CPXV clusters and OPXV species calculated from the Maximum likelihood (ML) and Bayesian inference (BI) trees of 62 conserved genes, 87 OPXV whole genomes, core genomes and orthologous genes.

ML tree of 62 conserved genes															
	VACV	VACV-like	CPXV-like1	CPXV-like2	VARV-like	TATV	CMLV	ABATINO	MPXV	ECTV	IV-Abatino-	VARV	AKMV	AKPV	New World
VACV															
VACV-like	0.026														
CPXV-like1	0.045	0.037													
CPXV-like2	0.050	0.042	0.048												
VARV-like	0.031	0.021	0.043	0.049											
TATV	0.036	0.026	0.048	0.053	0.016										
CMLV	0.040	0.030	0.052	0.058	0.020	0.011									
ABATINO	0.046	0.038	0.049	0.055	0.044	0.049	0.053								
MPXV	0.034	0.030	0.043	0.048	0.033	0.037	0.041	0.044							
ECTV	0.044	0.038	0.048	0.053	0.043	0.047	0.052	0.028	0.045						
ECTV-Abatino-like	0.041	0.033	0.044	0.049	0.039	0.044	0.048	0.037	0.041	0.037					
VARV	0.046	0.037	0.059	0.064	0.026	0.018	0.022	0.059	0.052	0.060	0.054				
AKMV	0.082	0.074	0.085	0.091	0.080	0.085	0.089	0.084	0.083	0.084	0.078	0.095			
AKPV	0.170	0.162	0.174	0.179	0.169	0.173	0.178	0.172	0.171	0.173	0.167	0.184	0.148		
New World	0.693	0.685	0.697	0.702	0.692	0.696	0.700	0.695	0.694	0.696	0.690	0.707	0.671	0.703	
BI tree of 62 conserved genes															
	VACV	VACV-like	CPXV-like1	CPXV-like2	VARV-like	TATV	CMLV	ABATINO	MPXV	ECTV	IV-Abatino-	VARV	AKMV	AKPV	New World
VACV															
VACV-like	0.026														
CPXV-like1	0.044	0.036													
CPXV-like2	0.051	0.043	0.048												
VARV-like	0.030	0.021	0.042	0.049											
TATV	0.035	0.026	0.047	0.054	0.016										
CMLV	0.039	0.030	0.051	0.058	0.020	0.011									
ABATINO	0.045	0.038	0.048	0.055	0.044	0.048	0.052								
MPXV	0.038	0.030	0.045	0.052	0.036	0.041	0.045	0.046							
ECTV	0.046	0.038	0.048	0.055	0.044	0.049	0.053	0.023	0.047						
ECTV-Abatino-like	0.040	0.032	0.043	0.050	0.038	0.043	0.047	0.036	0.041	0.037					
VARV	0.046	0.036	0.057	0.064	0.026	0.018	0.022	0.059	0.051	0.059	0.054				
AKMV	0.080	0.073	0.083	0.090	0.079	0.083	0.087	0.082	0.081	0.083	0.077	0.094			
AKPV	0.166	0.158	0.169	0.176	0.165	0.169	0.173	0.168	0.167	0.168	0.163	0.180	0.220		
New World	0.427	0.419	0.430	0.437	0.426	0.430	0.434	0.429	0.428	0.429	0.424	0.441	0.405	0.435	
ML tree of 87 OPXV whole genomes															
	VACV	VACV-like	CPXV-like1	CPXV-like2	VARV-like	TATV	CMLV	ABATINO	MPXV	ECTV	IV-Abatino-	VARV	AKMV	AKPV	New World
VACV															
VACV-like	0.026														
CPXV-like1	0.043	0.034													
CPXV-like2	0.063	0.053	0.052												
VARV-like	0.037	0.027	0.031	0.051											
TATV	0.041	0.031	0.036	0.055	0.016										
CMLV	0.045	0.036	0.040	0.059	0.020	0.012									
ABATINO	0.060	0.051	0.049	0.061	0.048	0.053	0.057								
MPXV	0.039	0.072	0.050	0.069	0.043	0.048	0.052	0.067							
ECTV	0.066	0.056	0.055	0.066	0.054	0.058	0.062	0.030	0.072						
ECTV-Abatino-like	0.062	0.052	0.051	0.062	0.050	0.054	0.058	0.046	0.068	0.052					
VARV	0.052	0.043	0.047	0.066	0.027	0.019	0.023	0.064	0.059	0.070	0.065				
AKMV	0.096	0.087	0.085	0.096	0.084	0.089	0.093	0.088	0.103	0.093	0.089	0.100			
AKPV	0.188	0.179	0.178	0.189	0.177	0.181	0.185	0.180	0.195	0.185	0.181	0.192	0.161		
New World	0.744	0.735	0.733	0.745	0.733	0.737	0.741	0.736	0.751	0.741	0.737	0.748	0.717	0.740	
BI tree of 87 OPXV whole genomes															
	VACV	VACV-like	CPXV-like1	CPXV-like2	VARV-like	TATV	CMLV	ABATINO	MPXV	ECTV	IV-Abatino-	VARV	AKMV	AKPV	New World
VACV															
VACV-like	0.026														
CPXV-like1	0.043	0.033													
CPXV-like2	0.069	0.053	0.058												
VARV-like	0.036	0.027	0.031	0.050											
TATV	0.041	0.031	0.035	0.055	0.016										
CMLV	0.045	0.035	0.040	0.059	0.020	0.012									
ABATINO	0.060	0.050	0.049	0.060	0.048	0.052	0.056								
MPXV	0.039	0.032	0.049	0.069	0.043	0.047	0.051	0.066							
ECTV	0.065	0.056	0.054	0.065	0.053	0.058	0.062	0.030	0.072						
ECTV-Abatino-like	0.061	0.052	0.050	0.061	0.049	0.054	0.058	0.046	0.068	0.051					
VARV	0.052	0.042	0.047	0.066	0.027	0.019	0.023	0.063	0.058	0.069	0.065				
AKMV	0.095	0.086	0.084	0.095	0.083	0.088	0.092	0.086	0.102	0.092	0.088	0.099			
AKPV	0.185	0.176	0.175	0.186	0.174	0.178	0.182	0.177	0.192	0.182	0.178	0.189	0.158		
New World	0.469	0.460	0.459	0.470	0.458	0.462	0.466	0.461	0.476	0.466	0.462	0.473	0.442	0.464	

ML tree of 87 OPXV core genomes															
	VACV	VACV-like	CPXV-like1	CPXV-like2	VARV-like	TATV	CMLV	ABATINO	MPXV	ECTV	IV-Abatino-	VARV	AKMV	AKPV	New World
VACV															
VACV-like	0.026														
CPXV-like1	0.042	0.033													
CPXV-like2	0.040	0.053	0.034												
VARV-like	0.037	0.027	0.031	0.051											
TATV	0.041	0.031	0.035	0.055	0.016										
CMLV	0.045	0.035	0.039	0.059	0.020	0.012									
ABATINO	0.060	0.051	0.049	0.060	0.048	0.052	0.056								
MPXV	0.039	0.032	0.050	0.070	0.044	0.048	0.052	0.067							
ECTV	0.067	0.057	0.055	0.067	0.055	0.059	0.063	0.032	0.074						
ECTV-Abatino-like	0.057	0.052	0.045	0.049	0.045	0.049	0.053	0.046	0.063	0.053					
VARV	0.054	0.044	0.048	0.068	0.029	0.021	0.025	0.065	0.060	0.072	0.067				
AKMV	0.096	0.086	0.085	0.096	0.084	0.088	0.092	0.087	0.103	0.094	0.089	0.101			
AKPV	0.187	0.177	0.175	0.187	0.175	0.179	0.183	0.178	0.194	0.184	0.180	0.191	0.159		
New World	0.739	0.729	0.728	0.739	0.727	0.731	0.735	0.730	0.746	0.737	0.732	0.744	0.711	0.734	
BI tree of 87 OPXV core genomes															
	VACV	VACV-like	CPXV-like1	CPXV-like2	VARV-like	TATV	CMLV	ABATINO	MPXV	ECTV	IV-Abatino-	VARV	AKMV	AKPV	New World
VACV															
VACV-like	0.026														
CPXV-like1	0.043	0.033													
CPXV-like2	0.062	0.053	0.051												
VARV-like	0.037	0.027	0.031	0.051											
TATV	0.040	0.031	0.035	0.054	0.016										
CMLV	0.044	0.035	0.039	0.058	0.020	0.012									
ABATINO	0.052	0.050	0.040	0.045	0.040	0.044	0.048								
MPXV	0.039	0.031	0.049	0.069	0.043	0.047	0.051	0.066							
ECTV	0.066	0.057	0.055	0.066	0.054	0.058	0.062	0.031	0.073						
ECTV-Abatino-like	0.061	0.052	0.050	0.061	0.050	0.053	0.057	0.046	0.068	0.052					
VARV	0.053	0.043	0.047	0.067	0.028	0.020	0.024	0.064	0.059	0.070	0.066				
AKMV	0.095	0.085	0.083	0.095	0.083	0.087	0.091	0.086	0.101	0.092	0.087	0.099			
AKPV	0.183	0.174	0.172	0.183	0.171	0.175	0.179	0.174	0.190	0.181	0.176	0.188	0.155		
New World	0.464	0.454	0.452	0.464	0.452	0.456	0.460	0.455	0.470	0.461	0.456	0.468	0.436	0.458	
ML tree of OPXV orthologous genes															
	VACV	VACV-like	CPXV-like1	CPXV-like2	VARV-like	TATV	CMLV	ABATINO	MPXV	ECTV	IV-Abatino-	VARV	AKMV	AKPV	New World
VACV															
VACV-like	0.024														
CPXV-like1	0.042	0.034													
CPXV-like2	0.061	0.053	0.058												
VARV-like	0.038	0.030	0.029	0.054											
TATV	0.041	0.033	0.033	0.057	0.017										
CMLV	0.045	0.038	0.037	0.062	0.021	0.013									
ABATINO	0.056	0.048	0.054	0.062	0.049	0.053	0.057								
MPXV	0.039	0.023	0.049	0.068	0.045	0.048	0.052	0.063							
ECTV	0.061	0.053	0.058	0.067	0.054	0.057	0.062	0.030	0.061						
ECTV-Abatino-like	0.059	0.052	0.057	0.066	0.053	0.056	0.060	0.049	0.060	0.054					
VARV	0.052	0.044	0.043	0.068	0.027	0.018	0.023	0.063	0.052	0.068	0.066				
AKMV	0.092	0.084	0.089	0.098	0.085	0.088	0.093	0.087	0.092	0.092	0.091	0.099			
AKPV	0.189	0.181	0.187	0.195	0.182	0.186	0.190	0.185	0.190	0.189	0.188	0.196	0.164		
New World	0.762	0.754	0.760	0.768	0.755	0.759	0.763	0.758	0.763	0.762	0.761	0.769	0.737	0.762	

Table S7. Genetic distances between CPXV clusters and OPXV species estimated by p-distances from the alignment of 62 conserved genes (A), 87 OPXV whole genomes (B), core genomes (C) and orthologous genes (D).

A															
	VACV	VACV-like	CPXV-like1	CPXV-like2	VARV-like	TATV	CMLV	ABATINO	MPXV	ECTV	IV-Abatino	VARV	AKMV	AKPV	New World
VACV															
VACV-like	0.013														
CPXV-like1	0.016	0.014													
CPXV-like2	0.022	0.019	0.019												
VARV-like	0.015	0.013	0.014	0.021											
TATV	0.018	0.016	0.016	0.023	0.011										
CMLV	0.020	0.018	0.019	0.025	0.014	0.008									
ABATINO	0.025	0.022	0.023	0.023	0.023	0.026	0.028								
MPXV	0.021	0.018	0.021	0.024	0.020	0.023	0.025	0.027							
ECTV	0.024	0.021	0.023	0.025	0.022	0.025	0.028	0.016	0.026						
ECTV-Abatino-like	0.020	0.017	0.020	0.021	0.020	0.023	0.025	0.022	0.023	0.023					
VARV	0.024	0.022	0.022	0.029	0.017	0.012	0.015	0.032	0.028	0.031	0.029				
AKMV	0.042	0.040	0.039	0.043	0.039	0.041	0.043	0.044	0.045	0.044	0.044	0.046			
AKPV	0.075	0.073	0.073	0.075	0.074	0.075	0.076	0.075	0.077	0.077	0.074	0.079	0.068		
New World	0.127	0.125	0.126	0.126	0.125	0.126	0.127	0.127	0.128	0.128	0.126	0.128	0.126	0.130	
B															
	VACV	VACV-like	CPXV-like1	CPXV-like2	VARV-like	TATV	CMLV	ABATINO	MPXV	ECTV	IV-Abatino	VARV	AKMV	AKPV	New World
VACV															
VACV-like	0.015														
CPXV-like1	0.019	0.017													
CPXV-like2	0.026	0.023	0.021												
VARV-like	0.019	0.016	0.015	0.024											
TATV	0.022	0.019	0.018	0.027	0.012										
CMLV	0.025	0.022	0.021	0.030	0.015	0.009									
ABATINO	0.030	0.026	0.028	0.028	0.028	0.031	0.034								
MPXV	0.024	0.021	0.025	0.029	0.025	0.028	0.031	0.032							
ECTV	0.031	0.028	0.030	0.031	0.030	0.034	0.036	0.021	0.034						
ECTV-Abatino-like	0.030	0.027	0.027	0.027	0.029	0.032	0.035	0.028	0.033	0.032					
VARV	0.030	0.027	0.025	0.034	0.019	0.014	0.017	0.038	0.035	0.040	0.039				
AKMV	0.049	0.046	0.045	0.050	0.045	0.046	0.049	0.050	0.054	0.050	0.053	0.053			
AKPV	0.088	0.085	0.085	0.086	0.085	0.087	0.089	0.087	0.090	0.087	0.087	0.092	0.081		
New World	0.150	0.148	0.148	0.148	0.148	0.149	0.150	0.149	0.151	0.150	0.149	0.152	0.150	0.153	
B															
	VACV	VACV-like	CPXV-like1	CPXV-like2	VARV-like	TATV	CMLV	ABATINO	MPXV	ECTV	IV-Abatino	VARV	AKMV	AKPV	New World
VACV															
VACV-like	0.015														
CPXV-like1	0.019	0.017													
CPXV-like2	0.026	0.023	0.021												
VARV-like	0.019	0.016	0.015	0.024											
TATV	0.023	0.020	0.018	0.028	0.012										
CMLV	0.026	0.022	0.021	0.030	0.015	0.009									
ABATINO	0.030	0.026	0.027	0.028	0.028	0.031	0.034								
MPXV	0.024	0.021	0.026	0.030	0.026	0.029	0.031	0.032							
ECTV	0.032	0.029	0.030	0.032	0.031	0.034	0.037	0.022	0.035						
ECTV-Abatino-like	0.030	0.027	0.028	0.027	0.029	0.033	0.035	0.029	0.033	0.033					
VARV	0.031	0.028	0.026	0.036	0.021	0.015	0.018	0.039	0.036	0.042	0.040				
AKMV	0.049	0.047	0.045	0.050	0.045	0.047	0.049	0.050	0.054	0.049	0.053	0.054			
AKPV	0.088	0.086	0.086	0.086	0.086	0.087	0.089	0.087	0.090	0.087	0.087	0.093	0.081		
New World	0.151	0.149	0.149	0.150	0.149	0.151	0.152	0.150	0.152	0.152	0.151	0.154	0.151	0.154	
D															
	VACV	VACV-like	CPXV-like1	CPXV-like2	VARV-like	TATV	CMLV	ABATINO	MPXV	ECTV	IV-Abatino	VARV	AKMV	AKPV	New World
VACV															
VACV-like	0.014														
CPXV-like1	0.019	0.017													
CPXV-like2	0.026	0.024	0.022												
VARV-like	0.019	0.016	0.015	0.025											
TATV	0.022	0.019	0.017	0.028	0.012										
CMLV	0.025	0.022	0.020	0.030	0.015	0.009									
ABATINO	0.030	0.027	0.028	0.028	0.029	0.031	0.033								
MPXV	0.023	0.021	0.025	0.029	0.026	0.028	0.031	0.032							
ECTV	0.031	0.028	0.030	0.031	0.030	0.033	0.035	0.021	0.033						
ECTV-Abatino-like	0.031	0.028	0.029	0.027	0.030	0.033	0.036	0.030	0.033	0.032					
VARV	0.028	0.026	0.024	0.034	0.019	0.014	0.016	0.037	0.034	0.039	0.039				
AKMV	0.049	0.046	0.044	0.050	0.045	0.046	0.048	0.050	0.053	0.049	0.052	0.052			
AKPV	0.088	0.086	0.086	0.087	0.086	0.087	0.090	0.088	0.090	0.086	0.088	0.091	0.081		
New World	0.149	0.149	0.148	0.148	0.148	0.148	0.150	0.150	0.150	0.149	0.149	0.150	0.150	0.153	

Table S8. Patristic and genetic distances within CPXV clusters calculated from the Maximum likelihood (ML) and Bayesian inference (BI) trees of 62 conserved genes, 87 OPXV core genomes, whole genomes and orthologous genes and their alignments, respectively.

Cluster	Patristic distances						
	ML tree of 62 conserved genes	BI tree of 62 conserved genes	ML tree of 87 OPXV whole genomes	BI tree of 87 OPXV whole genomes	ML tree of 87 OPXV core genomes	BI tree of 87 OPXV core genomes	ML tree of OPXV orthologous genes
VACV-like	0.018	0.017	0.018	0.018	0.018	0.017	0.017
CPXV-like1	0.016	0.016	0.015	0.015	0.015	0.015	0.015
CPXV-like2	0.022	0.022	0.023	0.023	0.023	0.023	0.025
VARV-like	0.000	0.000	0.001	0.001	0.001	0.001	0.001
ECTV-Abatino like	0.012	0.012	0.016	0.016	0.016	0.016	0.016
TATV - CMLV	0.011	0.011	0.012	0.012	0.012	0.012	0.013
TATV-VARV	0.018	0.018	0.019	0.019	0.021	0.020	0.018

TATV: Taterapox virus, CMLV:Camelpox virus, VARV: Variola virus

Cluster	Genetic distances			
	62 conserved genes	87 OPXV whole genomes	87 OPXV core genomes	OPXV orthologous genes
VACV-like	0.010	0.012	0.012	0.011
CPXV-like1	0.008	0.008	0.008	0.008
CPXV-like2	0.012	0.013	0.013	0.014
VARV-like	0.000	0.000	0.000	0.001
ECTV-Abatino like	0.008	0.012	0.011	0.011
TATV - CMLV	0.008	0.009	0.009	0.009
TATV-VARV	0.012	0.014	0.015	0.014

TATV: Taterapox virus, CMLV:Camelpox virus, VARV: Variola virus

Table S9. Patristic distances within CPXV-like 2 calculated from the Maximum likelihood (ML) and Bayesian inference (BI) trees of 62 conserved genes, 87 OPXV whole genomes, core genomes and orthologous genes.

ML tree of 62 conserved genes																				
	1	8	9	10			11				7			5	4	6	3	2		
	CPXV_Ger1998_2_1998	CPXV_Fra2001_Nancy_2001	CPXV_FraAmiens_2016	CPXV_Br_1937	CPXV_Catpox5wv1_1982	CPXV_No_F2_1999	CPXV_Nor1994_Man_1994	CPXV_No_H1_1994	CPXV_No_F1_1994	CPXV_NorwayFeline_1994	CPXV_CheNova_DK_2014	CPXV_Swe_H2_1990	CPXV_Swe_H1_1990	CPXV_Ger1990_2_1990	CPXV_Ger2015_Cat1_2015	CPXV_HumLue09_1_2009	CPXV_Ger2014_Human_2014	CPXV_Ger91_1991	CPXV_Ger2007_Vole_2007	CPXV_FM2292_2011
1	CPXV_Ger1998_2_1998																			
8	CPXV_Fra2001_Nancy_2001	0.026																		
9	CPXV_FraAmiens_2016	0.027	0.014																	
	CPXV_Br_1937	0.032	0.023	0.024																
10	CPXV_Catpox5wv1_1982	0.032	0.023	0.024	0.007															
	CPXV_No_F2_1999	0.031	0.022	0.022	0.018	0.018														
	CPXV_Nor1994_Man_1994	0.031	0.022	0.023	0.019	0.018	0.000													
	CPXV_No_H1_1994	0.031	0.022	0.023	0.019	0.018	0.000	0.000												
	CPXV_No_F1_1994	0.031	0.022	0.022	0.019	0.018	0.003	0.003	0.003											
11	CPXV_NorwayFeline_1994	0.031	0.022	0.022	0.019	0.018	0.003	0.003	0.003	0.000										
	CPXV_CheNova_DK_2014	0.028	0.019	0.020	0.021	0.021	0.020	0.020	0.020	0.020	0.020									
	CPXV_Swe_H2_1990	0.028	0.019	0.020	0.021	0.020	0.019	0.019	0.019	0.019	0.007									
7	CPXV_Swe_H1_1990	0.028	0.019	0.020	0.020	0.020	0.019	0.019	0.019	0.019	0.007	0.000								
5	CPXV_Ger1990_2_1990	0.026	0.019	0.020	0.025	0.025	0.024	0.024	0.024	0.024	0.022	0.021	0.021							
4	CPXV_Ger2015_Cat1_2015	0.026	0.020	0.021	0.026	0.025	0.024	0.024	0.024	0.024	0.022	0.022	0.021	0.012						
6	CPXV_HumLue09_1_2009	0.024	0.018	0.019	0.024	0.023	0.022	0.022	0.022	0.022	0.020	0.019	0.019	0.014	0.015					
3	CPXV_Ger2014_Human_2014	0.021	0.026	0.027	0.032	0.032	0.030	0.031	0.031	0.031	0.028	0.028	0.028	0.026	0.026	0.024				
	CPXV_Ger91_1991	0.018	0.023	0.024	0.029	0.028	0.027	0.027	0.027	0.027	0.025	0.024	0.024	0.022	0.023	0.021	0.007			
	CPXV_Ger2007_Vole_2007	0.022	0.027	0.028	0.033	0.032	0.031	0.031	0.031	0.031	0.029	0.029	0.029	0.026	0.027	0.025	0.016	0.013		
2	CPXV_FM2292_2011	0.021	0.026	0.027	0.032	0.032	0.030	0.031	0.031	0.030	0.028	0.028	0.028	0.026	0.026	0.024	0.015	0.012	0.009	
BI tree of 62 conserved genes																				
	CPXV_FM2292_2011	CPXV_Ger2007_Vole_2007	CPXV_Ger91_1991	CPXV_Ger2014_Human_2014	CPXV_HumLue09_1_2009	CPXV_Ger1990_2_1990	CPXV_Br_1937	CPXV_Catpox5wv1_1982	CPXV_Nor1994_Man_1994	CPXV_No_H1_1994	CPXV_No_F2_1999	CPXV_NorwayFeline_1994	CPXV_No_F1_1994	CPXV_CheNova_DK_2014	CPXV_Swe_H1_1990	CPXV_Swe_H2_1990	CPXV_FraAmiens_2016	CPXV_Fra2001_Nancy_2001	CPXV_Ger2015_Cat1_2015	CPXV_Ger1998_2_1998
2	CPXV_FM2292_2011	0.0086																		
	CPXV_Ger2007_Vole_2007	0.0118	0.0127																	
3	CPXV_Ger91_1991	0.0150	0.0159	0.0071																
6	CPXV_HumLue09_1_2009	0.0254	0.0263	0.0222	0.0254															
5	CPXV_Ger1990_2_1990	0.0253	0.0262	0.0222	0.0254	0.0121														
	CPXV_Br_1937	0.0331	0.0340	0.0299	0.0331	0.0237	0.0236													
10	CPXV_Catpox5wv1_1982	0.0328	0.0337	0.0296	0.0328	0.0234	0.0233	0.0073												
	CPXV_Nor1994_Man_1994	0.0319	0.0328	0.0287	0.0319	0.0225	0.0224	0.0185	0.0182											
	CPXV_No_H1_1994	0.0319	0.0328	0.0287	0.0319	0.0225	0.0224	0.0185	0.0182	0.0000										
	CPXV_No_F2_1999	0.0317	0.0326	0.0285	0.0318	0.0223	0.0223	0.0183	0.0180	0.0003	0.0003									
	CPXV_NorwayFeline_1994	0.0318	0.0327	0.0286	0.0318	0.0224	0.0223	0.0184	0.0181	0.0030	0.0030	0.0028								
	CPXV_No_F1_1994	0.0318	0.0327	0.0286	0.0318	0.0224	0.0223	0.0184	0.0181	0.0030	0.0030	0.0028	0.0000							
	CPXV_CheNova_DK_2014	0.0294	0.0303	0.0262	0.0294	0.0200	0.0199	0.0207	0.0204	0.0195	0.0195	0.0194	0.0194	0.0068						
7	CPXV_Swe_H1_1990	0.0288	0.0297	0.0257	0.0289	0.0194	0.0194	0.0202	0.0199	0.0190	0.0190	0.0188	0.0189	0.0189	0.0068					
	CPXV_Swe_H2_1990	0.0289	0.0298	0.0258	0.0290	0.0195	0.0195	0.0203	0.0200	0.0191	0.0191	0.0189	0.0190	0.0190	0.0069	0.0004				
9	CPXV_FraAmiens_2016	0.0281	0.0290	0.0249	0.0281	0.0187	0.0186	0.0235	0.0232	0.0223	0.0223	0.0222	0.0222	0.0198	0.0193	0.0194				
8	CPXV_Fra2001_Nancy_2001	0.0274	0.0283	0.0242	0.0274	0.0180	0.0179	0.0229	0.0226	0.0217	0.0217	0.0215	0.0216	0.0216	0.0191	0.0186	0.0187	0.0140		
4	CPXV_Ger2015_Cat1_2015	0.0217	0.0226	0.0185	0.0217	0.0161	0.0160	0.0238	0.0235	0.0226	0.0226	0.0226	0.0224	0.0225	0.0225	0.0201	0.0195	0.0196	0.0188	0.0181
1	CPXV_Ger1998_2_1998	0.0208	0.0217	0.0177	0.0209	0.0257	0.0256	0.0334	0.0331	0.0322	0.0322	0.0320	0.0321	0.0321	0.0296	0.0291	0.0292	0.0284	0.0277	0.0220

ML tree of 87 OPXV whole genomes																				
	1	2			3	4	5	6	7		8	9	10		11					
	CPXV_Ger1 998_2	CPXV_Ger9 1	CPXV_Ger2 007_Vole	CPXV_FM2 292	CPXV_Ger2 014_Human	CPXV_Ger2 015_Cat1	CPXV_Ger1 990_2	CPXV_Hum Lue09_1	CPXV_Che Nova_DK_2 014	CPXV_Swe_ H1	CPXV_Swe_ H2	CPXV_Fra2 001_Nancy	CPXV_FraA miens_2016	CPXV_Catp ox_5sw1	CPXV_Br	CPXV_No_ F2	CPXV_NOR _1994_MAN	CPXV_No_ H1	CPXV_No_ F1	CPXV_Nor wayfeine
1	CPXV_Ger1998_2																			
	CPXV_Ger91	0.0175																		
2	CPXV_Ger2007_Vole	0.0203	0.0106																	
	CPXV_FM2292	0.0199	0.0102	0.0064																
3	CPXV_Ger2014_Human	0.0214	0.0155	0.0183	0.0179															
4	CPXV_Ger2015_Cat1	0.0268	0.0209	0.0237	0.0233	0.0140														
5	CPXV_Ger1990_2	0.0313	0.0254	0.0283	0.0278	0.0185	0.0164													
6	CPXV_HumLue09_1	0.0332	0.0273	0.0301	0.0297	0.0204	0.0183	0.0149												
	CPXV_CheNova_DK_2014	0.0361	0.0303	0.0331	0.0327	0.0234	0.0212	0.0178	0.0148											
	CPXV_Swe_H1	0.0361	0.0303	0.0331	0.0327	0.0234	0.0213	0.0178	0.0148	0.0063										
7	CPXV_Swe_H2	0.0362	0.0303	0.0331	0.0327	0.0234	0.0213	0.0179	0.0148	0.0063	0.0005									
8	CPXV_Fra2001_Nancy	0.0336	0.0278	0.0306	0.0302	0.0209	0.0187	0.0187	0.0206	0.0235	0.0235	0.0236								
9	CPXV_FraAmiens_2016	0.0333	0.0275	0.0303	0.0299	0.0206	0.0185	0.0184	0.0203	0.0232	0.0233	0.0233	0.0136							
	CPXV_Catpox_5sw1	0.0370	0.0311	0.0340	0.0335	0.0242	0.0221	0.0221	0.0239	0.0269	0.0269	0.0269	0.0220	0.0218						
10	CPXV_Br	0.0373	0.0315	0.0343	0.0339	0.0246	0.0224	0.0224	0.0243	0.0272	0.0272	0.0273	0.0224	0.0221	0.0064					
	CPXV_No_F2	0.0356	0.0297	0.0326	0.0321	0.0228	0.0207	0.0207	0.0226	0.0255	0.0255	0.0255	0.0206	0.0204	0.0182	0.0185				
	CPXV_NOR_1994_MAN	0.0356	0.0298	0.0326	0.0322	0.0229	0.0208	0.0207	0.0226	0.0255	0.0255	0.0256	0.0207	0.0204	0.0182	0.0185	0.0001			
	CPXV_No_H1	0.0356	0.0298	0.0326	0.0322	0.0229	0.0208	0.0207	0.0226	0.0255	0.0255	0.0256	0.0207	0.0204	0.0182	0.0185	0.0001	0.0000		
	CPXV_No_F1	0.0357	0.0298	0.0326	0.0322	0.0229	0.0208	0.0207	0.0226	0.0255	0.0256	0.0256	0.0207	0.0204	0.0182	0.0185	0.0034	0.0034	0.0034	
11	CPXV_Norwayfeine	0.0357	0.0298	0.0326	0.0322	0.0229	0.0208	0.0207	0.0226	0.0255	0.0256	0.0256	0.0207	0.0204	0.0182	0.0185	0.0034	0.0034	0.0034	0.0000
BI tree of 87 OPXV whole genomes																				
	1	2			7		6	5	9	8	11					10		4	3	
	CPXV_Ger1 998_2	CPXV_Ger2 007_Vole	CPXV_FM2 292	CPXV_Ger9 1	CPXV_Swe_ H2	CPXV_Swe_ H1	CPXV_Che Nova_DK_2 014	CPXV_Hum Lue09_1	CPXV_Ger1 990_2	CPXV_FraA miens_2016	CPXV_Fra2 001_Nancy	CPXV_Nor wayfeine	CPXV_No_ F1	CPXV_NOR _1994_MAN	CPXV_No_ H1	CPXV_No_ F2	CPXV_Catp ox_5sw1	CPXV_Br	CPXV_Ger2 015_Cat1	CPXV_Ger2 014_Human
1	CPXV_Ger1998_2																			
	CPXV_Ger2007_Vole	0.0201																		
	CPXV_FM2292	0.0197	0.0063																	
2	CPXV_Ger91	0.0173	0.0105	0.0101																
	CPXV_Swe_H2	0.0358	0.0328	0.0324	0.0300															
	CPXV_Swe_H1	0.0358	0.0328	0.0324	0.0300	0.0005														
7	CPXV_CheNova_DK_2014	0.0358	0.0327	0.0323	0.0300	0.0063	0.0062													
6	CPXV_HumLue09_1	0.0329	0.0298	0.0294	0.0271	0.0147	0.0146	0.0146												
5	CPXV_Ger1990_2	0.0310	0.0280	0.0276	0.0252	0.0177	0.0177	0.0176	0.0148											
9	CPXV_FraAmiens_2016	0.0330	0.0300	0.0296	0.0272	0.0231	0.0230	0.0230	0.0201	0.0182										
8	CPXV_Fra2001_Nancy	0.0333	0.0303	0.0299	0.0275	0.0233	0.0233	0.0204	0.0185	0.0135										
	CPXV_Norwayfeine	0.0353	0.0323	0.0319	0.0295	0.0254	0.0253	0.0253	0.0224	0.0205	0.0202	0.0205	0.0000							
	CPXV_No_F1	0.0353	0.0323	0.0319	0.0295	0.0254	0.0253	0.0253	0.0224	0.0205	0.0202	0.0205	0.0000							
	CPXV_NOR_1994_MAN	0.0353	0.0323	0.0319	0.0295	0.0253	0.0253	0.0253	0.0224	0.0205	0.0202	0.0205	0.0034	0.0034						
	CPXV_No_H1	0.0353	0.0323	0.0319	0.0295	0.0253	0.0253	0.0253	0.0224	0.0205	0.0202	0.0205	0.0034	0.0034	0.0000					
11	CPXV_No_F2	0.0352	0.0322	0.0318	0.0294	0.0253	0.0253	0.0252	0.0223	0.0205	0.0202	0.0204	0.0034	0.0034	0.0001	0.0001				
	CPXV_Catpox_5sw1	0.0366	0.0336	0.0332	0.0308	0.0267	0.0266	0.0266	0.0237	0.0218	0.0215	0.0218	0.0180	0.0180	0.0180	0.0180	0.0180			
10	CPXV_Br	0.0369	0.0339	0.0335	0.0311	0.0270	0.0270	0.0269	0.0240	0.0222	0.0219	0.0221	0.0184	0.0184	0.0183	0.0183	0.0183	0.0063		
4	CPXV_Ger2015_Cat1	0.0265	0.0235	0.0231	0.0207	0.0211	0.0211	0.0210	0.0181	0.0163	0.0183	0.0186	0.0206	0.0206	0.0206	0.0206	0.0206	0.0219	0.0222	
3	CPXV_Ger2014_Human	0.0211	0.0181	0.0177	0.0153	0.0232	0.0231	0.0231	0.0202	0.0183	0.0204	0.0206	0.0227	0.0227	0.0226	0.0226	0.0240	0.0243	0.0139	

ML tree of 87 OPXV core genomes																				
	1	2			3	4	5	6	7		8	9	10		11					
	CPXV_Ger1998_2	CPXV_Ger2007_Vole	CPXV_FM2292	CPXV_Ger91	CPXV_Ger2014_Human	CPXV_Ger2015_Cat1	CPXV_Ger1990_2	CPXV_HumLue09_1	CPXV_CheNova_DK_2014	CPXV_Swe_H1	CPXV_Swe_H2	CPXV_Fra2001_Nancy	CPXV_FraAmiens_2016	CPXV_Catpox5_wv1	CPXV_Br	CPXV_No_F1	CPXV_NorwayFeline	CPXV_No_F2	CPXV_Nor1994_Man	CPXV_No_H1
1	CPXV_Ger1998_2																			
2	CPXV_Ger2007_Vole	0.0207																		
	CPXV_FM2292	0.0203	0.0061																	
3	CPXV_Ger91	0.0179	0.0102	0.0098																
	CPXV_Ger2014_Human	0.0217	0.0181	0.0177	0.0153															
4	CPXV_Ger2015_Cat1	0.0271	0.0235	0.0231	0.0207	0.0140														
5	CPXV_Ger1990_2	0.0316	0.0279	0.0275	0.0251	0.0184	0.0163													
6	CPXV_HumLue09_1	0.0335	0.0299	0.0295	0.0270	0.0203	0.0183	0.0149												
7	CPXV_CheNova_DK_2014	0.0363	0.0327	0.0323	0.0299	0.0231	0.0211	0.0177	0.0147											
	CPXV_Swe_H1	0.0365	0.0329	0.0325	0.0301	0.0234	0.0213	0.0180	0.0149	0.0062										
	CPXV_Swe_H2	0.0366	0.0330	0.0326	0.0301	0.0234	0.0214	0.0180	0.0150	0.0063	0.0005									
8	CPXV_Fra2001_Nancy	0.0340	0.0304	0.0300	0.0276	0.0209	0.0188	0.0187	0.0207	0.0235	0.0237	0.0238								
9	CPXV_FraAmiens_2016	0.0338	0.0302	0.0298	0.0274	0.0207	0.0186	0.0185	0.0205	0.0233	0.0235	0.0236	0.0137							
10	CPXV_Catpox5_wv1	0.0373	0.0336	0.0332	0.0308	0.0241	0.0220	0.0220	0.0239	0.0267	0.0269	0.0270	0.0221	0.0218						
	CPXV_Br	0.0376	0.0340	0.0336	0.0311	0.0244	0.0223	0.0223	0.0242	0.0270	0.0273	0.0273	0.0224	0.0222	0.0064					
11	CPXV_No_F1	0.0359	0.0323	0.0319	0.0295	0.0228	0.0207	0.0206	0.0226	0.0254	0.0256	0.0257	0.0207	0.0205	0.0182	0.0185				
	CPXV_NorwayFeline	0.0359	0.0323	0.0319	0.0295	0.0228	0.0207	0.0206	0.0226	0.0254	0.0256	0.0257	0.0207	0.0205	0.0182	0.0185	0.0000			
	CPXV_No_F2	0.0358	0.0322	0.0318	0.0294	0.0227	0.0206	0.0206	0.0225	0.0253	0.0255	0.0256	0.0207	0.0204	0.0181	0.0184	0.0034	0.0034		
	CPXV_Nor1994_Man	0.0359	0.0323	0.0319	0.0294	0.0227	0.0206	0.0206	0.0225	0.0253	0.0256	0.0256	0.0207	0.0205	0.0181	0.0184	0.0034	0.0034	0.0001	
	CPXV_No_H1	0.0359	0.0323	0.0319	0.0294	0.0227	0.0206	0.0206	0.0225	0.0253	0.0256	0.0256	0.0207	0.0205	0.0181	0.0184	0.0034	0.0034	0.0001	0.0000

BI tree of 87 OPXV core genomes																				
	2			11					10		9	8	7		6	5	4	3	1	
	CPXV_Ger2007_Vole	CPXV_FM2292	CPXV_Ger91	CPXV_No_F1	CPXV_NorwayFeline	CPXV_Nor1994_Man	CPXV_No_H1	CPXV_No_F2_reversed_	CPXV_Catpox5_wv1	CPXV_Br	CPXV_FraAmiens_2016	CPXV_Fra2001_Nancy	CPXV_Swe_H2	CPXV_Swe_H1_reversed_	CPXV_CheNova_DK_2014	CPXV_HumLue09_1	CPXV_Ger1990_2	CPXV_Ger2015_Cat1	CPXV_Ger2014_Human	CPXV_Ger1998_2
2	CPXV_Ger2007_Vole																			
2	CPXV_FM2292	0.0061																		
	CPXV_Ger91	0.0101	0.0097																	
11	CPXV_No_F1	0.0319	0.0315	0.0291																
	CPXV_NorwayFeline	0.0319	0.0315	0.0291	0.0000															
	CPXV_Nor1994_Man	0.0319	0.0315	0.0291	0.0034	0.0034														
	CPXV_No_H1	0.0319	0.0315	0.0291	0.0034	0.0034	0.0000													
	CPXV_No_F2_reversed_	0.0318	0.0314	0.0290	0.0034	0.0034	0.0001	0.0001												
10	CPXV_Catpox5_wv1	0.0332	0.0328	0.0304	0.0179	0.0179	0.0179	0.0178												
	CPXV_Br	0.0335	0.0332	0.0308	0.0182	0.0182	0.0182	0.0182	0.0063											
9	CPXV_FraAmiens_2016	0.0298	0.0294	0.0270	0.0202	0.0202	0.0202	0.0202	0.0216	0.0219										
8	CPXV_Fra2001_Nancy	0.0300	0.0296	0.0272	0.0205	0.0205	0.0204	0.0204	0.0218	0.0221	0.0135									
7	CPXV_Swe_H2	0.0326	0.0322	0.0298	0.0254	0.0254	0.0253	0.0253	0.0267	0.0270	0.0233	0.0235								
	CPXV_Swe_H1_reversed_	0.0326	0.0322	0.0298	0.0253	0.0253	0.0253	0.0253	0.0267	0.0270	0.0232	0.0235	0.0005							
	CPXV_CheNova_DK_2014	0.0323	0.0319	0.0295	0.0251	0.0251	0.0251	0.0250	0.0264	0.0267	0.0230	0.0232	0.0062	0.0062						
6	CPXV_HumLue09_1	0.0295	0.0291	0.0267	0.0223	0.0223	0.0223	0.0223	0.0222	0.0236	0.0239	0.0202	0.0204	0.0148	0.0148	0.0145				
5	CPXV_Ger1990_2	0.0276	0.0272	0.0248	0.0204	0.0204	0.0203	0.0203	0.0217	0.0220	0.0183	0.0185	0.0178	0.0178	0.0175	0.0147				
4	CPXV_Ger2015_Cat1	0.0232	0.0228	0.0204	0.0204	0.0204	0.0204	0.0203	0.0217	0.0221	0.0183	0.0186	0.0211	0.0211	0.0208	0.0180	0.0161			
3	CPXV_Ger2014_Human	0.0179	0.0175	0.0151	0.0225	0.0225	0.0224	0.0224	0.0238	0.0241	0.0204	0.0206	0.0232	0.0231	0.0229	0.0201	0.0182	0.0138		
1	CPXV_Ger1998_2	0.0205	0.0201	0.0177	0.0355	0.0355	0.0354	0.0354	0.0354	0.0368	0.0371	0.0334	0.0336	0.0362	0.0361	0.0359	0.0331	0.0311	0.0268	0.0214

ML tree of OPXV orthologous genes																				
	1	3	4	6	7	5	9	8	10	11	2									
	CPXV_Ger1998_2	CPXV_Ger2014_Human	CPXV_Ger2015_Cat1	CPXV_HumLue09_1	CPXV_CheNova_DK_2014	CPXV_SweH2	CPXV_SweH1	CPXV_Ger1990_2	CPXV_FraAmiens_2016	CPXV_Fra2001_Nancy	CPXV_Br	CPXV_Catpox5_wv1	CPXV_Norwayfeline	CPXV_NoF1	CPXV_NoF2	CPXV_NoH1	CPXV_Nor1994_Man	CPXV_FM2292	CPXV_Ger2007_Vole	CPXV_Ger91
1																				
3	0.0223																			
4	0.0280	0.0156																		
6	0.0344	0.0219	0.0193																	
7	0.0374	0.0250	0.0223	0.0156																
	0.0376	0.0252	0.0225	0.0158	0.0069															
	0.0376	0.0251	0.0225	0.0157	0.0069	0.0006														
5	0.0329	0.0204	0.0178	0.0157	0.0188	0.0190	0.0189													
9	0.0349	0.0224	0.0198	0.0213	0.0244	0.0246	0.0245	0.0198												
8	0.0347	0.0222	0.0195	0.0211	0.0242	0.0244	0.0243	0.0196	0.0144											
10	0.0390	0.0266	0.0239	0.0255	0.0286	0.0287	0.0287	0.0240	0.0234	0.0232										
	0.0384	0.0260	0.0233	0.0249	0.0280	0.0281	0.0281	0.0234	0.0228	0.0226	0.0062									
	0.0377	0.0253	0.0226	0.0242	0.0273	0.0274	0.0274	0.0227	0.0221	0.0219	0.0201	0.0195								
11	0.0377	0.0253	0.0226	0.0242	0.0273	0.0274	0.0274	0.0227	0.0221	0.0219	0.0201	0.0195	0.0000							
	0.0375	0.0250	0.0223	0.0239	0.0270	0.0272	0.0271	0.0224	0.0218	0.0216	0.0198	0.0192	0.0037	0.0037						
	0.0375	0.0250	0.0224	0.0239	0.0270	0.0272	0.0271	0.0225	0.0218	0.0216	0.0198	0.0192	0.0037	0.0037	0.0001					
	0.0375	0.0250	0.0224	0.0239	0.0270	0.0272	0.0271	0.0225	0.0218	0.0216	0.0198	0.0192	0.0037	0.0037	0.0001	0.0000				
	0.0213	0.0195	0.0252	0.0316	0.0347	0.0348	0.0348	0.0301	0.0321	0.0319	0.0362	0.0356	0.0349	0.0349	0.0347	0.0347	0.0347			
2	0.0220	0.0202	0.0259	0.0323	0.0353	0.0355	0.0355	0.0308	0.0328	0.0326	0.0369	0.0363	0.0356	0.0356	0.0354	0.0354	0.0354	0.0066		
	0.0185	0.0167	0.0224	0.0288	0.0318	0.0320	0.0320	0.0273	0.0293	0.0291	0.0334	0.0328	0.0321	0.0321	0.0319	0.0319	0.0319	0.0116	0.0123	

Table S10. Genetic distances within CPXV-like 2 estimated by p-distances from the alignment of 62 conserved genes (A), 87 OPXV whole genomes (B), core genomes (C) and orthologous genes (D).

A																				
	1	2				3	9	4	5	10				8			7	6		
	CPXV_Ger1998_2	CPXV_FM2292	CPXV_Ger91	CPXV_Ger2007_Vole	CPXV_Ger2014_Human	CPXV_HumLae09_1	CPXV_Br	CPXV_Catpox5swv1	CPXV_Ger1990_2	CPXV_Ger2015_Cat1	CPXV_Nor1994_Man	CPXV_No_F2	CPXV_No_HI	CPXV_NorwayFeline	CPXV_No_F1	CPXV_CheNova_DK	CPXV_Swe_HI	CPXV_Swe_H2	CPXV_FraAmiens	CPXV_Fra2001_Nancy
1	CPXV_Ger1998_2																			
	CPXV_FM2292	0.0103																		
2	CPXV_Ger91	0.0102	0.0071																	
	CPXV_Ger2007_Vole	0.0124	0.0061	0.0080																
	CPXV_Ger2014_Human	0.0124	0.0099	0.0051	0.0101															
3	CPXV_HumLae09_1	0.0130	0.0136	0.0118	0.0133	0.0118														
	CPXV_Br	0.0163	0.0157	0.0143	0.0150	0.0137	0.0126													
	CPXV_Catpox5swv1	0.0165	0.0159	0.0143	0.0154	0.0139	0.0123	0.0053												
4	CPXV_Ger1990_2	0.0137	0.0148	0.0125	0.0142	0.0119	0.0086	0.0141	0.0140											
	CPXV_Ger2015_Cat1	0.0133	0.0133	0.0111	0.0127	0.0105	0.0094	0.0129	0.0129	0.0083										
	CPXV_Nor1994_Man	0.0161	0.0152	0.0135	0.0152	0.0132	0.0119	0.0117	0.0117	0.0133	0.0127									
	CPXV_No_F2	0.0160	0.0151	0.0134	0.0151	0.0131	0.0119	0.0116	0.0116	0.0132	0.0126	0.0002								
10	CPXV_No_HI	0.0161	0.0152	0.0135	0.0152	0.0132	0.0119	0.0117	0.0117	0.0133	0.0127	0.0000	0.0002							
	CPXV_NorwayFeline	0.0158	0.0149	0.0130	0.0149	0.0129	0.0118	0.0116	0.0116	0.0127	0.0124	0.0021	0.0020	0.0021						
	CPXV_No_F1	0.0158	0.0149	0.0130	0.0149	0.0129	0.0118	0.0116	0.0116	0.0127	0.0124	0.0021	0.0020	0.0021	0.0000					
	CPXV_CheNova_DK	0.0148	0.0150	0.0138	0.0150	0.0133	0.0100	0.0119	0.0119	0.0113	0.0116	0.0117	0.0117	0.0117	0.0120	0.0120				
8	CPXV_Swe_HI	0.0145	0.0147	0.0132	0.0142	0.0127	0.0097	0.0117	0.0116	0.0107	0.0112	0.0119	0.0119	0.0119	0.0121	0.0121	0.0049			
	CPXV_Swe_H2	0.0145	0.0148	0.0132	0.0143	0.0128	0.0098	0.0119	0.0117	0.0108	0.0112	0.0120	0.0120	0.0122	0.0122	0.0049	0.0003			
7	CPXV_FraAmiens	0.0151	0.0146	0.0128	0.0147	0.0126	0.0106	0.0121	0.0121	0.0109	0.0115	0.0119	0.0119	0.0119	0.0119	0.0117	0.0115	0.0114		
6	CPXV_Fra2001_Nancy	0.0134	0.0139	0.0123	0.0136	0.0120	0.0103	0.0132	0.0130	0.0094	0.0105	0.0126	0.0125	0.0126	0.0122	0.0122	0.0112	0.0110	0.0110	0.0098
B																				
	1	2				7		6	4	5	9	8	11				3	10		
	CPXV_Ger1998_2	CPXV_Ger2007_Vole	CPXV_FM2292	CPXV_Ger91	CPXV_Swe_H2	CPXV_Swe_HI	CPXV_CheNova_DK_2014	CPXV_HumLae09_1	CPXV_Ger2015_Cat1	CPXV_Ger1990_2	CPXV_FraAmiens_2016	CPXV_Fra2001_Nancy	CPXV_NorwayFeline	CPXV_NOR_1994_MAN	CPXV_No_HI	CPXV_No_F2	CPXV_No_F1	CPXV_Ger2014_Human	CPXV_Catpox_5swv1	CPXV_Br
1	CPXV_Ger1998_2																			
	CPXV_Ger2007_Vole	0.0126																		
2	CPXV_FM2292	0.0119	0.0048																	
	CPXV_Ger91	0.0109	0.0077	0.0070																
	CPXV_Swe_H2	0.0180	0.0170	0.0176	0.0173															
	CPXV_Swe_HI	0.0180	0.0169	0.0175	0.0172	0.0004														
	CPXV_CheNova_DK_2014	0.0180	0.0173	0.0177	0.0176	0.0047	0.0047													
6	CPXV_HumLae09_1	0.0170	0.0161	0.0164	0.0160	0.0106	0.0105	0.0106												
4	CPXV_Ger2015_Cat1	0.0157	0.0138	0.0145	0.0142	0.0126	0.0126	0.0129	0.0108											
5	CPXV_Ger1990_2	0.0165	0.0152	0.0154	0.0151	0.0118	0.0117	0.0120	0.0098	0.0094										
9	CPXV_FraAmiens_2016	0.0175	0.0163	0.0164	0.0159	0.0123	0.0123	0.0125	0.0119	0.0118	0.0119									
8	CPXV_Fra2001_Nancy	0.0169	0.0148	0.0153	0.0149	0.0130	0.0130	0.0129	0.0119	0.0113	0.0105	0.0101								
	CPXV_NorwayFeline	0.0182	0.0166	0.0171	0.0168	0.0133	0.0132	0.0130	0.0133	0.0126	0.0131	0.0125	0.0134							
	CPXV_NOR_1994_MAN	0.0184	0.0169	0.0174	0.0171	0.0131	0.0130	0.0127	0.0133	0.0130	0.0133	0.0122	0.0135	0.0026						
	CPXV_No_HI	0.0184	0.0169	0.0174	0.0171	0.0131	0.0130	0.0127	0.0133	0.0130	0.0133	0.0122	0.0135	0.0026	0.0000					
	CPXV_No_F2	0.0183	0.0169	0.0174	0.0171	0.0131	0.0130	0.0127	0.0133	0.0130	0.0133	0.0122	0.0134	0.0026	0.0001	0.0001				
	CPXV_No_F1	0.0182	0.0166	0.0171	0.0168	0.0133	0.0132	0.0130	0.0133	0.0126	0.0131	0.0125	0.0134	0.0000	0.0026	0.0026	0.0026			
3	CPXV_Ger2014_Human	0.0150	0.0114	0.0116	0.0096	0.0138	0.0137	0.0139	0.0123	0.0097	0.0114	0.0125	0.0121	0.0129	0.0130	0.0130	0.0130	0.0129		
	CPXV_Catpox_5swv1	0.0192	0.0173	0.0179	0.0176	0.0134	0.0132	0.0136	0.0140	0.0137	0.0143	0.0125	0.0140	0.0128	0.0126	0.0126	0.0125	0.0128	0.0143	
10	CPXV_Br	0.0197	0.0175	0.0179	0.0179	0.0138	0.0136	0.0136	0.0144	0.0140	0.0145	0.0125	0.0141	0.0129	0.0126	0.0126	0.0125	0.0129	0.0147	0.0049

C																				
		2		1	11					3	7			6	5	4	9	8	10	
	CPXV_Ger2007_Vole	CPXV_FM2292	CPXV_Ger91	CPXV_Ger1998_2	CPXV_NoF1	CPXV_NorwayFeline	CPXV_Nori994_Man	CPXV_No_H1	CPXV_No_F2	CPXV_Ger2014_Human	CPXV_Swe_H2	CPXV_Swe_H1	CPXV_CheNova_DK_2014	CPXV_HumLue09_1	CPXV_Ger1990_2	CPXV_Ger2015_Cat1	CPXV_FraAmiens_2016	CPXV_Fra2001_Nancy	CPXV_Catpox5_wvl	CPXV_Br
2	CPXV_Ger2007_Vole																			
	CPXV_FM2292	0.0047																		
	CPXV_Ger91	0.0075	0.0068																	
1	CPXV_Ger1998_2	0.0130	0.0123	0.0113																
	CPXV_NoF1	0.0167	0.0171	0.0168	0.0185															
	CPXV_NorwayFeline	0.0167	0.0171	0.0168	0.0185	0.0000														
11	CPXV_Nori994_Man	0.0170	0.0174	0.0170	0.0186	0.0027	0.0027													
	CPXV_No_H1	0.0170	0.0174	0.0170	0.0186	0.0027	0.0027	0.0000												
	CPXV_No_F2	0.0170	0.0174	0.0170	0.0186	0.0026	0.0026	0.0001	0.0001											
3	CPXV_Ger2014_Human	0.0113	0.0115	0.0096	0.0153	0.0130	0.0130	0.0130	0.0130	0.0130										
	CPXV_Swe_H2	0.0172	0.0177	0.0174	0.0183	0.0135	0.0135	0.0133	0.0133	0.0133	0.0139									
7	CPXV_Swe_H1	0.0171	0.0176	0.0173	0.0183	0.0134	0.0134	0.0132	0.0132	0.0132	0.0139	0.0004								
	CPXV_CheNova_DK_2014	0.0175	0.0178	0.0177	0.0182	0.0131	0.0131	0.0127	0.0127	0.0127	0.0139	0.0048	0.0048							
6	CPXV_HumLue09_1	0.0162	0.0165	0.0160	0.0172	0.0135	0.0135	0.0134	0.0134	0.0134	0.0124	0.0108	0.0107	0.0106						
5	CPXV_Ger1990_2	0.0152	0.0154	0.0151	0.0167	0.0132	0.0132	0.0134	0.0134	0.0133	0.0114	0.0120	0.0119	0.0121	0.0099					
4	CPXV_Ger2015_Cat1	0.0138	0.0145	0.0141	0.0159	0.0126	0.0126	0.0130	0.0130	0.0130	0.0097	0.0128	0.0127	0.0129	0.0109	0.0094				
9	CPXV_FraAmiens_2016	0.0164	0.0164	0.0160	0.0179	0.0126	0.0126	0.0123	0.0123	0.0123	0.0126	0.0126	0.0126	0.0126	0.0121	0.0120	0.0120			
8	CPXV_Fra2001_Nancy	0.0150	0.0154	0.0150	0.0171	0.0135	0.0135	0.0136	0.0136	0.0136	0.0122	0.0132	0.0131	0.0130	0.0120	0.0106	0.0114	0.0102		
10	CPXV_Catpox5_wvl	0.0174	0.0179	0.0176	0.0195	0.0128	0.0128	0.0126	0.0126	0.0126	0.0144	0.0135	0.0134	0.0136	0.0141	0.0143	0.0137	0.0126	0.0142	
	CPXV_Br	0.0176	0.0180	0.0179	0.0200	0.0129	0.0129	0.0126	0.0126	0.0126	0.0148	0.0139	0.0138	0.0136	0.0145	0.0145	0.0141	0.0126	0.0142	0.0049

D																				
		2		1	10	4	11			7			5	6	11		8	9	3	
	CPXV_FM2292	CPXV_Ger2007_Vole	CPXV_Ger91	CPXV_Ger1998_2	CPXV_Br	CPXV_Catpox5_wvl	CPXV_Ger2015_Cat1	CPXV_Nori994_Man	CPXV_NoF2	CPXV_NoH1	CPXV_SweH1	CPXV_SweH2	CPXV_CheNova_DK_2014	CPXV_Ger1990_2	CPXV_HumLue09_1	CPXV_NoF1	CPXV_NorwayFeline	CPXV_Fra2001_Nancy	CPXV_FraAmiens_2016	CPXV_Ger2014_Human
	CPXV_FM2292																			
2	CPXV_Ger2007_Vole	0.0049																		
	CPXV_Ger91	0.0079	0.0089																	
1	CPXV_Ger1998_2	0.0124	0.0131	0.0113																
	CPXV_Br	0.0185	0.0180	0.0186	0.0199															
10	CPXV_Catpox5_wvl	0.0185	0.0179	0.0182	0.0195	0.0046														
4	CPXV_Ger2015_Cat1	0.0152	0.0145	0.0149	0.0165	0.0145	0.0139													
	CPXV_Nori994_Man	0.0183	0.0180	0.0181	0.0190	0.0133	0.0130	0.0137												
11	CPXV_NoF2	0.0183	0.0179	0.0181	0.0189	0.0133	0.0129	0.0137	0.0001											
	CPXV_NoH1	0.0183	0.0180	0.0181	0.0190	0.0133	0.0130	0.0137	0.0000	0.0001										
	CPXV_SweH1	0.0181	0.0178	0.0180	0.0187	0.0140	0.0133	0.0133	0.0138	0.0138	0.0138									
7	CPXV_SweH2	0.0182	0.0179	0.0181	0.0187	0.0141	0.0134	0.0133	0.0138	0.0138	0.0138	0.0005								
	CPXV_CheNova_DK_2014	0.0178	0.0177	0.0181	0.0183	0.0138	0.0134	0.0133	0.0128	0.0128	0.0128	0.0051	0.0051							
5	CPXV_Ger1990_2	0.0162	0.0161	0.0159	0.0169	0.0152	0.0147	0.0101	0.0143	0.0143	0.0143	0.0124	0.0124	0.0125						
6	CPXV_HumLue09_1	0.0169	0.0168	0.0164	0.0174	0.0145	0.0140	0.0114	0.0135	0.0136	0.0135	0.0110	0.0112	0.0108	0.0101					
	CPXV_NoF1	0.0181	0.0177	0.0179	0.0189	0.0136	0.0132	0.0135	0.0028	0.0028	0.0028	0.0139	0.0141	0.0133	0.0142	0.0137				
11	CPXV_NorwayFeline	0.0160	0.0160	0.0165	0.0180	0.0123	0.0122	0.0127	0.0028	0.0027	0.0028	0.0132	0.0133	0.0128	0.0134	0.0130	0.0000			
8	CPXV_Fra2001_Nancy	0.0160	0.0156	0.0155	0.0174	0.0145	0.0140	0.0116	0.0139	0.0139	0.0139	0.0134	0.0134	0.0132	0.0110	0.0122	0.0140	0.0131		
9	CPXV_FraAmiens_2016	0.0166	0.0165	0.0161	0.0179	0.0131	0.0129	0.0123	0.0130	0.0130	0.0130	0.0129	0.0129	0.0129	0.0127	0.0125	0.0133	0.0121	0.0105	
3	CPXV_Ger2014_Human	0.0119	0.0118	0.0097	0.0155	0.0156	0.0150	0.0105	0.0140	0.0140	0.0144	0.0145	0.0142	0.0122	0.0127	0.0141	0.0136	0.0129	0.0133	

Table S11. Patristic and genetic distances within ECTV-Abatino-like calculated from the Maximum likelihood (ML) and Bayesian inference (BI) trees of 62 conserved genes, 87 OPXV whole genomes, core genomes and orthologous genes and their alignments, respectively.

	Patristic distances						
	ML tree of 62 conserved genes	BI tree of 62 conserved genes	ML tree of 87 OPXV whole genomes	BI tree of 87 OPXV whole genomes	ML tree of 87 OPXV core genomes	BI tree of 87 OPXV core genomes	ML tree of OPXV orthologous genes
CPXV-No-H2 - CPXV_GerMygEK938_17	0.016	0.016	0.022	0.022	0.022	0.021	0.022
CPXV-No-H2 - CPXV_Ger2010_MKY	0.016	0.016	0.022	0.022	0.022	0.021	0.022
CPXV_GerMygEK938_17 - CPXV_Ger2010_MKY	0.004	0.004	0.004	0.004	0.004	0.004	0.004
TATV - CMLV	0.011	0.011	0.012	0.012	0.012	0.012	0.013
TATV-VARV	0.018	0.018	0.019	0.019	0.021	0.020	0.018

TATV: Taterapox virus, CMLV:Camelpox virus, VARV: Variola virus

	Genetic distances			
	62 conserved genes	87 OPXV whole genomes	87 OPXV core genomes	OPXV orthologous genes
CPXV-No-H2 - CPXV_GerMygEK938_17	0.011	0.016	0.016	0.015
CPXV-No-H2 - CPXV_Ger2010_MKY	0.011	0.016	0.016	0.016
CPXV_GerMygEK938_17 - CPXV_Ger2010_MKY	0.003	0.003	0.003	0.003
TATV - CMLV	0.008	0.009	0.009	0.009
TATV-VARV	0.012	0.014	0.015	0.014

TATV: Taterapox virus, CMLV:Camelpox virus, VARV: Variola virus

Table S12. Patristic distances within VACV-like calculated from the Maximum likelihood (ML) and Bayesian inference (BI) trees of 62 conserved genes, 87 OPXV whole genomes, core genomes and orthologous genes.

ML tree of 62 conserved genes				
	CPXV_Fin2000_Man_2000	CPXV_Gri_1990	CPXV_HumLit08_1_2008	CPXV_Aus_1999
CPXV_Fin2000_Man_2000				
CPXV_Gri_1990	0.0090			
CPXV_HumLit08_1_2008	0.0181	0.0182		
CPXV_Aus_1999	0.0201	0.0203	0.0150	
BI tree of 62 conserved genes				
	CPXV_Fin2000_Man_2000	CPXV_Gri_1990	CPXV_HumLit08_1_2008	CPXV_Aus_1999
CPXV_Fin2000_Man_2000				
CPXV_Gri_1990	0.0089			
CPXV_HumLit08_1_2008	0.0179	0.0180		
CPXV_Aus_1999	0.0199	0.0200	0.0148	
ML tree of 87 OPXV whole genomes				
	CPXV_HumLit08_1	CPXV_Aus_1999	CPXV_Fin2000_Man	CPXV_Gri
CPXV_HumLit08_1				
CPXV_Aus_1999	0.0185			
CPXV_Fin2000_Man	0.0201	0.0185		
CPXV_Gri	0.0207	0.0191	0.0094	
BI tree of 87 OPXV whole genomes				
	CPXV_Gri	CPXV_Fin2000_Man	CPXV_Aus_1999	CPXV_HumLit08_1
CPXV_Gri				
CPXV_Fin2000_Man	0.0092			
CPXV_Aus_1999	0.0189	0.0183		
CPXV_HumLit08_1	0.0205	0.0199	0.0184	
ML tree of 87 OPXV core genomes				
	CPXV_HumLit08_1	CPXV_Aus_1999	CPXV_Fin2000_Man	CPXV_Gri
CPXV_HumLit08_1				
CPXV_Aus_1999	0.0186			
CPXV_Fin2000_Man	0.0201	0.0182		
CPXV_Gri	0.0208	0.0189	0.0094	
BI tree of 87 OPXV core genomes				
	CPXV_Gri	CPXV_Fin2000_Man	CPXV_Aus_1999	CPXV_HumLit08_1
CPXV_Gri				
CPXV_Fin2000_Man	0.0092			
CPXV_Aus_1999	0.0187	0.0180		
CPXV_HumLit08_1	0.0205	0.0199	0.0184	
ML tree of OPXV orthologous genes				
	CPXV_HumLit08_1	CPXV_Gri	CPXV_Fin2000_Man	CPXV_Aus_1999
CPXV_HumLit08_1				
CPXV_Gri	0.0194			
CPXV_Fin2000_Man	0.0179	0.0097		
CPXV_Aus_1999	0.0192	0.0197	0.0182	

Table S13. Genetic distances within VACV-like clade estimated by p-distances from the alignment of 62 conserved genes (A), 87 OPXV whole genomes (B), core genomes(C), orthologous genes (D).

A				
	CPXV_Gri	CPXV_Fin2000_Man	CPXV_Aus_1999	CPXV_HumLit08_1
CPXV_Gri				
CPXV_Fin2000_Man	0.006			
CPXV_Aus_1999	0.012	0.012		
CPXV_HumLit08_1	0.010	0.010	0.010	
B				
	CPXV_Gri	CPXV_Fin2000_Man	CPXV_HumLit08_1	CPXV_Aus_1999
CPXV_Gri				
CPXV_Fin2000_Man	0.007			
CPXV_HumLit08_1	0.013	0.012		
CPXV_Aus_1999	0.012	0.012	0.013	
C				
	CPXV_Gri	CPXV_Fin2000_Man	CPXV_HumLit08_1	CPXV_Aus_1999
CPXV_Gri				
CPXV_Fin2000_Man	0.007			
CPXV_HumLit08_1	0.013	0.012		
CPXV_Aus_1999	0.012	0.012	0.013	
D				
	CPXV_Gri	CPXV_Fin2000_Man	CPXV_Aus_1999	CPXV_HumLit08_1
CPXV_Gri				
CPXV_Fin2000_Man	0.007			
CPXV_Aus_1999	0.012	0.012		
CPXV_HumLit08_1	0.013	0.011	0.013	

Table S14. Patristic and genetic distances within CPXV-like 1 calculated from the Maximum likelihood (ML) and Bayesian inference (BI) trees of 87 OPXV whole genomes, core genomes and orthologous genes and their alignments, respectively.

	Patristic distances						
	ML tree of 62 conserved genes	BI tree of 62 conserved genes	ML tree of 87 OPXV whole genomes	BI tree of 87 OPXV whole genomes	ML tree of 87 OPXV core genomes	BI tree of 87 OPXV core genomes	ML tree of OPXV orthologous genes
CPXV_Ger_1971_EPI - CPXV-like 1*	0.0229	0.0219	0.0193	0.0191	0.0187	0.0185	0.0201
TATV - CMLV	0.0114	0.0113	0.0121	0.0120	0.0123	0.0121	0.0130
TATV-VARV	0.0179	0.0175	0.0193	0.0191	0.0207	0.0204	0.0182

* All CPXV-like1 strains without CPXV_Ger_1971_EPI

	Genetic distances			
	OPXV conserved genes	87 OPXV whole genomes	87 OPXV core genomes	OPXV orthologous genes
CPXV_Ger_1971_EPI - CPXV-like 1*	0.0105	0.0102	0.0101	0.0105
TATV - CMLV	0.0080	0.0090	0.0092	0.0094
TATV-VARV	0.0121	0.0141	0.0152	0.0136

* All CPXV-like1 strains without CPXV_Ger_1971_EPI

Table S15. Patristic distances within CPXV-like 1 calculated from the Maximum likelihood (ML) and Bayesian inference (BI) trees of 62 conserved genes, 87 OPXV whole genomes, core genomes and orthologous genes.

ML tree of 62 conserved genes																												
	CPXV_Ger2010_Racoon_2010	CPXV_EleGri07_1_2007	CPXV_Ger2014_Cat1_2014	CPXV_Ger2017_Vole_2017	CPXV_Ger2017_Alpacaca2_2017	CPXV_Ger2014_Cat2_2014	CPXV_HumLan08_1_2008	CPXV_JagKre08_1_2008	CPXV_MonKre08_4_2008	CPXV_JagKre08_2_2008	CPXV_MonKre08_4_2008	CPXV_JagKre08_2_2008	CPXV_Ger2015_Cat2_2015	CPXV_Ger2015_Human2_2015	CPXV_Ger2012_Alpacaca_2012	CPXV_Ama2015	CPXV_CatPot07_1_2007	CPXV_HumMag07_1_2007	CPXV_BeaBer04_1_2004	CPXV_Ger1980_EP4_1980	CPXV_Ger2010_Rat_2010	CPXV_Ger2002_MKY_2002	CPXV_Ger2013_Alpacaca_2013	CPXV_HumBer07_1_2007	CPXV_Ger2010_Alpacaca_2010	CPXV_Ger1971_EP1_1971		
CPXV_Ger2010_Racoon_2010																												
CPXV_EleGri07_1_2007	0.016																											
CPXV_Ger2014_Cat1_2014	0.020	0.008																										
CPXV_Ger2017_Vole_2017	0.015	0.006	0.010																									
CPXV_Ger2017_Alpacaca2_2017	0.016	0.007	0.011	0.005																								
CPXV_Ger2014_Cat2_2014	0.024	0.014	0.018	0.012	0.010																							
CPXV_HumLan08_1_2008	0.023	0.014	0.018	0.012	0.010	0.015																						
CPXV_JagKre08_1_2008	0.023	0.014	0.018	0.012	0.010	0.015	0.000																					
CPXV_MonKre08_4_2008	0.023	0.014	0.018	0.012	0.010	0.015	0.000	0.000																				
CPXV_JagKre08_2_2008	0.023	0.014	0.018	0.012	0.010	0.015	0.000	0.000	0.000																			
CPXV_Ger2015_Cat2_2015	0.019	0.010	0.014	0.008	0.006	0.011	0.009	0.008	0.008	0.008																		
CPXV_Ger2015_Human2_2015	0.020	0.011	0.015	0.009	0.008	0.015	0.015	0.015	0.015	0.015	0.011																	
CPXV_Ger2012_Alpacaca_2012	0.018	0.009	0.012	0.006	0.005	0.012	0.012	0.012	0.012	0.012	0.008	0.004																
CPXV_Ama2015	0.015	0.008	0.012	0.008	0.009	0.016	0.016	0.016	0.016	0.016	0.012	0.013	0.010															
CPXV_CatPot07_1_2007	0.015	0.009	0.013	0.008	0.009	0.017	0.017	0.017	0.017	0.017	0.013	0.014	0.011	0.004														
CPXV_HumMag07_1_2007	0.016	0.009	0.013	0.009	0.010	0.017	0.017	0.017	0.017	0.017	0.013	0.014	0.011	0.004	0.001													
CPXV_BeaBer04_1_2004	0.016	0.010	0.014	0.010	0.011	0.018	0.018	0.018	0.018	0.018	0.014	0.015	0.012	0.005	0.002	0.002												
CPXV_Ger1980_EP4_1980	0.032	0.025	0.029	0.025	0.026	0.033	0.033	0.033	0.033	0.033	0.029	0.030	0.027	0.020	0.017	0.018	0.016											
CPXV_Ger2010_Rat_2010	0.028	0.022	0.026	0.021	0.023	0.030	0.030	0.030	0.030	0.026	0.027	0.024	0.017	0.014	0.014	0.012	0.007											
CPXV_Ger2002_MKY_2002	0.028	0.021	0.025	0.021	0.022	0.029	0.029	0.029	0.029	0.025	0.026	0.023	0.016	0.013	0.014	0.012	0.011	0.008										
CPXV_Ger2013_Alpacaca_2013	0.027	0.021	0.025	0.021	0.022	0.029	0.029	0.029	0.029	0.025	0.026	0.023	0.016	0.013	0.014	0.011	0.011	0.008	0.004									
CPXV_HumBer07_1_2007	0.016	0.009	0.013	0.009	0.010	0.017	0.017	0.017	0.017	0.013	0.014	0.011	0.004	0.001	0.002	0.002	0.017	0.014	0.013	0.013								
CPXV_Ger2010_Alpacaca_2010	0.015	0.013	0.017	0.012	0.013	0.021	0.020	0.020	0.020	0.016	0.017	0.015	0.012	0.012	0.013	0.013	0.028	0.025	0.025	0.024	0.013							
CPXV_Ger1971_EP1_1971	0.016	0.019	0.022	0.018	0.019	0.026	0.026	0.026	0.026	0.022	0.023	0.021	0.017	0.018	0.019	0.019	0.034	0.031	0.030	0.030	0.018	0.017						
BI tree of 62 conserved genes																												
	CPXV_Ger2014_Cat2_2014	CPXV_Ger2012_Alpacaca_2012	CPXV_Ger2015_Human2_2015	CPXV_Ger2015_Cat2_2015	CPXV_Ger2017_Alpacaca2_2017	CPXV_Ger2017_Vole_2017	CPXV_HumLan08_1_2008	CPXV_JagKre08_1_2008	CPXV_JagKre08_2_2008	CPXV_MonKre08_4_2008	CPXV_EleGri07_1_2007	CPXV_Ger2014_Cat1_2014	CPXV_Ama2015	CPXV_BeaBer04_1_2004	CPXV_Ger1980_EP4_1980	CPXV_Ger2010_Rat_2010	CPXV_Ger2002_MKY_2002	CPXV_Ger2013_Alpacaca_2013	CPXV_HumBer07_1_2007	CPXV_CatPot07_1_2007	CPXV_HumMag07_1_2007	CPXV_Ger2010_Alpacaca_2010	CPXV_Ger2010_Racoon_2010	CPXV_Ger1971_EP1_1971				
CPXV_Ger2014_Cat2_2014																												
CPXV_Ger2012_Alpacaca_2012	0.010																											
CPXV_Ger2015_Human2_2015	0.013	0.004																										
CPXV_Ger2015_Cat2_2015	0.013	0.008	0.011																									
CPXV_Ger2017_Alpacaca2_2017	0.010	0.005	0.008	0.004																								
CPXV_Ger2017_Vole_2017	0.012	0.006	0.009	0.007	0.004																							
CPXV_HumLan08_1_2008	0.018	0.013	0.015	0.014	0.011	0.010																						
CPXV_JagKre08_1_2008	0.018	0.013	0.015	0.014	0.011	0.010	0.000																					
CPXV_JagKre08_2_2008	0.018	0.013	0.015	0.014	0.011	0.010	0.000	0.000																				
CPXV_MonKre08_4_2008	0.018	0.013	0.015	0.014	0.011	0.010	0.000	0.000	0.000																			
CPXV_EleGri07_1_2007	0.015	0.010	0.012	0.010	0.008	0.007	0.010	0.010	0.010	0.010																		
CPXV_Ger2014_Cat1_2014	0.018	0.013	0.015	0.014	0.011	0.010	0.013	0.013	0.013	0.013	0.008																	
CPXV_Ama2015	0.015	0.010	0.013	0.011	0.008	0.008	0.012	0.012	0.012	0.012	0.008	0.012																
CPXV_BeaBer04_1_2004	0.017	0.012	0.015	0.013	0.010	0.010	0.014	0.014	0.014	0.014	0.010	0.014	0.005															
CPXV_Ger1980_EP4_1980	0.032	0.027	0.030	0.028	0.025	0.025	0.029	0.029	0.029	0.025	0.029	0.020	0.016															
CPXV_Ger2010_Rat_2010	0.029	0.024	0.027	0.025	0.022	0.021	0.026	0.026	0.026	0.026	0.022	0.026	0.017	0.012	0.007													
CPXV_Ger2002_MKY_2002	0.028	0.023	0.026	0.024	0.021	0.021	0.025	0.025	0.025	0.025	0.021	0.025	0.016	0.012	0.011	0.008												
CPXV_Ger2013_Alpacaca_2013	0.028	0.023	0.026	0.024	0.021	0.020	0.025	0.025	0.025	0.025	0.021	0.025	0.016	0.011	0.011	0.008	0.004											
CPXV_HumBer07_1_2007	0.016	0.011	0.014	0.012	0.009	0.009	0.013	0.013	0.013	0.013	0.010	0.013	0.004	0.002	0.017	0.014	0.013	0.013										
CPXV_CatPot07_1_2007	0.016	0.011	0.014	0.012	0.009	0.009	0.013	0.013	0.013	0.013	0.009	0.013	0.004	0.002	0.017	0.014	0.013	0.013	0.001									
CPXV_HumMag07_1_2007	0.016	0.011	0.014	0.012	0.009	0.009	0.013	0.013	0.013	0.013	0.010	0.013	0.004	0.003	0.018	0.015	0.014	0.013	0.002	0.001								
CPXV_Ger2010_Alpacaca_2010	0.020	0.015	0.017	0.016	0.013	0.012	0.016	0.016	0.016	0.016	0.013	0.016	0.011	0.013	0.028	0.025	0.024	0.024	0.012	0.012	0.013							
CPXV_Ger2010_Racoon_2010	0.023	0.018	0.020	0.019	0.016	0.015	0.019	0.019	0.019	0.019	0.016	0.019	0.014	0.016	0.031	0.028	0.027	0.027	0.016	0.015	0.016	0.014						
CPXV_Ger1971_EP1_1971	0.026	0.021	0.023	0.022	0.019	0.018	0.022	0.022	0.022	0.022	0.019	0.022	0.017	0.019	0.034	0.031	0.030	0.030	0.018	0.018	0.018	0.017	0.016					

ML tree of 87 CPXV whole genomes																									
	CPXV_Ger1971_EP1	CPXV_Jagkre08_2	CPXV_MonKre08_4	CPXV_Jagkre08_1	CPXV_HumLan08_1	CPXV_Ger2017_Vole	CPXV_Ger2015_Cat2	CPXV_Ger2017_Alpacaca2	CPXV_Ger2010_Alpacaca	CPXV_Ger2010_Racoon	CPXV_Ger2014_Cat2	CPXV_Ger2015_Human2	CPXV_Ger2012_Alpacaca	CPXV_Ger2014_Cat1	CPXV_Ger2013_Alpacaca	CPXV_Ger1980_EP4	CPXV_Ger2010_Rat	CPXV_Ger2002_MKY	CPXV_HumMag07_1	CPXV_HumBer07_1	CPXV_CatPot07_1	CPXV_BeaBer04_1	CPXV_Ama_2015	CPXV_EleGri07_1	
CPXV_Ger1971_EP1																									
CPXV_Jagkre08_2	0.015																								
CPXV_MonKre08_4	0.015	0.000																							
CPXV_Jagkre08_1	0.015	0.000	0.000																						
CPXV_HumLan08_1	0.015	0.000	0.000	0.000																					
CPXV_Ger2017_Vole	0.016	0.012	0.012	0.012	0.012																				
CPXV_Ger2015_Cat2	0.019	0.015	0.015	0.015	0.015	0.007																			
CPXV_Ger2017_Alpacaca2	0.017	0.013	0.013	0.013	0.013	0.006	0.005																		
CPXV_Ger2010_Alpacaca	0.023	0.019	0.019	0.019	0.019	0.014	0.017	0.015																	
CPXV_Ger2010_Racoon	0.023	0.020	0.020	0.020	0.020	0.014	0.017	0.015	0.015																
CPXV_Ger2014_Cat2	0.023	0.019	0.019	0.019	0.019	0.014	0.017	0.015	0.015	0.010															
CPXV_Ger2015_Human2	0.019	0.015	0.015	0.015	0.015	0.010	0.013	0.011	0.013	0.014	0.014														
CPXV_Ger2012_Alpacaca	0.017	0.014	0.014	0.014	0.014	0.008	0.011	0.009	0.012	0.012	0.012	0.004													
CPXV_Ger2014_Cat1	0.018	0.014	0.014	0.014	0.014	0.011	0.014	0.012	0.018	0.018	0.018	0.014	0.012												
CPXV_Ger2013_Alpacaca	0.020	0.016	0.016	0.016	0.016	0.013	0.016	0.014	0.020	0.020	0.020	0.016	0.014	0.012											
CPXV_Ger1980_EP4	0.029	0.026	0.026	0.026	0.026	0.022	0.025	0.023	0.029	0.030	0.029	0.025	0.023	0.021	0.012										
CPXV_Ger2010_Rat	0.027	0.024	0.024	0.024	0.024	0.020	0.023	0.021	0.027	0.027	0.027	0.023	0.021	0.019	0.009	0.006									
CPXV_Ger2002_MKY	0.024	0.020	0.020	0.020	0.020	0.016	0.019	0.017	0.023	0.024	0.023	0.019	0.018	0.015	0.006	0.009	0.007								
CPXV_HumMag07_1	0.018	0.014	0.014	0.014	0.014	0.010	0.013	0.011	0.017	0.018	0.017	0.013	0.012	0.009	0.008	0.017	0.015	0.011							
CPXV_HumBer07_1	0.018	0.015	0.015	0.015	0.015	0.011	0.014	0.012	0.018	0.019	0.018	0.014	0.013	0.010	0.008	0.018	0.016	0.012	0.002						
CPXV_CatPot07_1	0.018	0.014	0.014	0.014	0.014	0.011	0.013	0.012	0.018	0.018	0.018	0.014	0.012	0.010	0.008	0.017	0.015	0.011	0.001	0.002					
CPXV_BeaBer04_1	0.018	0.015	0.015	0.015	0.015	0.011	0.014	0.012	0.018	0.019	0.018	0.014	0.012	0.010	0.008	0.018	0.016	0.012	0.002	0.002	0.001				
CPXV_Ama_2015	0.021	0.017	0.017	0.017	0.017	0.014	0.016	0.015	0.021	0.021	0.021	0.017	0.015	0.012	0.011	0.020	0.018	0.014	0.006	0.007	0.006	0.007			
CPXV_EleGri07_1	0.015	0.011	0.011	0.011	0.011	0.009	0.012	0.010	0.016	0.017	0.016	0.012	0.011	0.012	0.014	0.023	0.021	0.017	0.011	0.012	0.011	0.012	0.014		
BI tree of 87 CPXV whole genomes																									
	CPXV_MonKre08_4	CPXV_Jagkre08_2	CPXV_Jagkre08_1	CPXV_HumLan08_1	CPXV_Ger2017_Vole	CPXV_Ger2017_Alpacaca2	CPXV_Ger2015_Cat2	CPXV_Ger2015_Human2	CPXV_Ger2012_Alpacaca	CPXV_Ger2014_Cat2	CPXV_Ger2010_Racoon	CPXV_Ger2010_Alpacaca	CPXV_HumMag07_1	CPXV_HumBer07_1	CPXV_BeaBer04_1	CPXV_CatPot07_1	CPXV_Ama_2015	CPXV_Ger2013_Alpacaca	CPXV_Ger2010_Rat	CPXV_Ger1980_EP4	CPXV_Ger2002_MKY	CPXV_Ger2014_Cat1	CPXV_EleGri07_1	CPXV_Ger1971_EP1	
CPXV_MonKre08_4																									
CPXV_Jagkre08_2	0.00001																								
CPXV_Jagkre08_1	0.00001	0.00001																							
CPXV_HumLan08_1	0.00002	0.00002	0.00002																						
CPXV_Ger2017_Vole	0.012	0.012	0.012	0.012																					
CPXV_Ger2017_Alpacaca2	0.013	0.013	0.013	0.013	0.005																				
CPXV_Ger2015_Cat2	0.015	0.015	0.015	0.015	0.007	0.005																			
CPXV_Ger2015_Human2	0.015	0.015	0.015	0.015	0.010	0.011	0.013																		
CPXV_Ger2012_Alpacaca	0.013	0.013	0.013	0.013	0.008	0.009	0.011	0.004																	
CPXV_Ger2014_Cat2	0.019	0.019	0.019	0.019	0.014	0.015	0.017	0.013	0.012																
CPXV_Ger2010_Racoon	0.019	0.019	0.019	0.019	0.014	0.015	0.017	0.014	0.012	0.010															
CPXV_Ger2010_Alpacaca	0.019	0.019	0.019	0.019	0.014	0.015	0.016	0.013	0.012	0.015	0.015														
CPXV_HumMag07_1	0.014	0.014	0.014	0.014	0.010	0.011	0.013	0.013	0.012	0.017	0.018	0.017													
CPXV_HumBer07_1	0.015	0.015	0.015	0.015	0.011	0.012	0.014	0.014	0.012	0.018	0.019	0.018	0.002	0.002											
CPXV_BeaBer04_1	0.015	0.015	0.015	0.015	0.011	0.012	0.014	0.014	0.012	0.018	0.018	0.018	0.002	0.002	0.001										
CPXV_CatPot07_1	0.014	0.014	0.014	0.014	0.011	0.012	0.013	0.014	0.012	0.018	0.018	0.018	0.001	0.002	0.001										
CPXV_Ama_2015	0.017	0.017	0.017	0.017	0.013	0.015	0.016	0.017	0.015	0.021	0.021	0.020	0.006	0.007	0.007	0.006									
CPXV_Ger2013_Alpacaca	0.016	0.016	0.016	0.016	0.013	0.014	0.015	0.016	0.014	0.020	0.020	0.020	0.007	0.008	0.008	0.008	0.011								
CPXV_Ger2010_Rat	0.023	0.023	0.023	0.023	0.020	0.021	0.023	0.023	0.021	0.027	0.027	0.027	0.015	0.016	0.015	0.015	0.018	0.009							
CPXV_Ger1980_EP4	0.026	0.026	0.026	0.026	0.022	0.023	0.025	0.025	0.023	0.029	0.029	0.029	0.017	0.018	0.018	0.017	0.020	0.011	0.006						
CPXV_Ger2002_MKY	0.020	0.020	0.020	0.020	0.016	0.017	0.019	0.019	0.017	0.023	0.023	0.023	0.011	0.012	0.012	0.011	0.014	0.006	0.007	0.009					
CPXV_Ger2014_Cat1	0.014	0.014	0.014	0.014	0.011	0.012	0.013	0.014	0.012	0.018	0.018	0.018	0.009	0.010	0.010	0.009	0.012	0.011	0.019	0.021	0.015				
CPXV_EleGri07_1	0.011	0.011	0.011	0.011	0.009	0.010	0.012	0.012	0.010	0.016	0.017	0.016	0.011	0.012	0.012	0.011	0.014	0.013	0.020	0.023	0.017	0.011			
CPXV_Ger1971_EP1	0.015	0.015	0.015	0.015	0.016	0.017	0.018	0.019	0.017	0.023	0.023	0.023	0.017	0.018	0.018	0.018	0.021	0.020	0.027	0.029	0.023	0.018	0.015		

Table S16. Genetic distances within CPXV-like 1 estimated by p-distances from the alignment of the conserved genes (A), 87 OPXV whole genomes (B), core genomes (C) and orthologous genes (D).

A																									
	CPXV_Ger20 14_Cat2_201 4	CPXV_Ger20 15_Cat2_201 5	CPXV_HumL an08_1_200 8	CPXV_JagKr e08_1_2008	CPXV_JagKr e08_2_2008	CPXV_MonK re08_4_2008	CPXV_Ama 2015	CPXV_Ger20 10_Alpac a_2010	CPXV_Ger20 12_Alpac a_2012	CPXV_Ger20 17_Alpac a_2017	CPXV_Ger20 17_Vole_2 017	CPXV_BeaB er04_1_2004	CPXV_CatPo t07_1_2007	CPXV_EleGr i07_1_2007	CPXV_Ger20 15_Human2 _2015	CPXV_Ger19 71_EP1_197 1	CPXV_Hum Ber07_1_20 07	CPXV_Hum Mag07_1_20 07	CPXV_Ger20 14_Cat1_201 4	CPXV_Ger19 80_EP4_198 0	CPXV_Ger20 10_Racoon 2010	CPXV_Ger20 02_MKY_200 2	CPXV_Ger20 13_Alpac a_2013	CPXV_Ge r2010_Ra t_2010	
CPXV_Ger2014_Cat2_2014																									
CPXV_Ger2015_Cat2_2015	0.007																								
CPXV_HumLan08_1_2008	0.009	0.006																							
CPXV_JagKre08_1_2008	0.009	0.006	0.000																						
CPXV_JagKre08_2_2008	0.009	0.006	0.000	0.000																					
CPXV_MonKre08_4_2008	0.009	0.006	0.000	0.000	0.000																				
CPXV_Ama_2015	0.008	0.006	0.007	0.007	0.007	0.007																			
CPXV_Ger2010_Alpac a_2010	0.009	0.009	0.010	0.010	0.010	0.010	0.007																		
CPXV_Ger2012_Alpac a_2012	0.007	0.005	0.007	0.007	0.007	0.007	0.005	0.007																	
CPXV_Ger2017_Alpac a_2017	0.007	0.003	0.006	0.006	0.006	0.006	0.004	0.007	0.003																
CPXV_Ger2017_Vole_2017	0.008	0.005	0.006	0.006	0.006	0.006	0.005	0.008	0.004	0.003															
CPXV_BeaBer04_1_2004	0.008	0.008	0.009	0.009	0.009	0.009	0.003	0.008	0.007	0.007	0.006														
CPXV_CatPot07_1_2007	0.008	0.007	0.008	0.008	0.008	0.008	0.003	0.007	0.007	0.006	0.005	0.001													
CPXV_EleGr07_1_2007	0.008	0.006	0.007	0.007	0.007	0.007	0.006	0.007	0.005	0.004	0.006	0.006	0.005												
CPXV_Ger2015_Human2_2015	0.007	0.007	0.007	0.007	0.007	0.007	0.006	0.009	0.003	0.005	0.006	0.008	0.007	0.006											
CPXV_Ger1971_EP1_1971	0.012	0.010	0.011	0.011	0.011	0.011	0.010	0.010	0.009	0.009	0.010	0.010	0.010	0.009	0.010										
CPXV_HumBer07_1_2007	0.008	0.007	0.008	0.008	0.008	0.008	0.003	0.007	0.007	0.006	0.006	0.001	0.001	0.006	0.007	0.010									
CPXV_HumMag07_1_2007	0.008	0.008	0.008	0.008	0.008	0.008	0.003	0.007	0.007	0.006	0.006	0.002	0.001	0.006	0.007	0.010	0.001								
CPXV_Ger2014_Cat1_2014	0.010	0.009	0.009	0.009	0.009	0.009	0.007	0.009	0.008	0.007	0.006	0.007	0.006	0.005	0.008	0.010	0.007	0.006							
CPXV_Ger1980_EP4_1980	0.011	0.013	0.013	0.013	0.013	0.013	0.010	0.011	0.011	0.012	0.012	0.008	0.009	0.012	0.011	0.012	0.009	0.009	0.010						
CPXV_Ger2010_Racoon_2010	0.010	0.010	0.010	0.010	0.010	0.010	0.009	0.009	0.009	0.009	0.009	0.009	0.008	0.009	0.007	0.010	0.009	0.009	0.010	0.010					
CPXV_Ger2002_MKY_2002	0.011	0.011	0.011	0.011	0.011	0.011	0.009	0.010	0.010	0.011	0.010	0.007	0.008	0.010	0.010	0.011	0.008	0.008	0.008	0.006	0.010				
CPXV_Ger2013_Alpac a_2013	0.010	0.011	0.011	0.011	0.011	0.011	0.009	0.010	0.010	0.010	0.009	0.007	0.007	0.009	0.010	0.012	0.007	0.007	0.009	0.007	0.011	0.003			
CPXV_Ger2010_Rat_2010	0.010	0.012	0.012	0.012	0.012	0.012	0.010	0.010	0.011	0.011	0.011	0.008	0.009	0.011	0.011	0.013	0.009	0.009	0.010	0.005	0.011	0.005	0.005	0.005	
B																									
	CPXV_MonK re08_4	CPXV_JagKr e08_2	CPXV_JagKr e08_1	CPXV_HumL an08_1	CPXV_Ger20 17_Vole	CPXV_EleGr i07_1	CPXV_Ger20 17_Alpac a_2	CPXV_Ger20 15_Cat2	CPXV_Ger20 15_Human2	CPXV_Ger20 12_Alpac a	CPXV_Ger20 14_Cat2	CPXV_Ger20 10_Racoon	CPXV_Ger20 10_Alpac a	CPXV_Hum Mag07_1	CPXV_Hum Ber07_1	CPXV_BeaB er04_1	CPXV_Ama 2015	CPXV_Ger20 13_Alpac a	CPXV_CatPo t07_1	CPXV_Ger20 10_Rat	CPXV_Ger19 80_EP4	CPXV_Ger20 02_MKY	CPXV_Ger20 14_Cat1	CPXV_Ge r1971_EP 1	
CPXV_MonKre08_4																									
CPXV_JagKre08_2	0.000																								
CPXV_JagKre08_1	0.000	0.000																							
CPXV_HumLan08_1	0.000	0.000	0.000																						
CPXV_Ger2017_Vole	0.007	0.007	0.007	0.007																					
CPXV_EleGr07_1	0.008	0.008	0.008	0.008	0.005	0.007																			
CPXV_Ger2017_Alpac a_2	0.007	0.007	0.007	0.007	0.004	0.007																			
CPXV_Ger2015_Cat2	0.007	0.007	0.007	0.007	0.005	0.008	0.004																		
CPXV_Ger2015_Human2	0.008	0.008	0.008	0.008	0.007	0.007	0.006	0.007																	
CPXV_Ger2012_Alpac a	0.008	0.008	0.008	0.008	0.005	0.007	0.005	0.006	0.003																
CPXV_Ger2014_Cat2	0.011	0.011	0.011	0.011	0.008	0.009	0.008	0.008	0.007	0.007															
CPXV_Ger2010_Racoon	0.011	0.011	0.011	0.011	0.009	0.010	0.009	0.010	0.007	0.008	0.008														
CPXV_Ger2010_Alpac a	0.011	0.011	0.011	0.011	0.008	0.010	0.008	0.010	0.010	0.008	0.010	0.009													
CPXV_HumMag07_1	0.009	0.009	0.009	0.009	0.006	0.007	0.007	0.008	0.008	0.007	0.009	0.009	0.009												
CPXV_HumBer07_1	0.009	0.009	0.009	0.009	0.006	0.007	0.007	0.008	0.008	0.007	0.009	0.009	0.009	0.001											
CPXV_BeaBer04_1	0.009	0.009	0.009	0.009	0.006	0.007	0.007	0.008	0.008	0.007	0.009	0.009	0.009	0.001	0.001										
CPXV_Ama_2015	0.009	0.009	0.009	0.009	0.007	0.008	0.007	0.008	0.008	0.007	0.009	0.010	0.009	0.005	0.005	0.005									
CPXV_Ger2013_Alpac a	0.010	0.010	0.010	0.010	0.008	0.009	0.009	0.009	0.009	0.008	0.010	0.010	0.009	0.005	0.005	0.005	0.008								
CPXV_CatPot07_1	0.009	0.009	0.009	0.009	0.006	0.007	0.007	0.008	0.008	0.007	0.009	0.009	0.009	0.001	0.001	0.001	0.005	0.005							
CPXV_Ger2010_Rat	0.012	0.012	0.012	0.012	0.011	0.011	0.011	0.012	0.011	0.011	0.011	0.010	0.010	0.009	0.009	0.009	0.010	0.007	0.009						
CPXV_Ger1980_EP4	0.013	0.013	0.013	0.013	0.011	0.012	0.011	0.012	0.011	0.011	0.010	0.009	0.010	0.009	0.010	0.009	0.011	0.008	0.009	0.004					
CPXV_Ger2002_MKY	0.011	0.011	0.011	0.011	0.009	0.009	0.010	0.010	0.010	0.009	0.010	0.009	0.010	0.007	0.008	0.007	0.009	0.004	0.007	0.005					
CPXV_Ger2014_Cat1	0.009	0.009	0.009	0.009	0.006	0.007	0.008	0.009	0.008	0.008	0.009	0.009	0.010	0.006	0.007	0.006	0.008	0.007	0.006	0.009	0.009	0.007			
CPXV_Ger1971_EP1	0.011	0.011	0.011	0.011	0.009	0.009	0.010	0.010	0.010	0.010	0.012	0.010	0.011	0.009	0.009	0.009	0.010	0.010	0.009	0.012	0.012	0.010	0.010	0.010	

C																										
	CPXV_HumBer07_1	CPXV_CatPot07_1	CPXV_HumMag07_1	CPXV_BeaBer04_1	CPXV_Ger2013_Alpac	CPXV_Ger2010_Rat	CPXV_Ger1980_EP4	CPXV_Ger2002_MKY	CPXV_Ama2015	CPXV_Ger2014_Cat1	CPXV_EleGr07_1	CPXV_Ger2017_Vole	CPXV_Ger2017_Alpac	CPXV_Ger2015_Cat2	CPXV_Ger2010_Alpac	CPXV_Ger2015_Human2	CPXV_Ger2012_Alpac	CPXV_Ger2014_Cat2	CPXV_Ger2010_Raccoon	CPXV_MonKre08_4	CPXV_JagKre08_1	CPXV_JagKre08_2	CPXV_HumLan08_1	CPXV_Ger1971_EP1		
CPXV_HumBer07_1																										
CPXV_CatPot07_1	0.001																									
CPXV_HumMag07_1	0.001	0.001																								
CPXV_BeaBer04_1	0.001	0.001	0.001																							
CPXV_Ger2013_Alpac	0.005	0.005	0.005	0.005																						
CPXV_Ger2010_Rat	0.009	0.009	0.009	0.009	0.007																					
CPXV_Ger1980_EP4	0.010	0.009	0.009	0.009	0.008	0.004																				
CPXV_Ger2002_MKY	0.008	0.007	0.007	0.007	0.004	0.005	0.006																			
CPXV_Ama2015	0.005	0.005	0.004	0.005	0.008	0.010	0.010	0.009																		
CPXV_Ger2014_Cat1	0.007	0.006	0.006	0.006	0.007	0.009	0.009	0.007	0.008																	
CPXV_EleGr07_1	0.007	0.007	0.007	0.007	0.008	0.011	0.012	0.009	0.008	0.007																
CPXV_Ger2017_Vole	0.006	0.006	0.006	0.006	0.008	0.010	0.011	0.009	0.006	0.006	0.005															
CPXV_Ger2017_Alpac2	0.007	0.007	0.007	0.007	0.008	0.011	0.011	0.010	0.006	0.008	0.007	0.004														
CPXV_Ger2015_Cat2	0.008	0.008	0.007	0.008	0.009	0.011	0.012	0.010	0.007	0.008	0.008	0.005	0.004													
CPXV_Ger2010_Alpac	0.009	0.009	0.009	0.009	0.009	0.010	0.009	0.010	0.009	0.010	0.010	0.008	0.008	0.010												
CPXV_Ger2015_Human2	0.008	0.008	0.008	0.008	0.009	0.011	0.011	0.010	0.008	0.008	0.007	0.008	0.006	0.007	0.009											
CPXV_Ger2012_Alpac	0.007	0.007	0.007	0.007	0.008	0.011	0.011	0.009	0.007	0.007	0.007	0.005	0.005	0.006	0.008	0.003										
CPXV_Ger2014_Cat2	0.009	0.009	0.009	0.009	0.010	0.010	0.010	0.009	0.009	0.009	0.009	0.008	0.007	0.008	0.010	0.007	0.007									
CPXV_Ger2010_Raccoon	0.009	0.009	0.009	0.009	0.010	0.010	0.009	0.009	0.009	0.009	0.009	0.010	0.009	0.009	0.009	0.009	0.007	0.008	0.010	0.007	0.008	0.008	0.007	0.007	0.007	
CPXV_MonKre08_4	0.009	0.009	0.009	0.009	0.010	0.012	0.013	0.011	0.009	0.009	0.008	0.007	0.007	0.006	0.011	0.008	0.008	0.011	0.010							
CPXV_JagKre08_1	0.009	0.009	0.009	0.009	0.010	0.012	0.013	0.011	0.009	0.009	0.008	0.007	0.007	0.006	0.011	0.008	0.008	0.011	0.010	0.000						
CPXV_JagKre08_2	0.009	0.009	0.009	0.009	0.010	0.012	0.013	0.011	0.009	0.009	0.008	0.007	0.007	0.006	0.011	0.008	0.008	0.011	0.010	0.000	0.000					
CPXV_HumLan08_1	0.009	0.009	0.009	0.009	0.010	0.012	0.013	0.011	0.009	0.009	0.008	0.007	0.007	0.006	0.011	0.008	0.008	0.011	0.010	0.000	0.000	0.000				
CPXV_Ger1971_EP1	0.009	0.009	0.009	0.009	0.010	0.012	0.012	0.010	0.010	0.010	0.009	0.009	0.010	0.011	0.009	0.010	0.011	0.010	0.011	0.011	0.011	0.011	0.011	0.011	0.011	
D																										
	CPXV_EleGr07_1	CPXV_Ger1980_EP4	CPXV_Ger2002_MKY	CPXV_Ger1971_EP1	CPXV_Ger2010_Raccoon	CPXV_Ger2010_Rat	CPXV_Ger2014_Cat1	CPXV_Ger2015_Human2	CPXV_HumLan08_1	CPXV_JagKre08_1	CPXV_JagKre08_2	CPXV_MonKre08_4	CPXV_Ama2015	CPXV_Ger2010_Alpac	CPXV_Ger2012_Alpac	CPXV_Ger2014_Cat2	CPXV_Ger2015_Cat2	CPXV_Ger2017_Alpac2	CPXV_Ger2017_Vole	CPXV_BeaBer04_1	CPXV_CatPot07_1	CPXV_Ger2013_Alpac	CPXV_HumBer07_1	CPXV_HumMag07_1		
CPXV_EleGr07_1																										
CPXV_Ger1980_EP4	0.012																									
CPXV_Ger2002_MKY	0.009	0.006																								
CPXV_Ger1971_EP1	0.009	0.012	0.011																							
CPXV_Ger2010_Raccoon	0.010	0.010	0.009	0.011																						
CPXV_Ger2010_Rat	0.011	0.004	0.005	0.012	0.010																					
CPXV_Ger2014_Cat1	0.007	0.009	0.007	0.010	0.010	0.009																				
CPXV_Ger2015_Human2	0.007	0.010	0.009	0.010	0.007	0.011	0.008																			
CPXV_HumLan08_1	0.008	0.012	0.011	0.011	0.010	0.012	0.009	0.007																		
CPXV_JagKre08_1	0.008	0.012	0.011	0.011	0.010	0.012	0.009	0.007	0.000																	
CPXV_JagKre08_2	0.008	0.012	0.011	0.011	0.010	0.012	0.009	0.007	0.000	0.000																
CPXV_MonKre08_4	0.008	0.012	0.011	0.011	0.010	0.012	0.009	0.007	0.000	0.000	0.000															
CPXV_Ama2015	0.008	0.010	0.009	0.010	0.009	0.010	0.008	0.007	0.009	0.009	0.009	0.009														
CPXV_Ger2010_Alpac	0.010	0.009	0.009	0.011	0.008	0.010	0.009	0.010	0.010	0.010	0.010	0.010	0.009													
CPXV_Ger2012_Alpac	0.006	0.010	0.009	0.010	0.008	0.010	0.007	0.003	0.007	0.007	0.007	0.007	0.006	0.008												
CPXV_Ger2014_Cat2	0.009	0.010	0.010	0.012	0.008	0.010	0.010	0.007	0.010	0.010	0.010	0.011	0.009	0.010	0.007											
CPXV_Ger2015_Cat2	0.008	0.012	0.010	0.010	0.010	0.012	0.009	0.006	0.006	0.006	0.006	0.006	0.007	0.010	0.006	0.008										
CPXV_Ger2017_Alpac2	0.007	0.011	0.009	0.010	0.009	0.011	0.008	0.006	0.007	0.007	0.007	0.007	0.006	0.008	0.004	0.008	0.004									
CPXV_Ger2017_Vole	0.005	0.011	0.009	0.010	0.009	0.011	0.006	0.006	0.007	0.007	0.007	0.007	0.006	0.008	0.005	0.008	0.005	0.004								
CPXV_BeaBer04_1	0.008	0.008	0.007	0.010	0.009	0.009	0.006	0.008	0.009	0.009	0.009	0.009	0.004	0.008	0.007	0.009	0.008	0.007	0.006							
CPXV_CatPot07_1	0.007	0.009	0.007	0.010	0.009	0.009	0.006	0.008	0.009	0.009	0.009	0.009	0.004	0.009	0.007	0.009	0.008	0.007	0.006	0.001						
CPXV_Ger2013_Alpac	0.009	0.007	0.004	0.011	0.010	0.006	0.007	0.009	0.010	0.010	0.010	0.010	0.008	0.009	0.008	0.010	0.009	0.008	0.008	0.005	0.005					
CPXV_HumBer07_1	0.008	0.009	0.008	0.010	0.009	0.009	0.006	0.008	0.009	0.009	0.009	0.009	0.005	0.009	0.007	0.009	0.008	0.007	0.006	0.002	0.001	0.006				
CPXV_HumMag07_1	0.007	0.009	0.007	0.010	0.009	0.009	0.006	0.007	0.009	0.009	0.009	0.009	0.004	0.008	0.006	0.009	0.008	0.007	0.006	0.001	0.001	0.005	0.001			

Paper III

1 **Whole genome sequencing of recombinant viruses obtained from co-**
2 **infection and superinfection of Vero cells with Modified Vaccinia virus**
3 **Ankara vectored influenza vaccine and a naturally occurring cowpox virus**

4 Diana Diaz-Cánova, Ugo Moens*, Annika Brinkmann, Andreas Nitsche and Malachy Ifeanyi
5 Okeke*

6 **Abstract:**

7 **Background:**

8 Modified vaccinia virus Ankara (MVA) has been widely tested in clinical trials as recombinant vector
9 vaccine against infectious diseases and cancers in humans and animals. However, one biosafety concern
10 about the use of MVA vectored vaccine is the potential for MVA to recombine with naturally occurring
11 orthopoxviruses in cells and hosts in which it multiplies poorly. We previously conducted co-infection
12 and superinfection experiments with MVA vectored influenza vaccine (MVA-HANP) and a feline
13 Cowpox virus (CPXV-No-F1) in Vero cells (that were semi-permissive to MVA infection) and showed
14 that recombination occurred in both co-infected and superinfected cells.

15 **Results:**

16 In this study, we selected the progeny viruses and performed genomic characterization of these viruses.
17 Some progeny viruses displayed plaque morphology distinct of that of the parental viruses. Our analysis
18 demonstrated that they had mosaic genomes of different lengths. The *HA*-transgene-expressing progeny
19 viruses contained the transgene expression cassette. Furthermore, the recombinant viruses, with a
20 genome more similar to MVA-HANP (>50%), rescued deleted and/or fragmented genes in MVA and
21 gained new host ranges genes. Our analysis also revealed that some MVA-HANP contained a partially
22 deleted transgene expression cassette and one progeny virus contained part of the transgene expression
23 cassette similar to that incomplete MVA-HANP.

24 **Conclusion:**

25 The recombination in co-infected and superinfected Vero cells resulted in recombinant viruses with
26 unpredictable biological and genetic properties as well as recovery of delete/fragmented genes in MVA
27 and transfer of the transgene into replication competent CPXV. These results are relevant to hazard
28 characterization and risk assessment of MVA vectored biologicals.

29 Background:

30 The *Orthopoxvirus* genus belongs to the *Poxviridae* family. The orthopoxviruses (OPXV) are viruses
31 with large linear double stranded DNA genome (170 to 250 kbp) [1]. OPXV can infect vertebrates and
32 insects [2]. Among the OPXV that cause human diseases, *Variola virus* (VARV), vaccinia-like virus,
33 *Cowpox virus* (CPXV) and *Monkeypox virus* (MPXV) are the most common [3–6]. VARV is the
34 causative agent of smallpox, a deadly viral disease, which was eradicated in 1980 as a result of a massive
35 vaccination campaign [7]. During the smallpox campaign, *Vaccinia virus* (VACV) was used as the
36 smallpox vaccine and several VACV strains have been developed and used in different countries, such
37 as New York City Board of Health (NYCBH) was used in the America, Tian tan in China, Ankara in
38 Turkey, and Lister and modified vaccinia virus Ankara (MVA) in Europe [8–10].

39 MVA was administrated to over 120,000 people in Germany with no reported major side effects [10–
40 13]. MVA was derived from Chorioallantois vaccinia virus Ankara (CVA) by over 570 passages in primary
41 chicken embryo fibroblasts [14]. In this process, CVA genome suffered modifications including six large
42 deletions and other mutations that lead to the reduction of the genome from 208 kbp in CVA to 170kbp
43 in MVA [15,16]. These mutations affected many genes involved in virus–host interaction and other
44 genes responsible for evasion of the host immune response [16,17].

45 As a result, MVA is unable to replicate productively in most mammalian cell lines [15,17–21]. Although
46 some mammalian cell lines have been reported as permissive to MVA, such as Baby Hamster Kidney
47 (BHK-21) cells [21,22], and semi-permissive to MVA, such as Vero cells (African green monkey kidney
48 epithelial cells) [15,20]. Recently, it was shown that a repair of the inactivated C16R/B22R in
49 conjunction with the restoration of the deleted *C12L* gene restores production infection of many human
50 cells with MVA [23]. The host range restriction of MVA is considered the major biosafety advantage for
51 its use as a vaccine vector along with its immunogenicity, its incapability to cause illness *in vivo* and its
52 safety record [24–26].

53 Since the nineties, MVA has been widely tested in clinical trials as recombinant vector for vaccination
54 against infectious diseases and cancers in both humans and animals [27,28]. Today, several MVA
55 vaccines against HIV [29,30], Ebola [31–34], respiratory syncytial virus [35], Middle East Respiratory
56 Syndrome [36], cytomegalovirus [37], influenza [38,39], tuberculosis [40] and malaria [41–43] are in

57 different phases of clinical trials. MVA-BN (JYNNEUS or Imvanex) is licensed as a vaccine against Mpox
58 and smallpox in both Europe and USA, and is currently being used for immunization against current
59 global Mpox outbreak [44,45]. Even though MVA is already deployed as a vaccine and is a promising
60 viral vector, there are still some biosafety aspects that should be considered during the biological hazard
61 characterization of MVA and recombinant MVA (rMVA). One is the potential for MVA or rMVA to
62 recombine with naturally occurring OPXV, which could lead to the rescue of interrupted or deleted genes
63 in MVA or to transfer of the transgene to multiplication competent OPXV [46]. Hence, the
64 recombination could result in the emergence of novel mosaic viruses with atypical virulence and host
65 range characteristics. Recombination is not a rare event between OPXV. Natural occurring
66 recombination events between OPXV have been reported [47,48,57,49–56]. However, the possibility of
67 recombination was considered negligible due to the low likelihood of co-localization of the viruses in the
68 same cell, poor or no multiplication of MVA in many mammalian cells and superinfection exclusion
69 [58,59].

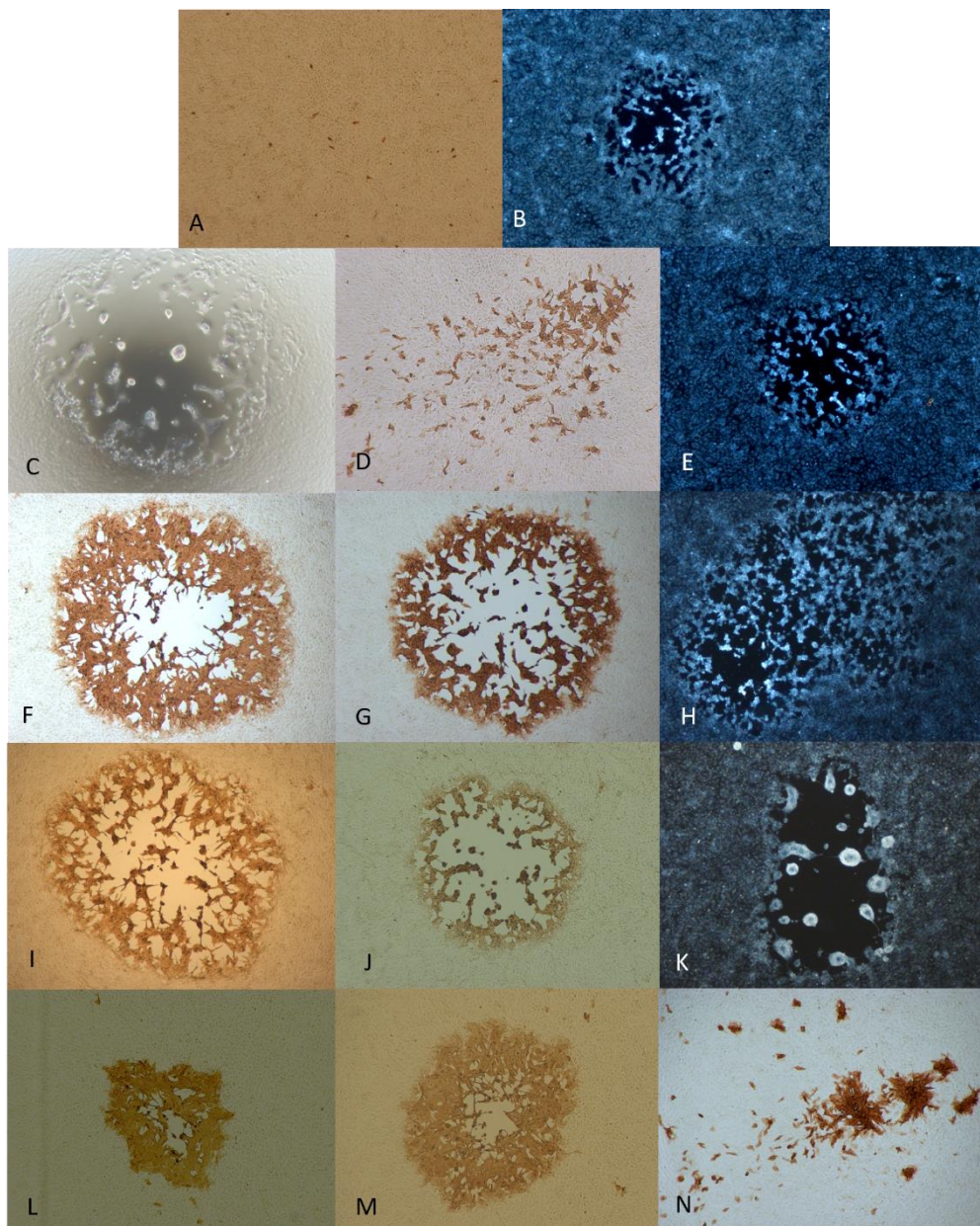
70 The circulation of naturally zoonotic OPXV, such as CPXV and MPXV, has increased in recent years [6].
71 Several cases of human cowpox infections caused by infected animals have been reported in Europe
72 [57,60–68] and the global outbreak of human Mpox has been reported in 110 countries [69] followed by
73 increased vaccination with MVA. Therefore, the possibility of co-localization and recombination could
74 have increased. We highlight that there is a need to better understand the mechanism of recombination
75 and possible public health threat of recombination after co- and superinfection of two poxviruses.

76 In a previous study, we have demonstrated recombination in Vero cells co-infected and superinfected
77 with recombinant MVA expressing the influenza virus *haemagglutinin (HA)* and *nucleoprotein (NP)*
78 proteins (MVA-HANP) and feline CPXV [27]. In the present study, we sequenced the genome of progeny
79 viruses produced in semipermissive Vero cells co-infected and superinfected with MVA-HANP and
80 feline CPXV-No-F1, conducted genomic characterization of parental and progeny viruses and mapped
81 genome-wide recombination events in the hybrid progeny viruses.

82 Results:

83 Plaque phenotype formed by progeny viruses after co-infected and superinfected Vero
84 cells

85 The plaque phenotype caused by progeny viruses and the parental viruses were examined in Vero cells.
86 The parental CPXV-No-F1 forms medium, semilytic plaques. Whereas MVA-HANP do not produce
87 plaques; however, some Vero cells have positive immunostaining for the HA transgene as a result of
88 MVA-HANP limited infection and expression of its HA transgene (Fig. 1).



89

90 **Fig. 1.** Plaque phenotypes of the parental viruses (MVA-HANP and CPXV-No-F1) and the progeny viruses obtained from either
91 co-infection or superinfection with MVA-HANP and CPXV-No-F1 in Vero cells. **A**, The parental virus MVA-HANP. **B**, The parental
92 virus CPXV-No-F1. **C**, Recombinant virus R1 from co-infection MVA-HANP and CPXV-No-F1. **D**, **E** Recombinant virus R2 and
93 R3 from superinfection 1 (primary infection with CPXV-No-F1 and secondary infection with MVA-HANP at 4h post primary
94 infection, ppi). **F-H** Recombinant virus R4, R5 and R6 from superinfection 2 (primary infection with MVA-HANP and secondary
95 infection with CPXV-No-F1 at 4h ppi). **I-M** Recombinant virus R7, R8, R9, R10 and R11 from superinfection 3 (primary infection
96 with CPXV-No-F1 and secondary infection with MVA-HANP at 6h ppi). **N** Recombinant virus R12 from superinfection 4 (primary
97 infection with MVA-HANP and secondary infection with CPXV-No-F1 at 6h ppi).

98 Different plaques phenotypes and transgene-expressing plaques were observed in co-infected Vero cells.
99 One progeny virus was isolated from co-infected Vero cells, which was named R1. The plaque of this
100 recombinant virus is large, lytic, and characterized by syncytium formation and cell lysis (Fig. 1C). In
101 addition, this recombinant forms HA transgene negative plaques.

102 Similarly, different plaque phenotypes were observed in superinfected Vero cells regardless the virus
103 strain used for the primary infection and the timing (4 and 6 hours ppi). Additionally, both the
104 transgene-expressing and non-transgene-expressing progeny viruses display different plaque
105 phenotypes (Fig. 1D-N). Two, three, five and one viruses were selected from superinfection 1,
106 superinfection 2, superinfection 3 and superinfection 4, respectively (see methods for details). We
107 referred to these progeny viruses as R2, R3, R4, R5, R6, R7, R8, R9, R10, R11 and R12.

108 The progeny virus R2 from the superinfection 1 expresses the HA transgene and produced small and
109 non-lytic plaques with secondary spread (comet formation). Whereas progeny virus R3 from the same
110 experiment is transgene negative and forms medium and lytic plaques (Fig. 1E). The plaques of the
111 progeny virus R4 and R5 from superinfection 2 are large, lytic and transgene positive. Unlike progeny
112 virus R4 and R5, the progeny virus R6 is transgene negative and forms medium and semilytic plaques
113 with extensive secondary spread (Fig. 1F-H).

114 The progeny virus R7, R8 and R9 from superinfection 3 form large and lytic plaques (Fig. 1I-K).
115 However, compared to the progeny virus R7 and R8, R9 do not express the transgene and forms syncytia.
116 The other two progeny viruses were chosen from superinfection 3, progeny virus R10 and R11. Both
117 progeny viruses express the *HA* transgene and form semilytic plaques (Fig. 1L-M). However, the size of
118 their plaques is different. The progeny virus R11 produces large plaques, whereas the progeny virus R10

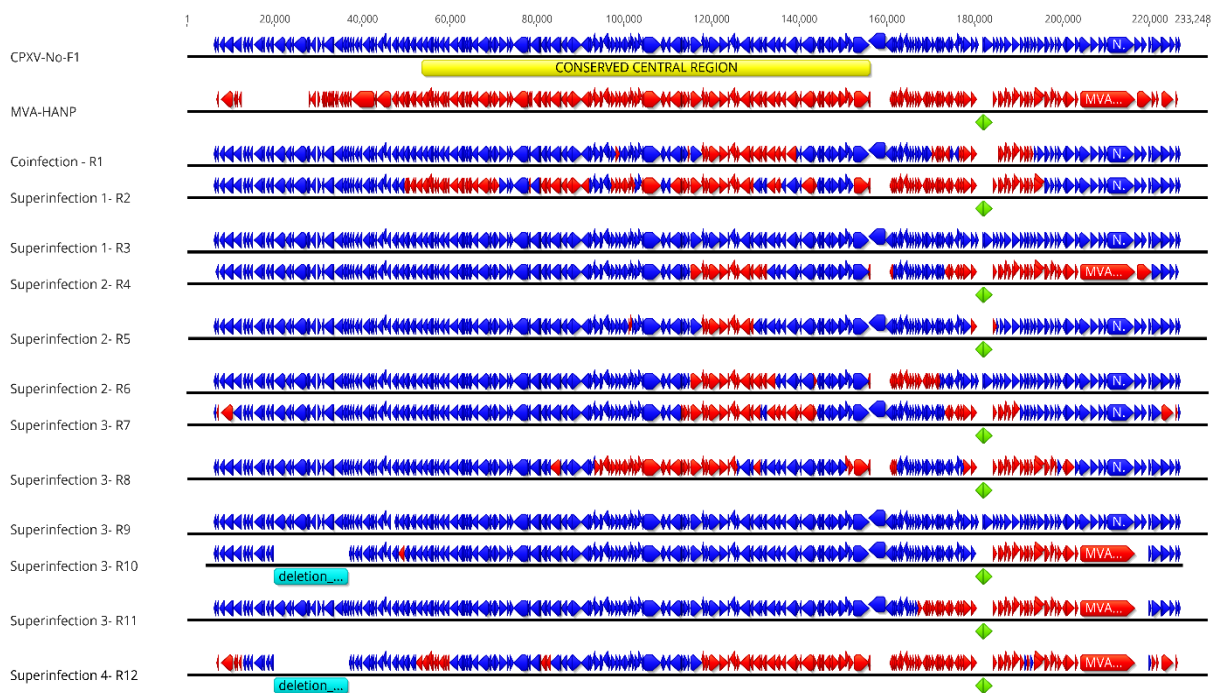
119 generates medium plaques. The progeny virus R12 from superinfection 4 expresses the *HA* transgene
120 and displays small and non-lytic plaques with comet formation (Fig. 1N).

121

122 Different genome size of the progeny viruses

123 The complete genomes of thirteen progeny viruses and the parental virus MVA-HANP were sequenced,
124 assembled, and annotated (Fig. 2). The assembled genome of the parental MVA-HANP has a length of
125 181,712 bp, with inverted terminal repeats (ITR) of 9.8 kbp. Genome annotation predicted 199 coding
126 sequences (CDS) in MVA-HANP genome (Table S1). The sequencing analysis of the parental MVA-
127 HANP showed that the double expression cassette containing the influenza *HA* and *NP* transgenes was
128 inserted in *A51R/A55R* hybrid gene. However, the assembly of MVA-HANP showed that there are two
129 populations of MVA-HANP, one with the complete double expression cassette (181,712 bp) and other
130 with an incomplete double expression cassette (178,579 bp). The small part of *NP* transgene (~6%),
131 whole *HA* transgene and downstream MVA-HANP flanking sequence (containing *VACV-Cop A56R*
132 gene) are deleted in the latter. It only contains major part of the *NP* transgene (94%) and the upstream
133 flanking MVA sequence (Fig. S1).

134



135 **Fig. 2.** Genome map of the parental viruses (CPXV-No-F1 and MVA-HANP) and the progeny viruses. The progeny viruses were
136 produced in Vero cells either co-infected or superinfected with CPXV-NoH1 and MVA-HANP. Superinfection 1, primary infection
137 with CPXV-No-F1 and secondary infection with MVA-HANP at 4h post primary infection (ppi); Superinfection 2, primary
138 infection with MVA-HANP and secondary infection with CPXV-No-F1 at 4h ppi; Superinfection 3, primary infection with CPXV-
139 No-F1 and secondary infection with MVA-HANP at 6h ppi; Superinfection 4, primary infection with MVA-HANP and secondary
140 infection with CPXV-No-F1 at 6h ppi. Blue blocks represent the coding sequences (CDS) from CPXV-No-F1. Red blocks represent
141 CDS from MVA-HANP. Green blocks represent the influenza virus *hemagglutinin (HA)* and *nucleoprotein (NP)* transgenes.
142 Turquoise blocks represent deleted regions in the progeny viruses. Yellow block represents the conserved central region (*VACV-
143 Cop F4L – VACV-Cop A24R*) in orthopoxvirus genomes.

144

145 The genome size and the number of predicted CDS of the parental and progeny virus genomes are shown
146 in the Table 1 and Table S2. The length of progeny virus genomes was not uniform, ranging from 176.9
147 kbp to 221 kbp. Three progeny viruses (R3, R5 and R9) have similar genome size to that of the parental
148 CPXV-No-F1 and one recombinant virus (R12) possesses a smaller genome than that of the parental
149 MVA-HANP (Table 1). No progeny virus has a bigger genome than the parental viruses. The ITR of the
150 progeny viruses ranged from 4.7 kbp to 8.3 kbp.

151

152 **Table 1. Genome size and number of predicted CDS of CPXV-No-F1, MVA-HANP and the progeny viruses**

Experiment		Virus	Genome (bp)	Inverted terminal repeat (bp)	CDS	Expressing HA transgene
		MVA-HANP	181,712	9882	199	Yes
		CPXV-No-F1	221,334	7929	217	-
Co-infection	CPXV-NO-F1/ MVA-HANP	R1	218,322	8219	216	No
Superinfection	Superinfection 1 (CPXV-NO-F1/ MVA-HANP 4h)	R2	215,275	8251	220	Yes
		R3	221,213	7929	217	No
		R4	199,702	7045	210	Yes
	Superinfection 2 (MVA-HANP/ CPXV-NO-F1-4h)	R5	220,926	7813	214	Yes
		R6	218,106	8365	217	No
		R7	216,643	5908	213	Yes
	Superinfection 3 (CPXV-NO-F1/ MVA-HANP-6h)	R8	216,086	8339	218	Yes
		R9	221,198	7853	217	No
		R10	185,955	6959	198	Yes
		R11	204,628	8054	212	Yes
	Superinfection 4 (MVA-HANP/ CPXV-NO-F1-6h)	R12	176,918	4694	197	Yes

153

154 The number of predicted CDS in the genomes of the progeny viruses varied from 197 to 220 CDS (Table
155 1). The progeny virus genomes included more CDS than the parental MVA-HANP, with exception of the
156 recombinant viruses R10 and R12. Furthermore, there were three recombinant viruses (R3, R6 and R9)
157 that contained the same number of predicted CDS as the parental CPXV-No-F1.

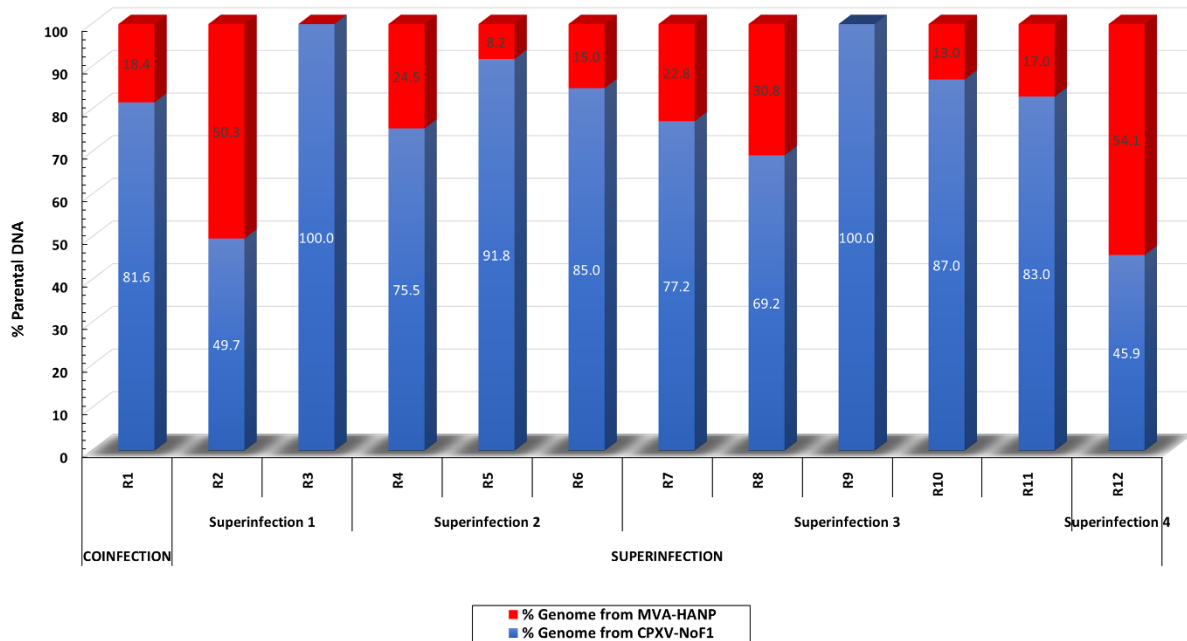
158

159 Mosaic genome of the progeny viruses

160 In order to localize the possible recombination events in the progeny virus, the thirteen progeny viruses
161 were examined for recombination. The analysis confirmed recombination across the genome of twelve
162 progeny viruses (Table S3). Only one progeny virus, R9 from superinfection 3, do not show any
163 recombination event based on the recombination analysis. The location of recombinant events in the
164 genome of the progeny viruses are aleatory, there are no recombination distribution pattern along their
165 genomes. The recombination events occur both in the conserved central region (*VACV-Cop F4L* to
166 *VACV-Cop A24L*) and the variable regions, including ITR (Table S3, Fig. 2). The number of recombinant
167 breakpoints distribute in the central region varied from 0 to 16, whereas the number of breakpoints in
168 the variable regions ranges from 1 to 6. Curiously, no recombination event is detected in the genomic
169 region from *VACV-Cop N2L* gene (*CPXV-Br010*) to *VACV-Cop K3L* gene (*CPXV-Br034*) in any of the
170 progeny viruses.

171 The genomes of the progeny viruses are a mosaic of the two parental strains (CPXV-No-F1 and MVA-
172 HANP), except for progeny virus R9. The lengths of the DNA segments exchanged between the parental
173 viruses range from approximately 200 bp to 36 kbp (Fig. 2). The percentage of DNA derived from the
174 parental strains in the progeny viruses is variable (Fig. 3). The majority of the recombinant progeny
175 viruses have more DNA from the parental CPXV-No-F1 than that from the parental MVA-HANP;
176 nevertheless, some of them contain the *HA* and *NP* transgenes. Only two recombinant progeny viruses,
177 R2 from superinfection 1 and R12 from superinfection 4, contain more DNA from the parental MVA-
178 HANP (Fig. 3, Table S4).

179



180

181 **Fig. 3.** Percentage of DNA derived from the parental viruses (CPXV-No-F1 and MVA-HANP) in the progeny viruses. The progeny
 182 viruses were produced in Vero cells co-infected and superinfected with CPXV-NoH1 and MVA-HANP. Superinfection 1, primary
 183 infection with CPXV-No-F1 and secondary infection with MVA-HANP at 4h post primary infection (ppi); Superinfection 2,
 184 primary infection with MVA-HANP and secondary infection with CPXV-No-F1 at 4h ppi; Superinfection 3, primary infection with
 185 CPXV-No-F1 and secondary infection with MVA-HANP at 6h ppi; Superinfection 4, primary infection with MVA-HANP and
 186 secondary infection with CPXV-No-F1 at 6h ppi. Blue blocks represent the coding sequences (CDS) from CPXV-No-F1.

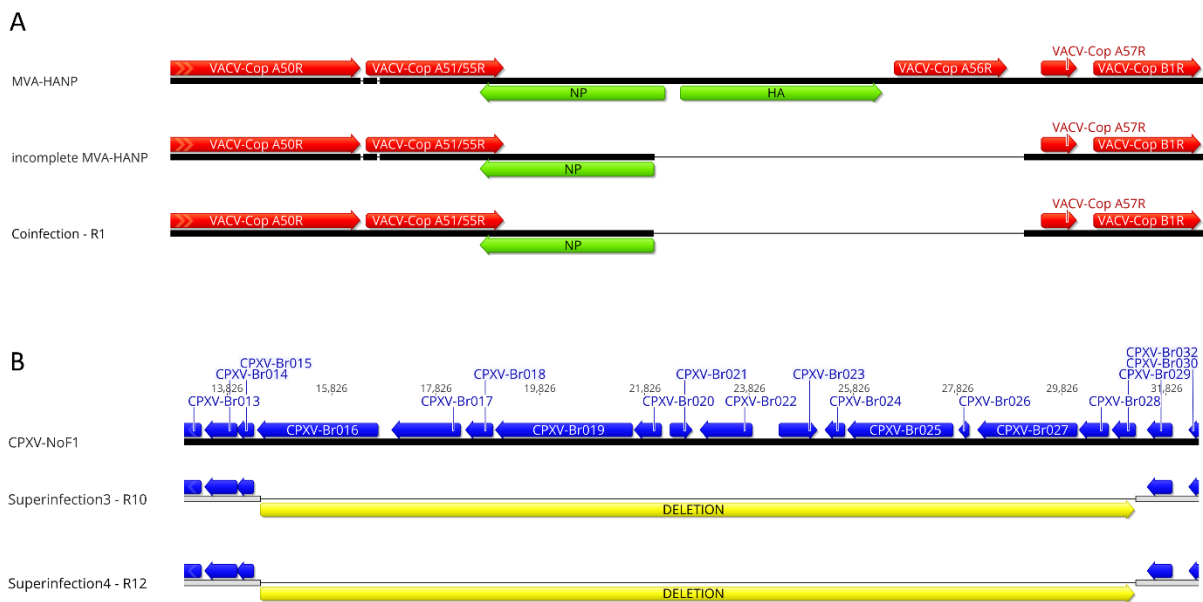
187

188 The influenza *HA* and *NP* transgenes were inserted in the same position in many of the
 189 progeny viruses, but other genetic changes outside of recombination were present

190 The parental MVA-HANP harbored a double expression cassette containing the influenza *HA* and *NP*
 191 transgenes. Several progeny viruses from both co-infected and superinfected Vero cells expressed the
 192 *HA* transgene in Vero cells. The sequencing analysis of the seven *HA* transgene expressing recombinant
 193 viruses (R2, R4, R5, R7, R8, R10, R11 and R12) confirmed that these viruses contain an intact double
 194 expression cassette and its flanking sequences. The *HA-NP* transgene sequences are identical to those
 195 of the parental MVA-HANP. The intergenic region between the *HA* and *NP* transgenes of MVA-HANP
 196 is only identical to that of recombinant virus R2. Whereas the other recombinant viruses (R4, R5, R7,
 197 R8, R11 and R12) have a single nucleotide deletion in that region. Moreover, the length of MVA

198 recombinant region containing the *HA-NP* transgenes in the progeny virus genomes ranges from 5.4
 199 kbp to 68.5 kbp.

200 In co-infected and superinfected Vero cells, there are non-*HA*-transgene expressing progeny viruses that
 201 formed plaques distinct from that of the parental viruses. The sequencing analysis of non-*HA*-transgene
 202 expressing recombinant viruses (R1, R3, R6 and R9) revealed that the *HA-NP* insert is absent in the
 203 recombinant viruses R3, R6 and R9, but not in the recombinant virus R1. Interestingly, the latter (R1)
 204 contains part of the double expression cassette. It comprises major part of the *NP* transgene (94%) and
 205 the upstream flanking MVA sequence (Fig. 4A) similar to the incomplete MVA-HANP (178,579 bp). The
 206 presence of the incomplete MVA-HANP population with a partial deleted double cassette expression
 207 was corroborated by the occurrence of recombinant progeny virus R1.



208
 209 **Fig. 4.** Comparison of the progeny viruses with the parental virus. **A**, Comparison of the recombinant region of progeny virus R1
 210 with MVA-HANP and incomplete MVA-HANP. The progeny virus R1 was produced in Vero cells co-infected with CPXV-No-F1
 211 and MVA-HANP. Green blocks represent the influenza virus *hemagglutinin* (*HA*) and *nucleoprotein* (*NP*) transgenes. Red blocks
 212 represent the coding sequences (CDS) from MVA-HANP. **B**, Deletion in progeny viruses R10 and R12. The progeny virus R10 was
 213 produced in Vero cells infected with CPXV-No-F1 and superinfected with MVA-HANP at 6h post primary infection (ppi)
 214 (superinfection 3). The progeny virus R12 was produced in Vero cells infected with MVA-HANP and superinfected with CPXV-
 215 No-F1 at 6h ppi (superinfection 4). Yellow blocks represent the deleted sequence in the progeny viruses.

216

217 In addition to the recombination events, our analyses revealed that the twelve progeny genomes
218 underwent other genetic variations, such as deletions. Although most of them are located outside of the
219 CDS regions (Table S5). A large deletion of 16,761 bp is found close to the left terminal genomic region
220 of recombinant viruses R10 and R12 from superinfection 3 and 4, respectively (Fig. 4B). The deleted
221 sequence comprises from *CXPV-BR016* gene to *CPXV-BR029* gene. Most of these genes encode proteins
222 involve in host range. Additional small deletions and insertions are also detected within these two
223 progeny genomes (Table S5). For instance, the *VACV-Cop N2L* gene of recombinant virus R10 has
224 suffered an internal deletion of 27 bp.

225 The other recombinant viruses also contain deletions, insertions and/or non-synonymous single-
226 nucleotide mutations (nsSNMs). We found two nsSNMs in *VACV-Cop N2L* and *VACV-Cop K2L* genes
227 of the progeny virus R9, that did not undergo recombination (Table S5). The nsSNM in the *VACV-Cop*
228 *K2L* gene resulted in the introduction of a premature stop codon and consequently the truncation of the
229 protein.

230

231 [Rescue of loss genes and fragment/disrupted genes:](#)

232 As mentioned before there are two recombinant progeny viruses with >50% of their genome derived
233 from MVA-HANP. These two recombinant viruses rescued disrupted/deleted genes and, furthermore,
234 gained genes that were absence in MVA-HANP. The recombinant virus R12 rescued *CPXV-Br009*,
235 *CPXV-Br032*, *CPXV-Br033*, *CPXV-Br034*, *CPXV-Br035* and *CPXV-Br036* genes (homologs to *VACV-*
236 *Cop C16L*, *C5L*, *C4L*, *C3L*, *C2L* and *C1L* genes, respectively) that were lost in MVA during the attenuation
237 process. Additionally, four fragmented/disrupted genes, *CPXV-Br037*, *CPXv-Br039*, *CPXV-Br043* and
238 *CPXV-Br078* (homologs to *VACV-Cop N1L*, *K1L*, *K5L* and *O1L* genes, respectively), were rescued in the
239 recombinant virus R12 by recombination. Although *O1L* gene is also fragmented in *VACV-CVA*.
240 Moreover, the recombinant virus gained seven more genes that were absent in MVA and *VACV-CVA*
241 strains: *CPXV-Br010*, *CPXV-Br011*, *CPXV-Br012*, *CPXV-Br013*, *CPXV-Br014*, *CXPV-Br015* genes and
242 one gene (*No-F1-009* gene) that encodes BTB Kelch-domain containing protein. Compared to
243 recombinant virus R12, the recombinant virus R1 gained six additional genes (*CPXV-Br002*, *CPXV-*
244 *Br016*, *CPXV-Br017*, *CPXV-Br018*, *CPXV-Br19* and *CPXV-Br020* genes) by recombination.

245 Furthermore, the recombination events in recombinant virus R1 rescued of deleted genes: *CPXV-Bro05*,
246 *CPXV-Bro09*, *CPXV-Bro32*, *CPXV-Bro33*, *CPXV-Bro34*, *CPXV-Bro35*, *CPXV-Bro36*, *CPXV-Bro39*,
247 *CPXV-Bro40*, *CPXV-Br213*, *CPXV-Br217* and *CPXV-Br226* genes (homologs to *VACV-Cop B28R*, *C16L*,
248 *C5L*, *C4L*, *C3L*, *C2L*, *C1L*, *M1L*, *M2L*, *B20R*, *C12L* and *C22L* genes). Additionally, twelve
249 fragmented/disrupted genes in MVA were also rescued in this recombinant virus (*CPXV-Bro03*, *CPXV-*
250 *Bro06*, *CPXV-Bro08*, *CPXV-Bro23*, *CPXV-025*, *CPXV-Bro27*, *CPXV-Bro41*, *CPXv-Bro78*, *CPXV-*
251 *Br207*, *CPXV-Br212*, *CXPV-Br223* and *CPXV-Br227* genes).

252

253 Discussion:

254 In our previous study, we performed co-infection and superinfection experiments with a naturally
255 circulating Fennoscandian CPXV-No-F1 and MVA carrying an influenza *HA* and *NP* transgene in semi-
256 permissive Vero cells. We have showed that recombination between these viruses occurred in both co-
257 infected and superinfected Vero cells. Although the likelihood of recombination in co-infected and
258 superinfected Vero cells was always considered low because (1) Vero cells are semi-permissive to MVA
259 [15,20] and (2) mechanisms as superinfection exclusion prevent the superinfection of the infected cell
260 with a second virus [58,59]. A previous study has reported recombination between human CPXV
261 (hCPXV) and MVA-HANP in co-infected BHK-21 cells [70]. Compared to Vero cells, those cells are fully
262 permissive to MVA-HANP and CPXV [20]. Viral DNA replication in non-permissive cells to MVA
263 infection is not blocked [71], therefore the likelihood of recombination increases since recombination
264 and viral DNA replication are connected [72,73]. In our superinfection experiments, the time gap
265 between the first and the second infection was 4h and 6h ppi to ensure the establishment of primary
266 infection since it has been reported that VACV DNA synthesis in HeLa cells starts 2 hours postinfection
267 [74]. Although the viral DNA synthesis of the primary virus is not needed for superinfection exclusion
268 [59,75]. A study demonstrated the time of superinfection of 4 and 6 hours after primary infection with
269 VACV produced 90% and 99% exclusion of superinfecting virus, respectively [75].

270

271 The recombination breakpoints along the genome of the recombinant viruses were found both in the
272 conserved central region and the variable regions. In orthopoxviral genomes the recombination events
273 have occurred mainly in terminal regions, although it has been reported in the central region of the
274 genome [47,48,57,49–56]. Interestingly, the only genomic region without any recombination event
275 («coldspot of recombination») was between *CXPV-Br010* to *CPXV-Br043* gene. Although this region in
276 two recombinant viruses had suffered a large deletion (from *CPXV-Br016* to *CPXV-Br029* gene).

277 The recombination between MVA-HANP and CPXV-NoH1 generated mosaic genomes containing
278 genomic material from both parental viruses. Additionally, DNA proportion of the parental genomes in
279 the recombinant viruses was not uniform. Most of them had more DNA from the parental CPXV-No-F1.
280 Several progeny viruses displayed plaque morphologies different from that of the parental viruses. This
281 was also observed in the progeny viruses arising from superinfected Vero cells with MVA-HANP and
282 CPXV-No-F1, using 2h ppi [27]. Similarly, the recombinant viruses from BHK-21 cells co-infected with
283 MVA-HANP and hCPXV displayed non-parental and parental traits with respect to plaque phenotype,
284 in vitro host range and cytopathogenicity [22,76].

285 Our recombinant viruses showed different plaque phenotypes. It has been reported that the proteins
286 encoded by *VACV-Cop F5L*, *F11L*, *F12L*, *F13L*, *A33R*, *A34R*, *A36R*, *A56R*, and *B5R* genes may be
287 involved in determining the plaque morphology [77–82]. Some of these genes were fragmented (i.e.
288 *VACV-Cop F5L* and *VACV-Cop F11L* gene) or encompassed some deletions (i.e. *VACV-Cop A36R*) in
289 MVA [16]. Two of our recombinant viruses (R2 and R12) formed small and non-lytic plaques. These
290 recombinant viruses contained the defective *VACV-Cop F5L*, *F11L* and *VACV-Cop A36R* genes from
291 MVA-HANP. F5L and F11L proteins are required to form normal plaques. They increase the plaque size
292 and only F5L protein promotes the formation of central plaque clearing [77–79]. The deletion of the
293 gene encoding A36R protein decreased the plaque size [83]. Additionally, these two recombinant viruses
294 displayed plaques with comet formation, similar to those of the recombinant virus R6. The genes
295 associated to the formation of comet-shaped plaques are *VACV-Cop A33R*, *A34R* and *B5R* [80,81,84].
296 Those recombinant viruses contained *VACV-Cop A33R*, *A34R* and *B5R* genes from MVA-HANP, except
297 for recombinant virus R6 that contained *VACV-Cop B5R* gene derived from CPXV-No-F1. Other
298 recombinant viruses that only have *VACV-Cop B5R* gene from MVA-HANP, as well as *VACV-Cop A33R*
299 and *VACV-Cop A34R* genes from CPXV-No-F1, did not show plaques with comet formation.

300 Two of the progeny viruses produced syncytial plaques, R1 and R9. The progeny virus R1, compared to
301 other progeny viruses, did not undergo recombination. However, this virus produces a truncated K2L
302 protein due to the introduction of an earlier stop codon in the *VACV-Cop K2L* gene as a result of a SNP.
303 It has been reported that the lack of K2L protein causes the fusion of infected cells [85–87]. This protein
304 forms a complex with A56 protein, and the heterodimer prevents syncytia formation [88] [85–87,89].
305 The *VACV-Cop A56R* gene of R9 was intact; in contrast, this gene was deleted in the recombinant virus
306 R1.

307 Several progeny viruses were transgene positive. The proportion of HA-expressing recombinant viruses
308 in the co-infected and superinfected Vero cells were reported elsewhere [27]. The HA-expressing
309 progeny viruses had the complete double expression cassette; however, the non-HA-expressing progeny
310 virus R1 retained the *NP* transgene (96%), but not the *HA* transgene similar to the incomplete MVA-
311 HANP. It seems that this progeny virus was the result of the recombination of CPXV-No-F1 and an
312 incomplete MVA-HANP. The instability of the transgene in MVA-HANP as well as in recombinant
313 progeny viruses from BHK-21 cells co-infected with MVA-HANP and CPXV-No-H1 has been previously
314 reported. MVA-HANP and the recombinant viruses were genetically unstable and lost the transgene
315 during cell culture passages [70,76]. The instability transgene is one of the major concerns in the
316 production of viral vector vaccines because any mutation in the expression cassette could lead to
317 unpredicted characteristics. Furthermore, the transgene is used as a tag to monitor the expression
318 cassette in the recombinant progeny viruses. Therefore, the loss or partial loss of the transgene hinders
319 the tracking of released recombinant progeny viruses. One possible solution to avoid transgene
320 instability is the insertion of the transgene(s) in the “coldspot of recombination” found in the
321 recombinant progeny viruses.

322 Another concern about the use of MVA-HANP is to transfer the transgene into a multiplication
323 competent OPXV (Goosens, 2013). In this study, we have shown that the transgenes were transferred to
324 the recombinant viruses with a genome mainly derived from CPXV-No-F1. Furthermore, the
325 recombinant progeny viruses with the transgene displayed new and non-parental plaque phenotypes. A
326 biological characterization of the recombinant viruses is required to investigate their host range, cell
327 tropism, transmissibility and virulence.

328 Compared to CVA, MVA had lost several genes and 25 genes were fragmented and/or suffered mutations
329 during the attenuation process, such as the host range genes *VACV-Cop K1L* and *C12L* [16,18]. The
330 recombination of MVA with a multiplication competent OPXV may lead to the restoration of
331 disrupted/deleted genes in MVA. In this study, we observed that two of our recombinant viruses, that
332 had >50% DNA from MVA-HANP, rescued deleted and fragment host range genes, such *CXPV-Bro09*
333 (*VACV-Cop C16L*) and *CPXV-Bro41* (*VACV-cop K1L*) [23,90]. Even these recombinant viruses gained
334 new host range genes, *crmB/CPXV-Br226* (*VACV-Cop B28R*) and *vCD30/CPXV015* [90,91]. The
335 recombination of MVA with a wild OPXV was considered negligent since smallpox was eradicated.
336 However, the circulation of the naturally OPXV [3,57,68,92–94] and the emergence of new OPVX in
337 the last few years [49,95,96], have increased the likelihood of recombination between MVA and a
338 naturally replication competent OPXV during co-infection or superinfection of the same cell or host. For
339 instance, the ongoing global outbreak of Mpox and prophylactic or post-exposure vaccination with
340 MVA-BN provide a good scenario for co-infection/superinfection and subsequent recombination
341 between MVA and MPXV. In addition, several orthopoxvirus outbreaks in humans have been reported
342 worldwide [6,97]. Our study has shown that insertion of the transgene into the genome of a co-infecting
343 or superinfecting OPXV was specific but recombination in other parts of the genome were nonspecific
344 and unpredictable. In addition, some of the progeny viruses lost some or part of the transgenic cassette
345 even when they were inserted into the intended genomic regions, and the loss of transgene may preclude
346 tracking of recombinant viruses. To evaluate the potential for recombination and robust monitoring of
347 potential recombinant viruses, hazard characterization and risk assessment of MVA vectored biologicals
348 should include genome wide characterization.

349 Finally, it is important to highlight the limitations of this study. First, the high moi used in our co-
350 infection and superinfection experiments may not be achievable under natural co-
351 infection/superinfection. Second, our experiments were done in cell cultures and an extrapolation
352 cannot be made to animals with an intact immune system. Thirdly, our use of selection markers like
353 plaque phenotype, expression or non-expression of the transgene may have introduced a selection bias
354 and thus underestimate the pattern and diversity of recombination between co-infecting or
355 superinfecting viruses. Future studies will address these limitations through metagenomic analysis of
356 cell cultures and animals co-infected or superinfected with MVA and CPXV under conditions that better
357 reflects natural scenario.

358

359 Conclusions

360 The superinfection exclusion and low permissivity of Vero cells to MVA did not prevent the
361 recombination between MVA vectored vaccines and the naturally circulating CPXV during
362 superinfection of cells. The recombination between MVA-HANP and the naturally circulating CPXV-
363 No-F1 in co-infected and superinfected Vero cells lead to the generation of progeny viruses with novel
364 biological and genetic characteristic as well as the regaining of delete/fragmented genes in MVA-HANP
365 and transfer of the transgene into CPXV.

366

367

368 METHODS:

369 **Co-infection and superinfection of Vero cells:**

370 The co-infection and superinfection experiments with MVA vectored influenza vaccine (MVA-HANP)
371 and the naturally circulating Fennoscandian feline cowpox strain (CPXV-No-F1) were performed in Vero
372 cells as previously described [27]. The origin of the cowpox strain was described elsewhere [68]. MVA-
373 HANP was kindly provided by Dr. Bernard Moss, National Institutes of Health, USA. MVA-HANP
374 contains the influenza virus *HA* (A/PR/8/34) and *NP* gene inserts [98]. MVA-HANP was propagated
375 in BHK-21 cells (ATCC CCL-10). CPXV-No-F1 and recombinant viruses were cultured on Vero cells
376 (ATCC CCL-81). Vero cells and BHK-21 cells were propagated in minimal essential medium (MEM)
377 supplemented with 10% fetal bovine serum (FBS). The cell cultures were maintained in a humidified 5%
378 CO₂ atmosphere at 37 °C.

379 Vero cells are semi-permissive to MVA-HANP [15,20] and permissive to CPXV [76]. Vero cells were co-
380 infected with MVA-HANP and CPXV-No-F1 at a multiplicity of infection (MOI) of 5 infection units per
381 cell for each virus strain. Superinfection with CPXV and MVA-HANP in Vero cells was performed in four
382 experiments. Vero cells were infected with CPXV-No-F1 at a MOI of 5. The infected Vero cells were
383 superinfected with MVA-HANP at same MOI (of 5) after 4-hours (superinfection 1) or 6-hours ppi
384 (superinfection 3). The cells were incubated for 72 hours at 37°C. The same procedure was repeated for
385 superinfection 2 and 4, but the primary infection was with MVA-HANP and the secondary infection with

386 CPXV-No-F1 after 4-hours (superinfection 2) or 6-hours ppi (superinfection 4). After 72 hours ppi, the
387 cells were harvested, freeze-thawed three times and sonicated.

388 **Selection of recombinant viruses, plaque purification and immunostaining:**

389 Progeny viruses were identified and selected in Vero Cells. The selection was based on (1) the expression
390 of the Influenza virus HA protein and (2) plaque phenotype. The progeny viruses that formed different
391 plaque phenotype from the parental viruses were selected. The sonicated cells suspensions were
392 inoculated on Vero cells and the progeny viruses were plaque-purified several times before plaque
393 amplification. The stock of the progeny viruses was prepared from plaque purified viruses. The progeny
394 viruses carrying the influenza virus HA protein were detected by immunostaining, as described
395 previously [22]. Moreover, the plaque phenotype of the parental viruses was also examined in Vero cells.

396 **Genome sequencing, genome assembly and annotation:**

397 Viral DNA of the plaque purified progeny viruses and the parental virus MVA-HANP was isolated using
398 QIAGEN Genomic-tip 100/G and QIAGEN Genomic DNA Buffer Set, following the manufacturer's
399 instructions (Qiagen, Hilden, Germany). The genomes were sequenced with Illumina MiSeq (Illumina
400 Inc., San Diego, CA, United States) using reagent kit v3 with 2 × 300 bp paired-end reads and Oxford
401 Nanopore Technology GridION (ONT; Oxford, United Kingdom), as previously described [57].
402 Nanopore and Illumina library preparation have been described elsewhere [57]. Nanopore sequencing
403 was performed at the Genomics Support Centre Tromsø at UiT—The Arctic University of Norway and
404 Illumina sequencing was conducted by the Norwegian Sequencing Centre, Oslo.

405 The genome assembly was performed using SPAdes v3.15.3 [99]. For the assembly of MVA-HANP, the
406 parameter trusted-contigs and the reference genome MVA were used. The viral genomes were annotated
407 using the Genome Annotation Transfer Utility (GATU) [100], as previously reported [57]. Vaccinia virus
408 Copenhagen (VACV-Cop), Choriollantois vaccinia virus Ankara (CVA) and MVA were used as reference
409 genomes for the genome annotation of MVA-HANP. VACV strains were retrieved from the Viral
410 Orthologous Clusters (VOCs) database [101]. The parental viruses, CPXV-No-F1
411 (Genbank accession number OP125538) and MVA-HANP, were used as reference genomes for the
412 genome annotation of the progeny viruses. The complete genome of the parental CPXV-No-F1 has been
413 published elsewhere [68].

414 **Recombination analysis:**

415 The progeny viral genomes were analyzed for possible recombination events using recombination
416 detection program 4 (RPD4) [102] and SimPlot v3.5.1 [103] as described previously [57]. The progeny
417 virus genomes were aligned to the parental viruses and other CPXV strains (CPXV-Br and CPXV-Gri)
418 with MAFFT v1.4.0 [104] implemented in Geneious Prime 2020.2.4. The CPXV strains were retrieved
419 from the Viral Orthologous Clusters (VOCs) database [101]. The gaps were not removed from the
420 alignments.

421 The recombination events identified by 5 of 7 methods (RDP [105], GENECONV [106], Bootscan [107],
422 MaxChi [108], Chimaera [109], SiScan [110], and 3Seq [111]) with significant p-values ($p \leq 0.01$) were
423 considered potential recombinant events. Furthermore, the breakpoints in the recombinant genomes
424 were checked manually in the alignments in case both programs could not detect the recombination
425 event.

426

427 **Availability of data and materials**

428 The original contributions presented in the study are publicly available. This data can be found
429 here: <https://www.ncbi.nlm.nih.gov/genbank/>, XX.

430

431 **Funding**

432 This study was supported by the University of Tromsø, the Arctic University of Norway (project
433 A212100108) and the National Graduate School in Infection Biology and Antimicrobials (grant no.
434 249062). Article processing charge was paid UiT - The Arctic University of Norway.

435

436 **Author information**

437 **Molecular Inflammation Research Group, Department of Medical Biology, UiT - The**
438 **Arctic University of Norway, Tromsø, Norway**

439 Diana Diaz-Cánova & Ugo Moens

440 **Highly Pathogenic Viruses, Centre for Biological Threats and Special Pathogens, WHO**
441 **Reference Laboratory for SARS-CoV-2 and WHO Collaborating Centre for Emerging**
442 **Infections and Biological Threats, Robert Koch Institute, Berlin, Germany**

443 Annika Brinkmann & Andreas Nitsche

444 **Section of Biomedical Sciences, Department of Natural and Environmental Sciences,**
445 **School of Arts and Sciences, American University of Nigeria, Yola, Nigeria**

446 Malachy Ifeanyi Okeke

447

448 **Contributions**

449 DD-C conducted the experiments, analyzed the data, and wrote the manuscript. MIO and UM
450 conceptualized the study, supervised the design and execution of the project, and wrote the manuscript.
451 AB and AN contributed to data interpretation and revision of the manuscript for improved intellectual
452 content. All authors contributed to the article and approved the submitted version.

453

454 **Corresponding authors**

455 *Correspondence to Ugo Moens or Malachy Ifeanyi Okeke.

456

457 **Ethics approval and consent to participate**

458 Not applicable.

459

460 **Consent for publication**

461 Not applicable.

462

463 **Competing interests**

464 The authors declare that they have no competing interests.

465

466 **Keywords**

467 orthopoxvirus, poxvirus, smallpox, superinfection exclusion

468

469 **Supplementary information**

470 Additional file 1. Supplementary tables.

471 Additional file 2. Fig. S1.

472

473 **References**

474 1. Hendrickson RC, Wang C, Hatcher EL, Lefkowitz EJ. Orthopoxvirus Genome Evolution:
475 The Role of Gene Loss. *Viruses* [Internet]. Multidisciplinary Digital Publishing Institute
476 (MDPI); 2010 [cited 2022 Jan 10];2:1933–67. Available from: /pmc/articles/PMC3185746/

477 2. MacLachlan NJ, Dubovi EJ, editors. *Poxviridae. Fenner's Vet Virol* [Internet]. Fifth. Boston:
478 Academic Press; 2017 [cited 2022 Jan 10]. p. 157–74. Available from:
479 <https://linkinghub.elsevier.com/retrieve/pii/B9780128009468000076>

480 3. Silva NIO, de Oliveira JS, Kroon EG, Trindade G de S, Drumond BP. Here, There, and
481 Everywhere: The Wide Host Range and Geographic Distribution of Zoonotic Orthopoxviruses.
482 *Viruses* [Internet]. Multidisciplinary Digital Publishing Institute (MDPI); 2021 [cited 2022 Jan
483 10];13. Available from: /pmc/articles/PMC7823380/

484 4. Vora NM, Li Y, Geleishvili M, Emerson GL, Khmaladze E, Maghlakelidze G, et al. Human

485 Infection with a Zoonotic Orthopoxvirus in the Country of Georgia. *N Engl J Med* [Internet].
486 NIH Public Access; 2015 [cited 2022 Jan 10];372:1223. Available from:
487 /pmc/articles/PMC4692157/

488 5. Reynolds MG, Guagliardo SAJ, Nakazawa YJ, Doty JB, Mauldin MR. Understanding
489 orthopoxvirus host range and evolution: from the enigmatic to the usual suspects. *Curr Opin*
490 *Virol*. Elsevier; 2018;28:108–15.

491 6. Diaz JH. The Disease Ecology, Epidemiology, Clinical Manifestations, Management,
492 Prevention, and Control of Increasing Human Infections with Animal Orthopoxviruses.
493 *Wilderness Environ Med* [Internet]. Elsevier; 2021 [cited 2022 Jan 10];32:528–36. Available
494 from: <http://www.wemjournal.org/article/S1080603221001575/fulltext>

495 7. Strassburg MA. The global eradication of smallpox. *Am J Infect Control*. Mosby;
496 1982;10:53–9.

497 8. Jacobs BL, Langland JO, Kibler K V., Denzler KL, White SD, Holechek SA, et al. *Vaccinia*
498 *Virus Vaccines: Past, Present and Future*. *Antiviral Res* [Internet]. NIH Public Access; 2009
499 [cited 2022 Mar 31];84:1. Available from: /pmc/articles/PMC2742674/

500 9. Sánchez-Sampedro L, Perdiguero B, Mejías-Pérez E, García-Arriaza J, Di Pilato M, Esteban
501 M. The evolution of poxvirus vaccines. *Viruses*. 2015;7.

502 10. Mayr A. Smallpox vaccination and bioterrorism with pox viruses. *Comp Immunol*
503 *Microbiol Infect Dis*. 2003;26.

504 11. Pittman PR, Hahn M, Lee HS, Koca C, Samy N, Schmidt D, et al. Phase 3 Efficacy Trial
505 of Modified *Vaccinia Ankara* as a Vaccine against Smallpox. *N Engl J Med*. 2019;381.

506 12. Mahnel H, Mayr A. Experiences with immunization against orthopox viruses of humans
507 and animals using vaccine strain MVA. *Berl Munch Tierarztl Wochenschr*. 1994;107.

508 13. Mayr A, Stickl H, Müller HK, Danner K, Singer H. [The smallpox vaccination strain MVA:
509 marker, genetic structure, experience gained with the parenteral vaccination and behavior in

510 organisms with a debilitated defence mechanism (author's transl)]. Zentralbl Bakteriol B.
511 1978;167.

512 14. Mayr A, Hochstein-Mintzel V, Stickl H. Abstammung, Eigenschaften und Verwendung des
513 attenuierten Vaccinia-Stammes MVA. Infection. 1975;3.

514 15. Meyer H, Sutter G, Mayr A. Mapping of deletions in the genome of the highly attenuated
515 vaccinia virus MVA and their influence on virulence. J Gen Virol. 1991;72.

516 16. Antoine G, Scheiflinger F, Dorner F, Falkner FG. The complete genomic sequence of the
517 modified vaccinia Ankara strain: Comparison with other orthopoxviruses. Virology. 1998;244.

518 17. Blanchard TJ, Alcamí A, Andrea P, Smith GL. Modified vaccinia virus Ankara undergoes
519 limited replication in human cells and lacks several immunomodulatory proteins: Implications
520 for use as a human vaccine. J Gen Virol. 1998;79.

521 18. Carroll MW, Moss B. Host range and cytopathogenicity of the highly attenuated MVA
522 strain of vaccinia virus: Propagation and generation of recombinant viruses in a nonhuman
523 mammalian cell line. Virology. 1997;238.

524 19. Jordan I, Horn D, Oehmke S, Leendertz FH, Sandig V. Cell lines from the Egyptian fruit
525 bat are permissive for modified vaccinia Ankara. Virus Res. 2009;145.

526 20. Okeke MI, Nilssen Ø, Traavik T. Modified vaccinia virus Ankara multiplies in the rat IEC-
527 6 cells and limited production of mature virions occurs in other mammalian cell lines. J Gen
528 Virol. 2006;87.

529 21. Drexler I, Heller K, Wahren B, Erfle V, Sutter G. Highly attenuated modified vaccinia virus
530 Ankara replicates in baby hamster kidney cells, a potential host for virus propagation, but not
531 in various human transformed and primary cells. J Gen Virol. 1998;79.

532 22. Hansen H, Okeke MI, Nilssen Ø, Traavik T. Recombinant viruses obtained from co-
533 infection in vitro with a live vaccinia-vectored influenza vaccine and a naturally occurring
534 cowpox virus display different plaque phenotypes and loss of the transgene. Vaccine. Elsevier;

535 2004;23:499–506.

536 23. Peng C, Moss B. Repair of a previously uncharacterized second host-range gene contributes
537 to full replication of modified vaccinia virus Ankara (MVA) in human cells. *Proc Natl Acad*
538 *Sci U S A*. 2020;117.

539 24. Suter M, Meisinger-Henschel C, Tzatzaris M, Hülsemann V, Lukassen S, Wulff NH, et al.
540 Modified vaccinia Ankara strains with identical coding sequences actually represent complex
541 mixtures of viruses that determine the biological properties of each strain. *Vaccine*. 2009;27.

542 25. Earl PL, Americo JL, Wyatt LS, Espenshade O, Bassler J, Gong K, et al. Rapid protection
543 in a monkeypox model by a single injection of a replication-deficient vaccinia virus. *Proc Natl*
544 *Acad Sci U S A*. 2008;105.

545 26. Guerra S, González JM, Climent N, Reyburn H, López-Fernández LA, Nájera JL, et al.
546 Selective Induction of Host Genes by MVA-B, a Candidate Vaccine against HIV/AIDS. *J Virol*.
547 2010;84.

548 27. Okeke MI, Okoli AS, Diaz D, Offor C, Oludotun TG, Tryland M, et al. Hazard
549 characterization of modified vaccinia virus ankara vector: What are the knowledge gaps?
550 *Viruses*. 2017.

551 28. Orlova OV, Glazkova DV, Bogoslovskaya EV, Shipulin GA, Yudin SM. Development of
552 Modified Vaccinia Virus Ankara-Based Vaccines: Advantages and Applications. *Vaccines*.
553 MDPI; 2022.

554 29. Joachim A, Nilsson C, Aboud S, Bakari M, Lyamuya EF, Robb ML, et al. Potent functional
555 antibody responses elicited by HIV-I DNA priming and boosting with heterologous HIV-1
556 recombinant MVA in healthy tanzanian adults. *PLoS One*. 2015;10.

557 30. Nilsson C, Godoy-Ramirez K, Hejdeman B, Bråve A, Gudmundsdotter L, Hallengård D, et
558 al. Broad and potent cellular and humoral immune responses after a second late HIV-modified
559 vaccinia virus ankara vaccination in HIV-DNA-primed and HIV-modified vaccinia virus

560 ankara-boosted swedish vaccinees. *AIDS Res Hum Retroviruses*. 2014;30.

561 31. Milligan ID, Gibani MM, Sewell R, Clutterbuck EA, Campbell D, Plested E, et al. Safety
562 and immunogenicity of novel adenovirus type 26-and modified vaccinia Ankara-vectored
563 Ebola vaccines: A randomized clinical trial. *JAMA - J Am Med Assoc*. 2016;315.

564 32. Tapia MD, Sow SO, Lyke KE, Haidara FC, Diallo F, Doumbia M, et al. Use of ChAd3-
565 EBO-Z Ebola virus vaccine in Malian and US adults, and boosting of Malian adults with MVA-
566 BN-Filo: a phase 1, single-blind, randomised trial, a phase 1b, open-label and double-blind,
567 dose-escalation trial, and a nested, randomised, double-blind, placebo-controlled trial. *Lancet*
568 *Infect Dis*. 2016;16.

569 33. Callendret B, Vellinga J, Wunderlich K, Rodriguez A, Steigerwald R, Dirmeier U, et al. A
570 prophylactic multivalent vaccine against different filovirus species is immunogenic and
571 provides protection from lethal infections with Ebolavirus and Marburgvirus species in non-
572 human primates. *PLoS One*. 2018;13.

573 34. Fuentes S, Ravichandran S, Coyle EM, Klenow L, Khurana S. Human Antibody Repertoire
574 following Ebola Virus Infection and Vaccination. *iScience*. 2020;23.

575 35. Jordan E, Lawrence SJ, Meyer TPH, Schmidt D, Schultz S, Mueller J, et al. Broad Antibody
576 and Cellular Immune Response from a Phase 2 Clinical Trial with a Novel Multivalent
577 Poxvirus-Based Respiratory Syncytial Virus Vaccine. *J Infect Dis*. 2021;223.

578 36. Koch T, Dahlke C, Fathi A, Kupke A, Krähling V, Okba NMA, et al. Safety and
579 immunogenicity of a modified vaccinia virus Ankara vector vaccine candidate for Middle East
580 respiratory syndrome: an open-label, phase 1 trial. *Lancet Infect Dis*. 2020;20.

581 37. Aldoss I, la Rosa C, Baden LR, Longmate J, Ariza-Heredia EJ, Rida WN, et al. Poxvirus
582 vectored cytomegalovirus vaccine to prevent cytomegalovirus viremia in transplant recipients:
583 A phase 2, randomized clinical trial. *Ann Intern Med*. 2020;172.

584 38. Kreijtz JHCM, Goeijenbier M, Moesker FM, van den Dries L, Goeijenbier S, De Gruyter

585 HLM, et al. Safety and immunogenicity of a modified-vaccinia-virus-Ankara-based influenza
586 A H5N1 vaccine: A randomised, double-blind phase 1/2a clinical trial. *Lancet Infect Dis.*
587 2014;14.

588 39. Pukhuriwong S, Ahmed MS, Sharma R, Krishnan M, Leong S, Lambe T, et al. Modified
589 vaccinia Ankara-vectored vaccine expressing nucleoprotein and matrix protein 1 (M1) activates
590 mucosal M1-specific T-Cell immunity and tissue-resident memory T Cells in human
591 nasopharynx-associated lymphoid tissue. *J Infect Dis.* 2020;222.

592 40. Tameris MD, Hatherill M, Landry BS, Scriba TJ, Snowden MA, Lockhart S, et al. Safety
593 and efficacy of MVA85A, a new tuberculosis vaccine, in infants previously vaccinated with
594 BCG: A randomised, placebo-controlled phase 2b trial. *Lancet.* 2013;381.

595 41. Hodgson SH, Ewer KJ, Bliss CM, Edwards NJ, Rampling T, Anagnostou NA, et al.
596 Evaluation of the efficacy of ChAd63-MVA vectored vaccines expressing circumsporozoite
597 protein and ME-TRAP against controlled human malaria infection in malaria-naive individuals.
598 *J Infect Dis.* 2015.

599 42. Biswas S, Choudhary P, Elias SC, Miura K, Milne KH, De Cassan SC, et al. Assessment of
600 humoral immune responses to blood-stage malaria antigens following ChAd63-MVA
601 immunization, controlled human malaria infection and natural exposure. *PLoS One.* 2014;9.

602 43. Sebastian S, Gilbert SC. Recombinant modified vaccinia virus Ankara-based malaria
603 vaccines. *Expert Rev. Vaccines.* 2016.

604 44. European Medicines Agency. EMA recommends approval of Imvanex for the prevention
605 of monkeypox disease [Internet]. 2022 [cited 2023 Jan 1]. Available from:
606 [https://www.ema.europa.eu/en/news/ema-recommends-approval-imvanex-prevention-](https://www.ema.europa.eu/en/news/ema-recommends-approval-imvanex-prevention-monkeypox-disease)
607 [monkeypox-disease](https://www.ema.europa.eu/en/news/ema-recommends-approval-imvanex-prevention-monkeypox-disease)

608 45. U.S. Food and Drugs. Vaccines Licensed for Use in the United States [Internet]. 2022.
609 Available from: <https://www.fda.gov/vaccines-blood-biologics/vaccines/vaccines-licensed->

610 use-united-states

611 46. Goossens M, Pauwels K, Willemarck N, Breyer D. Environmental Risk Assessment of
612 Clinical Trials Involving Modified Vaccinia Virus Ankara (MVA)-Based Vectors. *Curr Gene*
613 *Ther.* 2014;13.

614 47. Coulson D, Upton C. Characterization of indels in poxvirus genomes. *Virus Genes*
615 [Internet]. Springer; 2011 [cited 2022 Jan 10];42:171–7. Available from:
616 <https://link.springer.com/article/10.1007/s11262-010-0560-x>

617 48. Franke A, Pfaff F, Jenckel M, Hoffmann B, Höper D, Antwerpen M, et al. Classification of
618 cowpox viruses into several distinct clades and identification of a novel lineage. *Viruses.*
619 2017;9:1–14.

620 49. Gao J, Gigante C, Khmaladze E, Liu P, Tang S, Wilkins K, et al. Genome sequences of
621 Akhmeta virus, an early divergent old world orthopoxvirus. *Viruses.* 2018;10.

622 50. Gigante CM, Gao J, Tang S, McCollum AM, Wilkins K, Reynolds MG, et al. Genome of
623 Alaskapox Virus, a Novel Orthopoxvirus Isolated from Alaska. *Viruses* [Internet].
624 Multidisciplinary Digital Publishing Institute (MDPI); 2019 [cited 2022 Jan 10];11. Available
625 from: [/pmc/articles/PMC6723315/](https://pubmed.ncbi.nlm.nih.gov/323315/)

626 51. Gubser C, Hué S, Kellam P, Smith GL. Poxvirus genomes: A phylogenetic analysis. *J Gen*
627 *Virol* [Internet]. Microbiology Society; 2004 [cited 2022 Jan 10];85:105–17. Available from:
628 <https://www.microbiologyresearch.org/content/journal/jgv/10.1099/vir.0.19565-0>

629 52. Qin L, Evans DH. Genome Scale Patterns of Recombination between Coinfecting Vaccinia
630 *Viruses.* *J Virol.* 2014;88:5277–86.

631 53. Qin L, Upton C, Hazes B, Evans DH. Genomic Analysis of the Vaccinia Virus Strain
632 Variants Found in Dryvax Vaccine. *J Virol* [Internet]. American Society for Microbiology
633 (ASM); 2011 [cited 2022 Jan 10];85:13049. Available from: [/pmc/articles/PMC3233142/](https://pubmed.ncbi.nlm.nih.gov/2142/)

634 54. Qin L, Favis N, Famulski J, Evans DH. Evolution of and Evolutionary Relationships

635 between Extant Vaccinia Virus Strains. *J Virol* [Internet]. American Society for Microbiology
636 (ASM); 2015 [cited 2022 Jan 10];89:1809. Available from: /pmc/articles/PMC4300770/
637 55. Smithson C, Meyer H, Gigante CM, Gao J, Zhao H, Batra D, et al. Two novel poxviruses
638 with unusual genome rearrangements: NY_014 and Murmansk. *Virus Genes* [Internet].
639 Springer New York LLC; 2017 [cited 2022 Jan 10];53:883–97. Available from:
640 <https://link.springer.com/article/10.1007/s11262-017-1501-8>
641 56. Smithson C, Purdy A, Verster AJ, Upton C. Prediction of Steps in the Evolution of Variola
642 Virus Host Range. *PLoS One* [Internet]. Public Library of Science; 2014 [cited 2022 Jan
643 10];9:e91520. Available from:
644 <https://journals.plos.org/plosone/article?id=10.1371/journal.pone.0091520>
645 57. Diaz-Cánova D, Moens UL, Brinkmann A, Nitsche A, Okeke MI. Genomic Sequencing
646 and Analysis of a Novel Human Cowpox Virus With Mosaic Sequences From North America
647 and Old World Orthopoxvirus. *Front Microbiol* [Internet]. Frontiers Media SA; 2022 [cited
648 2022 May 23];13. Available from: /pmc/articles/PMC9112427/
649 58. Doceul V, Hollinshead M, Van Der Linden L, Smith GL. Repulsion of superinfecting
650 virions: A mechanism for rapid virus spread. *Science* (80-). 2010;327.
651 59. Laliberte JP, Moss B. A Novel Mode of Poxvirus Superinfection Exclusion That Prevents
652 Fusion of the Lipid Bilayers of Viral and Cellular Membranes. *J Virol*. 2014;88.
653 60. Campe H, Zimmermann P, Glos K, Bayer M, Bergemann H, Dreweck C, et al. Cowpox
654 Virus Transmission from Pet Rats to Humans, Germany. *Emerg Infect Dis* [Internet]. Centers
655 for Disease Control and Prevention; 2009 [cited 2022 Jan 10];15:777. Available from:
656 /pmc/articles/PMC2687013/
657 61. Ducournau C, Ferrier-Rembert A, Ferraris O, Joffre A, Favier AL, Flusin O, et al.
658 Concomitant human infections with 2 cowpox virus strains in related cases, France, 2011.
659 *Emerg Infect Dis*. 2013;19.

660 62. Gazzani P, Gach JE, Colmenero I, Martin J, Morton H, Brown K, et al. Fatal disseminated
661 cowpox virus infection in an adolescent renal transplant recipient. *Pediatr Nephrol.* 2017;32.

662 63. Andreani J, Arnault JP, Bou Khalil JY, Abrahão J, Tomei E, Vial E, et al. Atypical cowpox
663 virus infection in smallpox-vaccinated patient, France. *Emerg Infect Dis.* 2019;25.

664 64. Ferrier A, Frenois-Veyrat G, Schvoerer E, Henard S, Jarjaval F, Drouet I, et al. Fatal cowpox
665 virus infection in human fetus, France, 2017. *Emerg Infect Dis.* 2021;27:2570–7.

666 65. Krankowska DC, Woźniak PA, Cybula A, Izdebska J, Suchacz M, Samelska K, et al.
667 Cowpox: How dangerous could it be for humans? Case report. *Int J Infect Dis.* 2021;104.

668 66. Tryland M, Myrmel H, Holtet L, Haukenes G, Traavik T. Clinical cowpox cases in Norway.
669 *Scand J Infect Dis.* 1998;30:301–3.

670 67. Okeke MI, Hansen H, Traavik T. A naturally occurring cowpox virus with an ectromelia
671 virus A-type inclusion protein gene displays atypical A-type inclusions. *Infect Genet Evol.*
672 Elsevier; 2012;12:160–8.

673 68. Diaz-Cánova D, Mavian C, Brinkmann A, Nitsche A, Moens U, Okeke MI. Genomic
674 Sequencing and Phylogenomics of Cowpox Virus. *Viruses* 2022, Vol 14, Page 2134 [Internet].
675 Multidisciplinary Digital Publishing Institute; 2022 [cited 2022 Oct 12];14:2134. Available
676 from: <https://www.mdpi.com/1999-4915/14/10/2134/htm>

677 69. WHO. 2022 Mpox (Monkeypox) Outbreak: Global Trends [Internet]. 2023. Available from:
678 https://worldhealthorg.shinyapps.io/mpx_global/

679 70. Hansen H, Okeke MI, Nilssen Ø, Traavik T. Comparison and phylogenetic analysis of
680 cowpox viruses isolated from cats and humans in Fennoscandia. *Arch Virol* [Internet]. Springer;
681 2009 [cited 2022 Jan 10];154:1293–302. Available from:
682 <https://link.springer.com/article/10.1007/s00705-009-0442-5>

683 71. Sutter G, Moss B. Nonreplicating vaccinia vector efficiently expresses recombinant genes.
684 *Proc Natl Acad Sci U S A.* 1992;89.

685 72. Evans DH, Stuart D, McFadden G. High levels of genetic recombination among
686 cotransfected plasmid DNAs in poxvirus-infected mammalian cells. *J Virol.* 1988;62.

687 73. Willer DO, Mann MJ, Zhang W, Evans DH. Vaccinia virus DNA polymerase promotes
688 DNA pairing and strand-transfer reactions. *Virology.* 1999;257.

689 74. Tolonen N, Doglio L, Schleich S, Krijnse Locker J. Vaccinia virus DNA replication occurs
690 in endoplasmic reticulum-enclosed cytoplasmic mini-nuclei. *Mol Biol Cell.* 2001;12.

691 75. Christen L, Seto J, Niles EG. Superinfection exclusion of vaccinia virus in virus-infected
692 cell cultures. *Virology.* 1990;174.

693 76. Okeke MI, Nilssen I, Moens U, Tryland M, Traavik T. In vitro host range, multiplication
694 and virion forms of recombinant viruses obtained from co-infection in vitro with a vaccinia-
695 vectored influenza vaccine and a naturally occurring cowpox virus isolate. *Virol J.* 2009;6.

696 77. Dobson BM, Procter DJ, Hollett NA, Flesch IEA, Newsome TP, Tschärke DC. Vaccinia
697 virus F5 is required for normal plaque morphology in multiple cell lines but not replication in
698 culture or virulence in mice. *Virology.* 2014;456–457.

699 78. Dobson BM, Tschärke DC. Truncation of gene F5L partially masks rescue of vaccinia virus
700 strain MVA growth on mammalian cells by restricting plaque size. *J Gen Virol.* 2014;95.

701 79. Morales I, Carbajal MA, Bohn S, Holzer D, Kato SEM, Greco FAB, et al. The vaccinia
702 virus F11L gene product facilitates cell detachment and promotes migration. *Traffic.* 2008;9.

703 80. Blasco R, Sisler JR, Moss B. Dissociation of progeny vaccinia virus from the cell membrane
704 is regulated by a viral envelope glycoprotein: effect of a point mutation in the lectin homology
705 domain of the A34R gene. *J Virol.* 1993;67.

706 81. Roper RL, Wolffe EJ, Weisberg A, Moss B. The Envelope Protein Encoded by the A33R
707 Gene Is Required for Formation of Actin-Containing Microvilli and Efficient Cell-to-Cell
708 Spread of Vaccinia Virus. *J Virol.* 1998;72.

709 82. Zhang W-H, Wilcock D, Smith GL. Vaccinia Virus F12L Protein Is Required for Actin Tail

710 Formation, Normal Plaque Size, and Virulence. *J Virol.* 2000;74.

711 83. Parkinson JE, Smith GL. Vaccinia virus gene A36R encodes a M(r) 43-50 K protein on the
712 surface of extracellular enveloped virus. *Virology.* 1994;204.

713 84. Katz E, Wolffe E, Moss B. Identification of Second-Site Mutations That Enhance Release
714 and Spread of Vaccinia Virus. *J Virol.* 2002;76.

715 85. Zhou J, Sun XY, Fernando GJP, Frazer IH. The vaccinia virus K2L gene encodes a serine
716 protease inhibitor which inhibits cell-cell fusion. *Virology.* 1992;189.

717 86. Law KM, Smith GL. A vaccinia serine protease inhibitor which prevents virus-induced cell
718 fusion. *J Gen Virol.* 1992;73.

719 87. Turner PC, Moyer RW. An orthopoxvirus serpinlike gene controls the ability of infected
720 cells to fuse. *J Virol.* 1992;66.

721 88. Firth C, Kitchen A, Shapiro B, Suchard MA, Holmes EC, Rambaut A. Using Time-
722 Structured Data to Estimate Evolutionary Rates of Double-Stranded DNA Viruses. *Mol Biol*
723 *Evol* [Internet]. Oxford Academic; 2010 [cited 2022 Apr 5];27:2038–51. Available from:
724 <https://academic.oup.com/mbe/article/27/9/2038/1008481>

725 89. de Haven BC, Gupta K, Isaacs SN. The vaccinia virus A56 protein: A multifunctional
726 transmembrane glycoprotein that anchors two secreted viral proteins. *J. Gen. Virol.* 2011.

727 90. Bratke KA, McLysaght A, Rothenburg S. A survey of host range genes in poxvirus
728 genomes. *Infect Genet Evol* [Internet]. 2013;14:406–25. Available from:
729 <http://dx.doi.org/10.1016/j.meegid.2012.12.002>

730 91. Panus JF, Smith CA, Ray CA, Smith TD, Patel DD, Pickup DJ. Cowpox virus encodes a
731 fifth member of the tumor necrosis factor receptor family: A soluble, secreted CD30
732 homologue. *Proc Natl Acad Sci U S A.* 2002;99.

733 92. Abrahão JS, Campos RK, De Souza Trindade G, Da Fonseca FG, Ferreira PCP, Kroon EG.
734 Outbreak of Severe Zoonotic Vaccinia Virus Infection, Southeastern Brazil. *Emerg Infect Dis*

735 [Internet]. Centers for Disease Control and Prevention; 2015 [cited 2022 Jan 10];21:695.
736 Available from: /pmc/articles/PMC4378504/

737 93. Kalthan E, Tenguere J, Ndjapou SG, Koyazengbe TA, Mbomba J, Marada RM, et al.
738 Investigation of an outbreak of monkeypox in an area occupied by armed groups, Central
739 African Republic. *Médecine Mal Infect. Elsevier Masson*; 2018;48:263–8.

740 94. Alakunle E, Moens U, Nchinda G, Okeke MI. Monkeypox Virus in Nigeria: Infection
741 Biology, Epidemiology, and Evolution. *Viruses* [Internet]. Multidisciplinary Digital Publishing
742 Institute (MDPI); 2020 [cited 2022 Jan 12];12. Available from: /pmc/articles/PMC7694534/

743 95. Cardeti G, Gruber CEM, Eleni C, Carletti F, Castilletti C, Manna G, et al. Fatal Outbreak
744 in Tonkean Macaques Caused by Possibly Novel Orthopoxvirus, Italy, January 2015 - Volume
745 23, Number 12—December 2017 - *Emerging Infectious Diseases journal - CDC. Emerg Infect*
746 *Dis* [Internet]. Centers for Disease Control and Prevention (CDC); 2017 [cited 2022 Jan
747 10];23:1941–9. Available from: https://wwwnc.cdc.gov/eid/article/23/12/16-2098_article

748 96. Springer YP, Hsu CH, Werle ZR, Olson LE, Cooper MP, Castrodale LJ, et al. Novel
749 Orthopoxvirus Infection in an Alaska Resident. *Clin Infect Dis An Off Publ Infect Dis Soc Am*
750 [Internet]. Oxford University Press; 2017 [cited 2022 Jan 10];64:1737. Available from:
751 /pmc/articles/PMC5447873/

752 97. Alakunle E, Okeke M. Monkeypox virus: a neglected zoonotic pathogen spreads globally.
753 *Nat Rev Microbiol.* 2022;20:507–8.

754 98. Sutter G, Wyatt LS, Foley PL, Bennink JR, Moss B. A recombinant vector derived from
755 the host range-restricted and highly attenuated MVA strain of vaccinia virus stimulates
756 protective immunity in mice to influenza virus. *Vaccine. Elsevier*; 1994;12:1032–40.

757 99. Bankevich A, Nurk S, Antipov D, Gurevich AA, Dvorkin M, Kulikov AS, et al. SPAdes:
758 A New Genome Assembly Algorithm and Its Applications to Single-Cell Sequencing
759 [Internet]. *J. Comput. Biol.* Mary Ann Liebert, Inc.; 2012 [cited 2022 Jan 10]. p. 477. Available

760 from: /pmc/articles/PMC3342519/
761 100. Tcherepanov V, Ehlers A, Upton C. Genome Annotation Transfer Utility (GATU): rapid
762 annotation of viral genomes using a closely related reference genome [Internet]. BMC
763 Genomics. BioMed Central; 2006 [cited 2022 Jan 10]. p. 150. Available from:
764 /pmc/articles/PMC1534038/
765 101. Ehlers A, Osborne J, Slack S, Roper RL, Upton C. Poxvirus Orthologous Clusters (POCs)
766 [Internet]. Bioinformatics. Oxford Academic; 2002 [cited 2022 Jan 10]. p. 1544–5. Available
767 from: <https://academic.oup.com/bioinformatics/article/18/11/1544/178349>
768 102. Martin DP, Murrell B, Golden M, Khoosal A, Muhire B. RDP4: Detection and analysis of
769 recombination patterns in virus genomes [Internet]. Virus Evol. Oxford Academic; 2015 [cited
770 2021 Mar 2]. Available from: <https://academic.oup.com/ve/article/1/1/vev003/2568683>
771 103. Lole KS, Bollinger RC, Paranjape RS, Gadkari D, Kulkarni SS, Novak NG, et al. Full-
772 Length Human Immunodeficiency Virus Type 1 Genomes from Subtype C-Infected
773 Seroconverters in India, with Evidence of Intersubtype Recombination [Internet]. J. Virol.
774 American Society for Microbiology (ASM); 1999 [cited 2021 Mar 2]. p. 160. Available from:
775 /pmc/articles/PMC103818/
776 104. Katoh K, Standley DM. MAFFT Multiple Sequence Alignment Software Version 7:
777 Improvements in Performance and Usability [Internet]. Mol. Biol. Evol. Oxford University
778 Press; 2013 [cited 2022 Jan 10]. p. 772–80. Available from: /pmc/articles/PMC3603318/
779 105. Martin D, Rybicki E. RDP: detection of recombination amongst aligned sequences
780 [Internet]. Bioinformatics. Oxford Academic; 2000 [cited 2022 Jan 10]. p. 562–3. Available
781 from: <https://academic.oup.com/bioinformatics/article/16/6/562/178152>
782 106. Padidam M, Sawyer S, Fauquet CM. Possible Emergence of New Geminiviruses by
783 Frequent Recombination. Virology. Academic Press; 1999. p. 218–25.
784 107. Martin DP, Posada D, Crandall KA, Williamson C. A Modified Bootscan Algorithm for

785 Automated Identification of Recombinant Sequences and Recombination Breakpoints
786 [Internet]. <https://home.liebertpub.com/aid>. Mary Ann Liebert, Inc. 2 Madison Avenue
787 Larchmont, NY 10538 USA; 2005 [cited 2022 Jan 10]. p. 98–102. Available from:
788 <https://www.liebertpub.com/doi/abs/10.1089/aid.2005.21.98>

789 108. Smith JM. Analyzing the mosaic structure of genes [Internet]. *J. Mol. Evol.* 1992 342.
790 Springer; 1992 [cited 2022 Jan 10]. p. 126–9. Available from:
791 <https://link.springer.com/article/10.1007/BF00182389>

792 109. Posada D, Crandall KA. Evaluation of methods for detecting recombination from DNA
793 sequences: Computer simulations [Internet]. *Proc. Natl. Acad. Sci. National Academy of*
794 *Sciences*; 2001 [cited 2022 Jan 10]. p. 13757–62. Available from:
795 <https://www.pnas.org/content/98/24/13757>

796 110. Gibbs MJ, Armstrong JS, Gibbs AJ. Sister-Scanning: a Monte Carlo procedure for
797 assessing signals in recombinant sequences [Internet]. *Bioinformatics*. Oxford Academic; 2000
798 [cited 2022 Jan 10]. p. 573–82. Available from:
799 <https://academic.oup.com/bioinformatics/article/16/7/573/227862>

800 111. Boni MF, Posada D, Feldman MW. An Exact Nonparametric Method for Inferring Mosaic
801 Structure in Sequence Triplets [Internet]. *Genetics*. Oxford Academic; 2007 [cited 2022 Jan
802 10]. p. 1035–47. Available from:
803 <https://academic.oup.com/genetics/article/176/2/1035/6064558>
804

Supplementary Table 1. Predicted coding sequences (CDS) in CPXV-No-F1 and MVA-HANP compared to reference genomes CPXV-Brighton (CPXV_BR) and VACV-Copenhagen (VACV-Cop).

Function	VACV-Cop	CPXV-Br	CPXV-No-F1					VACV-MVA-HANP				
			CDS	Start	Stop	Length	Direction	CDS	Start	Stop	Length	Direction
CPV-B-002	-	CPXV002	NoF1-001	894	1121	228	reverse	-				
Chemokine binding protein (Cop-C23L)	B29R/C23L	vCCI/CPXV003	NoF1-002	1150	1887	738	reverse	MVA-HANP-001 ^f	6485	6895	411	reverse
CPV-B-004	-	CXPV004				overlap						
TNF receptor (CrmB) (Cop-C22L)	B28R/C22L	crmB/CPXV005	NoF1-003	1961	3034	1074	reverse	-				
Ankyrin (Cop-C19L)	B25R/C19L	CPXV006	NoF1-004	3112	4878	1767	reverse	MVA-HANP-002 ^f	7327	7857	531	reverse
Ankyrin-like repeat containing protein	-	CPXV007	NoF1-005	4960	5049	90	reverse	-				
Ankyrin (Cop-C17L)	B24R/C18L	CPXV008	NoF1-006	5089	7095	2007	reverse	MVA-HANP-003 ^f	8378	8515	138	reverse
								MVA-HANP-004 ^f	8545	8853	309	reverse
	B23R/C17L							MVA-HANP-005 ^f	8930	9631	702	reverse
Hypothetical protein (Cop-C16L)	C16L	CPXV009/CPXV222	NoF1-007	7310	7771	462	reverse	-				
Alpha amanatin target protein (Cop-N2L)	N2L	CPXV010	NoF1-008	7942	8595	654	reverse	-				
BTB Kelch-domain containing protein; CRL comple x (Cop-A55R)	-	-	NOF1-009	8908	9501	594	reverse	-				
Ankyrin (Cop-B20R)	B20R	CPXV011	NoF1-010	9828	11843	2016	reverse	-				
C-type lectin domain containing protein	-	CPXV012	NoF1-011	12070	12279	210	reverse	-				
BTB Kelch-domain containing protein; CRL comple x (Cop-A55R)	A55R	CPXV013	NoF1-012	12707	13318	612	reverse	-				
TNF receptor (CrmB) (Cop-C22L)	C22L	CPXV014	NoF1-013	13393	14001	609	reverse	-				
TNF-alpha receptor like protein	-	vCD30/CPXV015	NoF1-014	13998	14330	333	reverse	-				
Ankyrin (Cop-B18R)	B18R	CPXV016	NoF1-015	14405	16708	2304	reverse	-				
Ankyrin (CPXV-017)	-	CPXV017	NoF1-016	16984	18291	1308	reverse	-				
MPV-ZN3R	-	CPXV018	NoF1-017	18390	18905	516	reverse	-				
Ankyrin (Cop-B18R)	B18R	CPXV019	NoF1-018	18968	21583	2616	reverse	-				
Host range protein	-	CPXV020	NoF1-019	21631	22149	519	reverse	-				
Secreted EGF-like protein (Cop-C11R)	C11R	VGF/CPXV021	NoF1-020	22316	22741	426	forward	MVA-HANP-006	10276	10698	423	forward
IL-1 receptor antagonist (Cop-C10L)	C10L	CPXV022	NoF1-021	22894	23889	996	reverse	MVA-HANP-007	10851	11831	981	reverse
Zinc finger-like protein	-	CPXV023	NoF1-022	24404	25132	729	forward	MVA-HANP-008 ^f	12336	12611	276	forward
Soluble IL-18 binding protein (Bsh-D7L)	-	CPXV024	NoF1-023	25281	25661	381	reverse	MVA-HANP-009	13125	13487	363	reverse
Ankyrin/Host Range (Bang-D8L)	-	VHR1/CPXV025	NoF1-024	25720	27735	2016	reverse	MVA-HANP-010 ^f	13546	13818	273	reverse
								MVA-HANP-011 ^f	13831	14259	429	reverse
								MVA-HANP-012 ^f	14348	14755	408	reverse
								MVA-HANP-013 ^f	14984	15232	249	reverse
								MVA-HANP-014 ^f	15278	15493	216	reverse
ANK-containing protein	-	CPXV026	NoF1-025	27849	28040	192	reverse	MVA-HANP-015	15597	15776	180	reverse
Ankyrin; Type 1 IFN resistance (Cop-C9L)	C9L	CPXV027	NoF1-026	28214	30118	1905	reverse	MVA-HANP-016 ^f	15949	16278	330	reverse
								MVA-HANP-017 ^f	16569	16859	291	reverse
								MVA-HANP-018 ^f	16939	17832	894	reverse
Unknown (Cop-C8L)	C8L	CPXV028	NoF1-027	30160	30717	558	reverse	MVA-HANP-019	17875	18408	534	reverse
Type 1 IFN inhibitor (Cop-C7L)	C7L	CPXV029	NoF1-028	30789	31241	453	reverse	MVA-HANP-020	18480	18932	453	reverse
Bcl-2-like protein, IFN-beta inhibitor (Cop-C6L)	C6L	CPXV030	NoF1-029	31472	31939	468	reverse	MVA-HANP-021	19141	19614	474	reverse
Kelch-like protein (Cop-C5L)	C5L	CPXV031				overlap						
Kelch-like protein (Cop-C5L)	C5L	CPXV032	NoF1-030	32272	32649	378	reverse	-				
IL-1 receptor antagonist (Cop-C10L)	C4L	CPXV033	NoF1-031	32710	33657	948	reverse	-				
Complement binding (secreted) (Cop-C3L)	C3L	CPXV034	NoF1-032	33724	34518	795	reverse	-				
POZ/BTB Kelch domain protein (Cop-C2L)	C2L	CPXV035	NoF1-033	34581	36119	1539	reverse	-				
Putative TLR signalling inhibitor (Cop-C1L)	C1L	CPXV036	NoF1-034	36188	36826	639	reverse	-				
Anti-apoptotic Bcl-2-like protein (Cop-N1L)	N1L	CPXV037	NoF1-035	36868	37221	354	reverse	MVA-HANP-022 ^f	19757	20098	342	reverse
Alpha amanatin target protein (Cop-N2L)	N2L	CPXV038	NoF1-036	37343	37873	531	reverse	MVA-HANP-023	20217	20729	513	reverse
ANK-containing protein; apoptosis inhibitor (Cop-M1L)	M1L	CPXV039	NoF1-037	37916	39331	1416	reverse	-				
NFkB inhibitor (Cop-M2L)	M2L	CPXV040	NoF1-038	39309	39971	663	reverse	-				

Ankyrin/NFkB inhibitor (Cop-K1L)	K1L	CPXV041	NoF1-039	40095	40952	858	reverse	MVA-HANP-024 ^f	20758	21054	297	reverse
Serpin 1,2,3 (Cop-K2L)	K2L	SPI3/CPXV042	NoF1-040	41310	42431	1122	reverse	MVA-HANP-025	21260	22369	1110	reverse
IFN resistance, PKR/eIF-alpha inhibitor (Cop-K3 L)	K3L	CPXV043	NoF1-041	42482	42748	267	reverse	MVA-HANP-026	22419	22685	267	reverse
Phospholipase-D-like protein (Cop-K4L)	K4L	CPXV044	NoF1-042	42808	44082	1275	reverse	MVA-HANP-027	22737	24011	1275	reverse
Monoglyceride lipase (Cop-K5L/K6L)	K5L	CPXV045	NoF1-043	44110	44940	831	reverse	MVA-HANP-028 ^f	24039	24551	513	reverse
	K6L							MVA-HANP-029 ^f	24573	24767	195	reverse
Host immune response repressor (Cop-K7R)	K7R	CPXV046	NoF1-044	45078	45527	450	forward	MVA-HANP-030	24937	25386	450	forward
CPV-B-047	-	CPXV047	-	-	-	-	overlap	-	-	-	-	-
Caspase-9 (apoptosis) inhibitor (mitochondrial- associated) (Cop-F1L)	F1L	CPXV048	NoF1-045	45601	46344	744	reverse	MVA-HANP-031	25451	26119	669	reverse
dUTPase (Cop-F2L)	F2L	CPXV049	NoF1-046	46344	46787	444	reverse	MVA-HANP-032	26131	26574	444	reverse
Kelch-like protein (Cop-F3L)	F3L	CPXV050	NoF1-047	46811	48253	1443	reverse	MVA-HANP-033	26598	28028	1431	reverse
Ribonucleotide reductase small subunit (Cop-F4L)	F4L	CPXV051	NoF1-048	48264	49265	1002	reverse	MVA-HANP-034	28039	28998	960	reverse
36kDa major membrane protein (Cop-F5L)	F5L	CPXV052	NoF1-049	49255	50220	966	reverse	MVA-HANP-035 ^f	29030	29323	294	reverse
								MVA-HANP-036 ^f	29292	29948	657	reverse
Hypothetical protein (Cop-F6L)	F6L	CPXV053	NoF1-050	50250	50465	216	reverse	MVA-HANP-037	29978	30202	225	reverse
Hypothetical protein (Cop-F7L)	F7L	CPXV054	NoF1-051	50481	50726	246	reverse	MVA-HANP-038	30218	30460	243	reverse
Cytoplasmic protein (Cop-F8L)	F8L	CPXV055	NoF1-052	51003	51200	198	reverse	MVA-HANP-039	30607	30804	198	reverse
S-S bond formation pathway protein substrate (Cop-F9L)	F9L	CPXV056	NoF1-053	51261	51899	639	reverse	MVA-HANP-040	30864	31502	639	reverse
Essential Ser/Thr kinase morph (Cop-F10L)	F10L	CPXV057	NoF1-054	51886	53205	1320	reverse	MVA-HANP-041	31489	32808	1320	reverse
VV_Cop-F ORF D	-	CPXV058	-	-	-	-	overlap	-	-	-	-	-
RhoA signalling inhibitor, virus release protein (Cop-F11L)	F11L	CPXV059	NoF1-055	53228	54292	1065	reverse	MVA-HANP-042 ^f	32831	33085	255	reverse
								MVA-HANP-043 ^f	33542	33844	303	reverse
EEV maturation protein (Cop-F12L)	F12L	CPXV060	NoF1-056	54335	56239	1905	reverse	MVA-HANP-044	33887	35794	1908	reverse
Palmitoylated EEV membrane glycoprotein (Cop-F13 L)	F13L	CPXV061	NoF1-057	56273	57391	1119	reverse	MVA-HANP-045	35821	36939	1119	reverse
Unknown (Cop-F14L)	F14L	CPXV062	NoF1-058	57409	57630	222	reverse	MVA-HANP-046	36957	37178	222	reverse
IMV protein (Cop-F14.5L)	F14.5L	62.5	-	-	-	-	-	MVA-HANP-047	37228	37377	150	reverse
CPV-B-063	-	CPXV063	NoF1-059	57677	57835	159	forward	-	-	-	-	-
Unknown conserved protein (Cop-F15L)	F15L	CPXV064	NoF1-060	57903	58379	477	reverse	MVA-HANP-048	37450	37926	477	reverse
Non-functional Serine Recombinase (Cop-F16L)	F16L	CPXV065	NoF1-061	58379	59080	702	reverse	MVA-HANP-049	37933	38628	696	reverse
DNA-binding phosphoprotein (VP11); mTOR antagonist (Cop-F17R)	F17R	CPXV066	NoF1-062	59143	59448	306	forward	MVA-HANP-050	38692	38997	306	forward
Poly (A) polymerase catalytic subunit (VP55) (Cop-E1L)	E1L	CPXV067	NoF1-063	59445	60884	1440	reverse	MVA-HANP-051	38994	40433	1440	reverse
IEV morphogenesis (Cop-E2L)	E2L	CPXV068	NoF1-064	60881	63094	2214	reverse	MVA-HANP-052	40430	42643	2214	reverse
dsRNA-binding protein, IFN resistance/PKR inhibitor (Z-DNA binding)	E3L	CPXV069	NoF1-065	63225	63797	573	reverse	MVA-HANP-053	42770	43342	573	reverse
RNA polymerase subunit (RPO30) (Cop-E4L)	E4L	CPXV070	NoF1-066	63852	64637	786	reverse	MVA-HANP-054	43397	44176	780	reverse
Virosome component (Cop-E5R)	E5R	CPXV071	NoF1-067	64757	65710	954	forward	MVA-HANP-055	44253	45248	996	forward
Virion protein (Cop-E6R)	E6R	CPXV072	NoF1-068	65830	67533	1704	forward	MVA-HANP-056	45385	47088	1704	forward
Myristylated protein (Cop-E7R)	E7R	CPXV073	NoF1-069	67595	68092	498	forward	MVA-HANP-057	47155	47655	501	forward
ER-localized membrane protein, virion core protein (Cop-E8R)	E8R	CPXV074	NoF1-070	68203	69024	822	forward	MVA-HANP-058	47768	48589	822	forward
DNA polymerase (Cop-E9L)	E9L	CPXV075	NoF1-071	69031	72048	3018	reverse	MVA-HANP-059	48596	51616	3021	reverse
Sulfhydryl oxidase (FAD-linked) (Cop-E10R)	E10R	CPXV076	NoF1-072	72080	72367	288	forward	MVA-HANP-060	51648	51935	288	forward
Virion core protein (Cop-E11L)	E11L	CPXV077	NoF1-073	72362	72751	390	reverse	MVA-HANP-061	51930	52319	390	reverse
Membrane protein (Cop-O1L)	O1L	CPXV078	NoF1-074	72738	74738	2001	reverse	MVA-HANP-062 ^f	52306	52764	459	reverse
								MVA-HANP-063 ^f	53045	54262	1218	reverse
Glutaredoxin 1 (Cop-O2L)	O2L	CPXV079	NoF1-075	74786	75112	327	reverse	MVA-HANP-064	54302	54628	327	reverse
Virus entry/fusion complex component (Cop-O3L)	O3L	-	NoF1-076	75136	75243	108	reverse	MVA-HANP-065	54652	54759	108	reverse
DNA-binding core protein (Cop-I1L)	I1L	CPXV080	NoF1-077	75258	76196	939	reverse	MVA-HANP-066	54774	55712	939	reverse
IMV membrane protein (Cop-I2L)	I2L	CPXV081	NoF1-078	76203	76424	222	reverse	MVA-HANP-067	55719	55940	222	reverse
ssDNA-binding phosphoprotein (Cop-I3L)	I3L	CPXV082	NoF1-079	76425	77234	810	reverse	MVA-HANP-068	55941	56750	810	reverse
Ribonucleotide reductase large subunit (Cop-I4L)	I4L	CPXV083	NoF1-080	77317	79632	2316	reverse	MVA-HANP-069	56833	59148	2316	reverse
IMV protein VP13 (Cop-I5L)	I5L	CPXV084	NoF1-081	79659	79898	240	reverse	MVA-HANP-070	59176	59415	240	reverse
Telomere-binding protein (Cop-I6L)	I6L	CPXV085	NoF1-082	79917	81065	1149	reverse	MVA-HANP-071	59434	60582	1149	reverse
Virion core cysteine protease (Cop-I7L)	I7L	CPXV086	NoF1-083	81058	82329	1272	reverse	MVA-HANP-072	60575	61846	1272	reverse
RNA helicase, DEXH-NPH-II domain (Cop-I8R)	I8R	CPXV087	NoF1-084	82335	84365	2031	forward	MVA-HANP-073	61852	63882	2031	forward
Metalloprotease (Cop-G1L)	G1L	CPXV088	NoF1-085	84369	86144	1776	reverse	MVA-HANP-074	63886	65661	1776	reverse
Entry/fusion complex component (Cop-G3L)	G3L	CPXV089	NoF1-086	86141	86476	336	reverse	MVA-HANP-075	65658	65993	336	reverse
VLTF (late transcription elongation factor) (Cop-G2R)	G2R	CPXV090	NoF1-087	86470	87132	663	forward	MVA-HANP-076	65987	66649	663	forward
Glutaredoxin-like protein (Cop-G4L)	G4L	CPXV091	NoF1-088	87102	87476	375	reverse	MVA-HANP-077	66619	66993	375	reverse
FEN1-like nuclease (Cop-G5R)	G5R	CPXV092	NoF1-089	87479	88786	1308	forward	MVA-HANP-078	66996	68300	1305	forward

RNA polymerase subunit (RPO7) (Cop-G5.5R)	G5.5R	CPXV093	NoF1-090	88794	88985	192	forward	MVA-HANP-079	68308	68499	192	forward
NLPc[P60 superfamily protein (Cop-G6R)	G6R	CPXV094	NoF1-091	88987	89484	498	forward	MVA-HANP-080	68501	68998	498	forward
Virion phosphoprotein, early morphogenesis (Cop-G7L)	G7L	CPXV095	NoF1-092	89449	90564	1116	reverse	MVA-HANP-081	68963	70078	1116	reverse
CC_Cop-G ORF B	-	CPXV096					overlap	-				
VLTF-1 (late transcription factor 1) (Cop-G8R)	G8R	CPXV097	NoF1-093	90595	91377	783	forward	MVA-HANP-082	70109	70891	783	forward
Entry/fusion complex component, myristylprotein (Cop-G9R)	G9R	CPXV098	NoF1-094	91397	92419	1023	forward	MVA-HANP-083	70911	71933	1023	forward
IMV membrane protein (Cop-L1R)	L1R	CPXV099	NoF1-095	92420	93172	753	forward	MVA-HANP-084	71934	72686	753	forward
Virial membrane assembly proteins (VMAP) (Cop-L2R)	L2R	CPXV100	NoF1-096	93204	93470	267	forward	MVA-HANP-085	72718	72981	264	forward
Internal virion protein (Cop-L3L)	L3L	CPXV101	NoF1-097	93460	94512	1053	reverse	MVA-HANP-086	72971	74023	1053	reverse
ss/dsDNA binding protein (VP8) (Cop-L4R)	L4R	CPXV102	NoF1-098	94537	95292	756	forward	MVA-HANP-087	74048	74803	756	forward
Entry and Fusion IMV protein (Cop-L5R)	L5R	CPXV103	NoF1-099	95302	95688	387	forward	MVA-HANP-088	74813	75199	387	forward
Virion morph (Cop-J1R)	J1R	CPXV104	NoF1-100	95645	96106	462	forward	MVA-HANP-089	75156	75617	462	forward
Thymidine kinase (Cop-J2R)	J2R	CPXV105	NoF1-101	96122	96655	534	forward	MVA-HANP-090	75633	76166	534	forward
Poly (A) polymerase small subunit (VP39) (Cop-J3R)	J3R	CPXV106	NoF1-102	96723	97724	1002	forward	MVA-HANP-091	76232	77233	1002	forward
RNA polymerase subunit (RPO22) (Cop-J4R)	J4R	CPXV107	NoF1-103	97639	98196	558	forward	MVA-HANP-092	77148	77705	558	forward
IMV membrane protein (Cop-J5L)	J5L	CPXV108	NoF1-104	98257	98658	402	reverse	MVA-HANP-093	77773	78174	402	reverse
RNA polymerase subunit (RPO147) (Cop-J6R)	J6R	CPXV109	NoF1-105	98765	102625	3861	forward	MVA-HANP-094	78280	82140	3861	forward
Tyr/Ser phosphatase, IEN-gamma inhibitor (Cop-H1L)	H1L	CPXV110	NoF1-106	102622	103137	516	reverse	MVA-HANP-095	82137	82652	516	reverse
IMV membrane protein (Cop-H2R)	H2R	CPXV111	NoF1-107	103151	103720	570	forward	MVA-HANP-096	82666	83235	570	forward
IMV heparin binding surface protein (Cop-H3L)	H3L	CPXV112	NoF1-108	103723	104700	978	reverse	MVA-HANP-097	83238	84212	975	reverse
RAP94 (RNA pol assoc protein) (Cop-H4L)	H4L	CPXV113	NoF1-109	104701	107088	2388	reverse	MVA-HANP-098	84213	86600	2388	reverse
VLTF-4 (late transcription factor 4) (Cop-H5R)	H5R	CPXV114	NoF1-110	107274	107894	621	forward	MVA-HANP-099	86786	87397	612	forward
DNA topoisomerase type I (Cop-H6R)	H6R	CPXV115	NoF1-111	107895	108839	945	forward	MVA-HANP-100	87398	88342	945	forward
CPV-B-116	-	CPXV116					overlap	-				
Virial membrane assembly proteins (VMAP) (Cop-H7R)	H7R	CPXV117	NoF1-112	108877	109317	441	forward	MVA-HANP-101	88379	88819	441	forward
mRNA capping enzyme large subunit (Cop-D1R)	D1R	CPXV118	NoF1-113	109361	111895	2535	forward	MVA-HANP-102	88863	91397	2535	forward
Virion core (Cop-D2L)	D2L	CPXV119	NoF1-114	111854	112294	441	reverse	MVA-HANP-103	91356	91796	441	reverse
Virion core (Cop-D3R)	D3R	CPXV120	NoF1-115	112287	113000	714	forward	MVA-HANP-104	91789	92490	702	forward
Uracil-DNA glycosylase, DNA polymerase processivity factor (Cop-D4R)	D4R	CPXV121	NoF1-116	113000	113656	657	forward	MVA-HANP-105	92490	93146	657	forward
NTPase, DNA primase (Cop-D5R)	D5R	CPXV122	NoF1-117	113688	116045	2358	forward	MVA-HANP-106	93178	95535	2358	forward
Morphogenesis, VETF-s (early transcription factor or small) (Cop-D6R)	D6R	CPXV123	NoF1-118	116086	117999	1914	forward	MVA-HANP-107	95576	97489	1914	forward
RNA polymerase subunit (RPO18) (Cop-D7R)	D7R	CPXV124	NoF1-119	118026	118511	486	forward	MVA-HANP-108	97516	98001	486	forward
Carbonic anhydrase, GAG-binding IMV membrane protein (Cop-D8L)	D8L	CPXV125	NoF1-120	118474	119388	915	reverse	MVA-HANP-109	97964	98878	915	reverse
mRNA decapping enzyme (Cop-D9R)	D9R	CPXV126	NoF1-121	119430	120071	642	forward	MVA-HANP-110	98920	99561	642	forward
mRNA decapping enzyme (Cop-D10R)	D10R	CPXV127	NoF1-122	120068	120814	747	forward	MVA-HANP-111	99558	100304	747	forward
ATPase, NPH1 (Cop-D11L)	D11L	CPXV128	NoF1-123	120815	122710	1896	reverse	MVA-HANP-112	100305	102200	1896	reverse
mRNA capping enzyme small subunit (Cop-D12L)	D12L	CPXV129	NoF1-124	122744	123607	864	reverse	MVA-HANP-113	102235	103098	864	reverse
VV_Tan-unkown-16	-	CPXV130					overlap	-				
Trimeric virion coat protein (rifampicin res) (Cop-D13L)	D13L	CPXV131	NoF1-125	123638	125293	1656	reverse	MVA-HANP-114	103129	104784	1656	reverse
VLTF-2 (late transcription factor 2) (Cop-A1L)	A1L	CPXV132	NoF1-126	125317	125769	453	reverse	MVA-HANP-115	104808	105260	453	reverse
VLTF-3 (late transcription factor 3) (Cop-A2L)	A2L	CPXV133	NoF1-127	125790	126464	675	reverse	MVA-HANP-116	105281	105955	675	reverse
S-S bond formation pathway protein (Cop-A2.5L)	A2.5L	CPXV134	NoF1-128	126461	126694	234	reverse	MVA-HANP-117	105952	106182	231	reverse
P4b precursor (Cop-A3L)	A3L	CPXV135	NoF1-129	126709	128643	1935	reverse	MVA-HANP-118	106197	108131	1935	reverse
39kDa virion core protein (Cop-A4L)	A4L	CPXV136	NoF1-130	128696	129577	882	reverse	MVA-HANP-119	108184	109002	819	reverse
RNA polymerase subunit (RPO19) (Cop-A5R)	A5R	CPXV137	NoF1-131	129615	130109	495	forward	MVA-HANP-120	109040	109534	495	forward
Virial membrane assembly proteins (VMAP), core protein (Cop-A6L)	A6L	CPXV138	NoF1-132	130106	131224	1119	reverse	MVA-HANP-121	109531	110649	1119	reverse
VETF-L (early transcription factor large) (Cop- A7L)	A7L	CPXV139	NoF1-133	131248	133380	2133	reverse	MVA-HANP-122	110673	112805	2133	reverse
VLTF-3 34kda subunit (Cop-A8R)	A8R	CPXV140	NoF1-134	133434	134300	867	forward	MVA-HANP-123	112859	113725	867	forward
Virial membrane associated, early morphogenesis protein (Cop-A9L)	A9L	CPXV141	NoF1-135	134293	134640	348	reverse	MVA-HANP-124	113718	114002	285	reverse
P4a precursor (Cop-A10L)	A10L	CPXV142	NoF1-136	134641	137322	2682	reverse	MVA-HANP-125	114003	116678	2676	reverse
Virial membrane assembly proteins (VMAP) (Cop-A11R)	A11R	CPXV143	NoF1-137	137337	138293	957	forward	MVA-HANP-126	116693	117649	957	forward
Virion core and cleavage processing protein (Co p-A12L)	A12L	CPXV144	NoF1-138	138295	138873	579	reverse	MVA-HANP-127	117651	118214	564	reverse
IMV membrane protein, virion maturation (Cop-A13L)	A13L	CPXV145	NoF1-139	138897	139109	213	reverse	MVA-HANP-128	118238	118450	213	reverse
Essential IMV membrane protein (Cop-A14L)	A14L	CPXV146	NoF1-140	139217	139489	273	reverse	MVA-HANP-129	118558	118830	273	reverse
Non-essential IMV membrane protein (Cop-A14.5L)	A14.5L	CPXV147	NoF1-141	139506	139667	162	reverse	MVA-HANP-130	118847	119008	162	reverse
Core protein (Cop-A15L)	A15L	CPXV148	NoF1-142	139657	139941	285	reverse	MVA-HANP-131	118998	119282	285	reverse

Myristylated protein, essential for entry/fusion (Cop-A16L)	A16L	CPXV149	NoF1-143	139925	141058	1134	reverse	MVA-HANP-132	119266	120399	1134	reverse
IMV membrane protein (Cop-A17L)	A17L	CPXV150	NoF1-144	141061	141669	609	reverse	MVA-HANP-133	120402	121013	612	reverse
DNA helicase, transcript release factor (Cop-A18R)	A18R	CPXV151	NoF1-145	141684	143165	1482	forward	MVA-HANP-134	121028	122509	1482	forward
Zinc finger-like protein (Cop-A19L)	A19L	CPXV152	NoF1-146	143146	143379	234	reverse	MVA-HANP-135	122490	122723	234	reverse
IMV membrane protein, entry/fusion complex component (Cop-A21L)	A21L	CPXV153	NoF1-147	143380	143733	354	reverse	MVA-HANP-136	122724	123077	354	reverse
DNA polymerase processivity factor (Cop-A20R)	A20R	CPXV154	NoF1-148	143732	145012	1281	forward	MVA-HANP-137	123076	124356	1281	forward
Holliday junction resolvase (Cop-A22R)	A22R	CPXV155	NoF1-149	144942	145505	564	forward	MVA-HANP-138	124286	124849	564	forward
VITF-3 45kda subunit (Cop-A23R)	A23R	CPXV156	NoF1-150	145525	146673	1149	forward	MVA-HANP-139	124869	126017	1149	forward
RNA polymerase subunit (RPO132) (Cop-A24R)	A24R	rpo132/CPXV157	NoF1-151	146670	150164	3495	forward	MVA-HANP-140	126039	129509	3471	forward
A-type inclusion protein (Cop-A25L)	A25L	CPXV158	NoF1-152	150142	153918	3777	reverse	MVA-HANP-141 ^f	129514	129711	198	reverse
Unknown (CPV-B-160)	-	CPXV160			overlap			-				
P4c precursor (Cop-A26L)	A26L	CPXV161	NoF1-153	153964	155532	1569	reverse	MVA-HANP-142 ^f	130297	130989	693	reverse
IMV surface protein, fusion protein (Cop-A27L)	A27L	CPXV162	NoF1-154	155584	155916	333	reverse	MVA-HANP-143	131039	131371	333	reverse
IMV MPVirus entry (Cop-A28L)	A28L	CPXV163	NoF1-155	155917	156357	441	reverse	MVA-HANP-144	131372	131812	441	reverse
RNA polymerase subunit (RPO35) (Cop-A29L)	A29L	CPXV164	NoF1-156	156358	157275	918	reverse	MVA-HANP-145	131813	132730	918	reverse
IMV protein (Cop-A30L)	A30L	CPXV165	NoF1-157	157238	157468	231	reverse	MVA-HANP-146	132693	132926	234	reverse
Viral membrane assembly proteins (VMAP) (Cop-A30.5L)	A30.5L	165.5	NoF1-158	157501	157629	129	reverse	MVA-HANP-147	132959	133087	129	reverse
Hypothetical protein (Cop-A31R)	A31R	CPXV166	NoF1-159	157628	158041	414	forward	MVA-HANP-148	133086	133463	378	forward
ATPase/DNA packaging protein (Cop-A32L)	A32L	CPXV167	NoF1-160	158011	158820	810	reverse	MVA-HANP-149	133433	134242	810	reverse
EEV membrane phosphoglycoprotein, C-type lectin-like domain (Cop-A33R)	A33R	CPXV168	NoF1-161	158938	159513	576	forward	MVA-HANP-150	134360	134917	558	forward
C-type lectin-like IEV/EEV glycoprotein (Cop-A34R)	A34R	CPXV169	NoF1-162	159537	160043	507	forward	MVA-HANP-151	134941	135447	507	forward
VV-Cop-A ORF M	-	CPXV170			overlap			-				
MHC class II antigen presentation inhibitor (Co p-A35R)	A35R	CPXV171	NoF1-163	160089	160619	531	forward	MVA-HANP-152	135491	136021	531	forward
IEV transmembrane phosphoprotein (Cop-A36R)	A36R	CPXV172	NoF1-164	160683	161351	669	forward	MVA-HANP-153	136088	136714	627	forward
Hypothetical protein (Cop-A37R)	A37R	CPXV173	NoF1-165	161418	162209	792	forward	MVA-HANP-154	136778	137569	792	forward
Unknown (Gar-A43R)	-	CPXV174	NoF1-166	162317	162502	186	forward	-				
CD47-like, integral membrane protein (Cop-A38L)	A38L	CPXV175	NoF1-167	162499	163332	834	reverse	MVA-HANP-155	137829	138662	834	reverse
Semaphorin (Cop-A39R)	A39R	CPXV176	NoF1-168	163348	164559	1212	forward	MVA-HANP-156 ^f	138679	138930	252	forward
Lectin homolog (Cop-A40R)	A40R	CPXV177	NoF1-169	164581	165063	483	forward	MVA-HANP-157 ^f	139236	139868	633	forward
Chemokine binding protein (Cop-A41L)	A41L	CPXV178	NoF1-170	165161	165823	663	reverse	MVA-HANP-158	139894	140400	507	forward
Profilin-like protein, ATI-localized (Cop-A42R)	A42R	CPXV179	NoF1-171	166002	166403	402	forward	MVA-HANP-159	140439	141098	660	reverse
Type I membrane glycoprotein (Cop-A43R)	A43R	CPXV180	NoF1-172	166441	167022	582	forward	MVA-HANP-160	141270	141656	387	forward
Hypothetical protein (Cop-A43.5R)	A43.5R	CPXV181	NoF1-173	167025	167270	246	forward	MVA-HANP-161	141694	142266	573	forward
3 beta-hydroxysteroid dehydrogenase/delta 5->4 isomerase (Cop-A44L)	A44L	CPXV182	NoF1-174	167362	168402	1041	reverse	MVA-HANP-162	142274	142510	237	forward
Inactive Cu-Zn superoxide dismutase-like virion protein (Cop-A45R)	A45R	CPXV183	NoF1-175	168449	168826	378	forward	MVA-HANP-163	142610	143650	1041	reverse
IL-1/TLR signaling inhibitor (Cop-A46R)	A46R	CPXV184	NoF1-176	168816	169538	723	forward	MVA-HANP-164	143697	144062	366	forward
Immunoprevalent protein (Cop-A47L)	A47L	CPXV185	NoF1-177	169674	170408	735	reverse	MVA-HANP-165	144052	144774	723	forward
Thymidylate kinase (Cop-A48R)	A48R	CPXV186	NoF1-178	170281	171123	843	reverse	MVA-HANP-166	144822	145538	717	reverse
Putative phosphotransferase/anion transport protein (Cop-A49R)	A49R	CPXV187	NoF1-179	171172	171660	489	forward	MVA-HANP-167	145637	146251	615	forward
ATP-dependent DNA ligase (Cop-A50R)	A50R	CPXV188	NoF1-180	171693	173357	1665	forward	MVA-HANP-168	146275	146763	489	forward
Hypothetical protein (Cop-A51R)	A51R	CPXV189	NoF1-181	173410	174414	1005	forward	MVA-HANP-169	146795	148453	1659	forward
Toll/IL-1 receptor-like protein, IL-1, NFkB signaling inhibitor (Cop-A52R)	A52R	CPXV190	NoF1-182	174483	175055	573	forward	MVA-HANP-170	148499	149644	1146	forward
TNF receptor (CrmC) (Cop-A53R)	A53R	CrmC/CPXV191	-					-				
CPV-B-192	-	CPXV192	NoF1-183	175819	175989	171	forward	-				
BTB Kelch-domain containing protein; CRL complex (Cop-A55R)	A55R	CPXV193	NoF1-184	176193	177884	1692	forward	-				
Hemagglutinin (Cop-A56R)	A56R	CPXV194	NoF1-185	177936	178850	915	forward	MVA-HANP-171	152967	153914	948	forward
Guanylate kinase (Cop-A56.5R)	A57R	CPXV195	NoF1-186	178867	179460	594	forward	MVA-HANP-172 ^f	154210	154503	294	forward
Ser/Thr Kinase (Cop-B1R)	B1R	CPXV196	NoF1-187	179610	180509	900	forward	MVA-HANP-173	154654	155556	903	forward
Schlafen (Cop-B2R)	B2R	CPXV197	NoF1-188	180579	182096	1518	forward	MVA-HANP-174 ^f	155695	155985	291	forward
	B3R							MVA-HANP-175 ^f	155840	156271	432	forward
								MVA-HANP-176 ^f	156468	157007	540	forward
Ankyrin (Cop-B4R)	B4R	CPXV198	NoF1-189	182360	184045	1686	forward	MVA-HANP-177 ^f	157234	157767	534	forward
								MVA-HANP-178 ^f	157658	158887	1230	forward
EEV type-1 membrane glycoprotein, protective antigen (Cop-B5R)	B5R	CPXV199	NoF1-190	184149	185102	954	forward	MVA-HANP-179	158975	159928	954	forward
Ankyrin-like protein (Cop-B6R)	B6R	CPXV200	NoF1-191	185201	185500	300	forward	MVA-HANP-180	160025	160546	522	forward

Virulence, ER resident (Cop-B7R)	B7R	CPXV201	NoF1-192	185774	186319	546	forward	MVA-HANP-181	160584	161117	534	forward
Soluble IFN-g receptor-like protein (Cop-B8R)	B8R	CPXV202	NoF1-193	186371	187171	801	forward	MVA-HANP-182 ^f	161172	161852	681	forward
ER-localized apoptosis regulator (Cop-B9R)	B9R	CPXV203	NoF1-194	187192	187929	738	forward	MVA-HANP-183	162009	162227	219	forward
Kelch-like protein (Cop-B10R)	B10R	CPXV204	NoF1-195	188076	189581	1506	forward	MVA-HANP-184	162190	162666	477	forward
Hypothetical protein (Cop-B11R)	B11R	CPXV205	NoF1-196	189663	189887	225	forward	MVA-HANP-185	162738	162962	225	forward
Ser/Thr Kinase (Cop-B12R)	B12R	CPXV206	NoF1-197	189954	190817	864	forward	MVA-HANP-186	163029	163880	852	forward
Serp1n 1,2,3 (Cop-K2L)	B13R	CrmA/CPXV207	NoF1-198	190914	191948	1035	forward	MVA-HANP-187 ^f	163988	164338	351	forward
	B14R							MVA-HANP-188 ^f	164313	164981	669	forward
Hypothetical protein (Cop-C16L)	B15R	CPXV208	NoF1-199	192079	192528	450	forward	MVA-HANP-189	165057	165488	432	forward
IL-1 beta receptor (Cop-B16R)	B16R	CPXV209	NoF1-200	192612	193589	978	forward	MVA-HANP-190	165572	166552	981	forward
IL-1 beta inhibitor (Cop-B17L)	B17L	CPXV210	NoF1-201	193637	194659	1023	reverse	MVA-HANP-191	166598	167620	1023	reverse
Ankyrin (Cop-B18R)	B18R	CPXV211	NoF1-202	194801	196525	1725	forward	MVA-HANP-192	167760	169484	1725	forward
IFN-alpha beta receptor glycoprotein (Cop-B19R)	B19R	CPXV212	NoF1-203	196544	197641	1098	forward	MVA-HANP-193 ^f	169550	170254	705	forward
Ankyrin (Cop-B20R)	B20R	CPXV213	NoF1-204	197702	200059	2358	forward	-				
CPV-B-214	-	CPXV214		overlap				-				
kelch-like protein (EVM-167)	-	CPXV215	NoF1-205	200162	201835	1674	forward	-				
Hypothetical protein (Cop-C11.5R)	C11.5R	CPXV216	-					-				
Serp1n 1,2,3 (Cop-K2L)	C12L	CPXV217	NoF1-206	202015	203124	1110	forward	-				
Hypothetical protein (Cop-C14L)	C14L	CPXV218	NoF1-207	203301	203882	582	forward	-				
Surface glycoprotein	-	CPXV219	NoF1-208	204128	209893	5766	forward	MVA-HANP-194 ^f	170753	170965	213	forward
Ankyrin (Cop-C19L)	C19L	CPXV220	NoF1-209	210110	211915	1806	forward	-				
TNF receptor (CrmD)	-	CPXV221	NoF1-210	211922	212890	969	forward	-				
Hypothetical protein (Cop-C16L)	B22R	CPXV222	NoF1-211	213564	214025	462	forward	MVA-HANP-195	171448	172014	567	forward
Ankyrin (Cop-C17L)	B23R/C17L	CPXV223	NoF1-212	214240	216246	2007	forward	MVA-HANP-196 ^f	172082	172783	702	forward
								MVA-HANP-197 ^f	172860	173168	309	forward
Ankyrin-like repeat containing protein	-	CPXV224	NoF1-213	216286	216375	90	forward	-				
Ankyrin (Cop-C19L)	B25R/C19L	CPXV225	NoF1-214	216457	218223	1767	forward	MVA-HANP-198 ^f	173856	174386	531	forward
TNF receptor (CrmB) (Cop-C22L)	B28R/C22L	crmB/CPXV226	NoF1-215	218301	219374	1074	forward	-				
Chemokine binding protein (Cop-C23L)	B29R/C23L	vCCI/CPXV227	NoF1-216	219448	220185	738	forward	MVA-HANP-199 ^f	174818	175228	411	forward
CPV-B-002	-	CPXV228	NoF1-217	220214	220441	228	forward	-				

f= CDs was fragmented, disrupted or partially deleted

RAP94 (RNA pol assoc protein) (Cop-H4L)	NoF1-109	MVA-HANP-098	x		NoF1-109	104463	106850	2388	reverse	x		NoF1-109	104463	106850	2388	reverse	x	NoF1-109	105147	107534	2388	reverse	
VLTF-4 (late transcription factor 4) (Cop-H5R)	NoF1-110	MVA-HANP-099	x		NoF1-110	107036	107656	621	forward	x		NoF1-110	107036	107656	621	forward	x	NoF1-110	107720	108340	621	forward	
DNA topoisomerase type I (Cop-H6R)	NoF1-111	MVA-HANP-100	x		NoF1-111	107657	108601	945	forward	x		NoF1-111	107657	108601	945	forward	x	NoF1-111	108341	109285	945	forward	
CPV-B-116		-																					
Viral membrane assembly proteins (VMAP) (Cop-H7R)	NoF1-112	MVA-HANP-101	x		NoF1-112	108639	109079	441	forward	x		NoF1-112	108639	109079	441	forward	x	NoF1-112	109323	109763	441	forward	
mRNA capping enzyme large subunit (Cop-D1R)	NoF1-113	MVA-HANP-102	x	x	MVA-HANP-102	109123	111657	2535	forward	x		NoF1-113	109123	111657	2535	forward	x	MVA-HANP-10	109807	112341	2535	forward	
Virion core (Cop-D2L)	NoF1-114	MVA-HANP-103	x	x	MVA-HANP-103	111616	112056	441	reverse		x	MVA-HANP-10	111616	112056	441	reverse	x	MVA-HANP-10	112300	112740	441	reverse	
Virion core (Cop-D3R)	NoF1-115	MVA-HANP-104	x	x	MVA-HANP-104	112049	112750	702	forward	x	x	MVA-HANP-10	112049	112750	702	forward	x	MVA-HANP-10	112733	113434	702	forward	
Uracil-DNA glycosylase, DNA polymerase processivity factor (Cop-D4R)	NoF1-116	MVA-HANP-105	x	x	MVA-HANP-105	112750	113406	657	forward	x	x	MVA-HANP-10	112750	113406	657	forward	x	MVA-HANP-10	113434	114050	657	forward	
NTPase, DNA primase (Cop-D5R)	NoF1-117	MVA-HANP-106	x	x	MVA-HANP-106	113438	115795	2358	forward	x	x	MVA-HANP-10	113438	115795	2358	forward	x	MVA-HANP-10	114122	116479	2358	forward	
Morphogenesis, VETF-s (early transcription factor) (Cop-D6R)	NoF1-118	MVA-HANP-107	x	x	MVA-HANP-107	115836	117749	1914	forward		x	MVA-HANP-10	115836	117749	1914	forward		x	MVA-HANP-10	116520	118433	1914	forward
RNA polymerase subunit (RPO18) (Cop-D7R)	NoF1-119	MVA-HANP-108	x	x	MVA-HANP-108	117776	118261	486	forward		x	MVA-HANP-10	117776	118261	486	forward		x	MVA-HANP-10	118460	118945	486	forward
Carbonic anhydrase, GAG-binding IMV membrane protein (Cop-D8L)	NoF1-120	MVA-HANP-109	x	x	MVA-HANP-109	118224	119138	915	reverse		x	MVA-HANP-10	118224	119138	915	reverse		x	MVA-HANP-10	118908	119822	915	reverse
mRNA decapping enzyme (Cop-D9R)	NoF1-121	MVA-HANP-110	x	x	MVA-HANP-110	119180	119821	642	forward	x	x	MVA-HANP-11	119180	119821	642	forward	x	MVA-HANP-11	119864	120505	642	forward	
mRNA decapping enzyme (Cop-D10R)	NoF1-122	MVA-HANP-111	x	x	MVA-HANP-111	119818	120564	747	forward	x	x	MVA-HANP-11	119818	120564	747	forward	x	MVA-HANP-11	120502	121248	747	forward	
ATPase, NPH1 (Cop-D11L)	NoF1-123	MVA-HANP-112	x	x	MVA-HANP-112	120565	122460	1896	reverse	x	x	MVA-HANP-11	120565	122460	1896	reverse	x	MVA-HANP-11	121249	123144	1896	reverse	
mRNA capping enzyme small subunit (Cop-D12L)	NoF1-124	MVA-HANP-113	x	x	MVA-HANP-113	122495	123358	864	reverse	x	x	MVA-HANP-11	122495	123358	864	reverse	x	MVA-HANP-11	123179	124042	864	reverse	
VV_Tan-unkown-16		-																					
Trimeric virion coat protein (rifampicin res) (Cop-D13L)	NoF1-125	MVA-HANP-114	x	x	MVA-HANP-114	123389	125044	1656	reverse	x		NoF1-125	123389	125044	1656	reverse	x	MVA-HANP-11	124073	125728	1656	reverse	
VLTF-2 (late transcription factor 2) (Cop-A1L)	NoF1-126	MVA-HANP-115	x	x	MVA-HANP-115	125068	125520	453	reverse	x	x	MVA-HANP-11	125068	125520	453	reverse	x	MVA-HANP-11	125752	126204	453	reverse	
VLTF-3 (late transcription factor 3) (Cop-A2L)	NoF1-127	MVA-HANP-116	x	x	MVA-HANP-116	125541	126215	675	reverse	x	x	MVA-HANP-11	125541	126215	675	reverse	x	MVA-HANP-11	126225	126899	675	reverse	
S-S bond formation pathway protein (Cop-A2.5L)	NoF1-128	MVA-HANP-117	x	x	MVA-HANP-117	126212	126442	231	reverse	x	x	MVA-HANP-11	126212	126442	231	reverse	x	MVA-HANP-11	126896	127126	231	reverse	
P4b precursor (Cop-A3L)	NoF1-129	MVA-HANP-118	x		NoF1-129	126457	128391	1935	reverse	x		NoF1-129	126460	128394	1935	reverse		MVA-HANP-11	127141	129075	1935	reverse	
39kDa virion core protein (Cop-A4L)	NoF1-130	MVA-HANP-119	x		NoF1-130	128444	129325	882	reverse	x		NoF1-130	128447	129328	882	reverse	x	NoF1-130	129128	130009	882	reverse	
RNA polymerase subunit (RPO19) (Cop-A5R)	NoF1-131	MVA-HANP-120	x		NoF1-131	129363	129857	495	forward	x		NoF1-131	129366	129860	495	forward	x	NoF1-131	130047	130541	495	forward	
Viral membrane assembly proteins (VMAP), core protein (Cop-A6L)	NoF1-132	MVA-HANP-121	x		NoF1-132	129854	130972	1119	reverse	x		NoF1-132	129857	130975	1119	reverse	x	NoF1-132	130538	131656	1119	reverse	
VETF-L (early transcription factor large) (Cop-A7L)	NoF1-133	MVA-HANP-122	x		NoF1-133	130996	133128	2133	reverse	x		NoF1-133	130999	133121	2133	reverse	x	NoF1-133	131680	133812	2133	reverse	
VITF-3 34kDa subunit (Cop-A8R)	NoF1-134	MVA-HANP-123	x		NoF1-134	133182	134048	867	forward	x		NoF1-134	133185	134051	867	forward	x	NoF1-134	133866	134732	867	forward	
Viral membrane associated, early morphogenesis protein (Cop-A9L)	NoF1-135	MVA-HANP-124	x		NoF1-135	134041	134388	348	reverse	x		NoF1-135	134044	134391	348	reverse	x	NoF1-135	134725	135072	348	reverse	
P4a precursor (Cop-A10L)	NoF1-136	MVA-HANP-125	x		NoF1-136	134389	137070	2682	reverse	x		NoF1-136	134392	137073	2682	reverse	x	NoF1-136	135073	137554	2682	reverse	
Viral membrane assembly proteins (VMAP) (Cop-A11R)	NoF1-137	MVA-HANP-126	x		NoF1-137	137085	138041	957	forward	x		NoF1-137	137088	138044	957	forward	x	MVA-HANP-12	137769	138725	957	forward	
Virion core and cleavage processing protein (Cop-A12L)	NoF1-138	MVA-HANP-127	x		NoF1-138	138043	138621	579	reverse	x		NoF1-138	138046	138624	579	reverse	x	NoF1-138	138727	139305	579	reverse	
IMV membrane protein, virion maturation (Cop-A13L)	NoF1-139	MVA-HANP-128	x		NoF1-139	138645	138857	213	reverse	x		NoF1-139	138648	138860	213	reverse	x	NoF1-139	139329	139541	213	reverse	
Essential IMV membrane protein (Cop-A14L)	NoF1-140	MVA-HANP-129	x		NoF1-140	138965	139273	273	reverse	x		NoF1-140	138968	139240	273	reverse	x	NoF1-140	139649	139921	273	reverse	
Non-essential IMV membrane protein (Cop-A14.5L)	NoF1-141	MVA-HANP-130	x		NoF1-141	139254	139415	162	reverse	x		NoF1-141	139257	139418	162	reverse	x	NoF1-141	139938	140099	162	reverse	
Core protein (Cop-A15L)	NoF1-142	MVA-HANP-131	x		NoF1-142	139405	139689	285	reverse	x		NoF1-142	139408	139692	285	reverse	x	NoF1-142	140089	140373	285	reverse	
Myristylated protein, essential for entry/fusion (Cop-A16L)	NoF1-143	MVA-HANP-132	x		NoF1-143	139673	140806	1134	reverse	x		NoF1-143	139676	140809	1134	reverse	x	NoF1-143	140357	141490	1134	reverse	
IMV membrane protein (Cop-A17L)	NoF1-144	MVA-HANP-133	x		NoF1-144	140809	141417	609	reverse	x		NoF1-144	140812	141420	609	reverse	x	NoF1-144	141493	142101	609	reverse	
DNA helicase, transcript release factor (Cop-A18R)	NoF1-145	MVA-HANP-134	x		NoF1-145	141432	142913	1482	forward	x		NoF1-145	141435	142916	1482	forward	x	NoF1-145	142116	143597	1482	forward	
Zinc finger-like protein (Cop-A19L)	NoF1-146	MVA-HANP-135	x		NoF1-146	142894	143127	234	reverse	x		NoF1-146	142897	143130	234	reverse	x	NoF1-146	143578	143811	234	reverse	
IMV membrane protein, entry/fusion complex component (Cop-A21L)	NoF1-147	MVA-HANP-136	x		NoF1-147	143128	143481	354	reverse	x		NoF1-147	143131	143484	354	reverse	x	NoF1-147	143812	144165	354	reverse	
DNA polymerase processivity factor (Cop-A20R)	NoF1-148	MVA-HANP-137	x		NoF1-148	143480	144760	1281	forward	x		NoF1-148	143483	144763	1281	forward	x	NoF1-148	144164	145444	1281	forward	
Holiday junction resolvase (Cop-A22R)	NoF1-149	MVA-HANP-138	x		NoF1-149	144690	145253	564	forward	x		NoF1-149	144693	145256	564	forward	x	NoF1-149	145374	145937	564	forward	
VITF-3 45kDa subunit (Cop-A23R)	NoF1-150	MVA-HANP-139	x		NoF1-150	145273	146421	1149	forward	x		NoF1-150	145276	146424	1149	forward	x	NoF1-150	145957	147105	1149	forward	
RNA polymerase subunit (RPO132) (Cop-A24R)	NoF1-151	MVA-HANP-140	x		NoF1-151	146418	149912	3495	forward	x		NoF1-151	146421	149915	3495	forward	x	NoF1-151	147102	150596	3495	forward	
A-type inclusion protein (Cop-A25L)	NoF1-152	MVA-HANP-141	f	x	MVA-HANP-141	149917	150141	225	reverse	x		NoF1-152	149893	153669	3777	reverse	x	MVA-HANP-14	150601	150798	198	reverse	
Unknown (CPV-B-160)		-																					
P4c precursor (Cop-A26L)	NoF1-153	MVA-HANP-142	f	x	MVA-HANP-142	150727	151419	693	reverse	x		NoF1-153	153715	155283	1569	reverse	x	MVA-HANP-14	151384	152076	693	reverse	
IMV surface protein, fusion protein (Cop-A27L)	NoF1-154	MVA-HANP-143	x		NoF1-154	151471	151803	333	reverse	x		NoF1-154	155335	155667	333	reverse	x	MVA-HANP-14	152126	152458	333	reverse	
IMV MPVirus entry (Cop-A28L)	NoF1-155	MVA-HANP-144	x		NoF1-155	151804	152244	441	reverse	x		NoF1-155	155668	156108	441	reverse	x	MVA-HANP-14	152459	152899	441	reverse	
RNA polymerase subunit (RPO35) (Cop-A29L)	NoF1-156	MVA-HANP-145	x		NoF1-156	152245	153162	918	reverse	x		NoF1-156	156109	157026	918	reverse	x	MVA-HANP-14	152900	153817	918	reverse	
IMV protein (Cop-A30L)	NoF1-157	MVA-HANP-146	x		NoF1-157	153125	153855	231	reverse	x		NoF1-157	156989	157219	231	reverse	x	MVA-HANP-14	153780	154013	231	reverse	
Viral membrane assembly proteins (VMAP) (Cop-A30.5L)	NoF1-158	MVA-HANP-147	x		NoF1-158	153388	153516	129	reverse	x		NoF1-158	157252	157380	129	reverse	x	MVA-HANP-14	154046	15			

Semaphorin (Cop-A39R)	NoF1-168	MVA-HANP-156 ^f	x		NoF1-168	159235	160446	1212	forward	x		NoF1-168	163099	164310	1212	forward		x	MVA-HANP-155	159766	160017	252	forward		
		MVA-HANP-157 ^f																	x	MVA-HANP-155	160323	160955	633	forward	
Lectin homolog (Cop-A40R)	NoF1-169	MVA-HANP-158	x		NoF1-169	160468	160950	483	forward	x		NoF1-169	164332	164814	483	forward		x	MVA-HANP-155	160977	161483	507	forward		
Chemokine binding protein (Cop-A41L)	NoF1-170	MVA-HANP-159	x		NoF1-170	161048	161710	663	reverse	x		NoF1-170	164912	165574	663	reverse		x	MVA-HANP-155	161522	162181	660	reverse		
Profilin-like protein, ATI-localized (Cop-A42R)	NoF1-171	MVA-HANP-160	x		NoF1-171	161889	162290	402	forward	x		NoF1-171	165753	166154	402	forward		x	MVA-HANP-166	162353	162739	387	forward		
Type I membrane glycoprotein (Cop-A43R)	NoF1-172	MVA-HANP-161	x		NoF1-172	162328	162909	582	forward	x		NoF1-172	166192	166773	582	forward		x	MVA-HANP-166	162777	163358	582	forward		
Hypothetical protein (Cop-A43.5R)	NoF1-173	MVA-HANP-162	x		NoF1-173	162912	163157	246	forward	x		NoF1-173	166776	167021	246	forward		x	MVA-HANP-166	163361	163606	246	forward		
3 beta-hydroxysteroid dehydrogenase/delta 5->4 isomerase (Cop-A44L)	NoF1-174	MVA-HANP-163		x	MVA-HANP-163	163249	164289	1041	reverse	x		NoF1-174	167113	168153	1041	reverse		x	MVA-HANP-166	163698	164738	1041	reverse		
Inactive Cu-Zn superoxide dismutase-like virion protein (Cop-A45R)	NoF1-175	MVA-HANP-164		x	MVA-HANP-164	164336	164701	366	forward	x		NoF1-175	168200	168577	378	forward		x	MVA-HANP-166	164785	165162	378	forward		
IL-1/TLR signaling inhibitor (Cop-A46R)	NoF1-176	MVA-HANP-165		x	MVA-HANP-165	164691	165413	723	forward	x		NoF1-176	168967	169289	723	forward		x	MVA-HANP-166	165152	165874	723	forward		
Immunoprecipitant protein (Cop-A47L)	NoF1-177	MVA-HANP-166		x	MVA-HANP-166	165461	166177	717	reverse	x		NoF1-177	169425	170159	735	reverse		x	MVA-HANP-166	166010	166744	735	reverse		
Thymidylate kinase (Cop-A48R)	NoF1-178	MVA-HANP-167		x	MVA-HANP-167	166276	166890	615	forward	x		NoF1-178	170032	170874	843	forward		x	MVA-HANP-166	166617	167459	843	forward		
Putative phosphotransferase/anion transport protein (Cop-A49R)	NoF1-179	MVA-HANP-168		x	MVA-HANP-168	166914	167402	489	forward	x		NoF1-179	170923	171411	489	forward		x	MVA-HANP-166	167508	167996	489	forward		
ATP-dependent DNA ligase (Cop-A50R)	NoF1-180	MVA-HANP-169		x	MVA-HANP-169	167434	169092	1659	forward	x		NoF1-180	171444	173108	1665	forward		x	MVA-HANP-166	168029	169693	1665	forward		
Hypothetical protein (Cop-A51R)	NoF1-181	MVA-HANP-170		x	MVA-HANP-170	169138	170283	1146	forward		x	MVA-HANP-170	173154	174299	1146	forward		x	MVA-HANP-166	169746	170750	1005	forward		
TollIL-1 receptor-like protein, IL-1, NFkB signaling inhibitor (Cop-A52R)	NoF1-182	-																		NoF1-182	170819	171391	573	forward	
TNF receptor (CmC) (Cop-A53R)	-	-																							
CPV-B-192	NoF1-183	-																			NoF1-183	172155	172325	171	forward
BTB Kelch-domain containing protein, CRL complex (Cop-A55R)	NoF1-184	-																			NoF1-184	172529	174220	1692	forward
Hemagglutinin (Cop-A56R)	NoF1-185	MVA-HANP-171		x	MVA-HANP-171	173605	174552	948	forward		x	MVA-HANP-171	177621	178568	948	forward		x	MVA-HANP-166	174272	175186	915	forward		
Guanylate kinase (Cop-A56.5R)	NoF1-186	MVA-HANP-172		x	MVA-HANP-172	174848	175141	294	forward	x		NoF1-186	178586	178699	114	forward		x	MVA-HANP-166	175203	175796	594	forward		
SerThr Kinase (Cop-B1R)	NoF1-187	MVA-HANP-173		x	MVA-HANP-173	175292	176194	903	forward	x		NoF1-187	179318	180217	900	forward		x	MVA-HANP-166	175946	176845	900	forward		
Schlafen (Cop-B2R)	NoF1-188	MVA-HANP-174 ^f		x	MVA-HANP-174	176333	176623	291	forward	x		NoF1-188	180287	181804	1518	forward		x	MVA-HANP-166	176915	178432	1518	forward		
		MVA-HANP-175 ^f		x	MVA-HANP-175	176478	176909	432	forward																
		MVA-HANP-176		x	MVA-HANP-176	177106	177645	540	forward																
		MVA-HANP-177 ^f		x	MVA-HANP-177	177872	178405	534	forward	x		NoF1-189	182068	183753	1686	forward		x	MVA-HANP-166	178696	180381	1686	forward		
Ankyrin (Cop-B4R)	NoF1-189	MVA-HANP-178 ^f		x	MVA-HANP-178	178296	179525	1230	forward												NoF1-189	180485	181438	954	forward
EEV type-1 membrane glycoprotein, protective antigen (Cop-B5R)	NoF1-190	MVA-HANP-179		x	MVA-HANP-179	179613	180566	954	forward	x		NoF1-190	183857	184810	954	forward		x	MVA-HANP-166	180485	181438	954	forward		
Ankyrin-like protein (Cop-B6R)	NoF1-191	MVA-HANP-180		x	MVA-HANP-180	180663	181184	522	forward	x		NoF1-191	184909	185208	300	forward		x	MVA-HANP-166	181537	181836	300	forward		
Virulence, ER resident (Cop-B7R)	NoF1-192	MVA-HANP-181		x	MVA-HANP-181	181222	181755	534	forward	x		NoF1-192	185482	186027	546	forward		x	MVA-HANP-166	182110	182655	546	forward		
Soluble IFN-gamma receptor-like protein (Cop-B8R)	NoF1-193	MVA-HANP-182		x	MVA-HANP-182	181810	182490	681	forward	x		NoF1-193	186079	186879	801	forward		x	MVA-HANP-166	182707	183507	801	forward		
ER-localized apoptosis regulator (Cop-B9R)	NoF1-194	MVA-HANP-183		x	MVA-HANP-183	182647	182865	219	forward	x		NoF1-194	186900	187637	738	forward		x	MVA-HANP-166	183528	184265	738	forward		
Kelch-like protein (Cop-B10R)	NoF1-195	MVA-HANP-184		x	MVA-HANP-184	182828	183304	477	forward	x		NoF1-195	187784	189289	1506	forward		x	MVA-HANP-166	184412	185917	1506	forward		
Hypothetical protein (Cop-B11R)	NoF1-196	MVA-HANP-185		x	MVA-HANP-185	183376	183600	225	forward	x		NoF1-196	189371	189595	225	forward		x	MVA-HANP-166	185999	186223	225	forward		
SerThr Kinase (Cop-B12R)	NoF1-197	MVA-HANP-186		x	MVA-HANP-186	183667	184518	852	forward	x		NoF1-197	189662	190525	864	forward		x	MVA-HANP-166	186290	187153	864	forward		
Serpin 1,2,3 (Cop-K2L)	NoF1-198	MVA-HANP-187 ^f		x	MVA-HANP-187	184626	184976	351	forward	x		NoF1-198	190622	191656	1035	forward		x	MVA-HANP-166	187250	188284	1035	forward		
		MVA-HANP-188 ^f		x	MVA-HANP-188	184951	185619	669	forward																
Hypothetical protein (Cop-C16L)	NoF1-199	MVA-HANP-189		x	MVA-HANP-189	185695	186126	432	forward	x		NoF1-199	191787	192236	450	forward		x	MVA-HANP-166	188415	188864	450	forward		
IL-1 beta receptor (Cop-B16R)	NoF1-200	MVA-HANP-190		x	MVA-HANP-190	186210	187190	981	forward	x		NoF1-200	192320	193297	978	forward		x	MVA-HANP-166	188948	189925	978	forward		
IL-1 beta inhibitor (Cop-B17L)	NoF1-201	MVA-HANP-191		x	MVA-HANP-191	187236	188258	1023	reverse	x		NoF1-201	193345	194367	1023	reverse		x	MVA-HANP-166	189973	190995	1023	reverse		
Ankyrin (Cop-B18R)	NoF1-202	MVA-HANP-192		x	MVA-HANP-192	188398	190122	1725	forward	x		NoF1-202	194509	196233	1725	forward		x	MVA-HANP-166	191137	192861	1725	forward		
IFN-alpha/beta receptor glycoprotein (Cop-B19R)	NoF1-203	MVA-HANP-193 ^f		x	MVA-HANP-193	190188	190892	705	forward	x		NoF1-203	196252	197349	1098	forward		x	MVA-HANP-166	192880	193977	1098	forward		
Ankyrin (Cop-B20R)	NoF1-204	-										NoF1-204	197410	199767	2358	forward		x	MVA-HANP-166	194038	196395	2358	forward		
CPV-B-214	overlap	-																							
kelch-like protein (EVM-167)	NoF1-205	-										NoF1-205	199870	201543	1674	forward		x	MVA-HANP-166	196498	198171	1674	forward		
Hypothetical protein (Cop-C11.5R)	-	-																							
Serpin 1,2,3 (Cop-K2L)	NoF1-206	-										NoF1-206	201723	202832	1110	forward		x	MVA-HANP-166	198351	199460	1110	forward		
Hypothetical protein (Cop-C14L)	NoF1-207	-										NoF1-207	203009	203590	582	forward		x	MVA-HANP-166	199637	200218	582	forward		
Surface glycoprotein	NoF1-208	MVA-HANP-194 ^f		x	MVA-HANP-194	191391	191603	213	forward	x		NoF1-208	203836	209601	5766	forward		x	MVA-HANP-166	200464	206229	5766	forward		
Ankyrin (Cop-C19L)	NoF1-209	-										NoF1-209	209818	211623	1806	forward		x	MVA-HANP-166	206446	208251	1806	forward		
TNF receptor (CmD)	NoF1-210	-										NoF1-210	211630	212598	969	forward		x	MVA-HANP-166	208258	209226	969	forward		
Hypothetical protein (Cop-C16L)	NoF1-211	MVA-HANP-195		x	MVA-HANP-195	192086	192652	567	forward	x		NoF1-211	213272	213733	462	forward		x	MVA-HANP-166	209900	210361	462	forward		
Ankyrin (Cop-C17L)	NoF1-212	MVA-HANP-196 ^f		x	MVA-HANP-196	192869	194875	2007	forward	x		NoF1-212	213948	215954	2007	forward		x	MVA-HANP-166	210578	212584	2007	forward		
		MVA-HANP-197 ^f																							
Ankyrin-like repeat containing protein	NoF1-213	-		x	NoF1-213	194915	195004	90	forward	x		NoF1-213	215994	216083	90	forward		x	MVA-HANP-166	212624	212713	90	forward		
Ankyrin (Cop-C19L)																									

Function	CPXV-NoF1	MVA-HANP	R7							R8							R9						
	CDS	CDS	CPXV-NoF1	MVA-HANP	CDS	Start	Stop	Length	Direction	CPXV-NoF1	MVA-HANP	CDS	Start	Stop	Length	Direction	CPXV-NoF1	MVA-HANP	CDS	Start	Stop	Length	Direction
CPV-B-002	NoF1-001	-	x		NoF1-001	1302	1529	228	reverse	x		NoF1-001	1304	1531	228	reverse	x		NoF1-001	814	1041	228	reverse
Chemokine binding protein (Cop-C23L)	NoF1-002	MVA-HANP-001 ^f		x	MVA-HANP-002	1752	2162	411	reverse	x		NoF1-002	1560	2297	738	reverse	x		NoF1-002	1070	1807	738	reverse
CPV-B-004	overlap	-																					
TNF receptor (CrmB) (Cop-C22L)	NoF1-003	-								x		NoF1-003	2371	3444	1074	reverse	x		NoF1-003	1881	2954	1074	reverse
Ankyrin (Cop-C19L)	NoF1-004	MVA-HANP-002 ^f		x	MVA-HANP-003	2594	3124	531	reverse	x		NoF1-004	3522	5288	1767	reverse	x		NoF1-004	3032	4798	1767	reverse
Ankyrin-like repeat containing protein	NoF1-005	-								x		NoF1-005	5370	5459	90	reverse	x		NoF1-005	4880	4969	90	reverse
Ankyrin (Cop-C17L)	NoF1-006	MVA-HANP-003 ^f MVA-HANP-004 ^f MVA-HANP-005 ^f	x		NoF1-006	3232	5076	1845	reverse	x		NoF1-006	5499	7505	2007	reverse	x		NoF1-006	5009	7015	2007	reverse
Hypothetical protein (Cop-C16L)	NoF1-007	-	x		NoF1-007	5289	5750	462	reverse	x		NoF1-007	7720	8181	462	reverse	x		NoF1-007	7234	7695	462	reverse
Alpha amanitin target protein (Cop-N2L)	NoF1-008	-	x		NoF1-008	5921	6574	654	reverse	x		NoF1-008	8352	9005	654	reverse	x		NoF1-008	7856	8519	654	reverse
BTB Kelch-domain containing protein; CRL complex (Cop-A55R)	NoF1-009	-	x		NoF1-009	6887	7480	594	reverse	x		NoF1-009	9318	9911	594	reverse	x		NoF1-009	8832	9425	594	reverse
Ankyrin (Cop-B20R)	NoF1-010	-	x		NoF1-010	7807	9822	2016	reverse	x		NoF1-010	10238	12253	2016	reverse	x		NoF1-010	9752	11767	2016	reverse
C-type lectin domain containing protein	NoF1-011	-	x		NoF1-011	10049	10258	210	reverse	x		NoF1-011	12480	12689	210	reverse	x		NoF1-011	11994	12203	210	reverse
BTB Kelch-domain containing protein; CRL complex (Cop-A55R)	NoF1-012	-	x		NoF1-012	10686	11297	612	reverse	x		NoF1-012	13117	13728	612	reverse	x		NoF1-012	12631	13242	612	reverse
TNF receptor (CrmB) (Cop-C22L)	NoF1-013	-	x		NoF1-013	11372	11980	609	reverse	x		NoF1-013	13803	14411	609	reverse	x		NoF1-013	13317	13925	609	reverse
TNF-alpha receptor like protein	NoF1-014	-	x		NoF1-014	11977	12309	333	reverse	x		NoF1-014	14408	14740	333	reverse	x		NoF1-014	13922	14254	333	reverse
Ankyrin (Cop-B18R)	NoF1-015	-	x		NoF1-015	12384	14687	2304	reverse	x		NoF1-015	14815	17118	2304	reverse	x		NoF1-015	14329	16632	2304	reverse
Ankyrin (CPXV-017)	NoF1-016	-	x		NoF1-016	14963	16270	1308	reverse	x		NoF1-016	17394	18701	1308	reverse	x		NoF1-016	16908	18215	1308	reverse
MPV-Z-N3R	NoF1-017	-	x		NoF1-017	16369	16884	516	reverse	x		NoF1-017	18800	19315	516	reverse	x		NoF1-017	18314	18829	516	reverse
Ankyrin (Cop-B18R)	NoF1-018	-	x		NoF1-018	16947	19568	2622	reverse	x		NoF1-018	19378	21993	2616	reverse	x		NoF1-018	18892	21507	2616	reverse
Host range protein	NoF1-019	-	x		NoF1-019	19616	20134	519	reverse	x		NoF1-019	22041	22559	519	reverse	x		NoF1-019	21555	22073	519	reverse
Secreted EGF-like protein (Cop-C11R)	NoF1-020	MVA-HANP-006			NoF1-020	20301	20726	426	forward	x		NoF1-020	22726	23151	426	forward	x		NoF1-020	22240	22665	426	forward
IL-1 receptor antagonist (Cop-C10L)	NoF1-021	MVA-HANP-007	x		NoF1-021	20879	21874	996	reverse	x		NoF1-021	23304	24299	996	reverse	x		NoF1-021	22818	23813	996	reverse
Zinc finger-like protein	NoF1-022	MVA-HANP-008 ^f	x		NoF1-022	22389	23117	729	forward	x		NoF1-022	24814	25542	729	forward	x		NoF1-022	24328	25056	729	forward
Soluble IL 18 binding protein (Bsh-D7L)	NoF1-023	MVA-HANP-009	x		NoF1-023	23266	23646	381	reverse	x		NoF1-023	25691	26071	381	reverse	x		NoF1-023	25205	25585	381	reverse
Ankyrin/Host Range (Bang-D8L)	NoF1-024	MVA-HANP-010 ^f MVA-HANP-011 ^f MVA-HANP-012 ^f MVA-HANP-013 ^f MVA-HANP-014 ^f	x		NoF1-024	23705	25720	2016	reverse	x		NoF1-024	26130	28145	2016	reverse	x		NoF1-024	25644	27659	2016	reverse
ANK-containing protein	NoF1-025	MVA-HANP-015	x		NoF1-025	25834	26025	192	reverse	x		NoF1-025	28259	28450	192	reverse	x		NoF1-025	27773	27964	192	reverse
Ankyrin; Type I IFN resistance (Cop-C9L)	NoF1-026	MVA-HANP-016 ^f MVA-HANP-017 ^f MVA-HANP-018 ^f	x		NoF1-026	26199	28103	1905	reverse	x		NoF1-026	28624	30528	1905	reverse	x		NoF1-026	28138	30042	1905	reverse
Unknown (Cop-C8L)	NoF1-027	MVA-HANP-019	x		NoF1-027	28145	28702	558	reverse	x		NoF1-027	30570	31127	558	reverse	x		NoF1-027	30084	30641	558	reverse
Type I IFN inhibitor (Cop-C7L)	NoF1-028	MVA-HANP-020	x		NoF1-028	28774	29226	453	reverse	x		NoF1-028	31199	31651	453	reverse	x		NoF1-028	30713	31165	453	reverse
Bcl-2-like protein; IFN-beta inhibitor (Cop-C6L)	NoF1-029	MVA-HANP-021	x		NoF1-029	29457	29924	468	reverse	x		NoF1-029	31882	32349	468	reverse	x		NoF1-029	31396	31863	468	reverse
Kelch-like protein (Cop-C5L)	overlap	-																					
Kelch-like protein (Cop-C5L)	NoF1-030	-	x		NoF1-030	30257	30634	378	reverse	x		NoF1-030	32682	33059	378	reverse	x		NoF1-030	32196	32573	378	reverse
IL-1 receptor antagonist (Cop-C10L)	NoF1-031	-	x		NoF1-031	30695	31642	948	reverse	x		NoF1-031	33120	34067	948	reverse	x		NoF1-031	32634	33581	948	reverse
Complement binding (secreted) (Cop-C3L)	NoF1-032	-	x		NoF1-032	31709	32503	795	reverse	x		NoF1-032	34134	34928	795	reverse	x		NoF1-032	33648	34442	795	reverse
POZ/BTB Kelch domain protein (Cop-C2L)	NoF1-033	-	x		NoF1-033	32566	34104	1539	reverse	x		NoF1-033	34991	36529	1539	reverse	x		NoF1-033	34505	36043	1539	reverse
Putative TLR signalling inhibitor (Cop-C1L)	NoF1-034	-	x		NoF1-034	34173	34811	639	reverse	x		NoF1-034	36598	37236	639	reverse	x		NoF1-034	36112	36750	639	reverse
Anti-apoptotic Bcl-2-like protein (Cop-N1L)	NoF1-035	MVA-HANP-022 ^f	x		NoF1-035	34853	35206	354	reverse	x		NoF1-035	37278	37631	354	reverse	x		NoF1-035	36792	37145	354	reverse
Alpha amanitin target protein (Cop-N2L)	NoF1-036	MVA-HANP-023	x		NoF1-036	35328	35858	531	reverse	x		NoF1-036	37753	38283	531	reverse	x		NoF1-036	37267	37797	531	reverse
ANK-containing protein; apoptosis inhibitor (Cop-M1L)	NoF1-037	-	x		NoF1-037	35901	37316	1416	reverse	x		NoF1-037	38326	39741	1416	reverse	x		NoF1-037	37840	39255	1416	reverse
NFKB inhibitor (Cop-M2L)	NoF1-038	-	x		NoF1-038	37294	37956	663	reverse	x		NoF1-038	39719	40381	663	reverse	x		NoF1-038	39233	39895	663	reverse
Ankyrin/NFKB inhibitor (Cop-K1L)	NoF1-039	MVA-HANP-024 ^f	x		NoF1-039	38080	38937	858	reverse	x		NoF1-039	40505	41362	858	reverse	x		NoF1-039	40019	40876	858	reverse
Serpin I.2.3 (Cop-K2L)	NoF1-040	MVA-HANP-025	x		NoF1-040	39295	40416	1122	reverse	x		NoF1-040	41720	42841	1122	reverse	x		NoF1-040	42299	42355	57	reverse
IFN resistance; PKR/IFN-alpha inhibitor (Cop-K3 L)	NoF1-041	MVA-HANP-026	x		NoF1-041	40467	40733	267	reverse	x		NoF1-041	42892	43158	267	reverse	x		NoF1-041	42406	42672	267	reverse
Phospholipase-D-like protein (Cop-K4L)	NoF1-042	MVA-HANP-027	x		NoF1-042	40793	42067	1275	reverse	x		NoF1-042	43218	44492	1275	reverse	x		NoF1-042	42732	44006	1275	reverse
Monoglyceride lipase (Cop-K5L/K6L)	NoF1-043	MVA-HANP-028 ^f MVA-HANP-029 ^f	x		NoF1-043	42095	42925	831	reverse	x		NoF1-043	44520	45350	831	reverse	x		NoF1-043	44034	44864	831	reverse
Host immune response repressor (Cop-K7R)	NoF1-044	MVA-HANP-030	x		NoF1-044	43063	43512	450	forward	x		NoF1-044	45488	45937	450	forward	x		NoF1-044	45002	45451	450	forward
CPV-B-047	overlap	-																					
Caspase-9 (apoptosis) inhibitor (mitochondrial-associated) (Cop-F1L)	NoF1-045	MVA-HANP-031	x		NoF1-045	43586	44329	744	reverse	x		NoF1-045	46011	46754	744	reverse	x		NoF1-045	45525	46268	744	reverse
dUTPase (Cop-F2L)	NoF1-046	MVA-HANP-032	x		NoF1-046	44329	44772	444	reverse	x		NoF1-046	46754	47197	444	reverse	x		NoF1-046	46268	46711	444	reverse
Kelch-like protein (Cop-F3L)	NoF1-047	MVA-HANP-033	x		NoF1-047	44796	46238	1443	reverse	x		NoF1-047	47221	48663	1443	reverse	x		NoF1-047	46735	48177	1443	reverse
Ribonucleotide reductase small subunit (Cop-F4L)	NoF1-048	MVA-HANP-034	x		NoF1-048	46249	47250	1002	reverse	x		NoF1-048	48674	49675	1002	reverse	x		NoF1-048	48188	49189	1002	reverse
36Da major membrane protein (Cop-F5L)	NoF1-049	MVA-HANP-035 ^f MVA-HANP-036 ^f	x		NoF1-049	47240	48205	966	reverse	x		NoF1-049	49665	50630	966	reverse	x		NoF1-049	49179	50144	966	reverse
Hypothetical protein (Cop-F6L)	NoF1-050	MVA-HANP-037	x		NoF1-050	48235	48450	216	reverse	x		NoF1-050	50660	50875	216	reverse	x		NoF1-050	50174	50389	216	reverse

Hypothetical protein (Cop-F7L)	NoF1-051	MVA-HANP-038	x		NoF1-051	48466	48711	246	reverse	x		NoF1-051	50891	51136	246	reverse	x		NoF1-051	50405	50650	246	reverse
Cytoplasmic protein (Cop-F8L)	NoF1-052	MVA-HANP-039	x		NoF1-052	48868	49065	198	reverse	x		NoF1-052	51437	51634	198	reverse	x		NoF1-052	50943	51140	198	reverse
S-S bond formation pathway protein substrate (Cop-F9L)	NoF1-053	MVA-HANP-040	x		NoF1-053	49126	49764	639	reverse	x		NoF1-053	51695	52333	639	reverse	x		NoF1-053	51201	51839	639	reverse
Essential Ser/Thr kinase morph (Cop-F10L)	NoF1-054	MVA-HANP-041	x		NoF1-054	49751	51070	1320	reverse	x		NoF1-054	52320	53639	1320	reverse	x		NoF1-054	51826	53145	1320	reverse
VV_Cop-F ORF D	overlap	-																					
RhoA signalling inhibitor, virus release protein (Cop-F11L)	NoF1-055	MVA-HANP-042 [†]	x		NoF1-055	51093	52157	1065	reverse	x		NoF1-055	53662	54726	1065	reverse	x		NoF1-055	53168	54232	1065	reverse
		MVA-HANP-043 [†]																					
EEV maturation protein (Cop-F12L)	NoF1-056	MVA-HANP-044	x		NoF1-056	52200	54104	1905	reverse	x		NoF1-056	54769	56673	1905	reverse	x		NoF1-056	54275	56179	1905	reverse
Palmitoylated EEV membrane glycoprotein (Cop-F13L)	NoF1-057	MVA-HANP-045	x		NoF1-057	54138	55256	1119	reverse	x		NoF1-057	56707	57825	1119	reverse	x		NoF1-057	56213	57331	1119	reverse
Unknown (Cop-F14L)	NoF1-058	MVA-HANP-046	x		NoF1-058	55274	55495	222	reverse	x		NoF1-058	57843	58064	222	reverse	x		NoF1-058	57349	57570	222	reverse
IMV protein (Cop-F14.5L)	-	MVA-HANP-047																					
CPV-B-063	NoF1-059	-	x		NoF1-059	55542	55700	159	forward	x		NoF1-059	58111	58269	159	forward	x		NoF1-059	57617	57775	159	forward
Unknown conserved protein (Cop-F15L)	NoF1-060	MVA-HANP-048	x		NoF1-060	55768	56244	477	reverse	x		NoF1-060	58337	58813	477	reverse	x		NoF1-060	57843	58319	477	reverse
Non-functional Serine Recombinase (Cop-F16L)	NoF1-061	MVA-HANP-049	x		NoF1-061	56244	56945	702	reverse	x		NoF1-061	58813	59514	702	reverse	x		NoF1-061	58319	59020	702	reverse
DNA-binding phosphoprotein (VP11); mTOR antagonist (Cop-F17R)	NoF1-062	MVA-HANP-050	x		NoF1-062	57008	57313	306	forward	x		NoF1-062	59577	59882	306	forward	x		NoF1-062	59083	59388	306	forward
Poly (A) polymerase catalytic subunit (VP55) (Cop-E1L)	NoF1-063	MVA-HANP-051	x		NoF1-063	57310	58749	1440	reverse	x		NoF1-063	59879	61318	1440	reverse	x		NoF1-063	59385	60824	1440	reverse
IEV morphogenesis (Cop-E2L)	NoF1-064	MVA-HANP-052	x		NoF1-064	58746	60959	2214	reverse	x		NoF1-064	61315	63528	2214	reverse	x		NoF1-064	60821	63034	2214	reverse
dsRNA-binding protein, IFN resistance/PKR inhibitor (Z-DNA binding) (Cop-E3L)	NoF1-065	MVA-HANP-053	x		NoF1-065	61090	61662	573	reverse	x		NoF1-065	63659	64231	573	reverse	x		NoF1-065	63165	63737	573	reverse
RNA polymerase subunit (RPO30) (Cop-E4L)	NoF1-066	MVA-HANP-054	x		NoF1-066	61717	62502	786	reverse	x		NoF1-066	64286	65071	786	reverse	x		NoF1-066	63792	64577	786	reverse
Virusome component (Cop-E5R)	NoF1-067	MVA-HANP-055	x		NoF1-067	62622	63575	954	forward	x		NoF1-067	65191	66144	954	forward	x		NoF1-067	64697	65650	954	forward
Virion protein (Cop-E6R)	NoF1-068	MVA-HANP-056	x		NoF1-068	63695	65398	1704	forward	x		NoF1-068	66264	67967	1704	forward	x		NoF1-068	65770	67473	1704	forward
Myristylated protein (Cop-E7R)	NoF1-069	MVA-HANP-057	x		NoF1-069	65460	65957	498	forward	x		NoF1-069	68029	68526	498	forward	x		NoF1-069	67535	68032	498	forward
ER-localized membrane protein, virion core protein (Cop-E8R)	NoF1-070	MVA-HANP-058	x		NoF1-070	66068	66889	822	forward	x		NoF1-070	68637	69458	822	forward	x		NoF1-070	68143	68964	822	forward
DNA polymerase (Cop-E9L)	NoF1-071	MVA-HANP-059	x		NoF1-071	66896	69913	3018	reverse	x		NoF1-071	69465	72482	3018	reverse	x		NoF1-071	68971	71988	3018	reverse
Sulfhydryl oxidase (FAD-linked) (Cop-E10R)	NoF1-072	MVA-HANP-060	x		NoF1-072	69945	70232	288	forward	x		NoF1-072	72514	72801	288	forward	x		NoF1-072	72020	72307	288	forward
Virion core protein (Cop-E11L)	NoF1-073	MVA-HANP-061	x		NoF1-073	70227	70616	390	reverse	x		NoF1-073	72796	73185	390	reverse	x		NoF1-073	72302	72691	390	reverse
	NoF1-074	MVA-HANP-062 [†]	x		NoF1-074	70603	72603	2001	reverse	x		NoF1-074	73172	75172	2001	reverse	x		NoF1-074	72678	74678	2001	reverse
		MVA-HANP-063 [†]																					
Glutaredoxin I (Cop-O2L)	NoF1-075	MVA-HANP-064	x		NoF1-075	72651	72977	327	reverse	x		NoF1-075	75220	75546	327	reverse	x		NoF1-075	74726	75052	327	reverse
Virus entry/fusion complex component (Cop-O3L)	NoF1-076	MVA-HANP-065	x		NoF1-076	73001	73108	108	reverse	x		NoF1-076	75570	75677	108	reverse	x		NoF1-076	75076	75183	108	reverse
DNA-binding core protein (Cop-I1L)	NoF1-077	MVA-HANP-066	x		NoF1-077	73123	74061	939	reverse	x		NoF1-077	75692	76630	939	reverse	x		NoF1-077	75198	76136	939	reverse
IMV membrane protein (Cop-I2L)	NoF1-078	MVA-HANP-067	x		NoF1-078	74068	74289	222	reverse	x		NoF1-078	76637	76858	222	reverse	x		NoF1-078	76143	76364	222	reverse
ssDNA-binding phosphoprotein (Cop-I3L)	NoF1-079	MVA-HANP-068	x		NoF1-079	74290	75099	810	reverse	x		NoF1-079	76859	77668	810	reverse	x		NoF1-079	76365	77174	810	reverse
Ribonucleotide reductase large subunit (Cop-I4L)	NoF1-080	MVA-HANP-069	x		NoF1-080	75182	77497	2316	reverse	x	MVA-HANP-069	77751	80066	2316	reverse	x		NoF1-080	77257	79572	2316	reverse	
IMV protein VP13 (Cop-I5L)	NoF1-081	MVA-HANP-070	x		NoF1-081	77524	77763	240	reverse	x		NoF1-081	80093	80332	240	reverse	x		NoF1-081	79599	79838	240	reverse
Telomere-binding protein (Cop-I6L)	NoF1-082	MVA-HANP-071	x		NoF1-082	77782	78930	1149	reverse	x		NoF1-082	80351	81499	1149	reverse	x		NoF1-082	79857	81005	1149	reverse
Virion core cysteine protease (Cop-I7L)	NoF1-083	MVA-HANP-072	x		NoF1-083	78923	80194	1272	reverse	x		NoF1-083	81492	82763	1272	reverse	x		NoF1-083	80998	82269	1272	reverse
RNA helicase, DEAH-NPH-II domain (Cop-I8R)	NoF1-084	MVA-HANP-073	x		NoF1-084	80200	82230	2031	forward	x		NoF1-084	82769	84799	2031	forward	x		NoF1-084	82275	84305	2031	forward
Metalloprotease (Cop-G1L)	NoF1-085	MVA-HANP-074	x		NoF1-085	82234	84009	1776	reverse	x		NoF1-085	84803	86578	1776	reverse	x		NoF1-085	84309	86084	1776	reverse
Entry/fusion complex component (Cop-G3L)	NoF1-086	MVA-HANP-075	x		NoF1-086	84006	84341	336	reverse	x		NoF1-086	86575	86910	336	reverse	x		NoF1-086	86081	86416	336	reverse
VLTF (late transcription elongation factor) (Cop-G2R)	NoF1-087	MVA-HANP-076	x		NoF1-087	84335	84997	663	forward	x		NoF1-087	86904	87566	663	forward	x		NoF1-087	86410	87072	663	forward
Glutaredoxin-like protein (Cop-G4L)	NoF1-088	MVA-HANP-077	x		NoF1-088	84967	85341	375	reverse	x		NoF1-088	87536	87910	375	reverse	x		NoF1-088	87042	87416	375	reverse
FEN1-like nuclease (Cop-G5R)	NoF1-089	MVA-HANP-078	x		NoF1-089	85344	86651	1308	forward	x	MVA-HANP-078	87913	89217	1305	forward	x		NoF1-089	87419	88726	1308	forward	
RNA polymerase subunit (RPO7) (Cop-G5.5R)	NoF1-090	MVA-HANP-079	x		NoF1-090	86659	86850	192	forward	x		NoF1-090	89225	89416	192	forward	x		NoF1-090	88734	88925	192	forward
NLPcP60 superfamily protein (Cop-G6R)	NoF1-091	MVA-HANP-080	x		NoF1-091	86852	87349	498	forward	x	MVA-HANP-080	89418	89915	498	forward	x		NoF1-091	88927	89424	498	forward	
Virion phosphoprotein, early morphogenesis (Cop-G7L)	NoF1-092	MVA-HANP-081	x		NoF1-092	87314	88429	1116	reverse	x	MVA-HANP-081	89880	90995	1116	reverse	x		NoF1-092	89389	90504	1116	reverse	
CC_Cop-G ORF B	overlap	-																					
VLTF-1 (late transcription factor 1) (Cop-G8R)	NoF1-093	MVA-HANP-082	x		NoF1-093	88460	89242	783	forward	x	MVA-HANP-082	91026	91808	783	forward	x		NoF1-093	90535	91317	783	forward	
Entry/fusion complex component, myristylated protein (Cop-G9R)	NoF1-094	MVA-HANP-083	x		NoF1-094	89262	90284	1023	forward	x	MVA-HANP-083	91828	92850	1023	forward	x		NoF1-094	91337	92359	1023	forward	
IMV membrane protein (Cop-L1R)	NoF1-095	MVA-HANP-084	x		NoF1-095	90285	91037	753	forward	x	MVA-HANP-084	92851	93603	753	forward	x		NoF1-095	92360	93112	753	forward	
Viral membrane assembly proteins (VMAP) (Cop-L2R)	NoF1-096	MVA-HANP-085	x		NoF1-096	91069	91335	267	forward	x	MVA-HANP-085	93635	93898	264	forward	x		NoF1-096	93144	93410	267	forward	
Internal virion protein (Cop-L3L)	NoF1-097	MVA-HANP-086	x		NoF1-097	91325	92377	1053	reverse	x	MVA-HANP-086	93888	94940	1053	reverse	x		NoF1-097	93400	94452	1053	reverse	
ssDNA binding protein (VP8) (Cop-L4R)	NoF1-098	MVA-HANP-087	x		NoF1-098	92402	93157	756	forward	x	MVA-HANP-087	94955	95720	756	forward	x		NoF1-098	94477	95232	756	forward	
Entry and Fusion IMV protein (Cop-L5R)	NoF1-099	MVA-HANP-088	x		NoF1-099	93167	93553	387	forward	x	MVA-HANP-088	95730	96116	387	forward	x		NoF1-099	95242	95628	387	forward	
Virion morph (Cop-J1R)	NoF1-100	MVA-HANP-089	x		NoF1-100	93510	93971	462	forward	x	MVA-HANP-089	96073	96534	462</									

VLTF-4 (late transcription factor 4) (Cop-H5R)	NoF1-110	MVA-HANP-099		x	MVA-HANP-099	105139	105750	612	forward		x	MVA-HANP-099	107703	108314	612	forward	x		NoF1-110	107724	107834	621	forward
DNA topoisomerase type I (Cop-H6R)	NoF1-111	MVA-HANP-100		x	MVA-HANP-100	105751	106695	945	forward		x	MVA-HANP-100	108315	109259	945	forward	x		NoF1-111	107835	108779	945	forward
CPV-B-116 overlap																							
Viral membrane assembly proteins (VMAP) (Cop-H7R)	NoF1-112	MVA-HANP-101		x	MVA-HANP-101	106732	107172	441	forward		x	MVA-HANP-101	109296	109736	441	forward	x		NoF1-112	108817	109257	441	forward
mRNA capping enzyme large subunit (Cop-D1R)	NoF1-113	MVA-HANP-102		x	MVA-HANP-102	107216	109750	2535	forward		x	MVA-HANP-102	109780	112314	2535	forward	x		NoF1-113	109301	111835	2535	forward
Virion core (Cop-D2L)	NoF1-114	MVA-HANP-103		x	MVA-HANP-103	109709	110149	441	reverse		x	MVA-HANP-103	112273	112713	441	reverse	x		NoF1-114	111794	112234	441	reverse
Virion core (Cop-D3R)	NoF1-115	MVA-HANP-104		x	MVA-HANP-104	110142	110843	702	forward		x	MVA-HANP-104	112706	113407	702	forward	x		NoF1-115	112227	112940	714	forward
Uracil-DNA glycosylase, DNA polymerase processivity factor (Cop-D4R)	NoF1-116	MVA-HANP-105		x	MVA-HANP-105	111499	111499	657	forward		x	MVA-HANP-105	113407	114063	657	forward	x		NoF1-116	112940	113596	657	forward
NTase, DNA primase (Cop-D5R)	NoF1-117	MVA-HANP-106		x	MVA-HANP-106	111531	113888	2358	forward		x	MVA-HANP-106	114095	116452	2358	forward	x		NoF1-117	113628	115985	2358	forward
Morphogenesis, VETF-s (early transcription factor) (Cop-D6R)	NoF1-118	MVA-HANP-107		x	MVA-HANP-107	113929	115842	1914	forward		x	MVA-HANP-107	116493	118406	1914	forward	x		NoF1-118	116026	117939	1914	forward
RNA polymerase subunit (RPO18) (Cop-D7R)	NoF1-119	MVA-HANP-108		x	MVA-HANP-108	115869	116354	486	forward		x	MVA-HANP-108	118433	118918	486	forward	x		NoF1-119	117966	118451	486	forward
Carbonic anhydrase, GAG-binding IMV membrane protein (Cop-D8L)	NoF1-120	MVA-HANP-109		x	MVA-HANP-109	116317	117231	915	reverse		x	MVA-HANP-109	118881	119795	915	reverse	x		NoF1-120	118414	119328	915	reverse
mRNA decapping enzyme (Cop-D9R)	NoF1-121	MVA-HANP-110		x	MVA-HANP-110	117273	117914	642	forward		x	MVA-HANP-110	119837	120478	642	forward	x		NoF1-121	119370	120011	642	forward
mRNA decapping enzyme (Cop-D10R)	NoF1-122	MVA-HANP-111		x	MVA-HANP-111	117911	118657	747	forward		x	NoF1-122	120475	121221	747	forward	x		NoF1-122	120008	120754	747	forward
ATPase, NPH1 (Cop-D11L)	NoF1-123	MVA-HANP-112		x	MVA-HANP-112	118658	120553	1896	reverse		x	NoF1-123	121222	123117	1896	reverse	x		NoF1-123	120755	122650	1896	reverse
mRNA capping enzyme small subunit (Cop-D12L)	NoF1-124	MVA-HANP-113		x	MVA-HANP-113	120588	121451	864	reverse		x	NoF1-124	123151	124014	864	reverse	x		NoF1-124	122684	123547	864	reverse
VV_Tan-unknown-16 overlap																							
Trimeric virion coat protein (trifunctional) (Cop-D13L)	NoF1-125	MVA-HANP-114		x	MVA-HANP-114	121482	123137	1656	reverse		x	MVA-HANP-114	124045	125700	1656	reverse	x		NoF1-125	123578	125233	1656	reverse
VLTF-2 (late transcription factor 2) (Cop-A1L)	NoF1-126	MVA-HANP-115		x	NoF1-126	123161	123613	453	reverse		x	NoF1-126	125724	126176	453	reverse	x		NoF1-126	125257	125709	453	reverse
VLTF-3 (late transcription factor 3) (Cop-A2L)	NoF1-127	MVA-HANP-116		x	NoF1-127	123634	124308	675	reverse		x	NoF1-127	126197	126871	675	reverse	x		NoF1-127	125730	126404	675	reverse
S-S bond formation pathway protein (Cop-A2.5L)	NoF1-128	MVA-HANP-117		x	NoF1-128	124305	124538	234	reverse		x	NoF1-128	126868	127101	234	reverse	x		NoF1-128	126401	126634	234	reverse
P4b precursor (Cop-A3L)	NoF1-129	MVA-HANP-118		x	MVA-HANP-118	124553	126487	1935	reverse		x	NoF1-129	127116	129050	1935	reverse	x		NoF1-129	126649	128583	1935	reverse
39kDa virion core protein (Cop-A4L)	NoF1-130	MVA-HANP-119		x	MVA-HANP-119	126540	127358	819	reverse		x	NoF1-130	129103	129957	855	reverse	x		NoF1-130	128636	129517	882	reverse
RNA polymerase subunit (RPO19) (Cop-A5R)	NoF1-131	MVA-HANP-120		x	MVA-HANP-120	127396	127890	495	forward		x	NoF1-131	129995	130489	495	forward	x		NoF1-131	129555	130049	495	forward
Viral membrane assembly proteins (VMAP), core protein (Cop-A6L)	NoF1-132	MVA-HANP-121		x	MVA-HANP-121	127887	129005	1119	reverse		x	NoF1-132	130486	131604	1119	reverse	x		NoF1-132	130046	131164	1119	reverse
VETf-L (early transcription factor large) (Cop-A7L)	NoF1-133	MVA-HANP-122		x	MVA-HANP-122	129029	131161	2133	reverse		x	NoF1-133	131628	133760	2133	reverse	x		NoF1-133	131188	133320	2133	reverse
VITF-3 34kDa subunit (Cop-ASR)	NoF1-134	MVA-HANP-123		x	MVA-HANP-123	131215	132081	867	forward		x	NoF1-134	133814	134680	867	forward	x		NoF1-134	133374	134240	867	forward
Viral membrane associated, early morphogenesis protein (Cop-A9L)	NoF1-135	MVA-HANP-124		x	MVA-HANP-124	132074	132358	285	reverse		x	NoF1-135	134673	135020	348	reverse	x		NoF1-135	134233	134580	348	reverse
P4a precursor (Cop-A10L)	NoF1-136	MVA-HANP-125		x	MVA-HANP-125	132359	135034	2676	reverse		x	NoF1-136	135021	137702	2682	reverse	x		NoF1-136	134581	137262	2682	reverse
Viral membrane assembly proteins (VMAP) (Cop-A11R)	NoF1-137	MVA-HANP-126		x	MVA-HANP-126	135049	136005	957	forward		x	NoF1-137	137717	138673	957	forward	x		NoF1-137	137277	138233	957	forward
Virion core and cleavage processing protein (Cop-A12L)	NoF1-138	MVA-HANP-127		x	NoF1-138	136007	136585	579	reverse		x	NoF1-138	138675	139253	579	reverse	x		NoF1-138	138235	138813	579	reverse
IMV membrane protein, virion maturation (Cop-A13L)	NoF1-139	MVA-HANP-128		x	NoF1-139	136609	136821	213	reverse		x	NoF1-139	139277	139489	213	reverse	x		NoF1-139	138837	139049	213	reverse
Essential IMV membrane protein (Cop-A14L)	NoF1-140	MVA-HANP-129		x	NoF1-140	136929	137201	273	reverse		x	NoF1-140	139597	139869	273	reverse	x		NoF1-140	139157	139429	273	reverse
Non-essential IMV membrane protein (Cop-A14.5L)	NoF1-141	MVA-HANP-130		x	NoF1-141	137218	137379	162	reverse		x	NoF1-141	139886	140047	162	reverse	x		NoF1-141	139446	139607	162	reverse
Core protein (Cop-A15L)	NoF1-142	MVA-HANP-131		x	NoF1-142	137369	137653	285	reverse		x	NoF1-142	140037	140321	285	reverse	x		NoF1-142	139597	139881	285	reverse
Mystified protein, essential for entry/fusion (Cop-A16L)	NoF1-143	MVA-HANP-132		x	NoF1-143	137637	138770	1134	reverse		x	NoF1-143	140305	141438	1134	reverse	x		NoF1-143	139865	140998	1134	reverse
IMV membrane protein (Cop-A17L)	NoF1-144	MVA-HANP-133		x	NoF1-144	138773	139381	609	reverse		x	NoF1-144	141441	142049	609	reverse	x		NoF1-144	141001	141609	609	reverse
DNA helicase, transcript release factor (Cop-A18R)	NoF1-145	MVA-HANP-134		x	NoF1-145	139396	140877	1482	forward		x	NoF1-145	142064	143545	1482	forward	x		NoF1-145	141624	143105	1482	reverse
Zinc finger-like protein (Cop-A19L)	NoF1-146	MVA-HANP-135		x	NoF1-146	140858	141091	234	reverse		x	NoF1-146	143526	143759	234	reverse	x		NoF1-146	143086	143319	234	reverse
IMV membrane protein, entry/fusion complex component (Cop-A21L)	NoF1-147	MVA-HANP-136		x	NoF1-147	141092	141445	354	reverse		x	NoF1-147	143760	144113	354	reverse	x		NoF1-147	143320	143673	354	reverse
DNA polymerase processivity factor (Cop-A20R)	NoF1-148	MVA-HANP-137		x	NoF1-148	141444	142724	1281	forward		x	NoF1-148	144112	145392	1281	forward	x		NoF1-148	143672	144952	1281	forward
Holiday junction resolvase (Cop-A22R)	NoF1-149	MVA-HANP-138		x	NoF1-149	142654	143217	564	forward		x	MVA-HANP-138	145322	145885	564	forward	x		NoF1-149	144882	145445	564	forward
VITF-3 45kDa subunit (Cop-A23R)	NoF1-150	MVA-HANP-139		x	NoF1-150	143237	144385	1149	forward		x	MVA-HANP-139	145905	147053	1149	forward	x		NoF1-150	145465	146613	1149	forward
RNA polymerase subunit (RPO132) (Cop-A24R)	NoF1-151	MVA-HANP-140		x	NoF1-151	144382	147876	3495	forward		x	MVA-HANP-140	147075	150545	3471	forward	x		NoF1-151	146610	150104	3495	forward
A-type inclusion protein (Cop-A25L)	NoF1-152	MVA-HANP-141		x	NoF1-152	147854	151630	3777	reverse		x	MVA-HANP-141	150550	150747	198	reverse	x		NoF1-152	150082	153858	3777	reverse
Unknown (CPV-B-160) overlap																							
P4c precursor (Cop-A26L)	NoF1-153	MVA-HANP-142		x	NoF1-153	151676	153244	1569	reverse		x	MVA-HANP-142	151333	152025	693	reverse	x		NoF1-153	153904	155472	1569	reverse
IMV surface protein, fusion protein (Cop-A27L)	NoF1-154	MVA-HANP-143		x	NoF1-154	153296	153628	333	reverse		x	MVA-HANP-143	152075	152407	333	reverse	x		NoF1-154	155524	155856	333	reverse
IMV MPVirus entry (Cop-A28L)	NoF1-155	MVA-HANP-144		x	NoF1-155	153629	154069	441	reverse		x	MVA-HANP-144	152408	152848	441	reverse	x		NoF1-155	155857	156297	441	reverse
RNA polymerase subunit (RPO35) (Cop-A29L)	NoF1-156	MVA-HANP-145		x	NoF1-156	154070	154987	918	reverse		x	NoF1-156	152849	153766	918	reverse	x		NoF1-156	156298	157215	918	reverse
IMV protein (Cop-A30L)	NoF1-157	MVA-HANP-146		x	NoF1-157	154950	155180	231	reverse		x	NoF1-157	153729	153959	231	reverse	x		NoF1-157	157178	157408	231	reverse
Viral membrane assembly proteins (VMAP) (Cop-A30.5L)	NoF1-158	MVA-HANP-147		x	NoF1-158	155213	155341	129	reverse		x	NoF1-158	153992	154210	129	reverse	x		NoF1-158	157441	157569	129	reverse
Hypothetical protein (Cop-A31R)	NoF1-159	MVA-HANP-148		x	NoF1-159	155340	155753	414	forward		x	NoF1-159	154119	154532	414	forward	x		NoF1-159	157568	157981	414	forward
ATPase/DNA packaging protein (Cop-A32L)	NoF1-160	MVA-HANP-149		x	NoF1-160	155723	156532	810	reverse		x	NoF1-160	154502	155311	810	reverse	x		NoF1-160	157951	158760	810	reverse
EEV membrane phosphoglycoprotein, C-type lectin-like domain (Cop-A33R)	NoF1-161	MVA-HANP-150		x	NoF1-161	156650	157225	576	forward		x	NoF1-161	155429	156004	576	forward	x		NoF1-161	158878	159453	576	forward
C-type lectin-like IEV/EEV glycoprotein (Cop-A34R)	NoF1-162	MVA-HANP-151		x	NoF1-162	157249	157755	507	forward		x	NoF1-162	156028	156534	507	forward	x		NoF1-162	159477	159983	507	forward
VV-Cop-A ORF M overlap																							
MHC class II antigen presentation inhibitor (Cop-A35R)	NoF1-163	MVA-HANP-152		x	NoF1-163	157801	158331	531	forward		x	NoF1-163	156580	157110	531	forward	x		NoF1-163	160029	160559	531	forward
IEV transmembrane phosphoprotein (Cop-A36R)	NoF1-164	MVA-HANP-153		x	NoF1-164	158395	159063	669	forward		x	NoF1-164	157174	15									

Lectin homolog (Cop-A40R)	NoF1-169	MVA-HANP-158	x		NoF1-169	162293	162775	483	forward	x		NoF1-169	161072	161554	483	forward	x		NoF1-169	164521	165003	483	forward	
Chemokine binding protein (Cop-A41L)	NoF1-170	MVA-HANP-159	x		NoF1-170	162873	163535	663	reverse	x		NoF1-170	161652	162314	663	reverse	x		NoF1-170	165101	165763	663	reverse	
Profilin-like protein, ATI-localized (Cop-A42R)	NoF1-171	MVA-HANP-160	x		NoF1-171	163714	164115	402	forward	x		NoF1-171	162493	162894	402	forward	x		NoF1-171	165942	166343	402	forward	
Type I membrane glycoprotein (Cop-A43R)	NoF1-172	MVA-HANP-161	x		NoF1-172	164513	164734	582	forward	x		NoF1-172	162932	163513	582	forward	x		NoF1-172	166381	166962	582	forward	
Hypothetical protein (Cop-A43.5R)	NoF1-173	MVA-HANP-162	x		NoF1-173	164737	164982	246	forward	x		NoF1-173	163516	163761	246	forward	x		NoF1-173	166965	167210	246	forward	
3 beta-hydroxysteroid dehydrogenase/delta 5->4 isomerase (Cop-A44L)	NoF1-174	MVA-HANP-163		x	MVA-HANP-163	165074	166114	1041	reverse	x		NoF1-174	163853	164893	1041	reverse	x		NoF1-174	167302	168342	1041	reverse	
Inactive Cu-Zn superoxide dismutase-like virion protein (Cop-A45R)	NoF1-175	MVA-HANP-164		x	MVA-HANP-164	166161	166526	366	forward	x		NoF1-175	164940	165317	378	forward	x		NoF1-175	168389	168766	378	forward	
IL-1/TLR signaling inhibitor (Cop-A46R)	NoF1-176	MVA-HANP-165	x		MVA-HANP-165	166516	167238	723	forward	x		NoF1-176	165307	166029	723	forward	x		NoF1-176	168756	169478	723	forward	
Immunoprecipitant protein (Cop-A47L)	NoF1-177	MVA-HANP-166	x		MVA-HANP-166	167286	168002	717	reverse	x		NoF1-177	166165	166889	735	reverse	x		NoF1-177	169614	170348	735	reverse	
Thymidylate kinase (Cop-A48R)	NoF1-178	MVA-HANP-167	x		MVA-HANP-167	168101	168715	615	forward	x		NoF1-178	166772	167614	843	forward	x		NoF1-178	170221	171063	843	forward	
Putative phosphotransferase/anion transport protein (Cop-A49R)	NoF1-179	MVA-HANP-168		x	MVA-HANP-168	168739	169227	489	forward	x		NoF1-179	167663	168150	488	forward	x		NoF1-179	171112	171600	489	forward	
ATP-dependent DNA ligase (Cop-A50R)	NoF1-180	MVA-HANP-169	x		MVA-HANP-169	169259	170917	1659	forward		x	MVA-HANP-169	168183	169841	1659	forward	x		NoF1-180	171633	173297	1665	forward	
Hypothetical protein (Cop-A51R)	NoF1-181	MVA-HANP-170	x		MVA-HANP-170	170970	172115	1146	forward		x	MVA-HANP-170	169887	171032	1146	forward	x		NoF1-181	173730	174354	1005	forward	
Toll-like receptor-like protein, IL-1, NFkB signaling inhibitor (Cop-A52R)	NoF1-182	-																x		NoF1-182	174423	174995	573	forward
TNF receptor (CmC) (Cop-A53R)	-	-																						
CPV-B-192	NoF1-183	-																x		NoF1-183	175759	175929	171	forward
BTB Kelch-domain containing protein; CRL complex (Cop-A55R)	NoF1-184	-																						
Hemagglutinin (Cop-A56R)	NoF1-185	MVA-HANP-171		x	MVA-HANP-171	175437	176384	948	forward		x	MVA-HANP-171	174354	175301	948	forward	x			NoF1-184	176133	177824	1692	forward
Guanylate kinase (Cop-A56.5R)	NoF1-186	MVA-HANP-172 ^f		x	MVA-HANP-172	176680	176973	294	forward		x	MVA-HANP-172	175597	175890	294	forward	x			NoF1-185	177876	178790	915	forward
Ser/Thr Kinase (Cop-B1R)	NoF1-187	MVA-HANP-173		x	MVA-HANP-173	177124	178026	903	forward		x	MVA-HANP-173	176040	176942	903	forward	x			NoF1-186	178807	179400	594	forward
		MVA-HANP-174 ^f		x	MVA-HANP-174	178165	178455	291	forward		x	MVA-HANP-174	177081	177371	291	forward	x			NoF1-187	179550	180449	900	forward
Schlafen (Cop-B2R)	NoF1-188	MVA-HANP-175 ^f		x	MVA-HANP-175	178310	178741	432	forward		x	MVA-HANP-175	177226	177657	432	forward	x			NoF1-188	180519	182036	1518	forward
		MVA-HANP-176		x	MVA-HANP-176	178938	179477	540	forward		x	MVA-HANP-176	177854	178393	540	forward	x							
		MVA-HANP-177 ^f		x	MVA-HANP-177	179704	180237	534	forward		x	MVA-HANP-177	178620	179153	534	forward	x			NoF1-188	180519	182036	1518	forward
Ankyrin (Cop-B4R)	NoF1-189	MVA-HANP-178 ^f		x	MVA-HANP-178	180128	181375	1248	forward		x	MVA-HANP-178	179044	180273	1230	forward	x			NoF1-189	182300	183985	1686	forward
EEV type-1 membrane glycoprotein, protective antigen (Cop-B5R)	NoF1-190	MVA-HANP-179	x		NoF1-190	181479	182432	954	forward		x	MVA-HANP-179	180361	181314	954	forward	x			NoF1-189	182300	183985	1686	forward
Ankyrin-like protein (Cop-B6R)	NoF1-191	MVA-HANP-180	x		NoF1-191	182531	182830	300	forward		x	MVA-HANP-180	184411	184932	522	forward	x			NoF1-190	184089	185042	954	forward
Virulence, ER resident (Cop-B7R)	NoF1-192	MVA-HANP-181	x		NoF1-192	183104	183649	546	forward		x	MVA-HANP-181	181970	182503	534	forward	x			NoF1-191	185141	185440	300	forward
Soluble IFN-gamma receptor-like protein (Cop-B8R)	NoF1-193	MVA-HANP-182 ^f	x		NoF1-193	183701	184501	801	forward		x	MVA-HANP-182	182558	183238	681	forward	x			NoF1-192	185714	186259	546	forward
ER-localized apoptosis regulator (Cop-B9R)	NoF1-194	MVA-HANP-183	x		NoF1-194	184522	185259	738	forward		x	MVA-HANP-183	183395	183613	219	forward	x			NoF1-193	186311	187111	801	forward
Kelch-like protein (Cop-B10R)	NoF1-195	MVA-HANP-184	x		NoF1-195	185406	186911	1506	forward		x	MVA-HANP-184	183576	184052	477	forward	x			NoF1-194	187132	187869	738	forward
Hypothetical protein (Cop-B11R)	NoF1-196	MVA-HANP-185	x		NoF1-196	186993	187217	225	forward		x	MVA-HANP-185	184124	184348	225	forward	x			NoF1-195	188016	189521	1506	forward
Ser/Thr Kinase (Cop-B12R)	NoF1-197	MVA-HANP-186	x		NoF1-197	187284	188147	864	forward		x	MVA-HANP-186	184415	185266	852	forward	x			NoF1-196	189603	189827	225	forward
		MVA-HANP-187 ^f		x	NoF1-198	188244	189278	1035	forward		x	MVA-HANP-187	185374	185724	351	forward	x			NoF1-197	189894	190757	864	forward
Serpin 1,2,3 (Cop-K2L)	NoF1-198	MVA-HANP-188 ^f		x	MVA-HANP-188	185699	186367	669	forward		x	MVA-HANP-188	186443	186874	432	forward	x			NoF1-198	190854	191888	1035	forward
Hypothetical protein (Cop-C16L)	NoF1-199	MVA-HANP-189	x		NoF1-199	189409	189858	450	forward		x	MVA-HANP-189	186443	186874	432	forward	x			NoF1-198	190854	191888	1035	forward
IL-1 beta receptor (Cop-B16R)	NoF1-200	MVA-HANP-190	x		NoF1-200	189942	190919	978	forward	x		NoF1-200	186958	187935	978	forward	x			NoF1-199	192019	192468	450	forward
IL-1 beta inhibitor (Cop-B17L)	NoF1-201	MVA-HANP-191	x		NoF1-201	190967	191989	1023	reverse		x	MVA-HANP-190	187981	189003	1023	reverse	x			NoF1-200	192552	193529	978	forward
Ankyrin (Cop-B18R)	NoF1-202	MVA-HANP-192	x		NoF1-202	192131	193855	1725	forward		x	MVA-HANP-191	187981	189003	1023	reverse	x			NoF1-201	193577	194599	1023	reverse
IFN-alpha/beta receptor glycoprotein (Cop-B19R)	NoF1-203	MVA-HANP-193 ^f	x		NoF1-203	193874	194971	1098	forward	x		NoF1-202	189143	190867	1725	forward	x			NoF1-202	194741	196465	1725	forward
Ankyrin (Cop-B20R)	NoF1-204	-	x		NoF1-204	195032	197389	2358	forward	x		NoF1-203	190886	191983	1098	forward	x			NoF1-203	196484	197581	1098	forward
CPV-B-214	overlap	-			NoF1-204	192044	194401	2358	forward	x		NoF1-204	192044	194401	2358	forward	x			NoF1-204	197642	199999	2358	forward
kelch-like protein (EVM-167)	NoF1-205	-	x		NoF1-205	197492	199165	1674	forward	x		NoF1-204	192044	194401	2358	forward	x			NoF1-205	200102	201775	1674	forward
Hypothetical protein (Cop-C11.5R)	-	-																						
Serpin 1,2,3 (Cop-K2L)	NoF1-206	-	x		NoF1-206	199345	200454	1110	forward	x		NoF1-205	194504	196177	1674	forward	x			NoF1-206	201955	203064	1110	forward
Hypothetical protein (Cop-C14L)	NoF1-207	-	x		NoF1-207	200631	201212	582	forward	x		NoF1-206	196357	197466	1110	forward	x			NoF1-207	203241	203822	582	forward
Surface glycoprotein	NoF1-208	MVA-HANP-194 ^f	x		NoF1-208	201458	207223	5766	forward	x		NoF1-207	197643	198224	582	forward	x			NoF1-208	204068	208933	5766	forward
Ankyrin (Cop-C19L)	NoF1-209	-	x		NoF1-209	202945	209245	1806	forward	x		NoF1-208	198470	204235	5766	forward	x			NoF1-209	210050	211855	1806	forward
TNF receptor (CmD)	NoF1-210	-	x		NoF1-210	202952	210220	969	forward	x		NoF1-209	204452	206257	1806	forward	x			NoF1-210	211862	212830	969	forward
Hypothetical protein (Cop-C16L)	NoF1-211	MVA-HANP-195	x		NoF1-211	210894	211355	462	forward	x		NoF1-210	206264	207232	969	forward	x			NoF1-211	213504	213965	462	forward
Ankyrin (Cop-C17L)	NoF1-212	MVA-HANP-196 ^f	x		NoF1-212	211568	213412	1845	forward	x		NoF1-211	207906	208367	462	forward	x			NoF1-212	214184	216190	2007	forward
		MVA-HANP-197 ^f																						
Ankyrin-like repeat containing protein	NoF1-213	-								x		NoF1-212	208582	210588	2007	forward	x			NoF1-213	216230	216319	90	

Function	CPXV-NoF1	MVA-HANP	R10							R11					R12									
	CDS	CDS	CPXV-NoF1	MVA-HANP	CDS	Start	Stop	Length	Direction	CPXV-NoF1	MVA-HANP	CDS	Start	Stop	Length	Direction	CPXV-NoF1	MVA-HANP	CDS	Start	Stop	Length	Direction	
CPV-B-002	NoF1-001	-	x		NoF1-001	90	317	228	reverse	x		NoF1-001	1206	1433	228	reverse								
Chemokine binding protein (Cop-C23L)	NoF1-002	MVA-HANP-001 ^f	x		NoF1-002	346	1083	738	reverse	x		NoF1-002	1462	2199	738	reverse		x	MVA-HANP-001	1095	1505	411	reverse	
CPV-B-004	overlap	-																						
TNF receptor (CrmB) (Cop-C22L)	NoF1-003	-	x		NoF1-003	1157	2230	1074	reverse	x		NoF1-003	2273	3346	1074	reverse								
Ankyrin (Cop-C19L)	NoF1-004	MVA-HANP-002 ^f	x		NoF1-004	2308	4074	1767	reverse	x		NoF1-004	3424	5190	1767	reverse		x	MVA-HANP-002	1937	2467	531	reverse	
Ankyrin-like repeat containing protein	NoF1-005	-	x		NoF1-005	4156	4245	90	reverse	x		NoF1-005	5272	5361	90	reverse								
Ankyrin (Cop-C17L)	NoF1-006	MVA-HANP-003 ^f	x		NoF1-006	4285	6291	2007	reverse	x		NoF1-006	5401	7407	2007	reverse		x	MVA-HANP-003	2988	3125	138	reverse	
		MVA-HANP-004 ^f																x	MVA-HANP-004	3155	3463	309	reverse	
		MVA-HANP-005 ^f																x	MVA-HANP-005	3540	4241	702	reverse	
Hypothetical protein (Cop-C16L)	NoF1-007	-	x		NoF1-007	6506	6967	462	reverse	x		NoF1-007	7620	8081	462	reverse	x		NoF1-007	4309	4770	462	reverse	
Alpha amanitin target protein (Cop-N2L)	NoF1-008	-	x		NoF1-008	7138	7791	654	reverse	x		NoF1-008	8252	8905	654	reverse	x		NoF1-008	4941	5594	654	reverse	
BTB Kekk-domain containing protein; CRL complex (Cop-A55R)	NoF1-009	-	x		NoF1-009	8104	8697	594	reverse	x		NoF1-009	9218	9811	594	reverse	x		NoF1-009	5907	6500	594	reverse	
Ankyrin (Cop-B20R)	NoF1-010	-	x		NoF1-010	9024	11039	2016	reverse	x		NoF1-010	10138	12153	2016	reverse	x		NoF1-010	6827	8842	2016	reverse	
C-type lectin domain containing protein	NoF1-011	-	x		NoF1-011	11266	11475	210	reverse	x		NoF1-011	12380	12589	210	reverse	x		NoF1-011	9069	9278	210	reverse	
BTB Kekk-domain containing protein; CRL complex (Cop-A55R)	NoF1-012	-	x		NoF1-012	11909	12514	612	reverse	x		NoF1-012	13017	13628	612	reverse	x		NoF1-012	9706	10317	612	reverse	
TNF receptor (CrmB) (Cop-C22L)	NoF1-013	-	x		NoF1-013	12589	13197	609	reverse	x		NoF1-013	13703	14311	609	reverse	x		NoF1-013	10392	11000	609	reverse	
TNF-alpha receptor like protein	NoF1-014	-	x		NoF1-014	13194	13526	333	reverse	x		NoF1-014	14308	14640	333	reverse	x		NoF1-014	10997	11329	333	reverse	
Ankyrin (Cop-B18R)	NoF1-015	-			deleted					x		NoF1-015	14715	17018	2304	reverse			deleted					
Ankyrin (CPXV-017)	NoF1-016	-			deleted					x		NoF1-016	17294	18601	1308	reverse			deleted					
MPV-Z-N3R	NoF1-017	-			deleted					x		NoF1-017	18700	19215	516	reverse			deleted					
Ankyrin (Cop-B18R)	NoF1-018	-			deleted					x		NoF1-018	19278	21893	2616	reverse			deleted					
Host range protein	NoF1-019	-			deleted					x		NoF1-019	21941	22459	519	reverse			deleted					
Secreted EGF-like protein (Cop-C11R)	NoF1-020	MVA-HANP-006			deleted					x		NoF1-020	22626	23051	426	forward			deleted					
IL-1 receptor antagonist (Cop-C10L)	NoF1-021	MVA-HANP-007			deleted					x		NoF1-021	23204	24199	996	reverse			deleted					
Zinc finger-like protein	NoF1-022	MVA-HANP-008 ^f			deleted					x		NoF1-022	24714	25442	729	forward			deleted					
Soluble IL-18 binding protein (Bsh-D7L)	NoF1-023	MVA-HANP-009			deleted					x		NoF1-023	25591	25971	381	reverse			deleted					
Ankyrin/Host Range (Bang-D8L)	NoF1-024	MVA-HANP-010 ^f			deleted					x		NoF1-024	26030	28045	2016	reverse			deleted					
		MVA-HANP-011 ^f			deleted														deleted					
		MVA-HANP-012 ^f			deleted														deleted					
		MVA-HANP-013 ^f			deleted														deleted					
ANK-containing protein	NoF1-025	MVA-HANP-014 ^f			deleted														deleted					
		MVA-HANP-015			deleted					x		NoF1-025	28159	28350	192	reverse			deleted					
Ankyrin; Type I IFN resistance (Cop-C9L)	NoF1-026	MVA-HANP-016 ^f			deleted					x		NoF1-026	28524	30428	1905	reverse			deleted					
		MVA-HANP-017 ^f			deleted														deleted					
		MVA-HANP-018 ^f			deleted														deleted					
Unknown (Cop-C8L)	NoF1-027	MVA-HANP-019			deleted				x		NoF1-027	30470	31027	558	reverse			deleted						
Type I IFN inhibitor (Cop-C7L)	NoF1-028	MVA-HANP-020			deleted				x		NoF1-028	31099	31551	453	reverse			deleted						
Bcl-2-like protein; IFN-beta inhibitor (Cop-C6L)	NoF1-029	MVA-HANP-021	x		NoF1-029	13907	14374	468	reverse	x		NoF1-029	31782	32249	468	reverse	x		NoF1-029	11710	12177	468	reverse	
Kekk-like protein (Cop-C5L)	overlap	-																						
Kekk-like protein (Cop-C5L)	NoF1-030	-	x		NoF1-030	14707	15084	378	reverse	x		NoF1-030	32582	32959	378	reverse	x		NoF1-030	12510	12887	378	reverse	
IL-1 receptor antagonist (Cop-C10L)	NoF1-031	-	x		NoF1-031	15145	16092	948	reverse	x		NoF1-031	33020	33967	948	reverse	x		NoF1-031	12948	13895	948	reverse	
Complement binding (secreted) (Cop-C3L)	NoF1-032	-	x		NoF1-032	16159	16953	795	reverse	x		NoF1-032	34034	34828	795	reverse	x		NoF1-032	13962	14756	795	reverse	
POZ/BTB Kekk domain protein (Cop-C2L)	NoF1-033	-	x		NoF1-033	17016	18554	1539	reverse	x		NoF1-033	34891	36429	1539	reverse	x		NoF1-033	14819	16357	1539	reverse	
Putative TLR signalling inhibitor (Cop-C1L)	NoF1-034	-	x		NoF1-034	18623	19261	639	reverse	x		NoF1-034	36498	37136	639	reverse	x		NoF1-034	16426	17064	639	reverse	
Anti-apoptotic Bcl-2-like protein (Cop-N1L)	NoF1-035	MVA-HANP-022 ^f	x		NoF1-035	19303	19656	354	reverse	x		NoF1-035	37178	37531	354	reverse	x		NoF1-035	17106	17459	354	reverse	
Alpha amanitin target protein (Cop-N2L)	NoF1-036	MVA-HANP-023	x		NoF1-036	19778	20308	531	reverse	x		NoF1-036	37653	38183	531	reverse	x		NoF1-036	17581	18111	531	reverse	
ANK-containing protein; apoptosis inhibitor (Cop-M1L)	NoF1-037	-	x		NoF1-037	20351	21766	1416	reverse	x		NoF1-037	38226	39641	1416	reverse	x		NoF1-037	18154	19569	1416	reverse	
NFkB inhibitor (Cop-M2L)	NoF1-038	-	x		NoF1-038	21744	22406	663	reverse	x		NoF1-038	39619	40281	663	reverse	x		NoF1-038	19547	20209	663	reverse	
Ankyrin/NFkB inhibitor (Cop-K1L)	NoF1-039	MVA-HANP-024 ^f	x		NoF1-039	22530	23387	858	reverse	x		NoF1-039	40405	41262	858	reverse	x		NoF1-039	20333	21190	858	reverse	
Serpin 1.2.3 (Cop-K2L)	NoF1-040	MVA-HANP-025	x		NoF1-040	23745	24866	1122	reverse	x		NoF1-040	41620	42741	1122	reverse	x		NoF1-040	21548	22669	1122	reverse	
IFN resistance; PKR/IFN-alpha inhibitor (Cop-K3L)	NoF1-041	MVA-HANP-026	x		NoF1-041	24917	25183	267	reverse	x		NoF1-041	42792	43058	267	reverse	x		NoF1-041	22720	22986	267	reverse	
Phospholipase-D-like protein (Cop-K4L)	NoF1-042	MVA-HANP-027		x	MVA-HANP-02	25243	26517	1275	reverse	x		NoF1-042	43118	44392	1275	reverse	x		NoF1-042	23046	24320	1275	reverse	
Monoglyceride lipase (Cop-K5L/K6L)	NoF1-043	MVA-HANP-028 ^f	x		NoF1-043	26545	27375	831	reverse	x		NoF1-043	44420	45250	831	reverse	x		NoF1-043	24348	25178	831	reverse	
		MVA-HANP-029 ^f																						
Host immune response repressor (Cop-K7R)	NoF1-044	MVA-HANP-030	x		NoF1-044	27513	27962	450	forward	x		NoF1-044	45388	45837	450	forward	x		NoF1-044	25316	25765	450	forward	
CPV-B-047	overlap	-																						
Caspase-9 (apoptosis) inhibitor (mitochondrial-associated) (Cop-F1L)	NoF1-045	MVA-HANP-031	x		NoF1-045	28036	28779	744	reverse	x		NoF1-045	45911	46654	744	reverse	x		NoF1-045	25839	26582	744	reverse	
dUTPase (Cop-F2L)	NoF1-046	MVA-HANP-032	x		NoF1-046	28779	29222	444	reverse	x		NoF1-046	46654	47097	444	reverse	x		NoF1-046	26582	27025	444	reverse	
Kekk-like protein (Cop-F3L)	NoF1-047	MVA-HANP-033	x		NoF1-047	29246	30688	1443	reverse	x		NoF1-047	47121	48563	1443	reverse		x	MVA-HANP-033	27049	28479	1431	reverse	
Ribonucleotide reductase small subunit (Cop-F4L)	NoF1-048	MVA-HANP-034	x		NoF1-048	30699	31700	1002	reverse	x		NoF1-048	48574	49575	1002	reverse	x		MVA-HANP-034	28490	29449	960	reverse	

Hypothetical protein (Cop-F6L)	NoF1-050	MVA-HANP-037	x	NoF1-050	32685	32900	216	reverse	x	NoF1-050	50560	50775	216	reverse	x	MVA-HANP-037	30429	30653	225	reverse
Hypothetical protein (Cop-F7L)	NoF1-051	MVA-HANP-038	x	NoF1-051	32916	33161	246	reverse	x	NoF1-051	50791	51036	246	reverse	x	MVA-HANP-038	30669	30911	243	reverse
Cytoplasmic protein (Cop-F8L)	NoF1-052	MVA-HANP-039	x	NoF1-052	33444	33641	198	reverse	x	NoF1-052	51313	51510	198	reverse	x	MVA-HANP-039	31058	31255	198	reverse
S-S bond formation pathway protein substrate (Cop-F9L)	NoF1-053	MVA-HANP-040	x	NoF1-053	33702	34340	639	reverse	x	NoF1-053	51571	52209	639	reverse	x	MVA-HANP-040	31315	31953	639	reverse
Essential Ser/Thr kinase morph (Cop-F10L)	NoF1-054	MVA-HANP-041	x	NoF1-054	34327	35646	1320	reverse	x	NoF1-054	52196	53515	1320	reverse	x	MVA-HANP-041	31940	33259	1320	reverse
VV_Cop-F ORF D		-																		
RhoA signalling inhibitor, virus release protein i (Cop-F11L)	NoF1-055	MVA-HANP-042 ¹	x	NoF1-055	35669	36733	1065	reverse	x	NoF1-055	53538	54602	1065	reverse	x	MVA-HANP-042	33282	33536	255	reverse
EEV maturation protein (Cop-F12L)	NoF1-056	MVA-HANP-044	x	NoF1-056	36776	38680	1905	reverse	x	NoF1-056	54645	56549	1905	reverse	x	MVA-HANP-044	33993	34295	303	reverse
Palmitoylated EEV membrane glycoprotein (Cop-F13 L)	NoF1-057	MVA-HANP-045	x	NoF1-057	38714	39832	1119	reverse	x	NoF1-057	56583	57701	1119	reverse	x	MVA-HANP-045	34338	36242	1905	reverse
Unknown (Cop-F14L)	NoF1-058	MVA-HANP-046	x	NoF1-058	39850	40071	222	reverse	x	NoF1-058	57719	57940	222	reverse	x	MVA-HANP-046	36276	37394	1119	reverse
IMV protein (Cop-F14.5L)		-																		
CPV-B-063	NoF1-059	-	x	NoF1-059	40118	40276	159	forward	x	NoF1-059	57987	58145	159	forward	x	MVA-HANP-047	37412	37633	222	reverse
Unknown conserved protein (Cop-F15L)	NoF1-060	MVA-HANP-048	x	NoF1-060	40944	40820	477	reverse	x	NoF1-060	58213	58689	477	reverse	x	MVA-HANP-048	37680	37838	159	forward
Non-functional Serine Recombinase (Cop-F16L)	NoF1-061	MVA-HANP-049	x	NoF1-061	40820	41521	702	reverse	x	NoF1-061	58689	59390	702	reverse	x	MVA-HANP-049	37906	38382	477	reverse
DNA-binding phosphoprotein (VP11); mTOR antagonist (Cop-F17R)	NoF1-062	MVA-HANP-050	x	NoF1-062	41584	41889	306	forward	x	NoF1-062	59453	59758	306	forward	x	MVA-HANP-050	38382	39083	702	reverse
Poly (A) polymerase catalytic subunit (VP55) (Cop-E1L)	NoF1-063	MVA-HANP-051	x	NoF1-063	41886	43325	1440	reverse	x	NoF1-063	59755	61194	1440	reverse	x	MVA-HANP-051	39146	39451	306	forward
IEV morphogenesis (Cop-E2L)	NoF1-064	MVA-HANP-052	x	NoF1-064	43322	45535	2214	reverse	x	NoF1-064	61921	63404	2214	reverse	x	MVA-HANP-052	39448	40887	1440	reverse
dsRNA-binding protein, IFN resistance/PKR inhibitor (Z-DNA binding) (Cop-E3L)	NoF1-065	MVA-HANP-053	x	NoF1-065	45666	46238	573	reverse	x	NoF1-065	63535	64107	573	reverse	x	MVA-HANP-053	40884	43097	2214	reverse
RNA polymerase subunit (RPO30) (Cop-E4L)	NoF1-066	MVA-HANP-054	x	NoF1-066	46293	47078	786	reverse	x	NoF1-066	64162	64947	786	reverse	x	MVA-HANP-054	43228	43800	573	reverse
Virosome component (Cop-E5R)	NoF1-067	MVA-HANP-055	x	NoF1-067	47198	48151	954	forward	x	NoF1-067	65067	66020	954	forward	x	MVA-HANP-055	44670	45713	954	forward
Virion protein (Cop-E6R)	NoF1-068	MVA-HANP-056	x	NoF1-068	48271	49974	1704	forward	x	NoF1-068	66140	67843	1704	forward	x	MVA-HANP-056	45833	47536	1704	forward
Myristylated protein (Cop-E7R)	NoF1-069	MVA-HANP-057	x	NoF1-069	50036	50533	498	forward	x	NoF1-069	67905	68402	498	forward	x	MVA-HANP-057	47598	48095	498	forward
ER-localized membrane protein, virion core protein (Cop-E8R)	NoF1-070	MVA-HANP-058	x	NoF1-070	50644	51465	822	forward	x	NoF1-070	68513	69334	822	forward	x	MVA-HANP-058	48206	49027	822	forward
DNA polymerase (Cop-E9L)	NoF1-071	MVA-HANP-059	x	NoF1-071	51472	54492	3021	reverse	x	NoF1-071	69241	72358	3018	reverse	x	MVA-HANP-059	49034	52051	3018	reverse
Sulphydryl oxidase (FAD-linked) (Cop-E10R)	NoF1-072	MVA-HANP-060	x	NoF1-072	54524	54811	288	forward	x	NoF1-072	72390	72677	288	forward	x	MVA-HANP-060	52083	52370	288	forward
Virion core protein (Cop-E11L)	NoF1-073	MVA-HANP-061	x	NoF1-073	54806	55195	390	reverse	x	NoF1-073	72672	73061	390	reverse	x	MVA-HANP-061	52365	52754	390	reverse
Membrane protein (Cop-O1L)	NoF1-074	MVA-HANP-062 ¹	x	NoF1-074	55182	57182	2001	reverse	x	NoF1-074	73048	75048	2001	reverse	x	MVA-HANP-062	52741	54741	2001	reverse
Glutaredoxin 1 (Cop-O2L)	NoF1-075	MVA-HANP-064	x	NoF1-075	57230	57556	327	reverse	x	NoF1-075	75096	75422	327	reverse	x	MVA-HANP-064	54789	55115	327	reverse
Virus entry/fusion complex component (Cop-O3L)	NoF1-076	MVA-HANP-065	x	NoF1-076	57580	57687	108	reverse	x	NoF1-076	75446	75553	108	reverse	x	MVA-HANP-065	55139	55246	108	reverse
DNA-binding core protein (Cop-I1L)	NoF1-077	MVA-HANP-066	x	NoF1-077	57702	58640	939	reverse	x	NoF1-077	75568	76506	939	reverse	x	MVA-HANP-066	55261	56199	939	reverse
IMV membrane protein (Cop-I2L)	NoF1-078	MVA-HANP-067	x	NoF1-078	58647	58868	222	reverse	x	NoF1-078	76513	76734	222	reverse	x	MVA-HANP-067	56206	56427	222	reverse
ssDNA-binding phosphoprotein (Cop-I3L)	NoF1-079	MVA-HANP-068	x	NoF1-079	58869	59678	810	reverse	x	NoF1-079	76735	77544	810	reverse	x	MVA-HANP-068	56428	57237	810	reverse
Ribonucleotide reductase large subunit (Cop-I4L)	NoF1-080	MVA-HANP-069	x	NoF1-080	59761	62076	2316	reverse	x	NoF1-080	77627	79942	2316	reverse	x	MVA-HANP-069	57320	59635	2316	reverse
IMV protein VP13 (Cop-I5L)	NoF1-081	MVA-HANP-070	x	NoF1-081	62103	62342	240	reverse	x	NoF1-081	79969	80208	240	reverse	x	MVA-HANP-070	59662	59901	240	reverse
Tekomere-binding protein (Cop-I6L)	NoF1-082	MVA-HANP-071	x	NoF1-082	62361	63509	1149	reverse	x	NoF1-082	80227	81375	1149	reverse	x	MVA-HANP-071	59920	61068	1149	reverse
Virion core cysteine protease (Cop-I7L)	NoF1-083	MVA-HANP-072	x	NoF1-083	63502	64773	1272	reverse	x	NoF1-083	81368	82639	1272	reverse	x	MVA-HANP-072	61061	62332	1272	reverse
RNA helicase, DExH-NPH-II domain (Cop-I8R)	NoF1-084	MVA-HANP-073	x	NoF1-084	64779	66809	2031	forward	x	NoF1-084	82645	84675	2031	forward	x	MVA-HANP-073	62338	64368	2031	forward
Metalloprotease (Cop-G1L)	NoF1-085	MVA-HANP-074	x	NoF1-085	66813	68588	1776	reverse	x	NoF1-085	84679	86454	1776	reverse	x	MVA-HANP-074	64372	66147	1776	reverse
Entry/fusion complex component (Cop-G3L)	NoF1-086	MVA-HANP-075	x	NoF1-086	68585	68920	336	reverse	x	NoF1-086	86451	86786	336	reverse	x	MVA-HANP-075	66144	66479	336	reverse
VLTf (late transcription elongation factor) (Cop-G2R)	NoF1-087	MVA-HANP-076	x	NoF1-087	68914	69576	663	forward	x	NoF1-087	86780	87442	663	forward	x	MVA-HANP-076	66473	67135	663	forward
Glutaredoxin-like protein (Cop-G4L)	NoF1-088	MVA-HANP-077	x	NoF1-088	69546	69920	375	reverse	x	NoF1-088	87412	87786	375	reverse	x	MVA-HANP-077	67105	67479	375	reverse
FEN1-like nuclease (Cop-G5R)	NoF1-089	MVA-HANP-078	x	NoF1-089	69923	71230	1308	forward	x	NoF1-089	87789	89096	1308	forward	x	MVA-HANP-078	67482	68789	1308	forward
RNA polymerase subunit (RPO7) (Cop-G5.5R)	NoF1-090	MVA-HANP-079	x	NoF1-090	71238	71429	192	forward	x	NoF1-090	89104	89295	192	forward	x	MVA-HANP-079	68797	68988	192	forward
NLPcP60 superfamily protein (Cop-G6R)	NoF1-091	MVA-HANP-080	x	NoF1-091	71431	71928	498	forward	x	NoF1-091	89297	89794	498	forward	x	MVA-HANP-080	68990	69487	498	forward
Virion phosphoprotein, early morphogenesis (Cop-G7L)	NoF1-092	MVA-HANP-081	x	NoF1-092	71893	73008	1116	reverse	x	NoF1-092	89759	90874	1116	reverse	x	MVA-HANP-081	69452	70567	1116	reverse
CC_Cop-G ORF B		-																		
VLTf-1 (late transcription factor 1) (Cop-G8R)	NoF1-093	MVA-HANP-082	x	NoF1-093	73039	73821	783	forward	x	NoF1-093	90905	91687	783	forward	x	MVA-HANP-082	70598	71380	783	forward
Entry/fusion complex component, myristylated protein (Cop-G9R)	NoF1-094	MVA-HANP-083	x	NoF1-094	73841	74863	1023	forward	x	NoF1-094	91707	92729	1023	forward	x	MVA-HANP-083	71400	72422	1023	forward
IMV membrane protein (Cop-L1R)	NoF1-095	MVA-HANP-084	x	NoF1-095	74864	75616	753	forward	x	NoF1-095	92730	93482	753	forward	x	MVA-HANP-084	72423	73175	753	forward
Virial membrane assembly proteins (VMAP) (Cop-L2R)	NoF1-096	MVA-HANP-085	x	NoF1-096	75648	75914	267	forward	x	NoF1-096	93514	93780	267	forward	x	MVA-HANP-085	73207	73473	267	forward
Internal virion protein (Cop-L3L)	NoF1-097	MVA-HANP-086	x	NoF1-097	75904	76956	1053	reverse	x	NoF1-097	93770	94822	1053	reverse	x	MVA-HANP-086	73463	74515	1053	reverse
ssdsDNA binding protein (VP8) (Cop-L4R)	NoF1-098	MVA-HANP-087	x	NoF1-098	76981	77736	756	forward	x	NoF1-098	94847	95602	756	forward	x	MVA-HANP-087	74540	75295	756	forward
Entry and Fusion IMV protein (Cop-L5R)	NoF1-099	MVA-HANP-088	x	NoF1-099	77746	78132	387	forward	x	NoF1-099	95612	95998	387	forward	x	MVA-HANP-088	75305	75691	387	forward
Virion morph (Cop-J1R)	NoF1-100	MVA-HANP-089	x	NoF1-100	78089	78550	462	forward	x	NoF1-100	95955	96416	462	forward	x	MVA-HANP-089	75648	76109	462	forward
Thymidine kinase (Cop-J2R)	NoF1-101	MVA-HANP-090	x	NoF1-101	78566	79099	534	forward	x	NoF1-101	96432	96965	534	forward	x	MVA-HANP-090	76125	76658	534	forward
Poly (A) polymerase small subunit (VP39) (Cop-J3R)	NoF1-102	MVA-HANP-091	x	NoF1-102	79167	80168	1002	forward	x	NoF1-102	97033	98034	1002	forward	x	MVA-HANP-091	76726	77727	1002	forward
RNA polymerase subunit (RPO22) (Cop-J4R)	NoF1-103	MVA-HANP-092	x	NoF1-103	80083	80640	558	forward	x	NoF1-103	97949	98506	558	forward	x	MVA-HANP-092	77642	78		

Supplementary Table 3. Number of recombination breakpoints along the genome of progeny viruses.

Experiment		Virus	RDP4		Simplot		Manually	
			Core	ITR	Core	ITR	Core	ITR
Coinfection	CPXV-NOF1/ MVA-HANP	R1	10	-	14	-	14	-
	Superinfection 1 (CPXV-NOF1/ MVA-HANP 4h)	R2	20	-	20	-	20	-
		R3	0	-	2	-	2	-
		R4	7	1	9	3	9	3
	Superinfection 2 (MVA-HANP/ CPXV-NOF1-4h)	R5	6	-	6	-	6	-
		R6	4	-	8	-	8	-
		R7	8	2	14	2	14	2
	Superinfection 3 (CPXV-NOF1/ MVA-HANP-6h)	R8	12	-	22	-	22	-
		R9	-	-	-	-	-	-
		R10	6	-	10	-	12	-
		R11	2	-	4	2	8	2
	Superinfection 4 (MVA-HANP/ CPXV-NOF1-6h)	R12	6	-	9	1	11	1

Supplementary Table 4. Number of CDS derived from the parental viruses (CPXV-No-F1 and MVA-HANP) in the progeny viruses.

Experiment		Virus	CDS from CPXV-NoF1	CDS from MVA-HANP
Coinfection	CPXV-NOF1/ MVA-HANP	R1	173	43
Superinfection	Superinfection 1 (CPXV-NOF1/ MVA-HANP 4h)	R2	104	116
		R3	217	0
		R4	159	51
	Superinfection 2 (MVA-HANP/ CPXV-NOF1-4h)	R5	199	15
		R6	179	38
		R7	168	45
	Superinfection 3 (CPXV-NOF1/ MVA-HANP-6h)	R8	153	65
		R9	217	0
		R10	173	25
		R11	171	41
	Superinfection 4 (MVA-HANP/ CPXV-NOF1-6h)	R12	83	114

*R3 did not contain MVA-HANP CDS but it had a small recombination region from MVA-HANP

Supplementary Table 5. List of single-nucleotide polymorphisms (SNP), insertions and deletions detected in the progeny viruses

Experiment		Virus	Type	Progeny Genome	Parental genome	Location (bp)	Length (bp)	CDS	
Coinfection	CPXV-NOF1/ MVA-HANP	R1	deletion	<i>HA</i> transgene, partial <i>NP</i> transgene	<i>HA-NP</i> transgenes	14748-31510	3161	-	
			SNP	A	C	205360	1	<i>NoF1-208</i> (CPXV-Br219)	
Superinfection	Superinfection 1 (CPXV-NOF1/ MVA-HANP 4h)	R2	SNP	G	T	138235	1	<i>NoF1-138</i> (CPXV-Br144)	
			R3	insertion	ATC	-	154305-154307	3	<i>NoF1-153</i> (VACV-Cop A26L)
				insertion	GT	-	7446-7447	2	Intergenic region
	Superinfection 2 (MVA-HANP/ CPXV-NOF1-4h)	R4	deletion	-	T	172281	1	Intergenic region	
			insertion	CA	-	193258-193259	2	Intergenic region	
			deletion	-	T	176169	1	Intergenic region	
		R6	insertion	GT	-	7656-7657	2	Intergenic region	
			insertion	AC	-	210478-210479	2	Intergenic region	
	Superinfection 3 (CPXV-NOF1/ MVA-HANP-6h)	R7	deletion	-	T	181562	1	Intergenic region	
			deletion	-	T	172509	1	Intergenic region	
		R9	insertion	AGTG	-	7172-7175	4	Intergenic region	
			SNP	A	C	8097	1	<i>NoF1-oo8</i> (VACV-Cop N2L)	
			SNP	A	G	42301	1	<i>NoF1-040</i> (VACV-Cop K2L)	
			insertion	CTCA	-	213994-213997	4	Intergenic region	
		R10	deletion	-	long	13660	16761	<i>NoF1-015 - NoF1-028</i> (CPXV-Br016 - CPXV-Br029)	
			deletion	-	GGTGTAAGAATAGGAGCAGTACTACTA	111707	27	VACV-Cop A4L	
	deletion		-	T	158466	1	Intergenic region		
	R11	deletion	-	T	176071	1	Intergenic region		
	Superinfection 4 (MVA-HANP/ CPXV-NOF1-6h)	R12	deletion	-	long	13654	16761	<i>NoF1-015 - NoF1-028</i> (CPXV-Br016 - CPXV-Br029)	
insertion			A	-	126518	1	Intergenic region		
deletion			-	T	151622	1	Intergenic region		

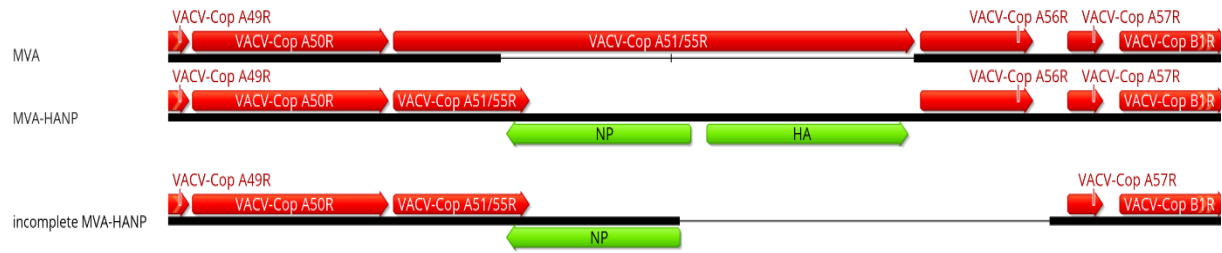


Fig S1. Comparison of the double expression cassette in MVA, MVA-HANP and incomplete MVA-HANP. Green blocks represent the influenza virus *hemagglutinin* (HA) and *nucleoprotein* (NP) transgenes. Red blocks represent the coding sequences (CDS) from MVA-HANP.

